

THEORETICAL AND NUMERICAL APPROACH OF ULTIMATE CAPACITY OF TRANSVERSELY PRESTRESSED CONCRETE DECK

Master Thesis

Georgia Petropoulou

Structural Engineering

Concrete Track

CITG



August 2013

THEORETICAL AND NUMERICAL APPROACH OF ULTIMATE CAPACITY OF TRANSVERSELY PRESTRESSED CONCRETE DECK

Date **26th of August 2013**

Student **Petropoulou D. Georgia**

Student I.D **4180763**

Delft University of Technology

Faculty Civil Engineering and Geosciences

Committee **Prof. Dr. Ir. D.A. Hordijk**

Dr. Ir. C. Van Der Veen

Dr. Ir. M.A.N. Hendriks

Acknowledgements

I would like to sincerely thank my supervisor Cor van der Veen for his precious advice and guidance throughout this endeavour. Many thanks to all members of the committee Prof. Hordijk and Dr. Hendriks for their assistance during the meetings. Last but not least, assistant professor Dr. P.J. Philip Vardon should be praised for always be willing to help about the numerical simulation.

Delft, August 2013
Petroplou D. Georgia

CONTENTS

TABLE OF FIGURES	6
CONTENT OF TABLES	10
NOTATION	11
1. INTRODUCTION	13
1.1. General.....	13
1.2. Basis for compressive membrane action.....	13
1.3. Basis for transverse prestressing	15
1.4. Literature Review.....	16
1.4.1. Kinnunen and Nylander’s Model.....	16
1.4.2. Hewitt-Batchelor’s Model.....	17
1.4.3. Plastic theory approach	20
1.4.4. Park and Garnble [1981]	22
1.4.5. New Zealand code.....	22
1.4.6. Eurocode 2	23
1.5. Objectives - Research Questions.....	23
1.6. Outline Of Thesis	24
PART I: PUNCHING SHEAR CAPACITY	26
2. COMPRESSIVE MEMBRANE ACTION IN PUNCHING SHEAR	26
2.1. Introduction.....	26
2.2. Failure Mechanism.....	26
2.3. Theoretical Approach of Punching Shear capacity	28
2.4. Analytical part of approach.....	33
2.4.1. Matlab flowchart.....	35
3. APPLICATION TO PRESENT EXPERIMENT.....	36
3.1. Introduction.....	36
3.2. Application at the applied prestress level: $\sigma_{cp} = 2.5$ MPa	37
3.2.1. Theoretical part of approach	37
3.2.2. Results for all the applied prestress levels	41
4. COMPARATIVE STUDY	43
4.1. Results.....	43
4.2. Comparison: Experimental – Theoretical approach.....	43
4.2.1. Graphs	46
PART II: BENDING CAPACITY OF TRANSVERELLY PRESTRSESSED SLAB	48
5. INTRODUCTION: FAILURE MECHANISM	48
5.1. Horizontal Elongation of Slab.....	49
5.2. Forces in the Slab.....	51

5.2.1.	Concrete Forces	51
5.2.2.	Forces in the Mild Steel Reinforcement.....	52
5.2.3.	Forces in Prestressing Steel.....	53
5.2.4.	Location of Neutral Axis at Plastic Hinges.....	55
5.3.	Determination of the Ultimate Capacity	57
5.3.1.	Axial Force and Moments.....	57
5.3.2.	Calculation of the Capacity.....	57
5.3.3.	Location of the Central Hinge.....	58
5.4.	Restrained Stiffness.....	58
5.4.1.	Interior bay loaded	60
5.4.2.	Exterior bay line loaded	63
6.	Computational Modelling	64
6.1.	Introduction.....	64
6.2.	Structure of the code	65
6.3.	Flowcharts.....	67
7.	APPLICATION OF THEORETICAL AND NUMERICAL APPROACH	69
7.1.	General.....	69
7.2.	Input data	70
7.3.	Determination of stiffness	72
8.	RESULTS	79
8.1.	CASE 1: Internal slab	79
8.1.1.	Effects of Compressive Membrane Action	79
8.1.2.	Effect of Lateral Restraint on the Ultimate capacity	83
8.1.3.	Capacity Enhancement Factor: Slenderness - Stiffness effect	90
8.2.	Case 2: Exterior slab	95
8.2.1.	Effects of Compressive Membrane Action	96
8.2.2.	Effect of Lateral Restraint on the Ultimate capacity	101
8.2.3.	Capacity Enhancement Factor: Slenderness - Stiffness effect	106
8.2.4.	Comparison: Load over Internal and External panel	109
9.	COMPARATIVE STUDY	111
9.1.	Comparison Bending results	111
9.2.	Graphs.....	112
9.3.	Comparison: Punching – Bending results	113
10.	PARAMETRIC STUDY.....	115
11.	CONCLUSIONS.....	118
	REFERENCES	120
	APPENDIX I	122
	APPENDIX II	142

TABLE OF FIGURES

Figure 1 Typical Load Deflection Curve for Restrained Slab [Park and Gamble, 1980] 14

Figure 2 Effect of Span to Depth Ratio on Capacity Enhancement 15

Figure 3 Typical Examples of Water Entry [Rogowsky, 1997] 15

Figure 4 η -TPL Relationship 16

Figure 5 Idealized displacement and Maximum boundary forces in fully restrained slab 18

Figure 6 Linear relation restraint factor and level of prestress 19

Figure 7 Analytical Methods.....	19
Figure 8 Kinnunen-Nylander model	27
Figure 9 Punching failure model modified by Hewitt-Batcelor (1975)	28
Figure 10 Failure Mode VE	28
Figure 12 Bending moments and slab deformation for a circular slab supported on the edge of a circular column	29
Figure 12 Stress-strain curve for concrete strength.....	32
Figure 13 Matlab flowchart.....	36
Figure 14 Apparatus of structure.....	37
Figure 15 V_e -TPL Relationship	46
Figure 16 V_e - δ Relationship	47
Figure 17 Restraint factor η -TPL Relationship	47
Figure 18 Compressive membrane action.....	48
Figure 19 Comparison: Punching shear capacity.....	48
Figure 20 Bending Failure Mechanism.....	49
Figure 21 Boundary restraints.....	49
Figure 22 Horizontal elongation of slab.....	50
Figure 23 Strains in the Mild Steel Reinforcement.....	52
Figure 24 Modified trilinear idealization for mild steel [Sargin, 1971].....	53
Figure 25 Increase in Tendon length for assumed failure mechanism.....	54
Figure 26 Modified Ramberg-Osgood function [Collins and Mitchell, 1991]	55
Figure 27 Geometry of the deformed slab and the forces present.....	55
Figure 28 Free Body Diagrams for Loaded Slab Segments.....	57
Figure 29 Linear springs at both ends of slab	59
Figure 30 Equivalent Model of Restraint.....	59
Figure 31 Shear influence	60
Figure 32 Lateral Displacement - Stiffness.....	62
Figure 33 Free body – Forces	63
Figure 34 Bridge model structure	70
Figure 35 Loaded panel.....	73
Figure 36 Shear deformation.....	75
Figure 37 Support deformation for varying stiffness ratio.....	76
Figure 38 $\Delta_{\text{support}} / \Delta_{\text{shear}}$ for varying stiffness ratio	76
Figure 39 Exterior bay line loaded.....	78
Figure 40 Deflection on Bending and Arching capacity.....	80
Figure 41 Compressive membrane force N_u - δ	81
Figure 42 Lateral displacement Δ_{13} - δ	81
Figure 43 Comparison: Effect of TPL and Deflection on Bending and Arching Capacities	82

Figure 44 Comparison: Effect of TPL and Deflection on Ultimate capacity	82
Figure 45 Comparison between compressive membrane force $Nu-\delta$ for different TPL	83
Figure 46 Comparison: Lateral displacement $\Delta_{13}-\delta$ for different TPL.....	83
Figure 47 Ultimate capacity-Restraint ratio	84
Figure 48 Ultimate capacity-Restraint ratio (in detail)	85
Figure 49 Enhancement factor-Restrained ratio.....	86
Figure 50 Load Deflections curves for varying S/Ss	86
Figure 51 Enhancement load factor for varying S/Ss	87
Figure 52 Comparison: Ultimate capacity-Restraint ratio for different TPL	88
Figure 53 Comparison: Ultimate capacity-Restraint ratio for different TPL (in detail)	88
Figure 54 Comparison: Enhancement load factor for varying S/Ss for different TPL.....	89
Figure 55 Comparison: Ultimate capacity for varying S/Ss for different TPL	89
Figure 56 Comparison: Enhancement load factor for varying S/Ss.....	90
Figure 57 Enhancement load factor for varying S/Ss and varying slenderness	91
Figure 58 Enhancement load factor for varying S/Ss and varying slenderness (in detail).....	91
Figure 59 Ultimate capacity for varying S/Ss and varying slenderness	92
Figure 60 Arching capacity for varying S/Ss and varying slenderness l/h	92
Figure 61 Bending capacity for varying S/Ss and varying slenderness l/h	93
Figure 62 Comparison: Enhancement load factor for varying S/Ss and varying slenderness l/h	93
Figure 63 Comparison: Ultimate capacity for varying S/Ss and varying slenderness (in detail).....	94
Figure 64 Comparison: Arching capacity for varying S/Ss, varying slenderness l/h and different TPL	94
Figure 65 Bending capacity for varying S/Ss and varying slenderness l/h	95
Figure 66 Effect of Deflection on Bending and Arching Capacities	98
Figure 67 Compressive membrane force $Nu-\delta$	98
Figure 68 Lateral displacement $\Delta_{13}-\delta$	99
Figure 69 Comparison: Effect of Deflection on Bending and Arching Capacities for different TPL... 99	99
Figure 70 Comparison: Compressive membrane force $Nu-\delta$ for different TPL	100
Figure 71 Comparison: Lateral displacement $\Delta_{13}-\delta$ for different TPL.....	100
Figure 72 Ultimate capacity-Restraint ratio	101
Figure 73 Ultimate capacity-Restraint ratio (in detail)	102
Figure 74 Effect of stiffness ratio on compressive membrane action	102
Figure 75 Effect of stiffness ratio on lateral displacement.....	103
Figure 76 Effect of stiffness ratio on enhancement load factor LE.....	103
Figure 77 Load Deflections curves for varying S/Ss	104
Figure 78 Comparison: Effect of Lateral Support Stiffness for different TPL	104
Figure 79 Comparison: Load enhancement factor for different TPL.....	105
Figure 80 Comparison: Compressive membrane force for different TPL	105

Figure 81 Comparison: Effect of stiffness ratio on lateral displacement	106
Figure 82 Comparison: Load Deflections curves for varying S/Ss and different TPL	106
Figure 83 Comparison: Ultimate capacity for varying l/h, varying S/Ss and different TPL.....	107
Figure 84 Comparison: Arching capacity for varying l/h, varying S/Ss and different TPL.....	108
Figure 85 Comparison: Bending capacity for varying l/h, varying S/Ss and different TPL	108
Figure 86 Comparison: Load deflection curves at Internal and External panel [TPL=2.5]	109
Figure 87 Comparison: Deflection on Bending and Arching Capacities at internal and external panel.....	109
Figure 88 Comparison: Effect of slenderness and stiffness over Arching Capacities [2.5MPa]	110
Figure 89 Comparison: Effect of slenderness and stiffness over Bending Capacities [2.5MPa].....	110
Figure 90 Compressive membrane force $Nu-\delta$	112
Figure 91 Comparison: Effect of Deflection on Bending and Arching Capacities for different TPL.	113
Figure 92 Ultimate capacity at bending	113
Figure 93 Comparison: Punching-Bending Results	114
Figure 94 Comparison: Punching-Bending Results	114
Figure 95 Punching failure mode.....	115
Figure 96 Enhancement load factor for varying S/Ss and varying slenderness (in detail).....	116
Figure 97 Comparison: Load deflection curves at Internal and External panel [TPL=2.5]	117
Figure 98 Comparison: Deflection on Bending and Arching Capacities at internal and external panel.....	117
Figure 99 Comparison: Effect of slenderness and stiffness over Arching Capacities [2.5MPa]	118
Figure 100 Comparison: Effect of slenderness and stiffness over Bending Capacities [2.5MPa].....	118
Figure 101 Apparatus of bridge model	123
Figure 102 BB-1 Apparatus of structure and load	123
Figure 103 Detail of the load position.....	124
Figure 104 Load – Midspan Deflection Response	125
Figure 105 Bottom side of deck slab after failure	126
Figure 106 Top side of deck slab after failure	126
Figure 107 BB-2 Apparatus of structure and load position	127
Figure 108 Load – Midspan Deflection Response	128
Figure 109 Crack width-Load curve	129
Figure 28 Top side of deck slab after failure	129
Figure 111 Bottom side of deck slab after failure.....	130
Figure 112 BB-16: Apparatus of structure and load	131
Figure 113 Load – Midspan Deflection Response ³	132
Figure 114 Load - Crack width	133
Figure 115 Top side of the deck slab	133
Figure 116 Bottom side of deck slab showing the cracks	134

Figure 117 Apparatus of structure and load.....	134
Figure 118 Detail of the load position.....	135
Figure 119 Load – Midspan Deflection Response.....	137
Figure 120 Bottom side of deck slab after failure.....	137
Figure 121 Top side of deck slab after failure	138
Figure 122 Apparatus of structure and load.....	139
Figure 123 Load – Midspan Deflection Response.....	140
Figure 124 Bottom side of deck slab after failure.....	141
Figure 125 Top side of deck slab after failure	141

CONTENT OF TABLES

Table 1 Input and Output Parameters.....	34
Table 2 Input data	37
Table 3: Theoretical Results	41
Table 4: Calculation of prestress force.....	42
Table 5: Results by Equilibrium	42
Table 6 Analytical Matlab Results.....	43
Table 7 Results of Experimental approach	43
Table 8 Results of Theoretical approach.....	43
Table 9 Input data	70
Table 10: Format and description of input file of the Program SLAB.....	72
Table 11: Values of input parameters	78
Table 12 Analytical results	79
Table 13 Results.....	95
Table 14 Results.....	96
Table 15 Experimental results.....	111
Table 16 Results of theoretical approach.....	111
Table 17 Response progress.....	124
Table 18 Summary results.....	125
Table 19 Response progress.....	127
Table 20 Summary results.....	128
Table 21 Response progress.....	131
Table 22 Summary results.....	132
Table 23 Response progress.....	135
Table 24 Response progress.....	139

NOTATION

d	effective depth of the cross-section	[mm]
d'	difference between the height and the effective depth of the cross-section	[mm]
d_0	length over which the concentrated load is spread	[mm]
d_1	outer diameter of the punched cone	[mm]
h	height of the cross-section	[mm]
f_{cc}	uni-axial concrete compression strength	[N/mm ²]
f_{ct}	uni-axial concrete tensile strength	[N/mm ²]
f_{cu}	cube strength of concrete	[N/mm ²]
f_s, f_y	yield strength of reinforcement steel	[N/mm ²]
f_c	cylindrical concrete tensile strength	[N/mm ²]
f'_c	cylindrical concrete compression strength	[N/mm ²]
kd	factor related to the height of the slab	[-]
n_a	dimensionless membrane force in the mid depth of a slab	[-]
n_r	dimensionless radial membrane force working on the surface of the failure cone	[-]
n_u	membrane force at the mid depth axis at the hogging moment per unit width	[N/mm]
n'_u	membrane force at the mid depth axis at the sagging moment per unit width	[N/mm]
p	perimeter	[mm]
p	punched out perimeter of cone	[mm]
q	reinforcement percentage in the code of New Zealand	[-]
r	radius	[mm]
r	function of the failure surface over the height	[mm]
t	outward lateral displacement at the restrained edge	[mm]
w_0	critical deflection, empirical determined as 0,5 h	[mm]
w_i	deflection at which membrane action starts, empirical determined as 0,03 h	[mm]
A	cross-sectional area	[mm ²]
A_{sh}	cross-sectional area of hoop steel per unit width	[mm ² /mm]
C	compression force at the sagging yield moment per unit width	[N/mm]
C'	compression force at the hogging yield moment per unit width	[N/mm]
D_A	the internal energy dissipation per unit area in the deforming zone	[N/mm]
E	modulus of elasticity	[N/mm ²]
F	concentrated load	[N]
I	impact factor in the code of New Zealand	[-]
L	length of the span	[mm]
M	moment	[Nmm]
N	internal force	[N]
N_{rs}	sum of the radial membrane forces	[N]

R_i unfactored ultimate resistance in the New Zealand code	[N]
P ultimate load in punching shear failure	[N]
P_a analytical ultimate load	[N]
P_e ultimate load from tests	[N]
P_p predicted ultimate load	[N]
S stiffness parameter of a laterally restrained slab	[N/mm]
W virtual work	[Nmm]

GREEK NOTATION

α angle between yield surface and displacement rate vector	[rad]
β factor ($0 < \beta < 0,5$)	[-]
β angle between relative displacement and vertical axes	[rad]
γ_0 overload factor in the code of New Zealand	[-]
γ_L live load factor in the code of New Zealand	[-]
δ deflection in the middle of the span	[mm]
ε strain	[-]
φ angular rotation	[rad]
τ shear stress	[N/mm ²]
τ_1 shear stress at with transverse reinforcement is necessary	[N/mm ²]
τ_2 ultimate shear stress capacity	[N/mm ²]
φ strength reduction factor in the code of New Zealand	[-]
φ_D strength reduction factor in the code of New Zealand	[-]
χ_u height of the compression zone of the concrete	[mm]
ω_0 reinforcement ratio	[-]
ΔL change in length [mm]	[mm]
θ virtual rotation [rad]	[rad]

1. INTRODUCTION

1.1. General

Composites bridge decks are a combination of slab and girder systems, which are designed to carry a concentrated wheel-load in bending and punching action. Formerly, the composite highway bridges were designed assuming that they obtain adequate shear capacity. Consequently, the decks had been considered as simply supported slabs failing entirely in flexure.

However, many researchers discovered that the effect of in-plane compressive membrane forces, induced by the lateral restrained boundary conditions, was considerable on the ultimate capacity of the slab. As a result bridge deck slabs which were designed to fail in bending, they mostly fail under punching mode at a higher load than that predicted for flexure failure, making the assumed bending design of the slab very conservative. Conclusively, the occurring compressive membrane forces enhance the strength of the deck slab and reduce its deformations. This phenomenon is termed “compressive membrane or arching action” and is going to be investigated at the present Master Thesis. Punching and bending failure modes are going to be analysed taken into account the enhancement due to compressive membrane action in combination with the transverse prestress effect.

1.2. Basis for compressive membrane action

Considering a concrete slab which the partially horizontal restraints at the ends do not allow horizontal movements, as illustrated in the figure 1.1. Due to high lateral restraints in plane compressive forces develop in the slab, increasing the ultimate load. According to experimental data the typical load deflection curve for a laterally restrained slab can be depicted at Fig.1

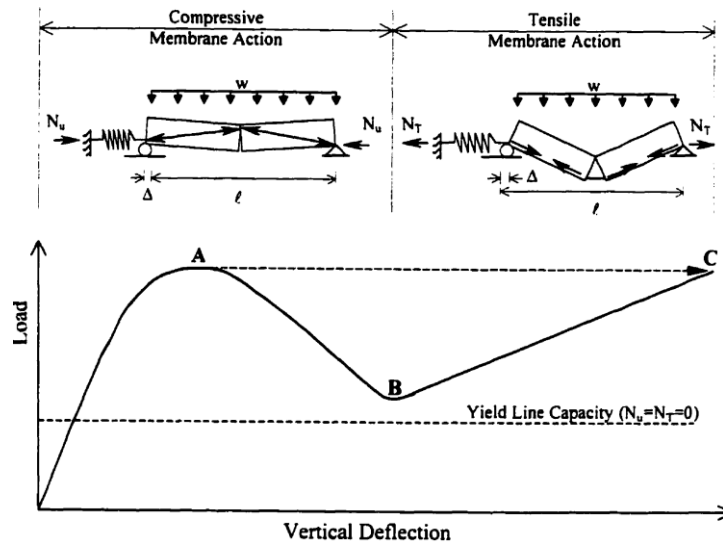


Figure 1 Typical Load Deflection Curve for Restrained Slab [Park and Gamble, 1980]

The dashed line expresses the capacity by predicting in the Yield Line Criterion. The Limit Analysis Method or Yield-Line theory is used to predict the ultimate load of slab systems by postulating a collapse mechanism and considering the principle of virtual work or equations of equilibrium. This method neglects the membrane action and strain hardening as the conventional design rules do. The load deflection curve is consisted of two parts: the compressive membrane action and the tensile membrane action. Comprehensively, while the load increases and the slab deflects vertically, the relative distance between the supports also increases, developing arching forces due to the horizontal restraints. This arching action explains the increase in the capacity of the concrete slab beyond the yield line.

The compressive forces take the maximum value in small vertical displacements, which has been experimentally proved to be equal to half of the slab's thickness. As the deflection increases, the ends of slab tend to move inward decreasing the compressive forces and finally converting to tensile forces. It is noticeable that the ultimate load is given by the load at the peak of the curve (point A).

Generally, it is accepted that the design criterion for the bridge decks should be governed by the serviceability limit state rather than the ultimate state for several reasons.

1. The minimum amount of reinforcement (mainly for shrinkage and temperature requirements) leads to high factors of safety against failure.
2. Compressive membrane action occurs at low deflections, in which the concrete is not fully cracked.
3. The development of tensile membrane action requires an adequate amount of the reinforcement and sufficient anchorage of it at the supports.

It is worth mentioning that the degree of compressive membrane action is dependent on the level of the lateral restraint and the span-to-depth ratio of the slab, the so-called slenderness. The higher

the lateral stiffness of the springs simulating the restraint, the higher the compressive in plane forces developed in the slab.

As have been mentioned, the development of compressive membrane action relies on the restraint of the horizontal elongation of the slab, which decreases as the span-to-depth ratio increases. Since the slenderness increases, the arching action becomes less effective inasmuch as the axial load decreases. The effect of the span-to-depth ratio on the capacity enhancement is shown in Fig 2. The ratio S/S_s represents the lateral support stiffness over the fully rigid stiffness.

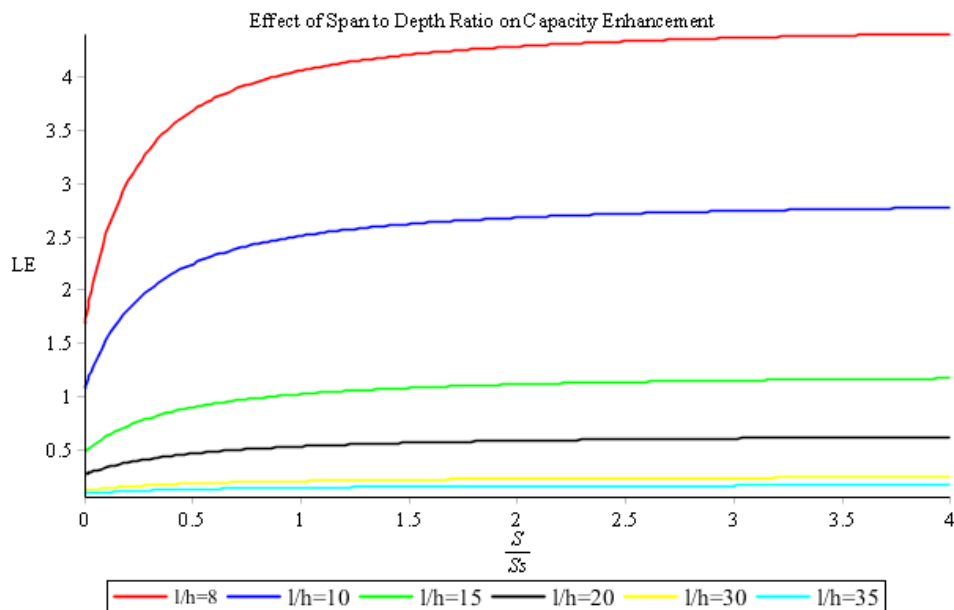


Figure 2 Effect of Span to Depth Ratio on Capacity Enhancement

1.3. Basis for transverse prestressing

It is generally recognized that bridge decks are suffered by wide cracking under moving loads, giving rise to penetration of water, oxygen and other chemical into concrete. This can be avoided by prestressing the deck slab so as to improve the structural response under service loads. The decks can be lighter reducing the dead loads and the deflection may be controlled reducing the cracking.

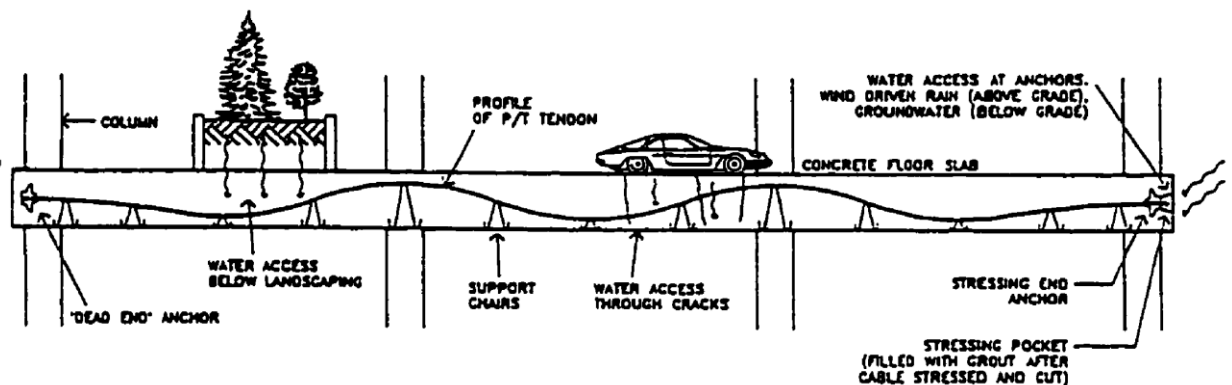


Figure 3 Typical Examples of Water Entry [Rogowsky, 1997]

Prestressed concrete systems commonly use unbonded post-tensioning tendons to improve the serviceability of the deck.

According to several experimental investigations, the development of the compressive membrane action is highly dependent on the level of transverse prestress. This dependence is proposed by Hewitt-Batchelor and can be expressed by linear regression as follows:

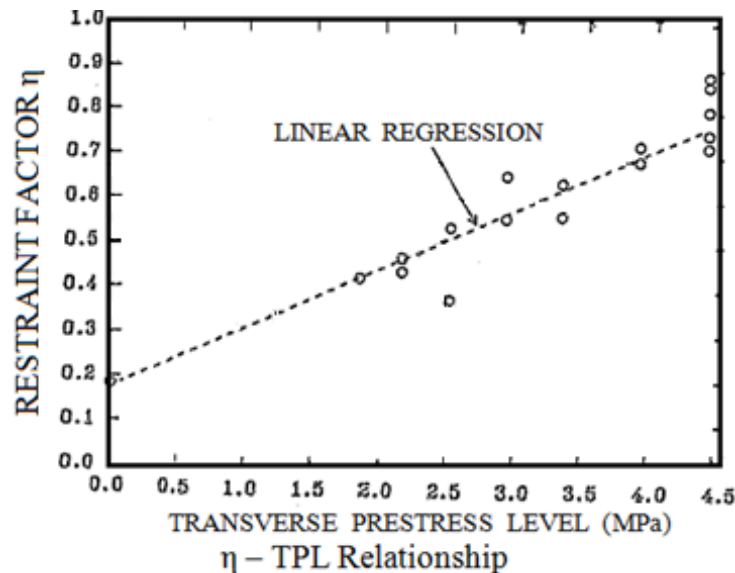


Figure 4 η -TPL Relationship

The transversely prestress can develop sufficient in-plane compressive stresses in the slab to counteract the tensile stresses induced by shrinkage and live loads. Thus, the higher the prestress applied, the higher the initial cracking loads, enhancing the cracking behaviour.

Moreover, one important factor influencing the ultimate capacity of the slab is the position of applied concentrated load with respect to the prestressed wires. It has been noticed that a deck panel is stronger when loaded directly above the wire than when loaded between the wires.

Generally, the effect of lateral restraint due to transversely prestress and the support conditions cooperate effectively to improve essentially the ultimate capacity of slab. The failure mode accounts for punching shear and flexure mode and both failure modes will be analysed at the next sections.

1.4. Literature Review

1.4.1. Kinnunen and Nylander's Model

Punching failure mechanism was primarily investigated by Kinnunen and Nylander in Royal Technical University (1960), carrying out an experimental study about an interior column supports of flat slab floors in a symmetric scheme. Kinnunen and Nylander developed an idealised model, the so-called triaxial state of compressive stresses in the conical shell based on the experimental

results. The failure mode of the slabs was punching failure, which occurred when the tangential strain at the top surface of the circular slabs in the root of the conical shell reaches a characteristic value. This would mean that the concrete has been crushed in the tangential direction.

However, the aforesaid model had to be improved further due to the restricted following assumptions:

1. Failure due to concrete crushing in the tangential direction
2. No size effect of the column is considered
3. Dowel forces are estimated 20% of the calculated resistance
4. The model can be applied to circular slabs with radial and circumferential reinforcement.

At later investigation a more realistic model was provided by Shegata and Regan (1989) as an improved version of the Kinnunen and Nylander's Model.

This model privileged over the initial because the dowel forces are not estimated but directly calculated from model equilibrium and the concrete fails in the critical zone by splitting due to the action of the principal tensile stresses or crushing in the tangential direction.

The improved model of Shegata and Regan corresponds better than the initial to the experimental results.

1.4.2. Hewitt-Batchelor's Model

Hewitt-Batchelor modified the proposed model by Kinnunen and Nylander so as to incorporate the compressive membrane action. It was achieved by introducing compressive forces (F_b) and fixed moments (M_b) at the level of compression reinforcement.

In order to take into account the variety of boundary conditions a restrained factor " η " was introduced accompanied by the maximum boundary forces, as expressed below:

$$F_b = \eta F_{b(\max)}$$

$$M_b = \eta M_{b(\max)}$$

where $F_{b(\max)}$ and $M_{b(\max)}$ correspond to fully rigid support giving maximum theoretically arching action

η : varies between 0 and 1, for simply supported and fully restrained slab respectively

The maximum theoretically arching action can be calculated by employing the model Brotchie and Holley (1971). This model based on the idealised geometry of displacements in the fully restrained slab, as illustrated below.

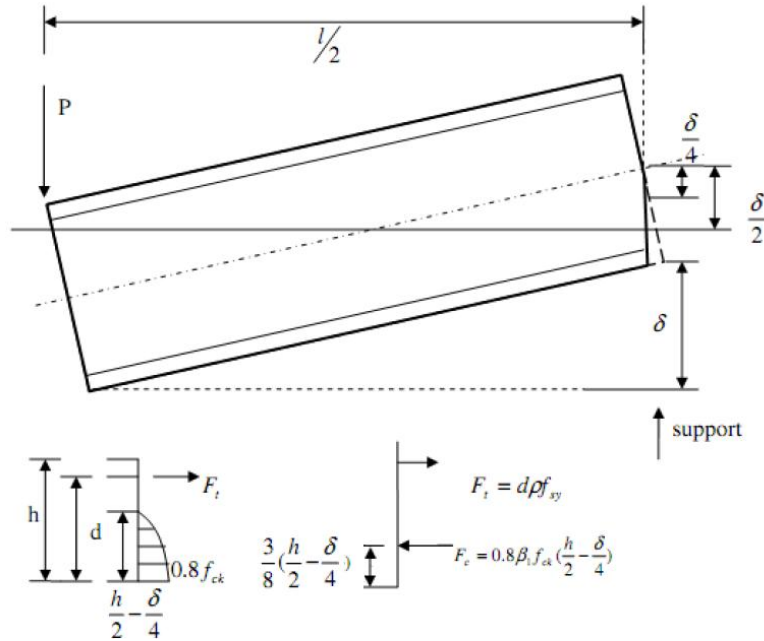


Figure 5 Idealized displacement and Maximum boundary forces in fully restrained slab [Hewitt-Batchelor 1975]

From equilibrium equations the maximum boundary restraints are obtained:

$$F_{b(\max)} = F_c - F_t$$

At the experiment of Hewitt-Batchelor there was not transverse reinforcement used. Thus, there is no contribution of reinforcement steel in the punching shear model. The concrete force is calculated according to NEN 1992-1-1:2005; art.3.1.7].

The concept proposed by Hewitt-Batchelor implies that the prestress steel area acts as normal reinforcement which effective yield stress is reduced insofar as a part of it contributes to the development of compressive forces. This assumption is valid because the positive effect of the applying prestress has already been considered as boundary restraints in the slab ($F_b=P$).

$$f_{sy} = f_{pk} - \frac{F_p}{A_p}$$

Taking into consideration that the ultimate punching shear load, as well as the relating forces are implicitly connected, Hewitt and Batchelor developed an analytical model, which calculated the ultimate load by executing an iteration process.

This model has been employed later in the study of He and Weishi, who proposed two methods to predict the ultimate punching load.

Comprehensively, in the first method the theoretical failure load is calculated for a variety of restraint factors. Then, a graph, which illustrates the relation of restraint factor and transverse prestress level is obtained, as depicted below. Having the experimental failure load the relating restraint factor can be determined.

The procedure briefly is the following:

1. For variety of η the failure loads are calculated
2. Plot the results: P_u - η
3. Plot the graph: η -TPL
4. Estimate the restraint factor by interpolation for the experimental failure load

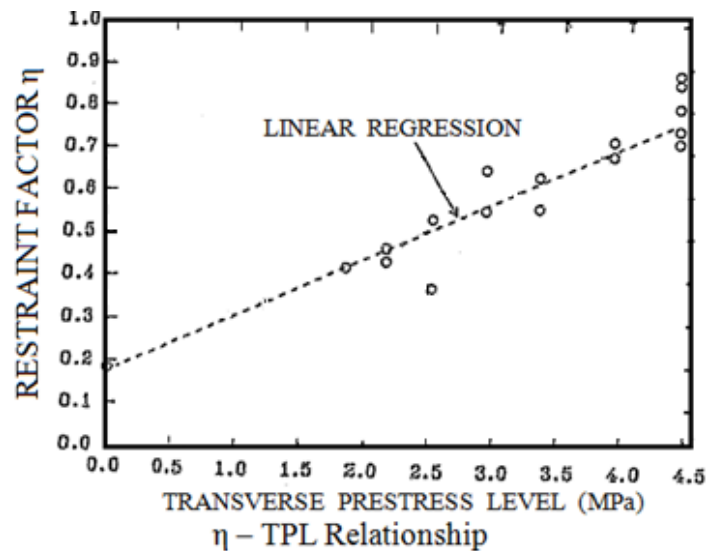


Figure 6 Linear relation restraint factor and level of prestress

In the second method the principle of superposition is employed, which the contribution of compressive membrane action in the reinforced concrete slab is examined separately from the contribution of the prestress. The latter is divided to two distinct trial approaches, as given diagrammatically below.

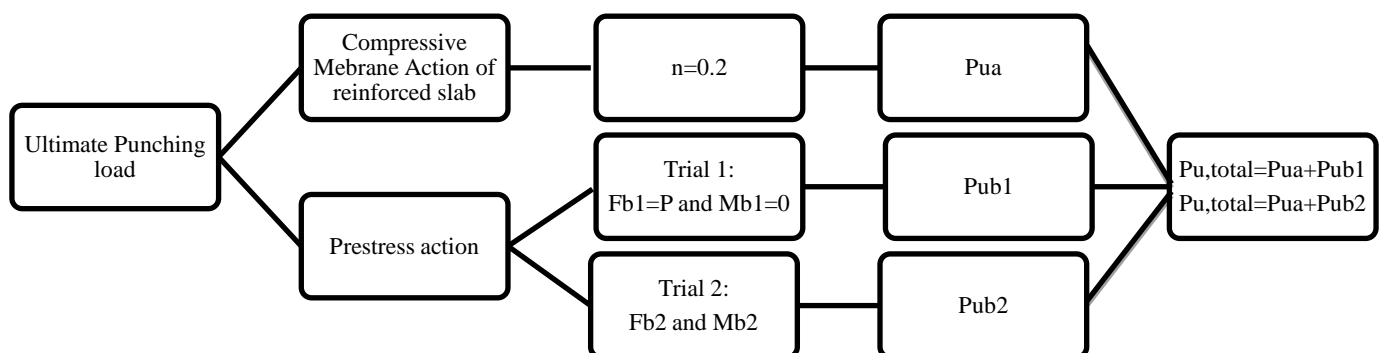


Figure 7 Analytical Methods

At the first step the slab is analysed as non-prestressed composite deck, considering compressive membrane action due to the supports. That is the case the restraint factor η is equal to 0.2 according to the above mentioned graph.

At the second step the effect of prestress action is considered and two approaches employed to predict the final load. The first trial is simplified since the boundary force is equal to the applied prestress force and the boundary moment is considered zero. It is worth mentioning that it has been proved by the test results that excluding the boundary moment is not appropriate while the arching action is underestimated. The ultimate load will be the summation of the first method the this trial.

At the second trial both compressive forces and moments are considered due to the prestressing load, given by the formula:

$$F_b = \eta F_{b(\max)}$$

$$M_b = \eta M_{b(\max)}$$

In order to evaluate them Hewitt and Batchelor were making use of the idealised model of Brotchie and Holley (1971). Moreover, setting again the compressive force F_b equal to prestress load F_p the restrained factor is the output of this iterative process.

$$\eta = \frac{F_p}{F_{b(\max)}}$$

1.4.3. Plastic theory approach

Braestrup and Nielsen [1976] developed a punching model to find an upper bound solution to an axisymmetric slab. The case is treated theoretically considering that a punching failure occurs with a vertical separation of the slab along a surface defined by a generatrix, described by the unknown function:

$$r = F(x)$$

Briefly, the main assumptions employed are:

- Concrete is considered as a modified Coulomb material.
- Proposed failure: punched-out of a solid of revolution whereas the rest of slab remains rigid.
- Yield criterion: with respect of tensile strains and stresses.

The upper bound failure load P is given by applying the theory of energy at the failure surface:

$$W_{\text{External}} = W_{\text{Internal}}$$

$$W_E = P u$$

The internal work can be expressed as a function of the geometry of the failure surface and the compressive and tensile strengths of the concrete.

It should be mentioned that the critical surface of the outer part of slab, which gives the minimum upper punching load, corresponds to the minimum work for a given displacement. The details of this calculation of the failure surface consists of the two parts: a straight line to a depth h_0 and a catenary curve from h_0 to h . The predicted failure surface is thus similar to that observed in punching shear tests.

The dissipation is found by integration over the failure surface. As the motion of failure is perpendicular to the tensile reinforcement, in terms of rigid plasticity, no work is produced by the steel. Thus, the predicted ultimate load is independent on the reinforcement ratio.

The area element can be taken as:

$$dA = 2\pi r \frac{dx}{\cos \alpha}$$

The work equation yields:

$$Pu = \int_0^h \frac{1}{2} f_c u (l - m \sin \alpha) 2\pi r \frac{dx}{\cos \alpha}$$

Conclusively, according to the plastic theory the ratio of flexural reinforcement has no influence on punching resistance and the compressive strength of the concrete is a decisive parameter for the surface of failure.

In 1986 Jiang and Shen modified the model of Braestrup and Nielsen by using a parabolic Coulomb – Mohr intrinsic curve of a modified Coulomb failure envelope.

The lowest upper bound was given as:

$$P = \pi f_t \left(\frac{d_1^2}{4} - \frac{d^2}{4} + \frac{2Kh^2}{\ln d_1 - \ln d} \right)$$

$$K = \frac{1}{4} \left(n + 2(1 - \sqrt{n+1}) \right)$$

$$n = \frac{f_c}{f_t}$$

By including the assumption of a straight yield line the formula was further simplified:

$$P = 0.21 f_c s h$$

where $s = \pi (d+h)$

f_c : an effective compression strength equals to: $f_c = v_c \cdot f_c'$

$v_c = 0.5$ from experimental study

Therefore, the equation of ultimate punching load is:

$$P = 0.074 f_c' s h$$

It is worth noting that the contribution of the prestressing steel is not taken into consideration, making the plastic model less realistic.

1.4.4. Park and Garnble [1981]

Considering a concrete slab which the partially horizontal restraints at the ends do not allow horizontal movements, as illustrated in the Fig 1. Due to lateral restraints high in plane compressive forces develop in the slab, increasing the ultimate load.

The dashed line expresses the capacity by employing the Yield Line Criterion. The Limit Analysis Method or Yield-Line theory is used to predict the ultimate load of slab systems by postulating a collapse mechanism and considering the principle of virtual work or equations of equilibrium. This method neglects the membrane action and strain hardening as the conventional design rules do. The load deflection curve is consisted of two parts: the compressive membrane action and the tensile membrane action. Comprehensively, while the load increases and the slab deflects vertically, the relative distance between the supports also increases, developing arching forces due to the horizontal restraints. This arching action explains the increase in the capacity of the concrete slab beyond the yield line.

The compressive forces take the maximum value in small vertical displacements, which has been experimentally proved to be equal to half of the slab's thickness. As the deflection increases, the ends of slab tend to move inward decreasing the compressive forces and finally converting to tensile forces.

1.4.5. New Zealand code

The New Zealand code is one of the first international codes that takes into account empirically the compressive membrane action in bridge decks by making use of test results. This empirical method can be used if the following conditions are met:

- the supporting beams are steel or concrete
- the diaphragms are continuous and present at all supports for pre-stressed concrete beams
- the slenderness does not exceed 20
- the span length does not exceed 4,5 meter
- the concrete strength $f'c$ is not less than 2 N/mm^2
- the minimum slab thickness is 150 mm
- the overhang of the outer beam is at least 80 mm

The above criteria are expressed by graphs which are categorised by the height of the slab and the compressive strength of the concrete.

It is noticeable that this code takes into account only the reinforcement ratio ρ . The prestressing steel and its effect are neglected, thus the prestressing area has to be converted to an equivalent

reinforcement area. This can be achieved by two ways: based on the force equilibrium and equal stiffness.

The New Zealand code considers only full scale bridge decks, consequently for the sake of comparison the experimental results have to scaled back according to the scale factors of He.

1.4.6. Eurocode 2

According to the Eurocode the ultimate punching shear capacity can be calculated by NEN-EN-1992-1-1 cl 6.4.4.

$$u_{Rd} = C_{Rd,c} \cdot k \cdot (100 \cdot \rho_1 \cdot f_{ck})^{1/3} + k_1 \cdot \sigma_{cp} \geq (u_{min} + k_1 \cdot \sigma_{cp})$$

The perimeter of the load area is u:

$$u = 2 \cdot (c_1 + c_2) + 4\pi d$$

The scaling coefficient:

$$k = 1 + \sqrt{\frac{200}{d}}$$

The reinforcement ratio: $\rho_1 = \sqrt{\rho_{lz} \cdot \rho_{ly}}$

In slab the mean transverse reinforcement is taken into account for the capacity, which in turn is based on the u_{min} and the level of prestress σ_{cp} .

$$\sigma_{cp,level} = \frac{\sigma_{cy} + \sigma_{cz}}{2}$$

$$P_{ulevel} = u_{Rd,2.50,min} \cdot d / \gamma_c \cdot u$$

As has been proved the Eurocode underestimates the ultimate punching load since it takes into account only the 10% of the prestressing $k_1 \cdot \sigma_{cp}$.

1.5. Objectives - Research Questions

The aim of this thesis is to investigate the effect of the compressive membrane action and transversely prestress over the ultimate punching and bending capacity. To develop the analysis of this scientific topic, research questions have been posed giving an orientation into the research and indicating the guiding components of the investigation.

- a. Develop an analytical model to predict the ultimate capacity of a slab accounting for the compressive membrane action and the transverse unbonded post-tensioned tendons.
- b. How can the punching shear and bending failure be defined in the terms of the effective stiffness provided by the supports and the surrounding slabs?
- c. To what extent can the compressive membrane action and the transverse prestress contribute to the punching shear and bending capacity of the slab?
- d. Parametric Study: How can the slenderness of the slab and the position of the load affect the development of compressive membrane action?

- e. Optimization of Structural Design: Which is the combination of the optimum dimensions of the slab for the maximum bending and punching shear capacity?
- f. Comparative Study: How realistic is the model compared to the experimental results?

To approach the research questions this thesis has been divided into two main parts to investigate the two failure modes: Punching shear capacity and Bending capacity. Numerical codes were necessary to be employed and modified to predict the ultimate capacities. These numerical codes were casted to take into account the compressive membrane forces, the prestress effect, the degree of stiffness and the loading conditions.

1.6. Outline Of Thesis

The present thesis is an attempt to estimate the punching shear capacity and bending capacity of a transversely prestressed concrete bridge under the development of compressive membrane action. Therefore, the thesis has been divided into two main parts: Punching shear capacity and Bending capacity.

The objective of this thesis is to investigate the effect of compressive membrane action (CMA) in combination with the transversely prestress under a static point load applied at the midspan of the bridge's slab. The challenge is to develop a physical model which could predict the mechanical response of the slab at punching and bending by taken into account the combination of compressive action and the prestress effect.

Chapter 2 describes the theoretical and analytical approach of punching shear capacity of a transversely prestressed slab under the effect of compressive membrane action. A combination of the models of Kinnunen and Nylander (1960), Hallgren (1996) and the Model Code 90 is employed for the theoretical approach and Hewitt-Batcelor (1975) for the analytical. The employed models were necessary to be adjusted at the conditions of the present thesis. Thus, modifications have taken place, presenting a different approach for the punching failure. The effect of prestress is introduced as imposed deformation in the total ultimate concrete compressive strain. Moreover, since the crushing of concrete characterizes the failure of the slab, the compressive concrete strain is expected to reach the maximum acceptable limit $3.5 \cdot 10^{-3}$. The compressive membrane force is calculated by making use of the principle of equilibrium and employing

In Chapter 3 the results of the theoretical approach regarding the punching shear mode are going to be compared with experimental results. Two prestress levels are applied (1.25-2.5MPa) during the experiments, which took place in the Stevin Lab II CITG, TUDelft, The Netherlands. Comparing the results of both cases many conclusions can be reached. Simulating the prestress as

an imposed strain, the ultimate punching capacity is hardly affected by different prestress levels and the compressive membrane force slightly changes.

Chapter 4 deals with the estimation of the bending capacity of the slab, employing the flexural failure of the approach of Park (1964). A direct solution is not possible due to the fact that the position of neutral axis is unknown. Thus, an iterative procedure should be followed to calculate the concrete and steel forces. Initially, the concrete force set equal to the crushing force and the steel forces equal to yielding force. Then, an incremental displacement is applied and new values of the forces are calculated until reaching the maximum capacity. Two cases are investigated related to the position of the load. When the load is applied at the exterior panel a lower stiffness is contributed to the capacity compared to that of the interior panel. This analysis has been carried out by making use of analytical modeling in Matlab, which is capable of making iterations and internal loops to estimate the ultimate capacity.

In *chapter 5* the structure and the functions of the Matlab code are thoroughly described. Executing a Matlab code for the iterative procedure, presented in the Master thesis Miltenburg [1998], the ultimate bending capacity and the vertical displacement are obtained. Then, the compressive membrane force can be found by making use of the horizontal equilibrium. Comparing the final results of the interior and exterior cases, conclusions can be made. The ultimate capacity of the interior panel is higher than the exterior but the displacement is smaller because the higher stiffness of the interior makes it stiffer and less ductile. The prestress is simulated as an additional stiffness in bending capacity. For different prestress levels, the ultimate capacity and arching action are slightly affected.

Chapter 6 presents the implementation of the theoretical approach to the present research. Employing the aforesaid models the ultimate capacity can be estimated for the given input data and compared to the experimental results.

In *chapter 7* a parametric study has been carried out to give an insight into the correlation of the governing parameters, such as the stiffness ratio and the slenderness. For higher stiffness ratio the ultimate capacity is abruptly increased, reaching the higher value at a stiffness ratio equal to 1, while for greater values of the ratio no effect is found. In order to achieve the peak of the capacity it is not necessary to provide extremely stiff supports. On the other hand, if the slenderness increases, the capacity substantially decreases because the slab becomes too slender to develop the compressive membrane forces.

Last but not least, in *chapter 8* a comparative study between punching shear and bending results takes place. Comparing the two failure modes the bending capacity exceeds the punching shear capacity, leading to the conclusion that depending on the loading conditions the most favourable failure could be the punching shear failure.

PART I: PUNCHING SHEAR CAPACITY

2. COMPRESSIVE MEMBRANE ACTION IN PUNCHING SHEAR

2.1. Introduction

The basic aim of this part of the thesis is to estimate theoretically the punching shear capacity V_E and analytically the effect of compressive membrane force of the transverse prestressed slab by combining the theory of Kinnunen and Nylander (1960) and Hallgren (1996) and the Model Code 90. The overall procedure has to deal with these phenomena: the bearing capacity under a vertical load, the compressive membrane action and their interaction. The parameters of the compressive membrane action are also going to be estimated by the analytical approach making use of a Matlab code, initially casted by Hewitt-Batcelor (1975). Both procedures are going to be explained in the following sections.

2.2. Failure Mechanism

Punching shear occurs when the compression zone near a column collapses, because the concrete strain in the slab reaches a critical level due to the bending moment or the inclined compression stress due to the column reaction.

According to the proposed model by Kinnunen and Nylander (1960) and Hallgren (1996) failure occurs when the tangential compression strain in the slab at the column edge reaches a critical value. The cracking at a critical tangential flexural strain softens the concrete at the column edge.

More comprehensively, at the ultimate stage the compression strain always exceeds the strain corresponding to the concrete strength f_{cc} . Thus, when the flexural tangential strain in the bottom of the slab reaches the critical value, the concrete loses the interface bond resulting in a vertical crack. This vertical crack is attributed to the combined action of the support reaction and the tangential strain. It has been observed that the radial compression strain at the bottom surface of the slab in the vicinity of the column suddenly decreases to zero when the load almost reaches the ultimate punching shear load. Therefore, the inclined compression strut cannot resist the support reaction, resulting progressively in the column collapse. Thus, the crack propagation takes place in

combination with the shear deformation of the compression zone. Due to the shear deformation the radial flexural strain in the bottom of the slab stops increasing while the load increases.

Conclusively, the failure mode is governed more by the circumferential crack at the slab/column interface rather than by propagation of an inclined flexural crack.

Hewitt-Batcelor (1975) extended the model of Kinnunen and Nylander by introducing compressive forces at the ends of the slab, as shown in Fig. 9.

Below the most representative failures models are presented, indicating the active forces and the plane of action.

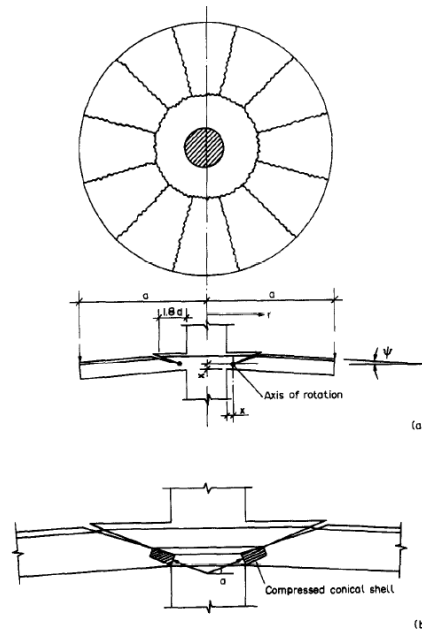
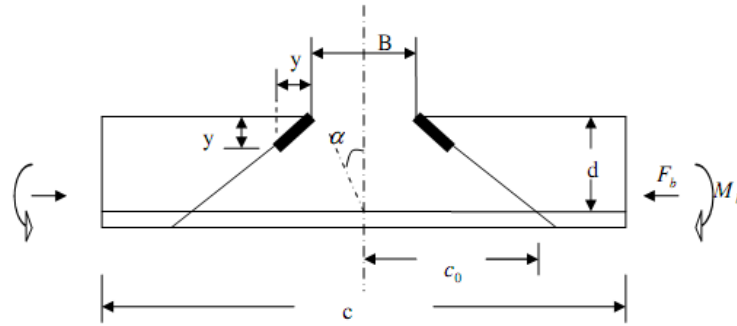
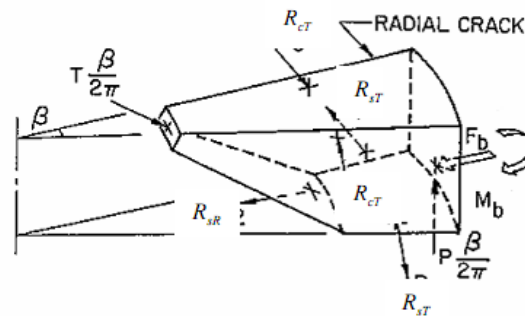


Figure 8 Kinnunen-Nylander model



a) Section Showing Boundary Forces



b) Forces on Sector Element

Figure 9 Punching failure model modified by Hewitt-Batcelor (1975)

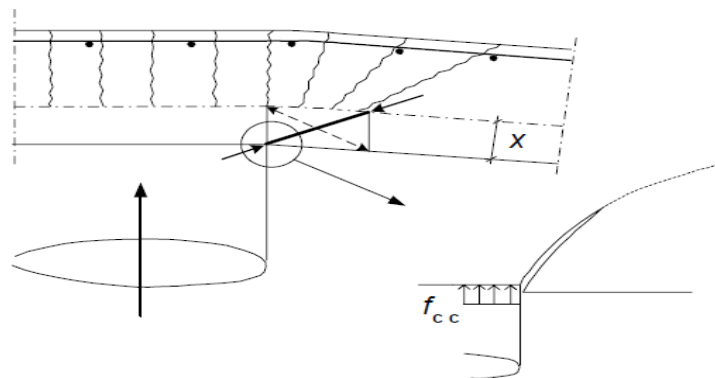


Figure 10 Failure Mode V_E

2.3. Theoretical Approach of Punching Shear capacity

The main objective of the theoretical approach is to estimate the punching shear capacity and the corresponding deflection. The basic assumptions for the material modelling are that at the ultimate stage the steel cannot yield and the concrete is crushing. Thus, the steel reinforcement is considered as an ideally elastic-plastic material.

According to punching theory the ultimate load is given by the following formula:

$$V\varepsilon = m\varepsilon \cdot \frac{8\pi}{2 \ln\left(\frac{c}{B}\right) + 1 - \frac{B^2}{c^2}} \quad (1)$$

Where m_ε : bending tangential and radial moment per unit width at column edge, given by the Eq 2.

y_u : compression zone at the ultimate stage, given by the Eq.6

It is worth mentioning that the employed models should be modified in order to be applicable and compatible with the present conditions of the slab. These modifications are based on assumptions accounting for simulation of the presence of the post-tensioning tendons and the compressive membrane action.

As can be noticed, the ultimate punching shear capacity V_e depends mainly on the compression zone at the failure stage, which in turn depends on the concrete compressive strain. Thus, any modification can take place with respect to the concrete strain in order to reflect this change in the ultimate capacity.

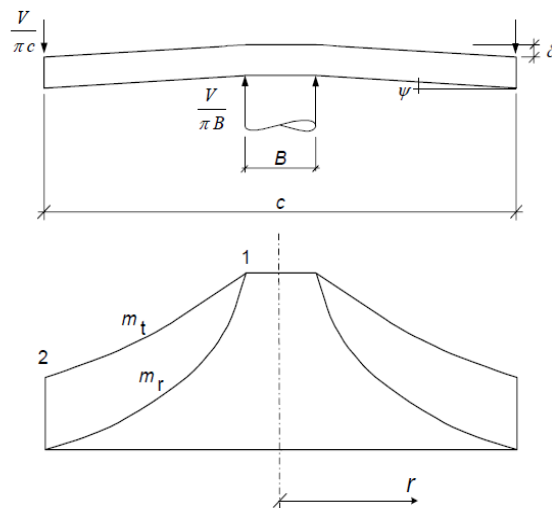


Figure 11 Bending moments and slab deformation for a circular slab supported on the edge of a circular column

According to the theory of elasticity for a circular slab of Timoshenko and Woinowsky-Krieger (1959) the moment can be expressed also as:

$$m_\varepsilon = EI \cdot f'' = \rho \sigma_s^* d^2 (1 - y_u/3d) \quad (2)$$

Where f'' : the curvature of the slab due to the bending moment m .

EI : the stiffness of the cracked cross section

ρ : reinforcement ratio including regular and prestressing steel, calculating as follows:

$$\rho = A_{pe} / A_c \quad (3)$$

$$A_{pe} = A_p + A_s$$

i. *Calculation of ultimate compression zone: y_u*

1st Assumption

The model *Kinnunen and Nylander, Hallgren and Model Code 90* deal with reinforced concrete structures. At the considering case, prestressed tendons are present, thus modifications of the equations should take place in order to adjust the models.

To estimate the punching shear capacity the depth of the compression zone should be found. The ultimate compression zone depends on the ultimate concrete compressive strain under the vertical load P_u and the applied prestress. The role of prestress is quite important since it neutralises the tensile strains induced by the external load P , which are responsible for the cracks and ultimately for the failure. When the prestress level increases the slab can carry more tensile strains, increasing the depth of compression zone, resulting to a higher capacity and better overall performance. This favourable effect has to be introduced in the equations of the compression zone. It can be achieved by superposing the strain of the reinforced concrete and the strain, carried by the prestress. Thanks to the elastic linear behaviour of the prestress steel, the strain compatibility can be employed. Thus, the neutralised strain is equal to the strain by the applied prestress. Then, it can be assumed that the ultimate compressive concrete strain $\epsilon_{u,total}$ is a summation of the concrete strain due to reinforcement and the induced strain due to the prestress at the concrete.

$$\epsilon_{neutralised} = \epsilon_{cp} \quad (4)$$

$$\epsilon_{u,total} = \epsilon_{cpu} + \epsilon_{cp} \quad (5)$$

2nd Assumption

Furthermore, since the crushing of concrete characterizes the failure of the slab, the compressive concrete strain is expected to reach the maximum acceptable limit $3.5 \cdot 10^{-3}$. Thus, at the failure stage the concrete has exhausted its capacity by reaching the maximum strain ϵ_{cpu} .

$$\epsilon_{u,total} = \epsilon_{cpu} + \epsilon_{cp} = 3.5 \cdot 10^{-3} + \epsilon_{cp}$$

The final compression zone is given by the Eq.(6) at the failure stage when the steel is not yielding and the concrete is crushing:

$$y_u = \frac{\rho \cdot E_s \cdot \epsilon_{cto}}{2 \cdot \alpha_{co} \cdot f_{cc}} \left(\sqrt{1 + \frac{4 \cdot \alpha_{co} \cdot f_{cc}}{\rho \cdot E_s \cdot \epsilon_{cto}}} - 1 \right) \cdot d \quad (6)$$

$$\alpha_{co} = 0.5$$

$$\epsilon_{cto} = C_1 / c_0$$

$$C_1 = \epsilon_{u,total} (B/2 + x)$$

$$x = y_{el} (1 + \tan \alpha)$$

Where ϵ_{cp} compressive strain at the concrete due to the applied prestress

d static effective depth at the level of the tendon: $d=0.45 \cdot 0.5h$

The elastic compression zone y_{el} is derived by the elastic conditions: If punching occurs without any yield of the equivalent reinforcement then both reinforcement and concrete behave elastically.

$$y_{el} = d \cdot n\rho \cdot \left(\sqrt{1 + \frac{2}{n\rho}} - 1 \right) \quad (7)$$

$$n = \frac{E_s}{E_{c10}}$$

ii. Steel stress at the ultimate stage: σ_s^*

3rd Assumption

It has been assumed that the steel cannot yield, so the linear elastic model can be used. The concrete force has to be balanced by a tensile force. Here, it is considered that the concrete force is in equilibrium with a fictitious tensile force which can be calculated making use the principle of the equilibrium assuming complete cooperation between concrete and steel (reinforcing and prestressing steel). As a result, the concrete strain gives a fictitious steel stress σ_s^* , given by the equilibrium as follows:

$$F_c = F_t^*$$

$$F_t^* = \rho \cdot d \cdot \sigma_s^* \quad (8)$$

$$F_c = 3/4 \cdot \lambda \cdot \eta_{EC} \cdot y_u \cdot E_{c10} \cdot \epsilon_{cpu} \quad (9)$$

Where λ is a factor defining the effective height of the compression zone, given by:

$$\lambda = 0.8 \quad f_{ck} \leq 50 \text{ MPa}$$

$$\lambda = 0.8 - (f_{ck} - 50) / 400 \quad 50 \leq f_{ck} \leq 90 \text{ MPa}$$

η is a parameters defining the effective strength

$$\eta_{EC} = 1.0 \quad f_{ck} \leq 50 \text{ MPa}$$

$$\eta_{EC} = 1.0 - (f_{ck} - 50) / 200 \quad 50 \leq f_{ck} \leq 90 \text{ MPa}$$

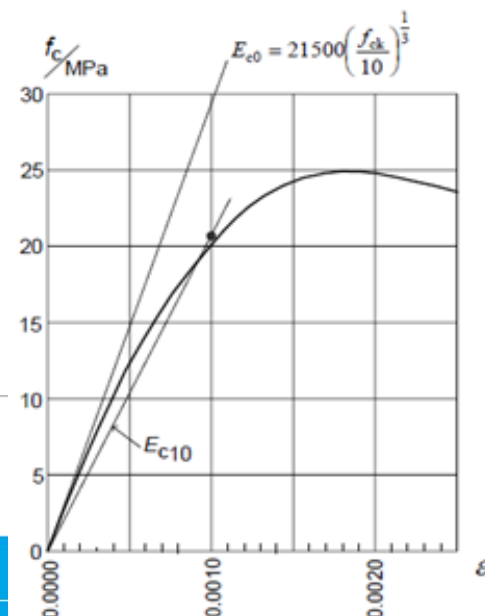
$$\sigma_s^* = \frac{E_{c10} \cdot \epsilon_{cpu} \cdot y_u \cdot \lambda \cdot \eta_{EC}}{\rho \cdot d} \quad (10)$$

The tangent modulus of elasticity E_{c0} for concrete at zero strain is taken as the value given in *Model Code 90 (1993)*:

$$E_{c0} = 21500 \cdot \left(\frac{f_{cc}}{10} \right)^{1/3}$$

$$E_{c10} = \left(1 - 0.6 \left(1 - \frac{f_{cc}}{150} \right)^4 \right) E_{c0}$$

This fictitious steel stress σ_s^* expresses the full cooperation between the governing actors: concrete-steel-restraint conditions of the supports.



These support conditions are introduced by the fact that there is a fictitious bond between concrete and steel.

Therefore, this fictitious tensile force F_t^* includes the steel force of the unbonded tendons, the support restraint and the effect of prestress as restraint. The effect of restraint, represented by the CMA compressive force F_b , can be isolated from the tensile steel force. Since the fictitious force is in equilibrium, the next equation is valid:

Figure 12 Stress-strain curve for concrete strength
(11)

$$F_t^* = F_b + F_{pt}$$

Where F_b : compressive membrane force

F_{pt} : prestress steel force, calculated according to the crack width theory as the tendon is unbonded.

iii. *Calculation of Ultimate Punching Shear capacity*

Now, the bending moment at the support can be calculated, as follows:

$$m_\varepsilon = EI \cdot f'' = \rho \sigma_s^* d^2 (1 - y_u/3d)$$

Finally, the punching shear capacity of the transverse prestressed slab can be estimated according to the following formula:

$$V_\varepsilon = m_\varepsilon \cdot \frac{8\pi}{2 \ln\left(\frac{c}{B}\right) + 1 - \frac{B^2}{c^2}}$$

Last but not least, the theoretical deflection δ represents the bending deformation and shear deformation where the latter cannot be considered negligible since it is important for the punching failure mode. This deflection is calculated as follows:

$$\delta = \frac{V_\varepsilon}{4\pi} \cdot \left(1 - \frac{B^2}{c^2}\right) \cdot \frac{c}{2EIcr} \cdot \frac{c - B}{2} \quad (12)$$

The effective (cracked) stiffness is given by the following formula:

$$EIcr = \frac{m}{f''} = \rho \cdot Es \cdot d^3 \cdot \left(1 - \frac{y_u}{d}\right) \cdot \left(1 - \frac{3 \cdot y_u}{d}\right) \quad (13)$$

iv. *Calculation of stress of unbonded tendon: Crack width theory F_{pt}*

The unbonded tendon is subjected to a vertical load and an initial axial imposed deformation. The total strain is constant along the length of the tendon as the deformation of the bridge is not enough to bend the tendon. Thus, it can be simulated as a spring, behaving in an elastic way and

accumulating all the strain at its ends. Consequently, the force that is carried by the tendon can be calculated directly by the total strain at the support. This strain is a superposition of the applied prestress and the strain due to the crack width.

$$\begin{aligned}\varepsilon_{\text{ptot}} &= \Delta\varepsilon_p + \sigma_s / E_s \\ \Delta\varepsilon_p &= w / L \\ w &= \Theta \cdot z \\ \Theta &= \theta_1 + \theta_2 = \delta/l_1 + \delta/l_2\end{aligned}\tag{14}$$

Where L_i : position of applied load

δ : vertical displacement

Due to symmetry the distances l_1 and l_2 are the same and half of the length of the intermediate slab.

$$L_{\text{tot}} = l_1 + l_2$$

Where z the level arm: $z = 0.4d$

$$d = 0.9 \cdot 0.5 \cdot h$$

$$\sigma_s = P_{m\infty} / A_p$$

$$P_{m\infty} = \sigma_{cp} \cdot A_c$$

A_{pe} : equivalent amount of reinforcement given by the summation of prestress and regular reinforcement

A_c : concrete area where the prestress applied

σ_{cp} : applied prestress level at the concrete as a result of the prestress working force $P_{m\infty}$

Total prestress of unbonded tendon:

$$\sigma_{pt} = \varepsilon_{\text{ptot}} \cdot E_s$$

$$F_{pt} = \varepsilon_{\text{ptot}} \cdot E_s\tag{15}$$

v. *Calculation of compressive membrane force F_b*

Two methods are going to be investigated for the calculation of compressive membrane action. The first method employs the principle of equilibrium as explained at the *Step 2* and the second method applies the analytical Matlab code of Hewitt-Batcelor (1975).

- Compressive membrane force by theoretical approach “Equilibrium”

$$F_b = F_t^* - F_{pt}\tag{16}$$

- Compressive membrane force by analytical approach Matlab

2.4. Analytical part of approach

The main objective of the analytical approach is to calculate the compressive forces and the relative factors according to method of Hewitt-Batcelor (1975). The effect of the compressive membrane action and the overall interaction will thoroughly investigated. Having obtained the

punching capacity and the corresponding deflection, an analytical procedure in Matlab can be followed. The value of compressive membrane force of theoretical analysis will be compared to that of method of Hewitt-Batcelor (1975).

4th Assumption

At the Matlab code of Hewitt-Batcelor (1975) the compressive membrane action is an input parameter F_b , which has been calculated by introducing an arbitrary value for the restrained factor n . Thus, the ultimate punching load is an output parameter that code calculates. At the present case study, the ultimate load has been calculated according to the theoretical model, giving above, so the code has been inverted and recasted in order to calculate the compressive membrane force. Consequently, the validation of the code is ensured because the equations of the model of Hewitt-Batcelor (1975) are employed to make them work in double way.

As has been mentioned above, the ultimate load P and the respective displacement are input parameters in the Matlab code, as a result no iterations are required to find the compressive force F_b and M_b .

Furthermore, the original code had to deal with bonded regular reinforcement, which was expected to yield, giving the steel stress equal to yield stress. At the considering case the tendons are unbonded, thus the steel stress will be given by the crack width control, since the unbonded tendon is always in the elastic zone.

Table 1 Input and Output Parameters

Input data	Output data
V_ε	F_b
y_{el}	M_b
y_u	F_{bmax}
$\varepsilon_{u,total}$	M_{bmax}
σ_s	η

Hereby, the inverted equations are presented to show the analytical procedure.

$$P_1 = T \sin \alpha = \pi \left(\frac{B}{d} \right) \left(\frac{y}{d} \right) \frac{B+2y}{B+y} f_i f(\alpha) d^2 \quad (17)$$

$$f(\alpha) = \frac{\tan \alpha (1 - \tan \alpha)}{1 + \tan^2 \alpha} \quad (18)$$

$$(K_z \tan \alpha - 1) \frac{1 - \tan \alpha}{1 + \tan^2 \alpha} = \frac{1}{4,7} \left(1 + \frac{y}{b} \right) \ln \left(\frac{c}{B+2y} \right) \quad (19)$$

$$X = \frac{4 \cdot (3 \cdot d - y)}{3} \cdot \frac{(ky - kz)}{1000} \quad (20)$$

$$Mb = \frac{P \cdot X}{4 \cdot \pi} \quad (21)$$

$$Fb = \left(\frac{P \cdot kz}{2 \cdot \pi} - R_1 \cdot 1000 - R_{2\text{overbeta}} \cdot 1000 \right) \cdot \frac{c}{2} \quad (22)$$

$$R_1 = (r_{ho} \cdot f_{sy} \cdot d \cdot ((rs - C_0) + r_s \cdot \log(c/(2 \cdot r_s))))/1000 \quad r_s > C_0 \quad (23)$$

$$R_{2\text{overBeta}} = r_{ho} \cdot f_{sy} \cdot d \cdot C_0/1000 \quad r_s > C_0 \quad (24)$$

$$R_1 = (r_{ho} \cdot f_{sy} \cdot d \cdot r_s \cdot \log(c/(2 \cdot C_0)))/1000 \quad r_s < C_0 \quad (25)$$

$$R_{2\text{overBeta}} = r_{ho} \cdot f_{sy} \cdot d \cdot r_s/1000 \quad r_s < C_0 \quad (26)$$

$$r_s = E_s / f_{sy} \cdot tasi \cdot (d - y) \quad (27)$$

$$f_{sy} = f_{pk} - (F_p / A_p) \quad (28)$$

$$F_p = \sigma_{cp} \cdot h \quad (29)$$

$$EI = \frac{m}{f''} = \rho \cdot Es \cdot d^3 \cdot \left(1 - \frac{y}{d} \right) \cdot \left(1 - \frac{3 \cdot y}{d} \right) \quad (30)$$

2.4.1. Matlab flowchart

Hewitt-Batcelor (1975) had casted a Matlab code to calculate the vertical ultimate load V_ϵ .

The whole procedure of the code is giving below in the flowchart:

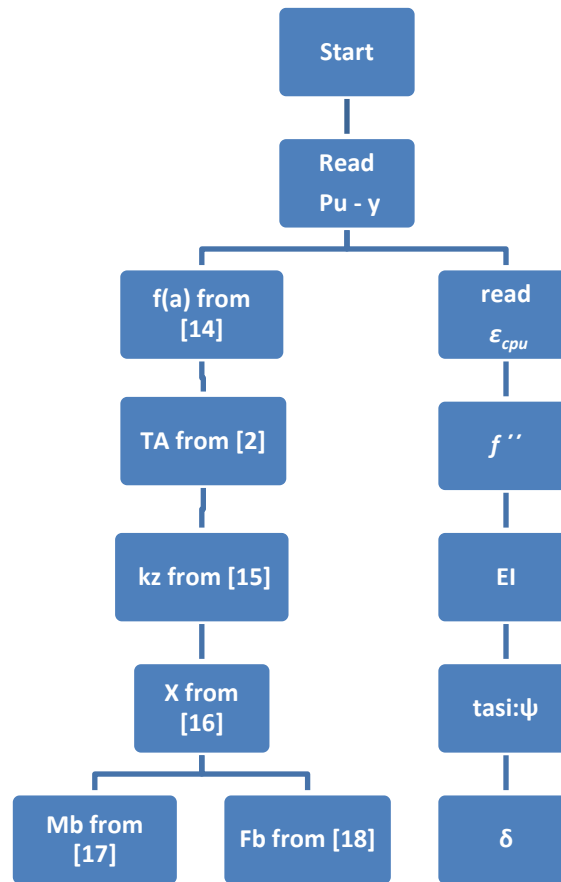


Figure 13 Matlab flowchart

At the Appendix III the initial and updated Matlab codes are presented to give an insight into the execution of the program.

3. APPLICATION TO PRESENT EXPERIMENT

3.1. Introduction

To investigate the punching shear capacity of a transversely prestressed slab, a bridge has been constructed at 1:2 scale model at Stevin II laboratory, CITG faculty, Delft University of Technology. The bridge model has 12m long and 6.4m width, consisting of four precast concrete girders placed at 1800 mm c/c distance. The slab has been casted in situ and prestressed in the transverse direction with clear span of 1050mm and thickness of 100mm, as can be observed below.

More specifically, the transversely prestressed slab has 3 intermediate slab panels. At the case of punching shear a point load has been applied at the midspan of the panels. The girders have been

designed and constructed to bear 11000kN, the load of which cannot be exceeded. Thus, the girders are going to remain uncracked during loading, which is also verified during the experiment. Since the supports are uncracked the conditions over them can be considered elastic. Consequently, the stiffness is not reduced, leading to greater restraint conditions.



Figure 14 Apparatus of structure

3.2. Application at the applied prestress level: $\sigma_{cp} = 2.5 \text{ MPa}$

The prestressing tendon is positioned at the mid-depth of the slab, resulting to a reduced effective depth about $d=0.9 \cdot 0.5 \cdot h=0.45 \cdot h$

3.2.1. Theoretical part of approach

Table 2 Input data

Description	Value [N/mm ²]
f_{ck} [N/mm ²]	82.54
f_{cd} [N/mm ²]	70.16

f_{ct} [N/mm ²]	5.68
E_{c0} [N/mm ²]	37957.37
E_{c10} [N/mm ²]	34297.30
E_{sp} [N/mm ²]	205000
ρ [-]	0.00583
$n\rho$ [-]	0.0277
h [mm]	100
d [mm]	45
a_{c0}	0.5
B [mm]	200
A_{pe} [mm ²]	0.5838
α	25°

i. Calculation of elastic zone: y_{el}

$$y_{el} = d \cdot n\rho \cdot \left(\sqrt{1 + \frac{2}{n\rho}} - 1 \right)$$

As mentioned above, due to the position of the tendon the effective depth of the slab is $d=0.45 \cdot h$

$$n\rho = \frac{E_{sp}}{E_{c10}} \cdot \rho$$

Where ρ is the total equivalent ratio taking into account both reinforcement and prestress steel area

$$\rho = A_{p+s}/A_c = 0.583/100 = 0.00583 \text{ per running mm}$$

$$A_{p+s} = A_p + A_s = 0.4425 + 0.141372 = 0.583 \text{ mm}^2/\text{mm}$$

$$y_{el} = 10.41 \text{ mm}$$

ii. Calculation of ultimate zone y_u

$$\alpha_{c0} = 0.5$$

$$\varepsilon_{ct0} = C_1/c_0$$

$$C_1 = \varepsilon_{u, \text{total}} (B/2 + x) = 0.411 \text{ mm}$$

$$x = y_{el} (1 + \tan \alpha) = 15.27 \text{ mm}$$

$$c_0 = B/2 + 1.8 \cdot d = 181 \text{ mm}$$

$$E_{c0} = 21500 \cdot \left(\frac{f_{cc}}{10}\right)^{1/3} = 37957.37 \text{ N/mm}^2$$

$$E_{c10} = \left(1 - 0.6 \left(1 - \frac{f_{cc}}{150}\right)^4\right) E_{c0} = 34297.30 \text{ N/mm}^2$$

$$\varepsilon_{cp} = \sigma_{cp} / E_{c10} = 5.929 \cdot 10^{-5}$$

It is worth mentioning again that the total ultimate compressive concrete strain of the concrete is the summation of the strain of the reinforced concrete and the strain, carried by the prestress.

Employing the strain compatibility it yields:

$$\varepsilon_{u, \text{total}} = \varepsilon_{ctu} + \varepsilon_{cp} = 3.57 \cdot 10^{-3}$$

$$y_u = \frac{\rho \cdot E_s \cdot \varepsilon_{cto}}{2 \cdot a c_0 \cdot f_{cc}} \left(\sqrt{1 + \frac{4 \cdot a c_0 \cdot f_{cc}}{\rho \cdot E_s \cdot \varepsilon_{cto}}} - 1 \right) \cdot d = 12.09 \text{ mm}$$

iii. Steel stress at the ultimate stage

Here, it is considered that the concrete force is in equilibrium with a fictitious tensile force which can be calculated making use the principle of the compatibility. As a result the concrete strain gives a fictitious steel stress σ_s^* , given by the formula below:

$$\sigma_s^* = \frac{E_{c10} \cdot \varepsilon_{cpu} \cdot y_u \cdot a c}{\rho d} = 2572.76 \text{ N/mm}^2$$

This fictitious tensile force F_t^* includes the steel force of the unbonded tendons, the support restraint and the effect of prestress as restraint. The effect of restraint, represented by the CMA compressive force F_b , can be isolated (support and prestress) from the tensile steel force. Since the fictitious force is in equilibrium, the next equation is valid:

$$F_c = F_t^*$$

$$F_t^* = \rho \cdot d \cdot \sigma_s^* \cdot 1000 = 0.583 \cdot 45 \cdot 2572.76 \cdot 1000 = 665190 \text{ N}$$

iv. Calculation of ultimate Punching shear capacity

Now, the bending moment at the support can be calculated, as follows:

$$m_\varepsilon = \rho d^2 \sigma_s^* (1 - y_u/3d) = 27651.60 \text{ N/mm}$$

Finally, the punching shear capacity of the slab can be estimated according to the following formula:

$$V_\varepsilon = m_\varepsilon \cdot \frac{8\pi}{2 \ln\left(\frac{c}{B}\right) + 1 - \frac{B^2}{c^2}} = 162367 \text{ N}$$

Last but not least, the theoretical deflection δ represents the bending deformation and shear deformation whereas the latter cannot be considered negligible since it is important for the punching failure mode. This deflection is calculated as follows:

$$\delta = \frac{V\varepsilon}{4\pi} \cdot \left(1 - \frac{B^2}{c^2}\right) \cdot \frac{c}{2EI_{cr}} \cdot \frac{c-B}{2} = 35.96\text{mm}$$

The effective (cracked) stiffness is given by the following formula:

$$EI_{cr} = \frac{m}{f''} = \rho \cdot Es \cdot d^3 \cdot \left(1 - \frac{yu}{d}\right) \cdot \left(1 - \frac{3yu}{d}\right) = 7.724 \cdot 10^7 \text{Nmm}$$

v. *Calculation of stress of unbonded tendon: Crack width theory*

The unbonded tendon is subjected to a vertical load and an initial axial imposed deformation. The total strain is constant along the length of the tendon as the deformation of the bridge is not enough to bend the tendon. Thus, it can be simulated as a spring, behaving in an elastic way and accumulating all the strain at its ends. Consequently, the force that is carried by the tendon can be calculated directly by the total strain at the support. This strain is a superposition of the applied prestress and the strain due to the crack width.

$$\varepsilon_{ptot} = \Delta\varepsilon_p + \sigma_s / E_s$$

$$\Theta = \theta_1 + \theta_2 = \delta/L_1 + \delta/L_2 = 2 \cdot \delta/L_1 = 0.096\text{rad}$$

Where L_i : position of applied load

$$L_{tot} = L_1 = L_2 = 1050/2 = 750\text{mm}$$

$$w = \Theta \cdot z = 1.72\text{mm}$$

Where z the level arm: $z = 0.4d = 18\text{mm}$

$$d = 0.45h = 45\text{mm}$$

$$\Delta\varepsilon_p = w/L = 1.72/6400 = 2.69\text{E-}04$$

$$P_{m\infty} = \sigma_{cp} \cdot A_c = 2.5 \cdot 100 \cdot 350 = 8.75\text{E}+04\text{N/mm}$$

A_c : concrete area where the prestress applied to the concrete (100x1000)

σ_{cp} : applied prestress level

The tensile steel and concrete forces are calculated per running meter of the slab, corresponding to 1000mm width of the slab. The distance between the tendons is 400mm which means that every 1m there are two tendons.

$$\sigma_s = P_{m\infty} / 2A_p = 707.41\text{MPa}$$

$$\varepsilon_{ptot} = \Delta\varepsilon_p + \sigma_s / E_s = 2.69\text{E-}04 + 707.41/205000 = 3.72\text{E-}04$$

Total prestress of unbonded tendon:

$$\sigma_{pt} = \varepsilon_{ptot} \cdot E_s = 3.72\text{E-}04 \cdot 205000 = 762.71\text{MPa}$$

$$F_{pt} = \sigma_{pt} \cdot A_p = 762.71 \cdot 0.5838 \cdot 1000 = 445272\text{N}$$

$$F_t^* = F_b + F_{pt}$$

At the previous stage the fictitious force has been calculated:

$$F_t^* = 674963\text{N}$$

Thus, the compressive membrane force is given by:

$$F_b = F_t^* - F_{pt} = 674963 - 445272 = 229691\text{N}$$

As mentioned in the section 1.4.2, the restrained factor is the ratio between the compressive membrane force F_b and the maximum F_{bmax} under ideal conditions.

Idealized compressive membrane force

$$F_{bmax} = F_c - F_s$$

$$F_c = \frac{3}{4} \cdot \lambda \cdot \eta_{EC} \cdot \left(\frac{2}{3} \cdot f_{ck} \right) \cdot \left(\frac{h}{2} - \frac{\delta}{4} \right)$$

Where λ is a factor defining the effective height of the compression zone, given by:

$$\lambda = 0,8 \quad f_{ck} \leq 50\text{MPa}$$

$$\lambda = 0,8 - \frac{(f_{ck} - 50)}{400} \quad 50 \leq f_{ck} \leq 90\text{MPa}$$

η is a parameters defining the effective strength

$$\eta_{EC} = 1,0 \quad f_{ck} \leq 50\text{MPa}$$

$$\eta_{EC} = 1,0 - \frac{(f_{ck} - 50)}{200} \quad 50 \leq f_{ck} \leq 90\text{MPa}$$

Thus, the concrete force can be evaluated, as follows:

$$F_c = \frac{3}{4} \cdot 0,721 \cdot 0,842 \cdot \left(\frac{2}{3} \cdot 82,54 \right) \cdot \left(\frac{100}{2} - \frac{35,96}{4} \right) \cdot 1000 = 684950\text{N}$$

At this point it is worth mentioning that the ideal conditions at the support has only effect on the concrete force. Due to the fact that the tendon is unbonded, it can be concluded that the prestressing steel is not going to yield. During loading, the steel stress will be in the linear stage and it is not governing for the failure. Thus, the failure is attributed to crushing of the concrete, which leads to punching shear failure. Conclusively, the steel force is not a function of the idealised conditions.

$$F_s = F_{pt} = 445272\text{N}$$

$$F_{bmax} = F_c - F_s = 1059.8981\text{N/mm}$$

The restrained factor is calculated by taken the ratio:

$$\eta = F_b / F_{bmax} = 229691 / 23967 = 0,95$$

3.2.2. Results for all the applied prestress levels

Table 3: Theoretical Results

Prestress level TPL [MPa]	ϵ_{cp} [10^{-5}]	ϵ_{cpu} [10^{-3}]	$\epsilon_{u,total}$ [10^{-3}]	y_u [mm]	σ_s^* [MPa]	m_ϵ [N]	V_ϵ [N]	δ [mm] by $EI_{cracked}$

0	-	3.5	3.5	11.99	2498.4	26875.3	157809	34.95
1,25	3.64	3.5	3.53	12.04	2535.5	27262.8	160084	35.46
2,5	7.28	3.5	3.57	12.09	2572.7	27651.6	162367	35.96

Table 4: Calculation of prestress force

Prestress level TPL [MPa]	Θ [rad]	w [mm]	$\Delta\varepsilon_p$ [10^{-4}]	$\varepsilon_{p,tot}$ [10^{-4}]	σ_{pt} [MPa]
0	0.093	1.67	2.62	2.62	53.74
1.25	0.0954	1.70	2.65	1.99	408.23
2.5	0,095	1.72	2.69	3.72	762.71

Following the above procedure the compressive membrane forces and the restrained factor can be found by equilibrium for every prestress level applied to the slab. The capacity and the deflection are used as an input data for the analytical approach. All the results from the analytical part for both cases are presented to the following table.

Table 5: Results by Equilibrium

Prestress level TPL [MPa]	$V_\varepsilon = P_u$ [N]	δ [mm]	F_t^* [N]	F_{pt} [N]	F_b [N]	F_{bmax} [N]	η
0	157809	34.95	655457	31378	624078	657788	0.94
1.25	160084	35.46	665190	238324	426865	448737	0.95
2.5	162367	35.96	674963	445272	229691	239677	0.95

- Analytical results by Hewitt-Batcelor

At this section the compressive membrane action is calculated according to Matlab code of Hewitt-Batcelor.

Table 6 Analytical Matlab Results

Prestress level TPL [MPa]	$V_{\epsilon} = P_u$ [N]	δ [mm]	F_b [N]	F_{bmax} [N]	η
0	157809	29.33	737900	1355900	0.54
1.25	160084	29.44	665230	1308400	0.50
2.5	162367	34.45	518276	1233000	0.42

4. COMPARATIVE STUDY

4.1. Results

Table 7 Results of Experimental approach

Experiment	TPL [N/mm ²]	Load P_u [N]	Deflection δ [mm]	Crack width w [mm]
BB-1 [Exterior]	2.5	348740	10.4	0.8
BB-2 [Exterior]	2.5	321400	9.1	0.7
BB-16 [Interior]	2.5	553400	9.97	1.5

Table 8 Results of Theoretical approach

Position of load	Failure mode	TPL [MPa]	$V_{\epsilon} = P_u$ [N]	Deflection δ [mm]	F_b [N]		F_{bmax} [N]		η	
					By Equilibrium	Hewitt-Batchelor	By Equilibrium	Hewitt-Batchelor	By Equilibrium	Hewitt-Batchelor
-	Punching	1.25	160084	35.4	426865	665230	657788	1308400	0.95	0.50
		2.5	162367	35.9	229691	518276	448737	1233000	0.95	0.42

4.2. Comparison: Experimental – Theoretical approach

Experimental results

At the specimens BB-1 and BB-2 the load is applied at the exterior panels at which there is only restraint from the edge beam and the one side panel. On the other hand, at the specimen BB-16 the load is applied at the interior panel, which is fully restrained by the panels and girders at both sides, which give higher restraint, leading to higher load capacity. The main difference between the specimens is the position of panel (exterior/interior). Therefore, the effect of the compressive membrane action and the effective stiffness are governing for the ultimate failure load, giving a deviation about 37% due to the additional stiffness of the interior slab.

Observations

- i. The experimental failure load is greater than the load prescribed at the Dutch code 52.5kN, which has been scaled down in compliance to the bridge model. Thus, a sufficient safety factor can be achieved with lower boundary $\gamma \geq 5.6$.
- ii. The skewed interface has sufficient capacity to bear the vertical load, since no interface failure occurred during the experiments.
- iii. No significant loss of prestressing steel occurred, verifying the initial assumption to neglect the prestress losses

Theoretical results

- i. The ultimate punching load V_{ε} depends on the steel stress, which in turn depends on the ultimate compressive zone, given by the concrete compressive strain. That means, every external effect such as prestress should be introduced as a strain in the concrete in order to be reflected at the ultimate capacity. This initial imposed deformation due to prestress is very small to increase the concrete strain, leading to slightly changes in the ultimate capacity.
- ii. The punching shear failure is governed more by circumferential cracks at the loaded area rather than by propagation of an inclined flexural crack. The stiffness should be defined in terms of parameters, which characterize the punching shear failure, such as the geometric dimensions of the conical area and the ultimate compressive zone. However, this stiffness cannot account for the boundary conditions and the additional stiffness of the surrounding slabs and concrete girders. Thus, the resulting stiffness does not reflect the real effective stiffness, which is higher than the assumed, leading to a higher vertical displacement than the experimental.
- iii. The theoretical approach cannot take into account the position of the slab, due to the deficiency to account for the boundary conditions. Therefore, the interior panel is assumed to have the same capacity with the exterior, which is not valid according to the experimental results.

- iv. The effect of compressive membrane action has been considered by taken the maximum theoretical capacity of the concrete, since the concrete is expected to crack at the ultimate stage. Thus, the concrete strain cannot exceed the value $3.5 \cdot 10^{-3}$ at the failure stage.
- vi. The compressive membrane force is the result of the restraint effect of support stiffness and prestress. The support stiffness is calculated at the cracked stage by taken into account the ultimate compressive zone and the prestress effect has been introduced as an initial imposed strain at the compressive zone. Thus, the ultimate punching shear capacity has been estimated by taken into account both effects. It is difficult to separate the nominal capacity and the additional due to prestress and CMA in punching shear, because at the approach of Kinnunen and Nylander (1960) CMA always occurs in the slab due to the fact that the stiffness is given by the cracked conical shell. Thus, the boundary conditions at the support are not included in the stiffness.

Comparison: Experiments – Theoretical Results

- i. According to the experimental results the position of loaded panel plays an important role at the failure load because of the contributed **effective stiffness** of the surrounding elements. Thus, the interior panel has 37% higher capacity than that of the exterior. On the other hand, the theoretical method cannot reflect the boundary conditions since the stiffness is given by the cracked conical shell due the shear failure mechanism, neglecting the position of the panel (interior/exterior).
- ii. In the theoretical approach the **TPL** has a low effect on the load capacity since it has been considered as initial imposed deformation, contributed both to concrete and steel force. The deviation between the ultimate punching capacities of the different prestress level is less than 1% (Fig.15). The prestress effect should be taken into account as a progressing effect since it introduces strains and restraint effect throughout all the loading process, delaying the failure stage.
- iii. In the theoretical approach the **deflection** has been estimated based on the cracked stiffness (effective stiffness) EI_{cracked} by taken into account the compressive zone at the ultimate stage when the concrete is crushing, as well as the TPL. The effective stiffness cannot be influenced by the effect of the prestress and CMA. Therefore, the stiffness occurs to be less than the real stiffness, provided by the support and the surrounding slabs. As a result the deflection is higher, almost double, than the observed to the experiments (Fig 16).
- iv. With respect to the two methods (by Equilibrium and Hewitt-Batchelor) for calculation of **compressive membrane action**, according to the literature review and the experimental results, the compressive membrane force is expected to increase while the prestress increases. However, both approaches analytically prove that in the case of unbonded tendons the

prestressing steel force F_{pt} increases. In the “Equilibrium” approach the fictitious steel force F_s^* increases at a lower rate than the increasing rate of steel force of the tendon with the increase of TPL. This results in a decreasing compressive force (Fig 18). Conclusively, the problem is attributed to the definition of the concrete force which cannot reflect the TPL levels.

4.2.1. Graphs

At the Fig 15-17 it can be observed the effect of TPL over ultimate punching capacity is weak due to the simulation of the prestress as imposed strain. The main weakness at the employed theoretical method is the definition of the concrete force. It depends mainly on the concrete strain, which in turn is replaced with the total strain, including the prestress strain. It is advisable to define the concrete force in terms of the effective stiffness, which directly reflect the prestress and arching action as a progressing contribution.

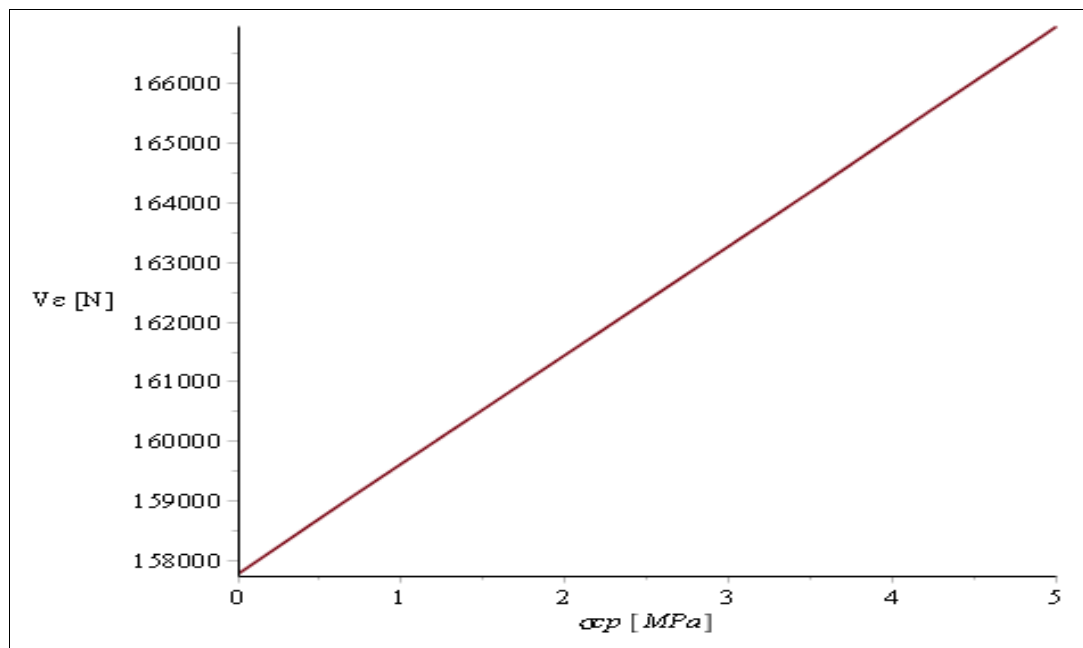


Figure 15 V_ε -TPL Relationship

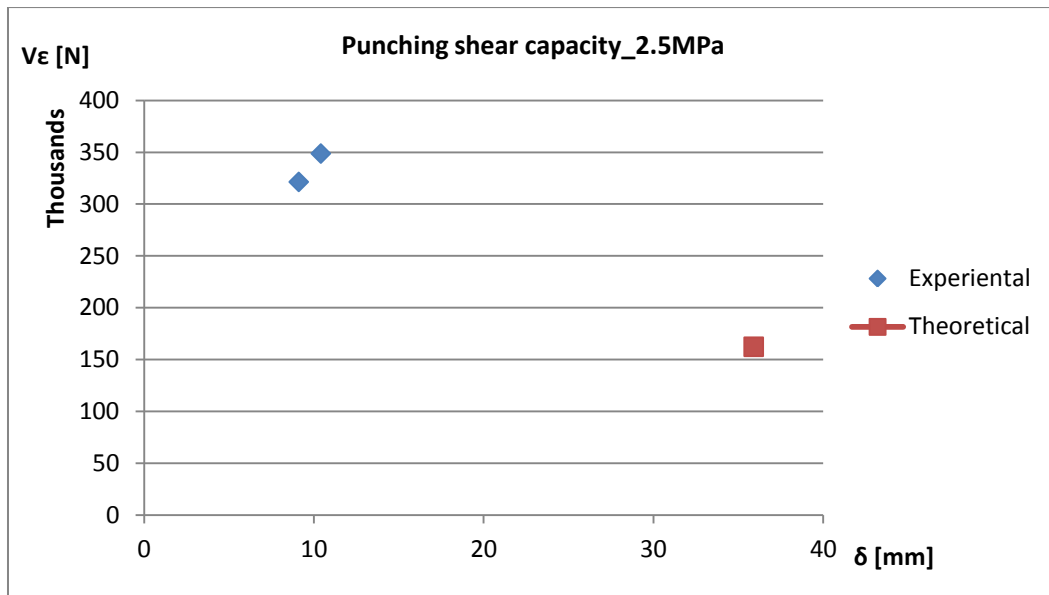


Figure 16 V_{ϵ} - δ Relationship

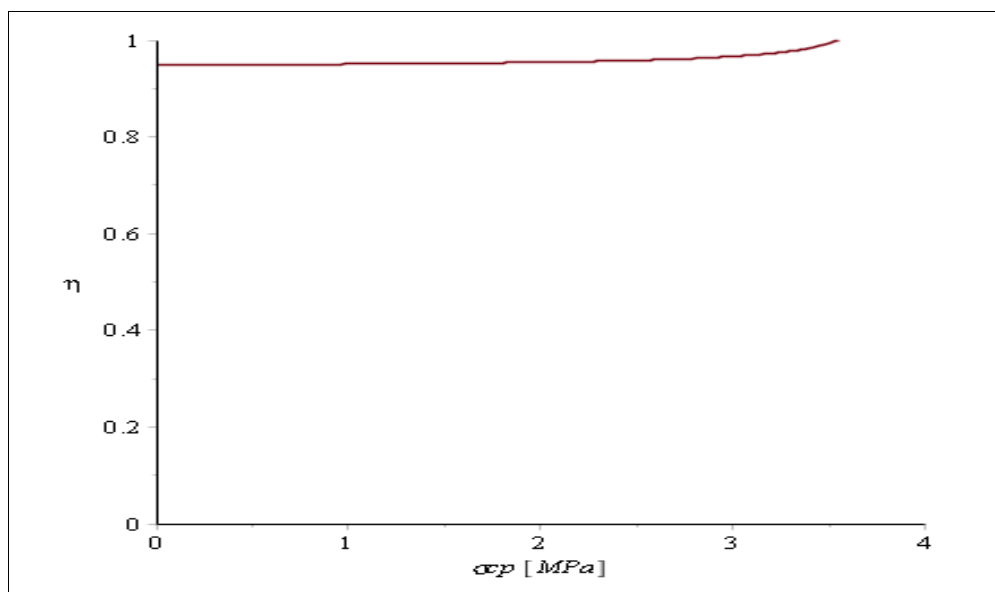


Figure 17 Restraint factor η -TPL Relationship

At the theoretical approach the compressive membrane force is calculated based on the equilibrium. On the other hand, at Hewitt-Batcelor approach the membrane force is calculated based on the in-plane steel resultants, which represent a better interaction of the steel to the punching shear plane. That is why the values of the latter approach are higher than the former.

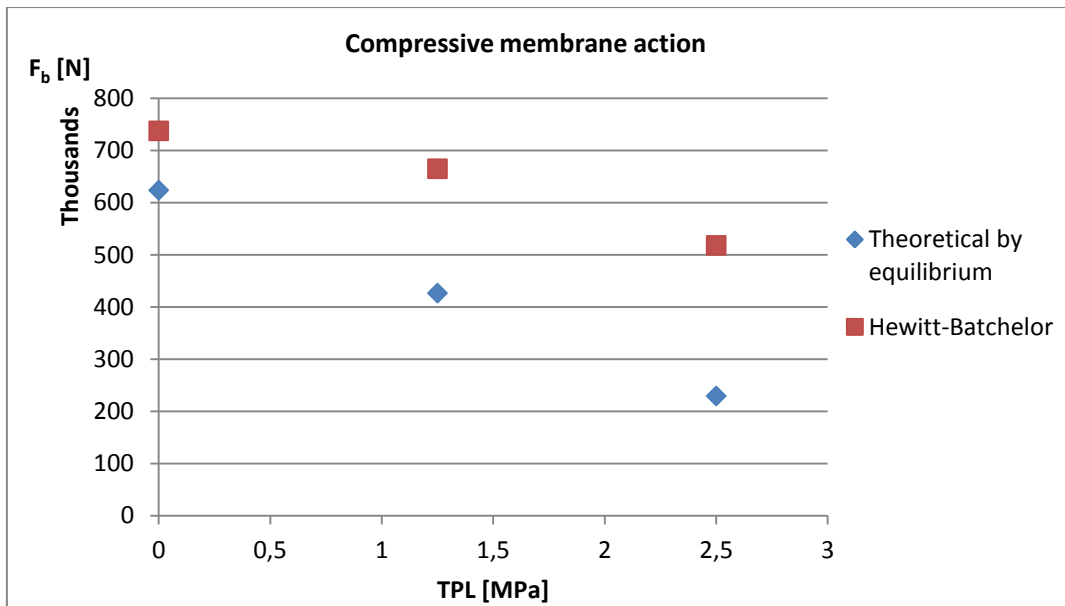


Figure 18 Compressive membrane action

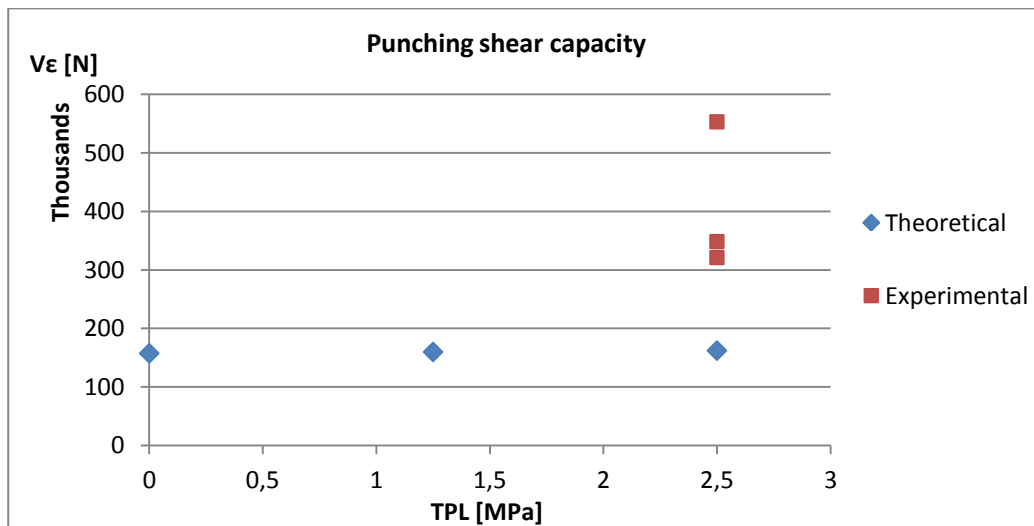


Figure 19 Comparison: Punching shear capacity

PART II: BENDING CAPACITY OF TRANSVERELLY PRESTRESSED SLAB

5. INTRODUCTION: FAILURE MECHANISM

At the present case the slab is subjected to a double load, applied at the midspan, assuming that it fails in bending. To investigate the flexural failure the approach of Park [Park, 1964] is employed. According to this theory the slab will form three plastic hinges, as presented below, at which large rotations concentrate, leading to the failure deformation. The segments of the panel between the slab can be considered that remains straight.

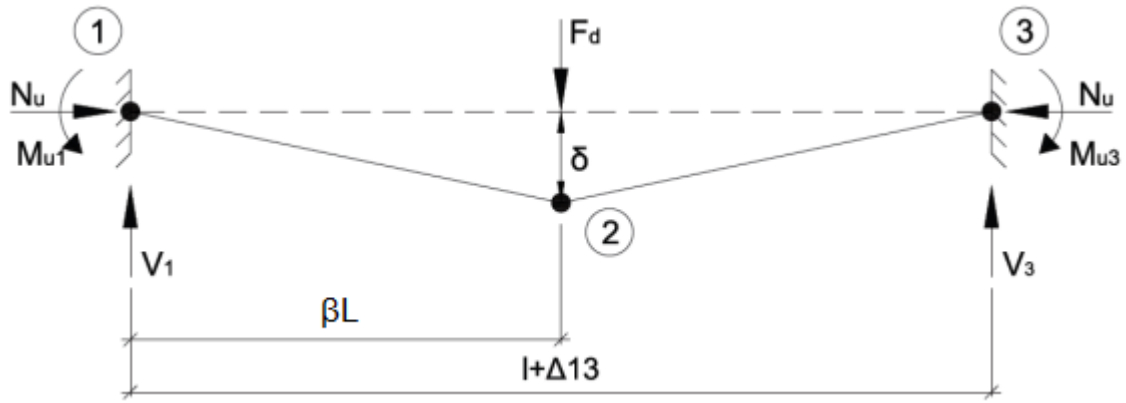


Figure 20 Bending Failure Mechanism

As can be seen at the Fig.20, while the deflection is incrementally increasing the slab moves horizontally outward Δ_{13} causing the development of compressive membrane action N_u due to significant horizontal stiffness. At the ultimate failure due to the vertical displacement δ the moments at the plastic hinges 1 and 3 are M_{u1} and M_{u3} , respectively.

5.1. Horizontal Elongation of Slab

The horizontal elongation is directly related to the geometric and kinematic conditions of the slab. According to the failure mechanism, three plastic hinges are formed at the critical locations 1, 2 and 3. The position of the central hinge (βL) varies with respect to symmetrical or unsymmetrical conditions at the supports. The fact that only the relative distance between the supports 1 and 3 is of interest, it can be assumed that the one end is fixed and the other is free to translate. The position of neutral axis is represented by notations: c_1 , c_2 and c_3 at plastic hinges 1, 2 and 3 respectively.

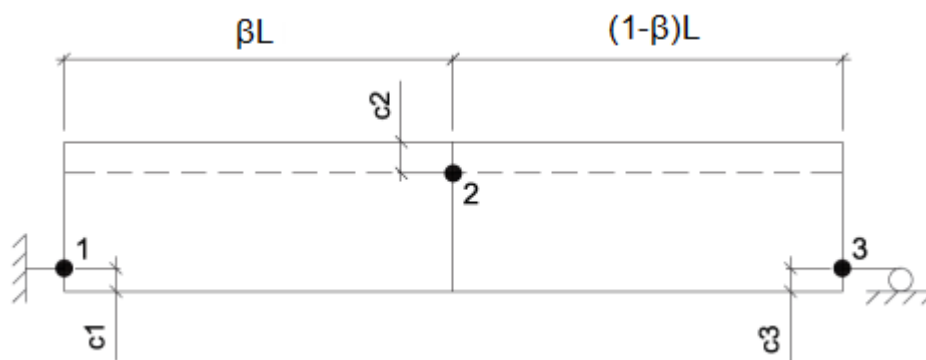


Figure 21 Boundary restraints

According to the failure mechanism, three plastic hinges are formed at the critical locations 1, 2 and 3. Idealizing the segments as rigid blocks, the profile of deformation can be considered linear, as illustrated below. The rotation of the segments leads to the elongation $\Delta_{11'}$ and $\Delta_{33'}$ of the segments 1-1' and 3-3'.

$$\Delta_{11'} = (h - c_2 - c_1) \sin \gamma$$

$$\Delta_{33'} = (h - c_2 - c_3) \sin \theta$$

In compatible to the geometric conditions the rotations γ and θ can be expressed as a function of the displacement δ , as follows:

$$\sin \gamma = \frac{\delta}{\beta * L}$$

$$\sin \theta = \frac{\delta}{(1 - \beta) * L}$$

$$\Delta_{11'} = (h - c_2 - c_1) \frac{\delta}{\beta * L}$$

$$\Delta_{33'} = (h - c_2 - c_3) \frac{\delta}{(1 - \beta) * L}$$

$$\Delta_{1'3'} = \beta L (1 - \cos \gamma) + (1 - \beta) L (1 - \cos \theta) = \beta L (2 \sin^2 \frac{\gamma}{2}) + (1 - \beta) L (2 \sin^2 \frac{\theta}{2})$$

At each incremental displacement δ the total horizontal deformation can be calculated as a summation of individual segment's deformations, as follows.

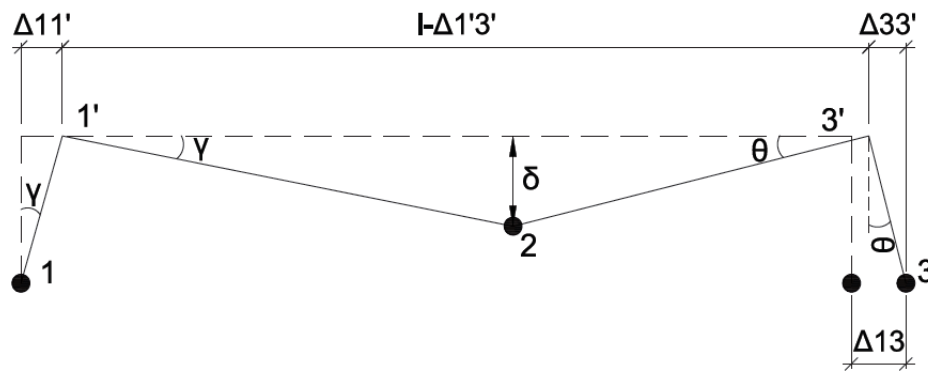


Figure 22 Horizontal elongation of slab

$$\text{Total elongation: } \Delta_{13} = \Delta_{11'} + \Delta_{33'} - \Delta_{1'3'}$$

$$2 \sin^2 \frac{\gamma}{2} = 2 \left(\frac{\gamma}{2} \right)^2 = \frac{\gamma^2}{2} \approx \frac{\delta^2}{2 \beta^2 L^2}$$

$$2 \sin^2 \frac{\theta}{2} = 2 \left(\frac{\theta}{2} \right)^2 = \frac{\theta^2}{2} \approx \frac{\delta^2}{2 (1 - \beta)^2 L^2}$$

$$\Delta_{1'3'} = \frac{\delta^2}{2 \beta (1 - \beta) L}$$

Thus, the total deformation can be expressed:

$$\Delta_{13} = (h - c_2 - c_1) \frac{\delta}{\beta * L} + (h - c_2 - c_3) \frac{\delta}{(1 - \beta) * L} - \frac{\delta^2}{2 \beta (1 - \beta) L} \quad (31)$$

The Eq.31 gives the outward deformation of the slab. The first two terms represent the increase in length and the third the decrease. It is worthy noticing that at low displacements the first two terms are determinant, explaining the strengthening effect of compressive membrane action at this range

of displacements. On the other hand, at large displacements the third term becomes very high due to the factor δ^2 , so the slab has the tendency to move inwards, giving rise to the tensile membrane force, as illustrated at Fig. 1.

Having defined the total horizontal displacement of the slab, the compressive membrane force can be expressed as:

$$\Delta_{13} = \frac{N_u}{K}$$

Any component of compressive membrane force N_u has to be constant along the entire length L (1800mm) of the slab because no other horizontal force is applied. Moreover, along the length of the slab the stiffness EA is considered constant since it has been assumed that cracks occur only at the plastic hinges.

The axial stiffness of the slab is consisted of the stiffness of the elements in the transverse direction: concrete, mild steel and prestress steel.

$$EA = E_s A_s + E_c (A_g - A_s - A_p) + E_p A_p$$

Where A_g gross cross sectional area

A_s cross section of the mild steel

A_p cross section of the prestress steel

Creep, shrinkage and temperature changes are not going to be taken into account in the present case study. For a scientific interest the final formula which includes all the strain changes is given by Mearnarian et. al [1994]:

$$\varepsilon = \frac{(1+k)N_u}{(1+(n-1)\rho)E_c h b} + \varepsilon_{S+T}$$

$$\Delta_{13} = (h - c_2 - c_1) \frac{\delta}{\beta^* L} + (h - c_2 - c_3) \frac{\delta}{(1-\beta)^* L} - \frac{\delta^2}{2\beta(1-\beta)L} - \left(\frac{(1+k)N_u}{(1+(n-1)\rho)E_c h b} + \varepsilon_{S+T} \right) L$$

5.2. Forces in the Slab

As has been mentioned above, the compressive membrane force N_u , expressed as a function of the total deformation Δ_{13} , depends on the position of neutral axes c_1, c_2 and c_3 . The rest of the forces: concrete, mild and prestressing steel are going to be derived at this section.

5.2.1. Concrete Forces

The concrete force can be estimated by the next formula according to Eurocode [prEN 1992-1-1]:

$$C_{ci} = \eta_{EC} f_{cd} \lambda c_i b$$

Where C_{ci} : the compressive concrete force in the hinge i

f_{cd} : the design value of concrete compressive strength, defined as:

$$f_{cd} = \frac{2}{3} f_{ck}$$

λ : a factor defining the effective height of the compression zone, given by:

$$\lambda = 0,8 \quad f_{ck} \leq 50 \text{MPa}$$

$$\lambda = 0,8 - (f_{ck} - 50) / 400 \quad 50 < f_{ck} \leq 90 \text{MPa}$$

η : a parameters defining the effective strength

$$\eta_{EC} = 1,0 \quad f_{ck} \leq 50 \text{MPa}$$

$$\eta_{EC} = 1,0 - (f_{ck} - 50) / 200 \quad 50 < f_{ck} \leq 90 \text{MPa}$$

The above formula implies a rectangular stress-strain distribution for concrete. It should be noted that this is not a true strain-deformation relationship because the extreme fibre of the concrete is always considered to be at the ultimate strain. However, the rectangular stress distribution is a good representation of the conditions of concrete in flexural compression at failure. Thus, it can be employed to approach a plastic failure mechanism.

5.2.2. Forces in the Mild Steel Reinforcement

The regular reinforcement is bonded to the concrete, as a result the steel strain is directly related to concrete strain, represented by a linear profile in compatible with Bernoulli's theory.

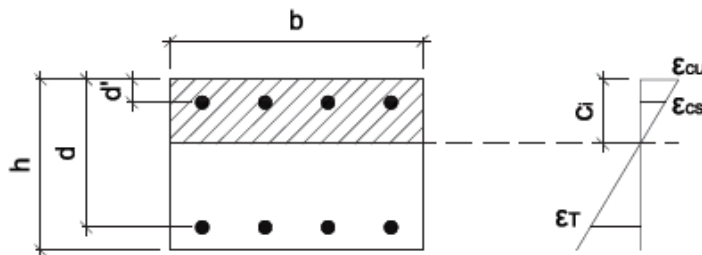


Figure 23 Strains in the Mild Steel Reinforcement

The strain in the tension and compression steel are expressed as follows:

$$\varepsilon_{Ti} = \varepsilon_{cu} \left(\frac{d_i - c_i}{c_i} \right) \quad i = 1,2,3$$

$$\varepsilon_{Csi} = \varepsilon_{cu} \left(\frac{c_i - d'_i}{c_i} \right) \quad i = 1,2,3$$

Where ε_{cu} : the ultimate compressive concrete strain

d_i : the depth from the extreme compression fibre to the centroid of the tension steel at

hinge i

d_i : the depth from the extreme compression fibre to the centroid of the compression steel at hinge i

Modeling of mild steel:

The regular reinforcement is bonded, implying that at the ultimate stage it definitely yields. To simulate the response of the mild steel during the bending test an elastic-plastic strain hardening relationship described by Sargin [1971] is employed.

According to this Sargin's approach the stress strain relationship is consisted of three parts the so-called Trilinear Idealization: elastic, plastic and hardening, as illustrated below.

$$f_s = E_s * \epsilon_s \quad \epsilon_s \leq \epsilon_y$$

$$f_s = f_y \quad \epsilon_y \leq \epsilon_s \leq \epsilon_{sh}$$

$$f_s = f_y + (\epsilon_s - \epsilon_{sh}) * E_{sh} \left[1 - \frac{E_{sh}(\epsilon_s - \epsilon_{sh})}{4(f_u - f_y)} \right] \quad \epsilon_s \geq \epsilon_{sh}$$

$$F = A_s * f_s$$

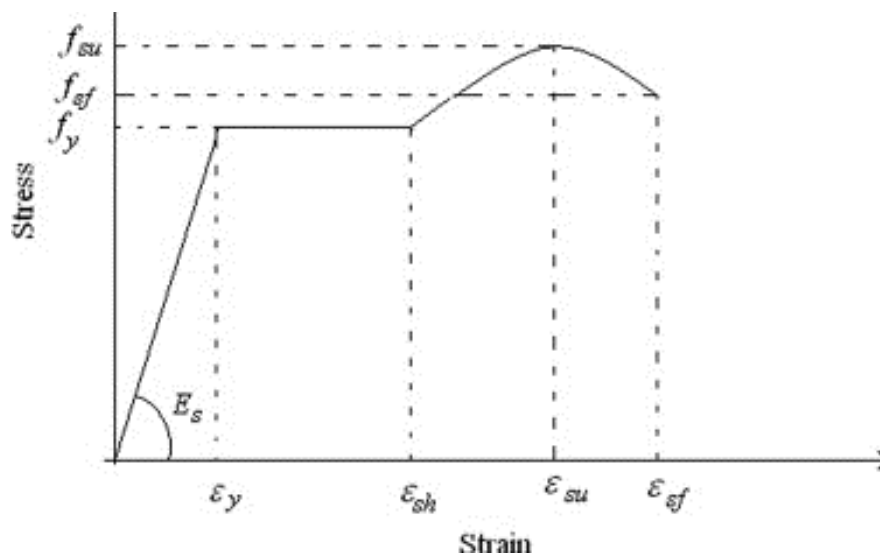


Figure 24 Modified trilinear idealization for mild steel [Sargin, 1971]

5.2.3. Forces in Prestressing Steel

Taking into account that the prestressing steel is unbonded, the strain cannot follow the concrete deformation, but it depends on the crack widths at the level of the tendon. The assumed failure mechanism in bending states that three plastic hinges are going to be formed at the ultimate stage. Due to the escalated deflection the tendon is increasing in length. This difference in length should be calculated in compatible with the plastic failure mechanism. Thus, the most suitable model to present the deflection of the entire member is that prescribed by Rogowsky and Daher, [1997], as presented below.

The total steel strain is the summation of the effective prestress ϵ_{pe} and the change in length Δp_i at each plastic hinge.

$$\epsilon_{pf} = \epsilon_{pe} + \Delta p_i$$

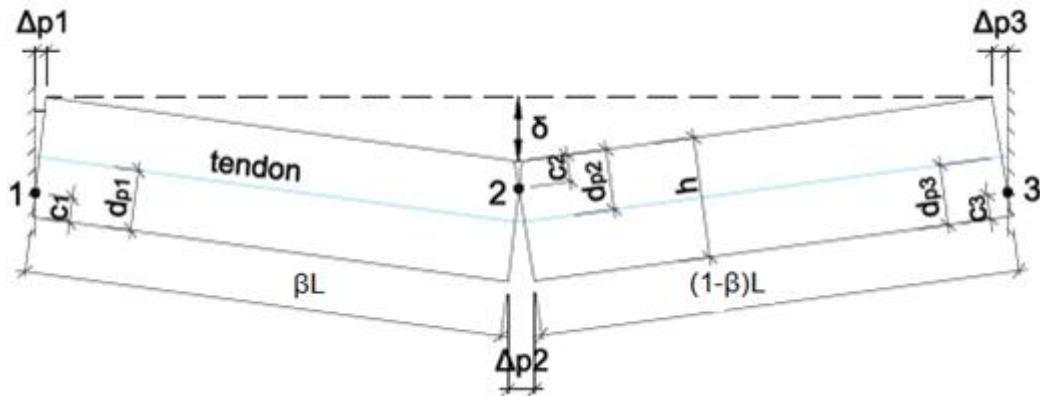


Figure 25 Increase in Tendon length for assumed failure mechanism

The increase in length of the tendons at each of the hinges is:

$$\Delta_{p1} = \left(\frac{h - 2c_1}{l} \right) \delta$$

$$\Delta_{p2} = \left(\frac{h - 2c_2}{l} \right) 2\delta$$

$$\Delta_{p3} = \left(\frac{h - 2c_3}{l} \right) \delta$$

Where d_{pi} : the depth from the extreme compression fibre to the centroid of the prestressing steel at hinge i.

At the present case no losses, such as friction, will be considered. Thus, the total strain in the tendon at failure is:

$$\epsilon_{pf} = \epsilon_{pe} + \frac{\Delta_{p1} + \Delta_{p2} + \Delta_{p3}}{l_t}$$

Modeling of prestressing steel:

The stress strain relationship is idealized by the model of Collins and Mitchell, [1991].

The stress for any strain can be calculated as:

$$f_{ps} = E_p \epsilon_{pf} \left\{ A + \frac{1 - A}{\left[1 + (B \epsilon_{pf})^C \right]^{1/C}} \right\} \quad f_{ps} \leq f_{pu}$$

$$F_{ps} = f_{ps} A_p$$

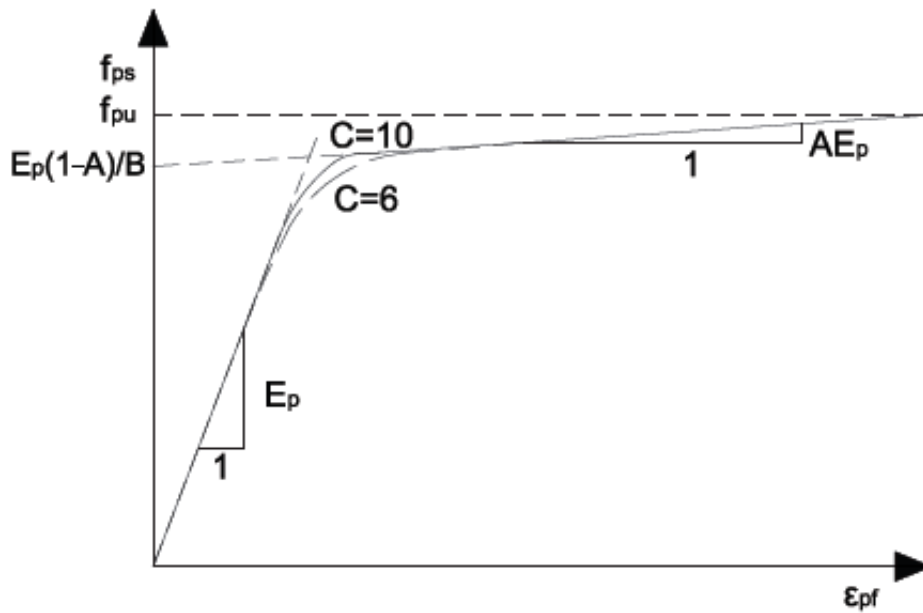


Figure 26 Modified Ramberg-Osgood function [Collins and Mitchell, 1991]

5.2.4. Location of Neutral Axis at Plastic Hinges

As has been defined in previous sections, the forces are given as a function of the vertical displacement δ , the position of the central hinge β and the position of neutral axis c_1, c_2 and c_3 . The position on neutral axis, in turn, can be calculated only when the forces are known. Thus, a direct solution is not possible leading to an iterative procedure for the calculation of the variables. This can be achieved by taking into account the equilibrium and the geometric compatibility.

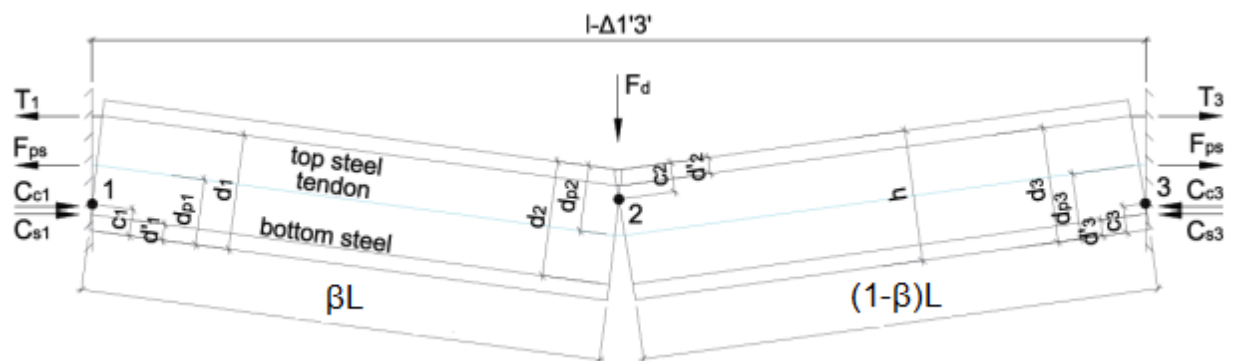


Figure 27 Geometry of the deformed slab and the forces present

Making use of the Fig.27 the equilibrium of forces can be derived.

$$C_{c1} + C_{s1} - T_1 - F_{ps} = C_{c2} + C_{s2} - T_2 - F_{ps} = C_{c3} + C_{s3} - T_3 - F_{ps}$$

Where C_{ci} compressive forces in the concrete
 C_{si} compressive forces in the mild steel reinforcement at hinge i
 T_i tensile forces in the mild steel reinforcement at hinge i
 F_{ps} prestress force

$$c_1 - c_2 = \frac{T_1 - T_2 - C_{s1} + C_{s2}}{\eta f_{cd} \lambda b}$$

$$c_3 - c_2 = \frac{T_3 - T_2 - C_{s3} + C_{s2}}{\eta f_{cd} \lambda b}$$

By solving the equations: the position of neutral axis results in the following equations:

$$c_1 = \frac{h}{2} - \frac{\delta}{4} - \frac{l}{8\delta} \left[\left(\frac{(1+k)N_u}{(1+(n-1)\rho)E_c h b} + \varepsilon_{S+T} \right) l + \frac{N_u}{bS} \right] + \frac{3T_1 - 2T_2 - T_3}{4\eta f_{cd} \lambda b}$$

$$c_2 = \frac{h}{2} - \frac{\delta}{4} - \frac{l}{8\delta} \left[\left(\frac{(1+k)N_u}{(1+(n-1)\rho)E_c h b} + \varepsilon_{S+T} \right) l + \frac{N_u}{bS} \right] - \frac{T_1 - 2T_2 + T_3}{4\eta f_{cd} \lambda b}$$

$$c_3 = \frac{h}{2} - \frac{\delta}{4} - \frac{l}{8\delta} \left[\left(\frac{(1+k)N_u}{(1+(n-1)\rho)E_c h b} + \varepsilon_{S+T} \right) l + \frac{N_u}{bS} \right] - \frac{T_1 + 2T_2 - 3T_3}{4\eta f_{cd} \lambda b}$$

$$\left(\frac{(1+k)N_u}{(1+(n-1)\rho)E_c h b} + \varepsilon_{S+T} \right) l + \Delta_{13} = \left[\frac{1}{1 + \frac{\eta f_{cd} \lambda}{8\delta} \frac{(1+k)l^2}{(1+(n-1)\rho)E_c h} + \frac{1}{S}} \right].$$

$$\left\{ \left(\frac{(1+k)l}{(1+(n-1)\rho)E_c h} + \frac{1}{S} \right) \left[\eta f_{cd} \lambda \left(\frac{h}{2} - \frac{\delta}{4} - \frac{T_1 - 2T_2 + T_3}{4\eta f_{cd} \lambda b} \right) - \frac{T_2 + F_{ps}}{b} \right] + l \varepsilon_{S+T} \right\}$$

$$N_u = \eta f_{cd} \lambda c_2 b - T_2 - F_{ps}$$

$$\left[\left(\frac{(1+k)N_u}{(1+(n-1)\rho)E_c h b} + \varepsilon_{S+T} \right) l + \Delta_{13} \right] = \left[\left(\frac{1}{1 + \frac{(\eta f_{cd} \lambda l)}{8\delta} \left(\frac{(1+k)l}{(1+(n-1)\rho)E_c h} + \frac{1}{S} \right)} \right) \left\{ \left(\frac{(1+k)l}{(1+(n-1)\rho)E_c h} + \frac{1}{S} \right) \left[\left(\eta f_{cd} \lambda b \left(\frac{h}{2} - \frac{\delta}{4} + \frac{(\beta-1)(T_1 - C_{s1}) + T_2 - C_{s2} - \beta(T_3 - C_{s3})}{2\eta f_{cd} \lambda b} \right) \right] \right\} \right]$$

All the above equations define the position of neutral axis as a function of the forces, which in turn depends on the position of neutral axis. That is the case, a direct solution of the equations cannot be possible which results in an iterative procedure. The iterations and the boundary criteria are going to be analysed at the numerical simulation section.

5.3. Determination of the Ultimate Capacity

At previous sections the forces of concrete, reinforcement and prestressing steel have been defined in terms of the deflection δ and central hinge location β . The ultimate capacity is calculated by the distribution of the aforesaid forces and their dependent parameters (δ and β). The determination of the capacity is according to the assumed failure mechanism, as presented below.

5.3.1. Axial Force and Moments

The axial forces of the concrete and steel can be observed below at a plastic hinge's cross section. By taking moment equilibrium the ultimate moment capacity can be expressed by the equation:

$$M_{ui} = 0.5 \eta f_{cd} \lambda c_i b (h - \lambda c_i) + T_1 (d_i - 0.5h) + C_{si} (0.5h - d_i') + F_{ps} (d_{pi} - 0.5h) \quad i=1..3$$

The compressive membrane force is given by the horizontal force equilibrium.

$$N_u = \eta f_{cd} \lambda c_2 b - T_2 - F_{ps}$$

5.3.2. Calculation of the Capacity

The failure vertical load, applied at the midspan, depends on the ultimate moments and the compressive arching force. By making use the principle of moment equilibrium at the left and the right of the central hinge, the capacity is calculated as follows:

$$F_d = \frac{2 \left(\frac{Mu_1}{\beta} + \frac{Mu_2}{(1-\beta)\beta} + \frac{Mu_3}{(1-\beta)} - \frac{Nu\delta}{(1-\beta)\beta} \right) \beta}{L}$$

The ultimate capacity as distributed load is given by the formula:

$$w_u = \frac{2 \left(\frac{Mu_1}{\beta} + \frac{Mu_2}{(1-\beta)\beta} + \frac{Mu_3}{(1-\beta)} - \frac{Nu\delta}{(1-\beta)\beta} \right)}{BL^2}$$

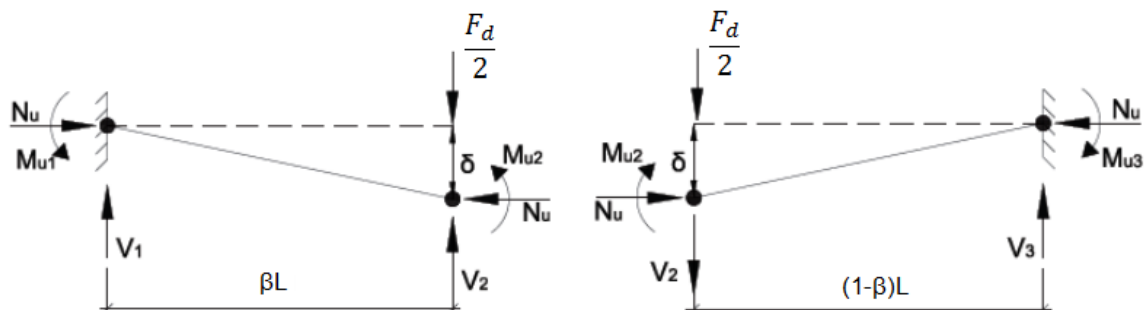


Figure 28 Free Body Diagrams for Loaded Slab Segments

As has already been observed, a direct solution of the capacity is not possible, because all the variables in the equations depend on the vertical deflection δ . However, the profile of the

deflection curve including the compressive membrane action is known beforehand by research, given at low deflections the arching action starts developing reaching a maximum value at a specific deflection and while the deflection keeps increasing the compressive membrane force converts to a tensile action. Thus, applying an iteration procedure the accurate deflection curve, giving the peak of the compressive action, can be obtained. The iterations are made by applying an incrementally increasing deflection at the midspan of the slab.

5.3.3. Location of the Central Hinge

At the previous sections, the assumed failure mechanism has been defined as a plastic collapse mechanism which requires the formation of three plastic hinges, Fig 30. According to the equations of the capacity, the failure load depends on the position of the central hinge β . The correct value of parameter β minimizes the collapse load, as a result it can be found by differentiating the equation of capacity with respect to the β and setting it equal to zero.

$$(Mu_1 - Mu_3) \beta^2 - 2(Mu_1 - Mu_2 - Nu\delta)\beta + (Mu_1 + Mu_2 - Nu\delta) = 0$$

Thus, the location of central hinge can be estimated by the expression:

$$\beta = \left(\frac{(Mu_1 + Mu_2 - Nu\delta) - \sqrt{(Mu_1 + Mu_2 - Nu\delta)^2 - (Mu_1 - Mu_3)(Mu_1 + Mu_2 - Nu\delta)}}{(Mu_1 - Mu_3)} \right) \quad (32)$$

When the reinforcement and the prestressing steel are symmetrical at both support, then the ultimate moments Mu_1 and Mu_3 are equal. At this case, the parameter β cannot be defined, taking the value 0.5 due to symmetrical conditions. For unsymmetrical conditions the Eq.32 can be employed to find the position or central hinge accurately.

5.4. Restrained Stiffness

An important parameter that governs the effect of compressive membrane force is the stiffness of the slab and of the surroundings elements. The slab is supported by the girders, which are assumed to behave linear elastic in order to develop full arching action. If the girders do not have sufficient capacity, the failure mechanism will be attributed to the composite failure slab-beam and the maximum ultimate capacity, explained at previous sections will not be reached. It is advisable to consider different cases of the position of the loaded part in order to estimate a proper distribution of (effective) stiffness during loading. The effective stiffness is given by the axial stiffness of the slab and the stiffness of the girders. Thus, the next cases are going to be examined at this section. The restraints of the loaded slab can be modelled as linear springs, the stiffness of which express the effective stiffness of the slab.



Figure 29 Linear springs at both ends of slab

Due to the fact that only the relative distance between the supports 1 and 3 is of interest, it can be assumed that the one end is fixed and the other is free to translate. Thus, the final model of the slab can be converted to the following one:

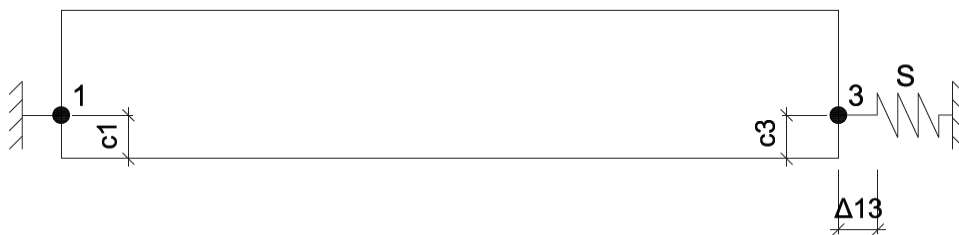


Figure 30 Equivalent Model of Restraint

Taking into account that axial force due to the arching action is the F_b compressive force, which has to be constant along span of the slab, since there are no other horizontal forces applied in the slab. This force is related to the total axial deformation and the stiffness is considered as the stiffness per unit width, as follows:

$$F_b = K \cdot \Delta_{13}$$

$$K = S \cdot B$$

Where S : the effective stiffness of the slab in the transverse direction per unit width B

L : length of the slab

Δ_{13} : the total deformation due to compressive force

The effective stiffness S is given as a function of the linear springs in series per unit width:

$$S = \left(\frac{1}{S_1} + \frac{1}{S_3} \right)^{-1} = \frac{S_1 S_3}{S_1 + S_3}$$

Having estimated the stiffness of the support the compressive membrane force can be defined:

$$N_u = bS \cdot \Delta_{13}$$

$$\Delta_{13} = \frac{N_u}{bS}$$

5.4.1. Interior bay loaded

Assuming that the loaded part is analyzed as an entire bay interior panel, the maximum compressive membrane action is expected since the surrounding slab panels will form a confining ring to resist the horizontal deformation. The overall stiffness is given by the axial stiffness of the slab and the flexural stiffness of the girders.

Axial stiffness of the slab

$$S_s = EA/L = (E_s A_s + E_c (A_g - A_s - A_p) + n * E_p A_p) / L$$

Where A_g gross cross sectional area

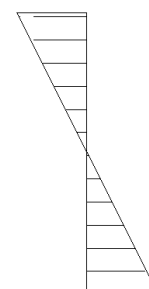
A_s cross section of the mild steel

A_p cross section of the prestress steel

n amplification factor, taking values 1 for TPL: 1.25 and 2 for TPL: 2.5

More specifically, the girders will not have any horizontal bending deflection since they will act as deep beams. At this stage, it is important to take two subcases: the load is applied at the centre and at the edge of the panel with respect to the longitudinal direction to investigate the shear effect over the horizontal displacement.

- If the load is applied at the centre of the panel, then there are many unloaded panels between the loaded and the edge structure as a result the shear deformation can be considered to be negligible. Thus, the axial forces are transferred to the support by bending only. Subsequently, the horizontal deflection along the entire width of the loaded panel is constant, and it can be modelled as a single slab strip with restrained stiffness equal to the axial stiffness of the slab. Moreover, the applied transverse prestress prevents cracking, so the restraint stiffness S can be considered as the full axial stiffness S_s .
- If the load is applied close to the edge of the panel, then the panel is restrained only by a single bay and the axial forces of the slab are transferred by shear and bending to the supports. To calculate the shear effect on the restraint, the shear stresses due to compressive force is considered linear, as plotted below. The compressive force is constant along the support.



As can be observed, the shear increases the deflection away from the ends of the panel, as the axial force is smaller and the restrained stiffness less than that of the ends of the panel.

Having assumed that the shear stress is uniformly distributed over the width of the panel, it can be expressed by the formula at any distance, x :

$$\tau = \frac{\frac{Nu}{2} - \frac{Nu \cdot x}{L}}{L \cdot h}$$

Thus, the shear strain is:

$$\gamma = \frac{\frac{Nu}{2} - \frac{Nu \cdot x}{L}}{L \cdot h \cdot G}$$

Where L : length of the single strip

B : width of the single strip

The total shear deformation at the loaded slab (1050x1000mm²) is given by the integration along the support:

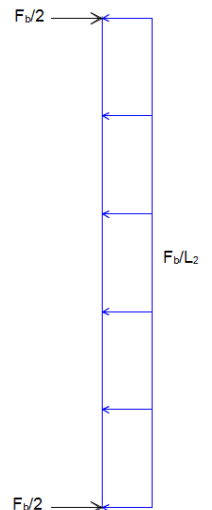
$$\Delta_{\text{shear}} = \int_0^x \frac{\tau}{G} dx = \frac{\frac{Nu}{2} \cdot x \cdot B - Nu \cdot x^2}{2 \cdot L \cdot B \cdot h \cdot G}$$

The total deflection of the support due to the compressive membrane force can be expressed as:

$$\Delta_{\text{support}} = \frac{Nu \cdot L}{2 \cdot B \cdot E \cdot h \cdot S / S_s}$$

The extent that the shear stress is important can be investigated by taking the ratio:

$$\Delta_{\text{support}} / \Delta_{\text{shear}} = \frac{2.3 \cdot L^2}{B^2 \cdot S / S_s}$$



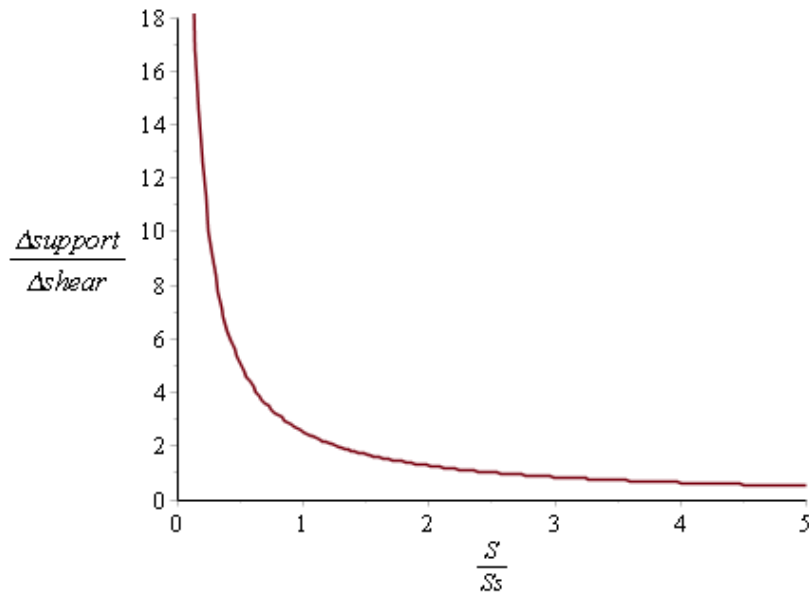


Figure 32 Lateral Displacement - Stiffness

As mentioned above, at the analysis of this slab the effective stiffness of the slab is equal to the full axial stiffness due to restraint prestress effect, so for the stiffness ratio $S/S_s=1$ the displacement ratio $\Delta_{support} / \Delta_{shear}$ becomes 2.53. Conclusively, the shear effect can be considered to be negligible either the load is positioned at the centre of the panel or close to the edge structure. Otherwise, the horizontal deformation should be calculated as a superposition of the support and the shear deformation.

Flexural stiffness of the girder

As has been mentioned above, the slab is supported by girders, which are considered to obtain sufficient capacity to avoid composite failure. The girders are restrained horizontally by the surrounding slabs at the upper flange and they are assumed fixed at the floor. Thus, the lateral stiffness can be calculated by the formula below:

$$k_{girder} = \frac{3EI}{h_g^3}$$

Where EI: the flexural rigidity of the girder

h_g : the height of the girder

Taking into account the fact that the inertia in the direction parallel to the length of the slab is of interest, the inertia of the girder can be estimated as follows:

$$I = I_{top,fl} + I_{web} + I_{bot,fl}$$

Having defined the flexural rigidity of the girder, the stiffness per unit width is:

$$S_i = \frac{k_{girder}}{B} \quad i=1..3$$

The total flexural stiffness of the girders is:

$$S = \left(\frac{1}{S_1} + \frac{1}{S_3} \right)^{-1} = \frac{S_1 S_3}{S_1 + S_3}$$

Total restraint stiffness:

Total restraint stiffness is given by the superposition of the contribution of the axial stiffness of the slab and the flexural stiffness of the girders. Thus, combining the equations, it is calculated by the next expression:

$$S_t = \frac{EA}{L} + \frac{S_1 S_3}{S_1 + S_3}$$

It should be noted that the flexural stiffness of the girders is much less than the axial stiffness of the slab. The slab should be designed with that high axial stiffness due to the fact that post-tensioning is applied and it has to be capable of resisting the induced compressive forces.

The compressive force will cause only lateral displacement at the adjacent slabs and the girders. The moment and the shear forces could cause a rotation of the girder towards the loaded slab, but due to the continuity of the girder with the slab, the rotation is quite negligible around the girder's axis. Also, to neglect this rotation is in the safety side since the rotation would lead to a reduced outward horizontal displacement.

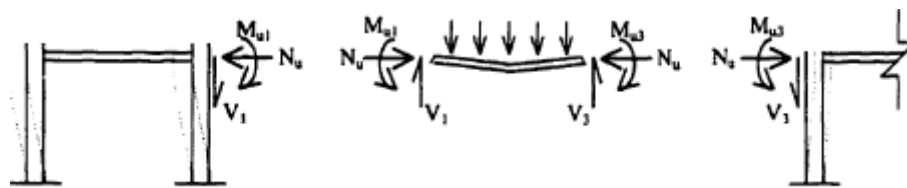


Figure 33 Free body – Forces

5.4.2. Exterior bay line loaded

At the case that the loaded panel is located at the exterior bay, the restrained stiffness depends on the stiffness of the edge beam from the one side, and the stiffness of the adjacent slab and girders from the other side. Along the interior edge, the stiffness has been analyzed at the previous section. Along the exterior edge is going to be described below:

Edge beam:

The stiffness at the edge beam is expected to be less than the stiffness of the interior line, since only the girders contribute to the horizontal resistance. Moreover, the stiffness along the length of the edge beam will vary, depending inversely on the deflection of the beam. To estimate the distribution of the stiffness the panel has been divided into strips. The lateral stiffness of each strip can be found by making use the geometric compatibility that the horizontal displacement at the neutral axis of the strip is equal to the horizontal displacement of the support at the same location. It is worth mentioning that the deflections are calculated under the loads applied by all the strips. The forces at the edge beam can cause both lateral deflection and rotation of the beam around its shear centre. Furthermore, the centroid of the edge beam does not coincide with the neutral axis of the slab, the horizontal displacement will be a combination of the lateral movement and the rotation of the edge beam. Thus, to take it into account the flexural rigidity EI and the torsional rigidity JG of the edge beam are calculated based on the gross concrete cross section using the equations:

$$(EI)_b = E_c \frac{1}{12} (h_b) (b_b)^3$$

$$(JG)_b = 0.43E_c \left(1 - 0.63 \frac{b_b}{h_b}\right) \left(\frac{b_b^3 h_b}{3}\right)$$

6. Computational Modelling

6.1. Introduction

The numerical simulation of the loaded slab is necessary for estimating the ultimate capacity since an iterative process gives an accurate solution. Thus, a code in Fortran 95 has been casted to estimate the bending resistance and the ultimate capacity of the slab. This code has taken into account the following important parameters, as well as their effects:

- Compressive membrane action (N_u)
- Effect of prestress (F_{ps})
- Strain hardening of reinforcement steel
- The position of the loaded part in the slab (case 1, case 2)
- The temperature changes, creep, shrinkage
- Symmetrical or unsymmetrical conditions at the supports

It is well-known that the capacity is directly dependent on the deflection. Therefore, the code calculates it by applying an incremental deflection at the midspan, using as a starting point the initial deflection: $\delta = h/300$. At each step the code extracts the capacity for a given deflection.

6.2. Structure of the code

The code, casted in Fortran 95, is consisted of the main program SLAB and six subroutines: INT, STRIP, REST, ISTRN and FMILDS.

SLAB

The main program SLAB initiates the procedure for the estimation of the capacity. It takes into account the presence of prestressing steel A_p and the position of the loaded part of the slab (exterior or interior). It contains the six subroutines, which are called depending on the different cases. Regarding the position of the load, the program calculates the capacity calling the subroutine INT or EXT.

INT

It calculates the ultimate capacity when the interior loaded slab can be simulated as a single strip. Initially, it estimated the ultimate capacity (w_{uo}) by calling the STRIP subroutine neglecting the effect of compressive membrane action and strain hardening of the mild steel, by employing an effective restraint stiffness S of 10^{-30} and ENSH equal to 0. Then, it takes into account these phenomena with the total effective stiffness and it finds the load enhancement LE. As has been mentioned at previous section the stiffness is a combination of the axial stiffness of the slab and the flexural stiffness of the girders, so it is given by the summation of them.

EXT

It calculates the ultimate capacity when the exterior loaded slab can be simulated as a number of strips in order to obtain a reliable distribution of the stiffness along the length of the edge beam. It calculated the ultimate capacity of the slab, by dividing the width and the area of reinforcement. Then, it calculates the ultimate capacity by calling the STRIP subroutine with and without the effect of CMA and strain hardening by setting an effective restraint stiffness S of 10^{-30} and ENSH equal to 0. For the exterior slab the flexural rigidity and the torsional stiffness are inserted as input data to calculate the overall response of the slab, by calling the subroutine REST. At the end of the analysis the average of the ultimate capacity and the load enhancement of the strips are calculated indicating the distribution of the stiffness along the support.

REST

It determines the horizontal displacement of the edge beam at the level of the neutral axis of the slab under the load applied by all the strips. The flexural rigidity and the torsional stiffness of the edge beam are calculated to form the flexibility matrix and finally to estimate the forces in compliance with the distribution of stiffness. Then, applying the geometric compatibility the criterion that the horizontal movement of the support has to be equal to that of strip.

STRIP

The subroutine STRIP mainly calculates the ultimate capacity and the moments at the reached failure deflection. Defining the restrained stiffness S , it calculates the position of neutral axis for a given deflection at each step. Totally it contains three loops:

Parameter β : Initially, it assumes that the position of central hinge is at the midspan, taking β equals to 0.5. At the present case the conditions at the support are symmetrical because of the same amount of regular and prestressing reinforcement. At the end, the ultimate moments will be known, so the parameter β can be updated using Eq. 32.

Deflection δ : The deflection is incrementally applied at the central hinge. It is increased at successive iterations until the full development of compressive membrane force.

Forces: In order to estimate the position of neutral axis at the starting point (first iteration), initial values for the regular and prestressing steel are assumed. Regarding the regular steel it is considered that it yields, but due to the very low initial applied deflection ($\delta = h/300$) the steel only yields and no strain hardening is considered yet (plateau part of curve). About the prestressing steel, the deflection is not able to cause yielding, thus the initial value is the effective prestress force, which takes into account the transverse prestress level, as explained later. Having obtained the initial forces the position of neutral axis can be found and then new values of the forces will be obtained and used as forces for the next iteration. If the difference between the assumed and the resulted is more than 0.01% then the average of the assumed and the calculated forces are taken as new values for the next iteration. The iterations stop when the difference between assumed and calculated is less than 0.01%. When the final position of neutral axis is known the ultimate capacity is calculated and checked with the previous so as to estimate the maximum reached.

The last step is to calculate the parameter β since all the moments and forces are known.

FMILDS

It determined the force in the mild steel at each incremental applied displacement at the midspan. The mild steel is modelled by employing the Modified Trilinear Idealization, allowing strain hardening of the steel.

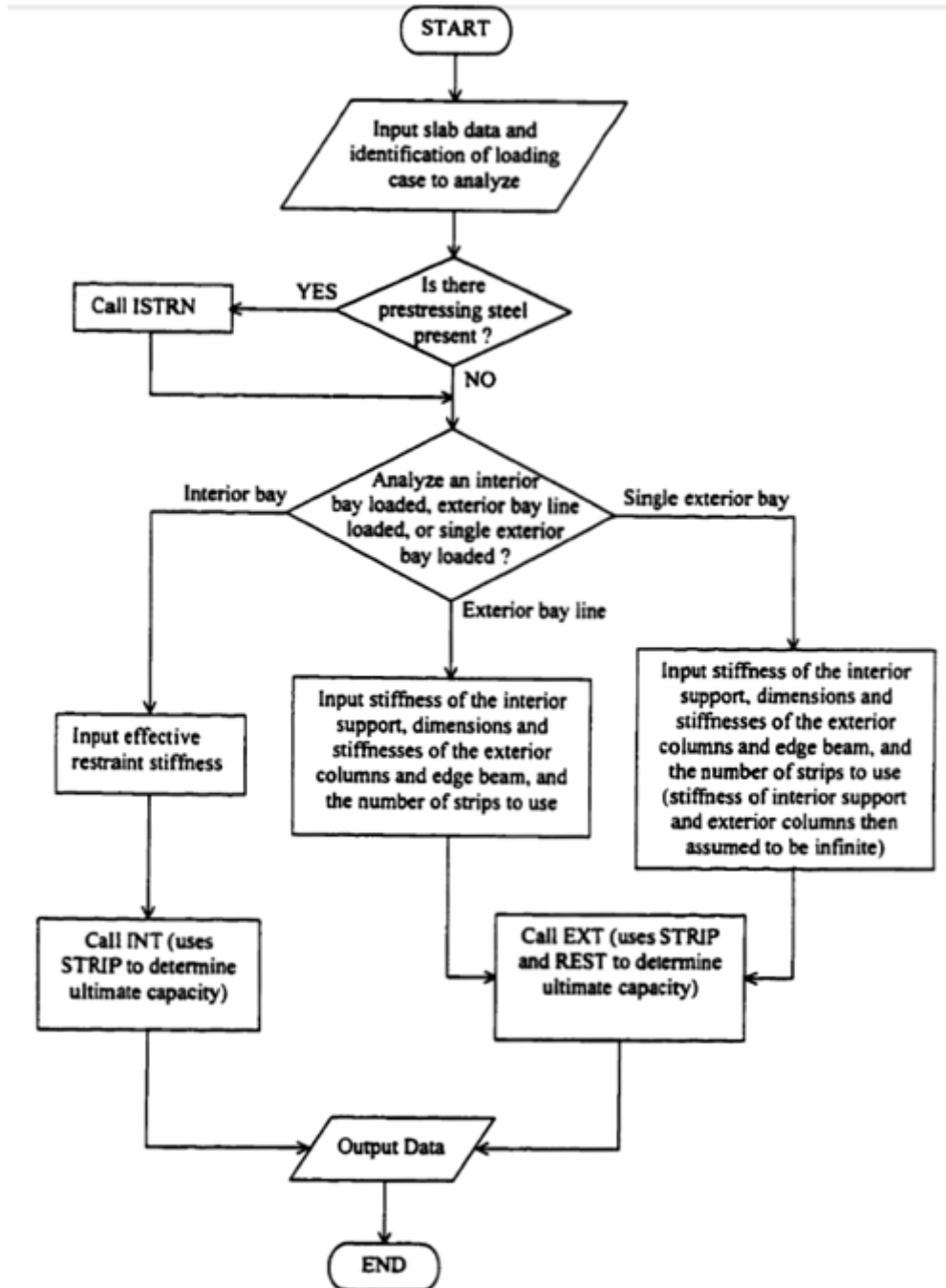
ISTRN

It determined the force in the prestressing steel at each incremental applied displacement. The prestressing steel is modelled by employing the Modified Ramberg-Osgood function. The transverse prestress level is introduced as imposed strain in the effective prestress force.

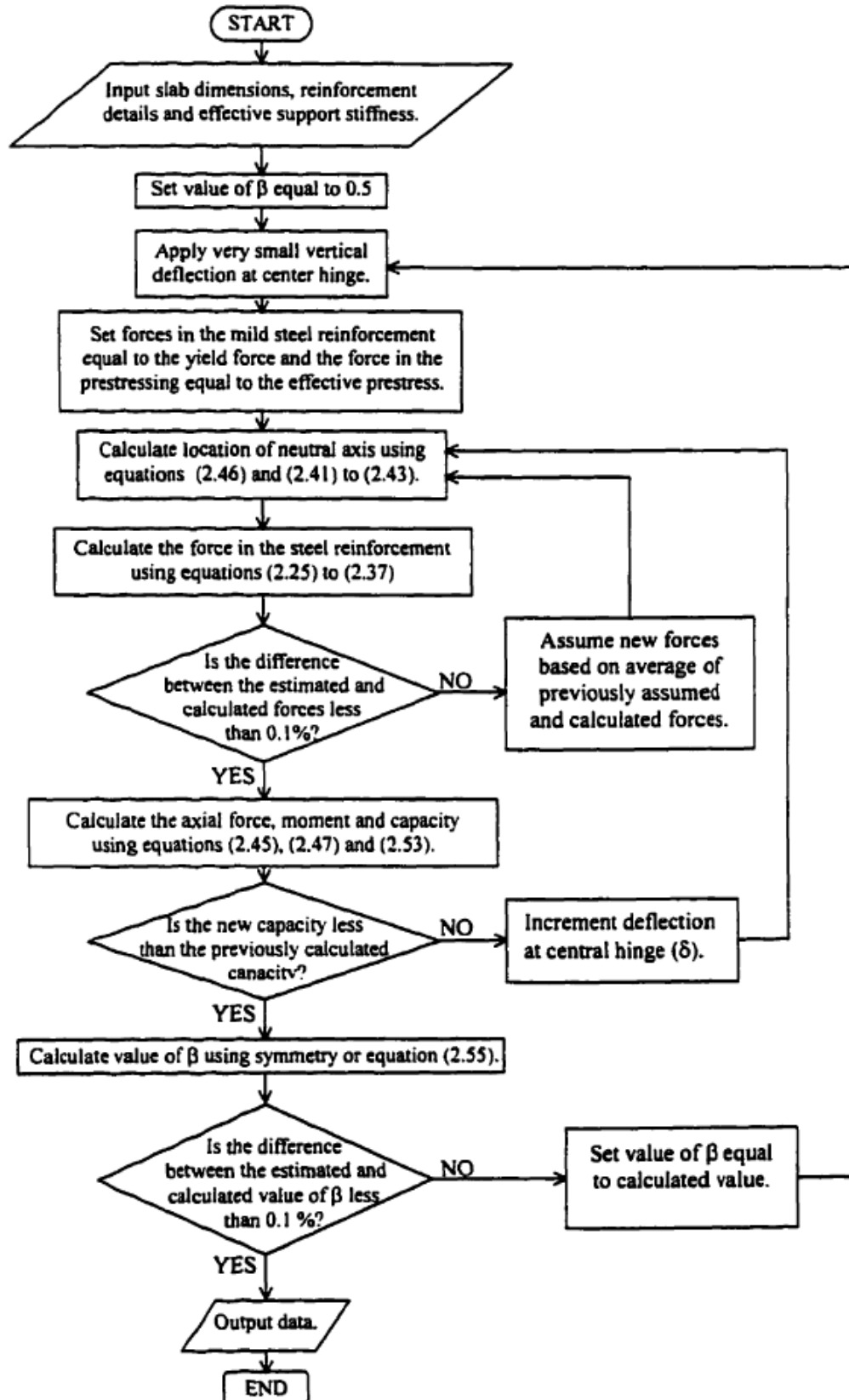
6.3. Flowcharts

Below the most important flowcharts of the code are presented:

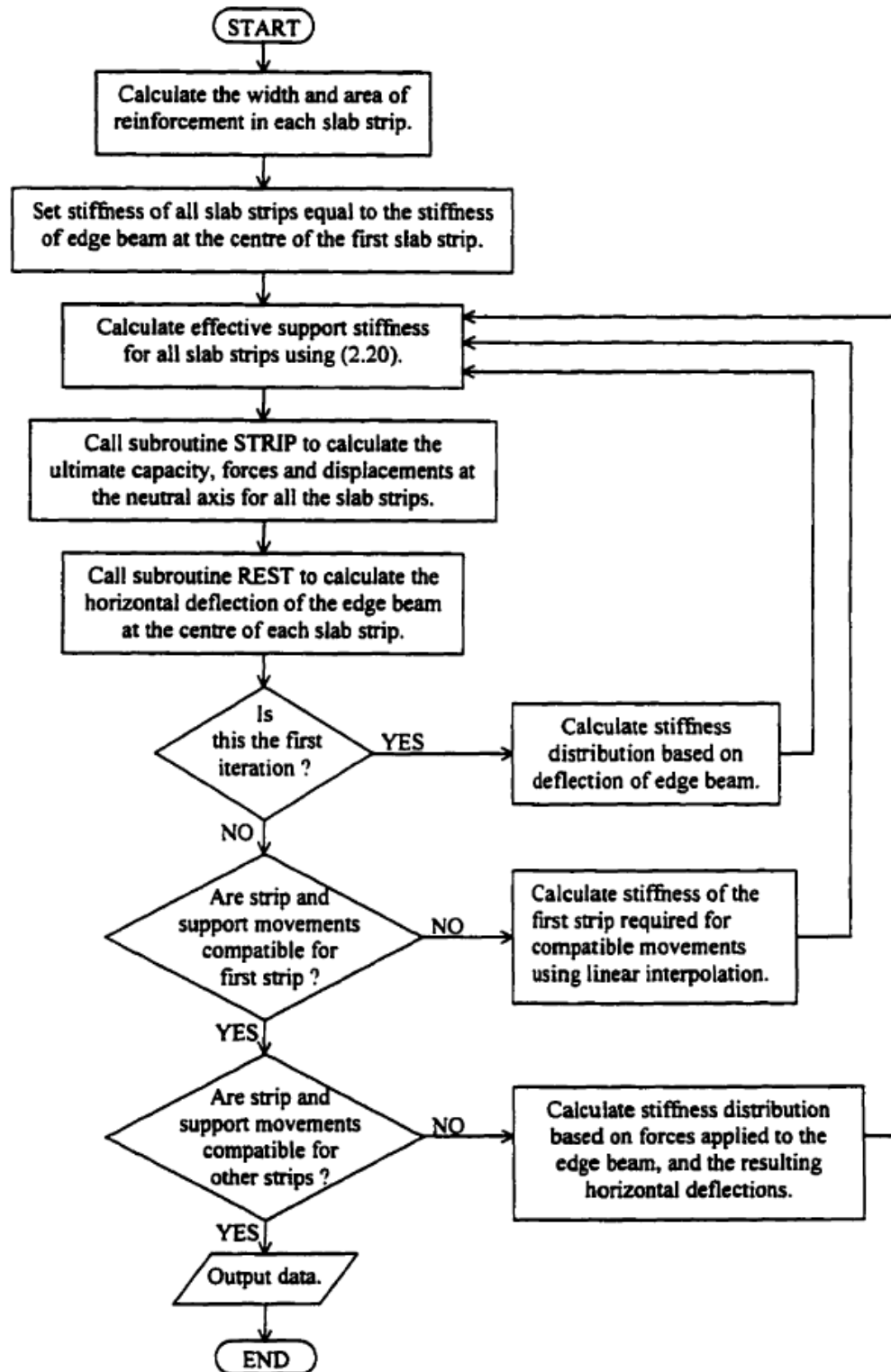
Main program: SLAB



Subroutine: STRIP



Subroutine: EXT



7. APPLICATION OF THEORETICAL AND NUMERICAL APPROACH

7.1. General

The theoretical approach is going to be applied at the present case study. A slab of 3 bays supported by girders is going to be analysed numerically in order to calculate the ultimate bending

capacity and compressive membrane action. As pictured below, the slab model has length 12000mm and width 6400mm. The concrete girders are located at centre-to-centre distance 1800mm. The thickness of the slab is 100mm.

The slab has been examined for different positions of loads: interior panel B and exterior panel A/C.

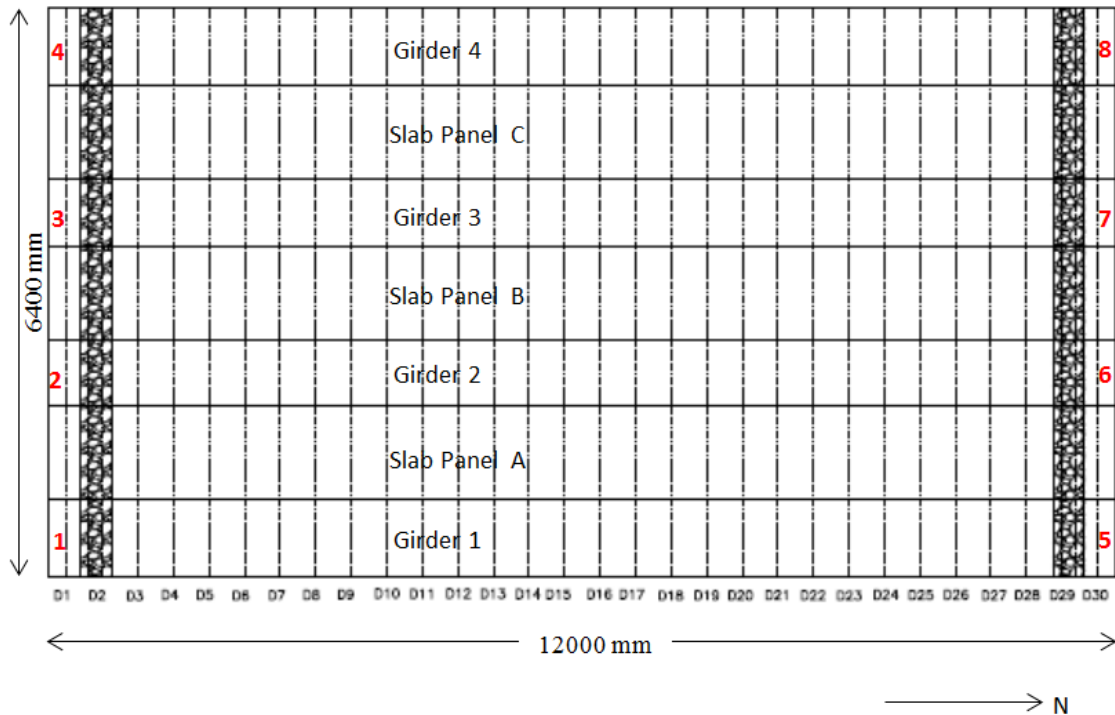


Figure 34 Bridge model structure

7.2. Input data

As has been presented in previous sections, the numerical simulation takes into account many governing parameters, which have already defined. These parameters are required to be introduced as input data to execute the main program SLAB. However, the concrete and steel properties, as well as the dimensions of the elements are also presented at the table below.

Table 9 Input data-Units in [N,mm]

Dimensions of slab	L	1050
	H	100
	b	12000

	I_t	6600
Dimensions of girder	h_b	1200
	b_b	300
	l_b	12000
Steel properties	A_{s1}	1725
	A_{s2}	1725
	A_{s3}	1725
	$A_{s1'}$	0
	$A_{s2'}$	0
	$A_{s3'}$	0
	E_s	200000
	E_{sh}	9000
	f_y	500
	f_u	700
	ϵ_y	0.0025
	ϵ_{sh}	0.006
	ϵ_u	0.045
	Prestressing steel	A_{sp}
E_p		205000
f_{pe}		818.18
f_{pu}		1100
Concrete properties	f_c	81.6
	E_c	40649.72

	α_1	0.7276
	β_1	0.766

Where $E_c = 4500(f_c)^{1/2}$

$$f_{pe}: 900/1.1=818.18\text{MPa}$$

The tables with the notification and the values of the input data are given below:

Table 10: Format and description of input file of the Program SLAB

Input file		Description of input data
S	l h b	Length, height, width of slab
L	d ₁ d' ₁ d ₂ d' ₂ d ₃ d' ₃	Depths of tension and compression steel at plastic hinges
A	d _{p1} d _{p2} l _t	Depths of prestressing at plastic hinges and length of tendon
B	A _{s1} A _{s2} A _{s3} A' _{s1} A' _{s1} A _{sp}	Areas of tension and compression steel and prestressing steel
D	f _c E _c α β	Concrete strength, modulus of elasticity and stress block constants
A	E _s E _{sh} f _y f _{cu}	Modulus of elasticity, strain hardening modulus, yield and ultimate stress
T	ε _y ε _{sh} ε _u	Strains corresponding to yield, start of strain-hardening and ultimate strain
A	F _{pe} F _{pu} E _p	Effective prestress force, ultimate stress and modulus of elasticity
A	A B C	Modified Ramberg-Osgood Function Constants
	k ε _{s+T}	Ratio of long term to short term axial strains, axial strain due to temper etc
Case 1: Interior slab loaded		
	S	Effective support stiffness
Case 1: Exterior slab loaded		
	S _{int}	Stiffness of the interior support
	l _c l _{cb} w _c (EI) _c	Dimensions and flexural stiffness of exterior columns
	h _{b1} b _b l _b (EI) _b (JG) _b	Dimensions, flexural and torsional stiffness of edge beam
	NUM	Number of slabs to be used

To fill the input data file, important calculations should be made to determine the required stiffness for both cases, as well as crucial and valid assumptions with respect to the transverse prestress level.

7.3. Determination of stiffness

Case 1: Interior slab

At this case the stiffness is considered the same at the right and left bay lines due to symmetrical conditions. It is given as a combination of the contribution of the axial stiffness of the slab and the flexural stiffness of the girders.

There are two subcases regarding the location of the load: centre and edge of the structure. When the load is applied at the centre shear deformation can be neglected and the lateral deformation is calculated only due to the bending and compressive action. But when the load is applied at the edge of the panel then the shear contribution should be checked since it can affect the lateral movement, which in turn has an impact on the compressive membrane force.

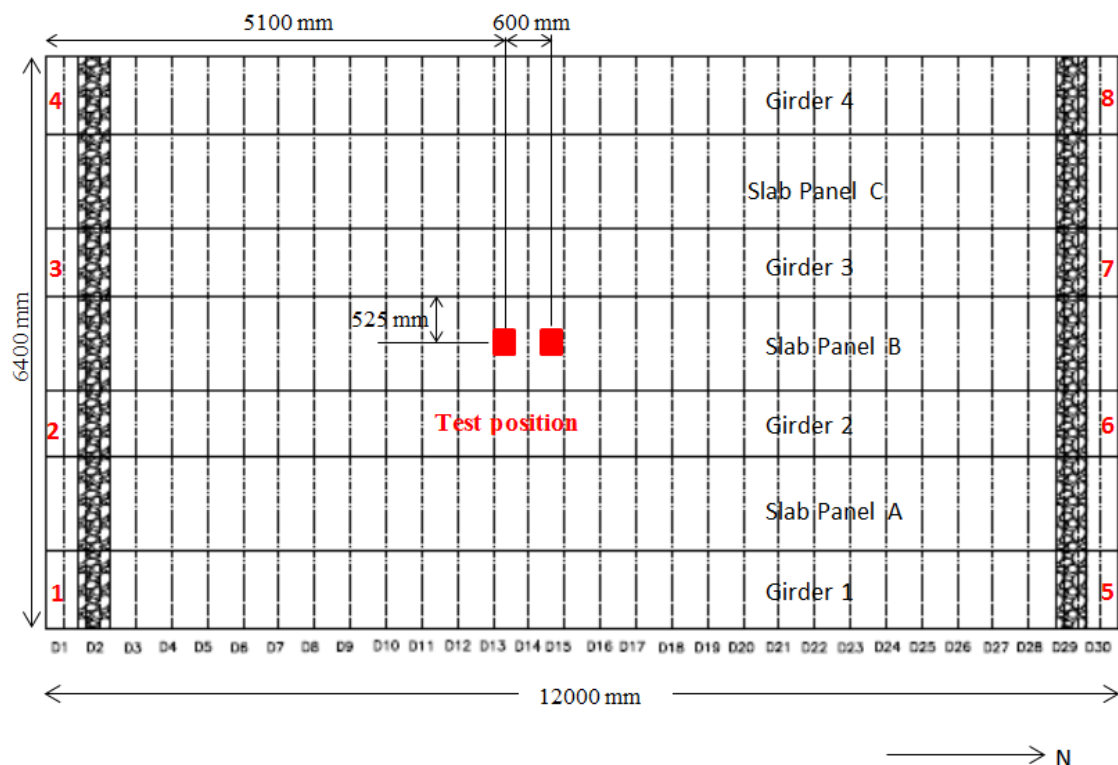


Figure 35 Loaded panel

- Load is applied at the centre of the slab

Due to axial stiffness of the slab:

$$S_s = EA/L = (E_s A_s + E_c (A_g - A_s - A_p) + n * E_p A_p) / L$$

At TPL: 1.25 => n=1

At TPL: 2.5 => n=2

$$n=1: S_s = [200000 * (1725 + 1725 + 1725) + 43285 * (105000 - (1725 + 1725 + 1725)) + 205000 * 4500] / 1050$$

$$S_s = 5793925.068 \text{ N/mm}^2$$

$$n=2: S_s = [200000*(1725+1725+1725)+43285*(105000-(1725+1725+1725)+2*205000*4500)]/1050$$

$$S_s = 6672496.496\text{N/mm}^2$$

Where : $A_g=L*h=1050*100=105000\text{mm}^2$

At the transverse direction 60 bars of reinforcement $\Phi 6/200$ along the entire length of the support have been used. Thus, the total amount of regular reinforcement is $A_s=1725\text{mm}^2$.

Regarding the prestressing steel, there have been installed 30 prestressing bars of cross section $A_p=150\text{mm}^2$. Thus, the total amount of prestressing area is 4500mm^2 .

Due to flexural stiffness of the girders:

Taking into account the fact that the inertia which participates to the horizontal resistance along the length of the slab is of interest, this inertia of the girder can be estimated as follows:

$$I = I_{\text{top,fl}} + I_{\text{web}} + I_{\text{bot,fl}} = 7.02 * 10^{10} \text{ mm}^4$$

$$k_{\text{girder}} = \frac{3EI}{h_g^3} = (3 * 37486 * 7.02 * 10^{10}) / 1200^3 = 4570526.106 \text{ N/mm}$$

where EI: the flexural rigidity of the girder

h_g : the height of the girder

Having defined the flexural rigidity of the girder and the slab at both sides, the total stiffness per unit width is:

$$\text{TPL:1.25} \quad S_i = \frac{2EA/L + 2k_{\text{girder}}}{B} = 1727.41 \text{ N/mm per unit width} \quad i=1..3$$

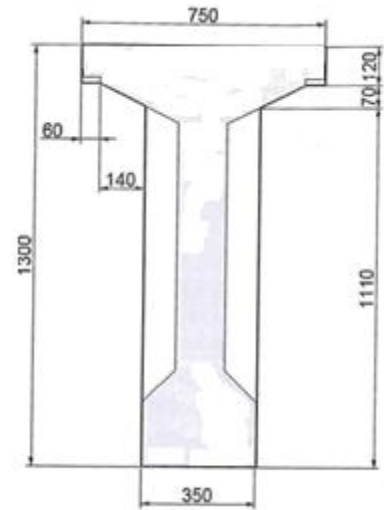
$$\text{TPL:2.5} \quad S_i = \frac{2EA/L + 2k_{\text{girder}}}{B} = 1873.84 \text{ N/mm per unit width} \quad i=1..3$$

Due to symmetrical conditions the flexural stiffness S will be the same at both supports: $S_1=S_3$

The total flexural stiffness of the girders is:

$$S = \left(\frac{1}{S_1} + \frac{1}{S_3} \right)^{-1} = \frac{S_1 S_3}{S_1 + S_3}$$

Total restrained stiffness for interior slab:



The total restrained stiffness is given by the superposition of the contribution of the axial stiffness of the slab and the flexural stiffness of the girders. Thus, combining the equations, it is calculated by the next expression:

$$\text{TPL: 1.25} \quad S_t = \frac{2EA/L+2kgirder}{2} = 863.7\text{N/mm}^2$$

$$\text{TPL: 2.5} \quad S_t = \frac{2EA/L+2kgirder}{2} = 936.92\text{N/mm}^2$$

- Load is applied at the edge of the slab:

$$\Delta_{\text{shear}} = \int_0^x \frac{\tau}{G} dx = \frac{\frac{Nu}{2} * x * B - Nu * x^2}{2 * L * B * h * G}$$

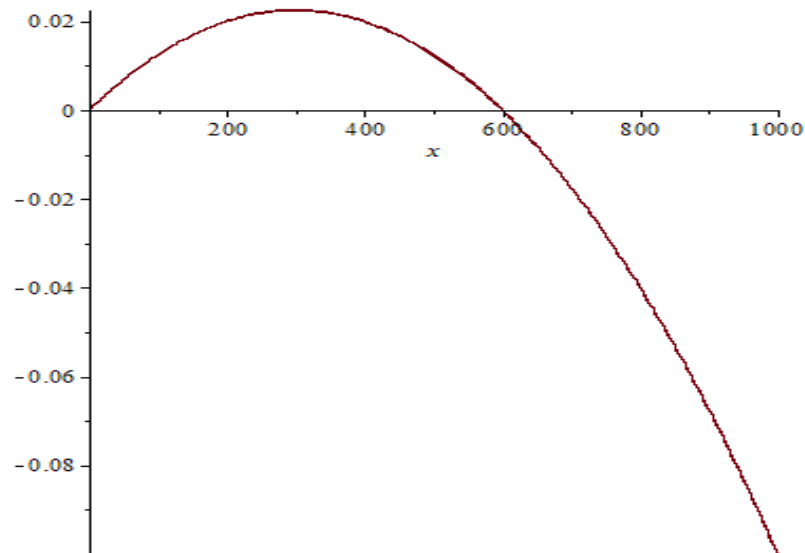


Figure 36 Shear deformation

The total deflection of the support due to the compressive membrane force can be expressed as:

$$\Delta_{\text{support}} = \frac{Nu * L}{2 * B * E * I * S / Ss}$$

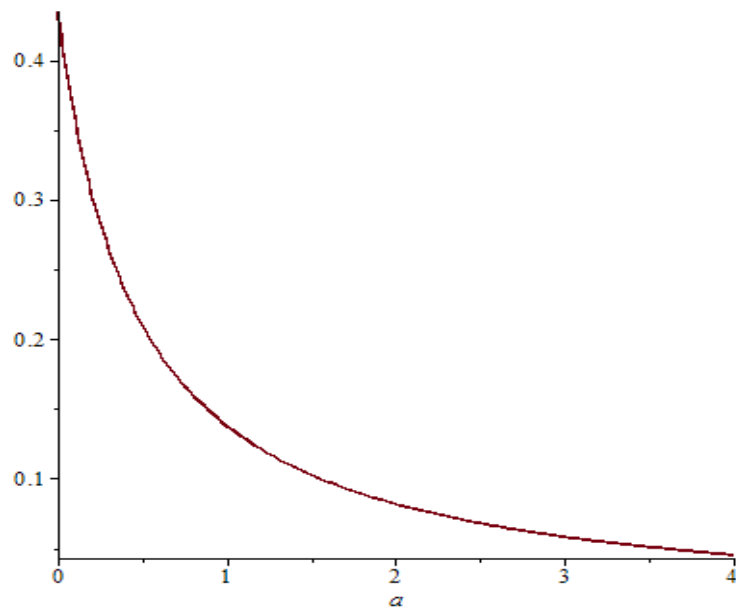


Figure 37 Support deformation for varying stiffness ratio

The extent that the shear stress is important can be investigated by taking the ratio:

$$\Delta_{\text{support}} / \Delta_{\text{shear}} = \frac{2.3 \cdot L^2}{B^2 \cdot S / S_s}$$

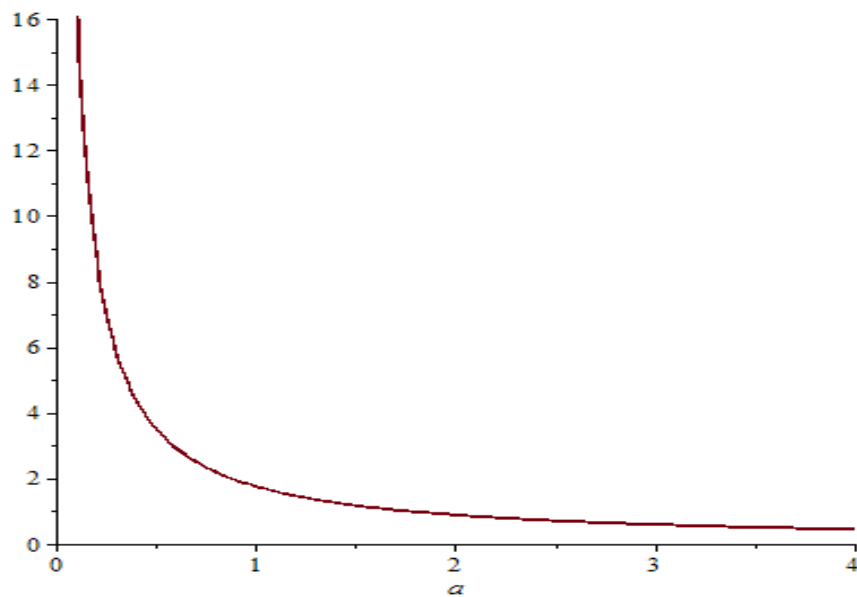


Figure 38 $\Delta_{\text{support}} / \Delta_{\text{shear}}$ for varying stiffness ratio

Case 2: Exterior slab

At the case that the loaded panel is located at the exterior bay, the restrained stiffness depends on the stiffness of the edge beam from the one side, and the stiffness of the adjacent slab and girders from the other side.

The stiffness at the interior bay line is calculated in the same as in case 1. Thus, only the half of the axial stiffness and both left and right girders contribute to the resistance.

$$\text{TPL: 1.25} \quad S_t = \frac{EA/L+2kgirder}{2} = 622.29\text{N/mm}^2$$

$$\text{TPL: 2.5} \quad S_t = \frac{EA/L+2kgirder}{2} = 658.89\text{N/mm}^2$$

About the exterior line, only the edge beam provide lateral stiffness against the horizontal deformation.

During loading the stiffness along the length of the edge beam will vary, depending inversely on the deflection of the beam. To estimate the distribution of the stiffness the panel has been divided into strips.

The forces at the edge beam can cause both lateral deflection and rotation of the beam around its shear centre. Furthermore, the centroid of the edge beam does not coincide with the neutral axis of the slab, the horizontal displacement will be a combination of the lateral movement and the rotation of the edge beam. Thus, to take it into account the flexural rigidity EI and the torsional rigidity JG of the edge beam are calculated based on the gross concrete cross section using the equations given in N and mm:

$$(EI)_b = E_c \frac{1}{12} (h_b) (b_b)^3 = 2.63262 * 10^{15}$$

$$(JG)_b = 0.43 E_c \left(1 - 0.63 \frac{b_b}{h_b} \right) \left(\frac{b_b^3 h_b}{3} \right) = 1.46667 * 10^{14}$$

Making use of the above equations the code can take into account the displacement and the rotation of the edge beam for the determination of the ultimate load and the compressive membrane action.

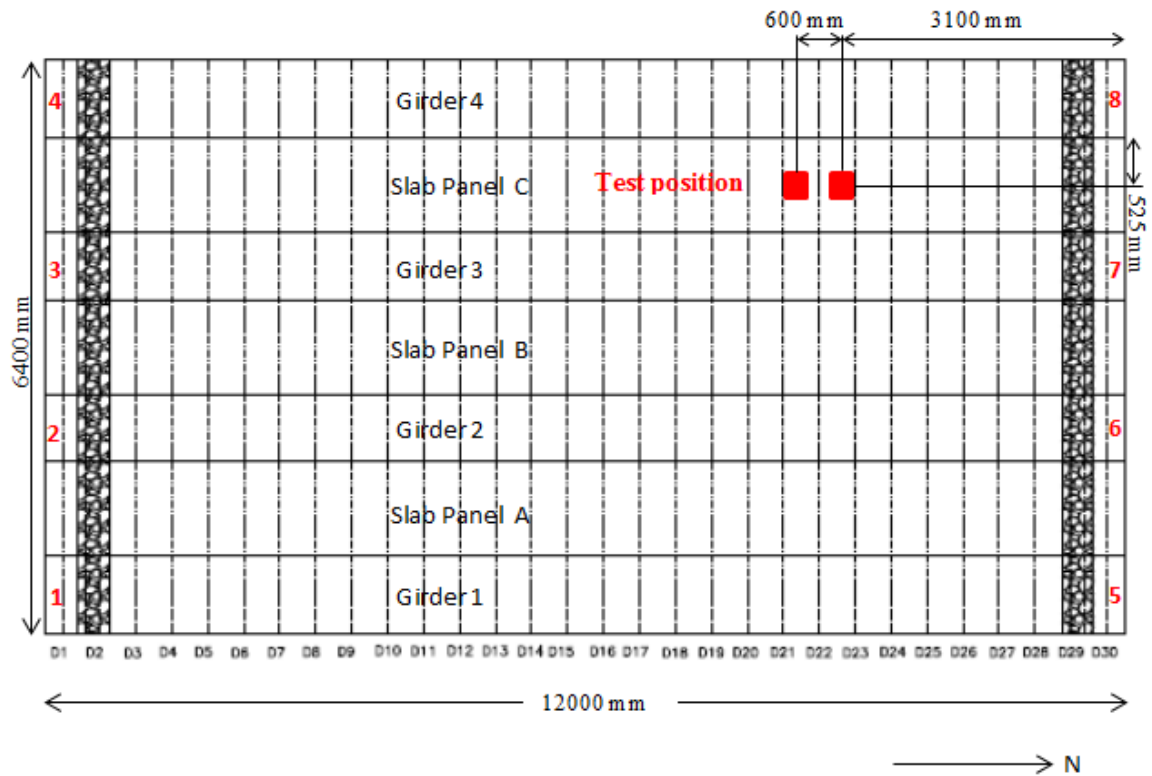


Figure 39 Exterior bay line loaded

At this stage all the required input data have defined to the code and given below:

Table 11: Values of input parameters

INPUT FILE							
S	1050	100	12000				
L	70	30	70	30	70	30	
A	56	66	56	6600			
B	1725	1725	1725	0	0	0	4500
	81.6	40650	0.7276	0.766			
D	200000	9000	500	700			
A	0.0025	0.006	0.045				
T	818.18	1100	205000				
A	0.025	118	10				
	0	0					
	Case						
S	Case 1: Interior slab loaded						
U	S						
P	Case 2: Exterior slab loaded						
P	S						

O	1200	1	300	$2.63262 \cdot 10^{15}$	
R	1200	300	12000	$2.63262 \cdot 10^{15}$	$1.46667 \cdot 10^{14}$
T	5				
DATA					

8. RESULTS

At this section the results of numerical analysis are plotted giving an insight into the overall performance of the structure. Moreover, the sensitivity of parameters is investigated and plotted in order to estimate the effect and the contribution of each parameter, such as the position of load, the restraint ratio, the slenderness and the TPL.

8.1. CASE 1: Internal slab

8.1.1. Effects of Compressive Membrane Action

Table 12 Analytical results

TPL	1.25	2.5
F_{dtot} [N]	479287.579	484260.85
F_{da} [N]	118159.46	117985
F_{db} [N]	361128.11	366275.65
M_{u1} [Nmm]	0.695E+09	0.701E+09
M_{u2} [Nmm]	0.732E+09	0.738E+09
M_{u3} [Nmm]	0.695E+09	0.701E+09
N_u [N]	0.127E+07	0.130E+07
δ [mm]	12.67	12.33
$c1=c2=c3$ [mm]	31.382	31.786
Δ_{13} [mm]	1.214	1.138

S	863.704	936.918
LE	2.29	2.32

The ultimate capacity will be noticed when the rate of arching is equal and opposite to that of bending capacity. Due to the fact that slab obtains very low regular reinforcement area the total bending capacity is reached later than the maximum value of the arching capacity. The maximum ultimate capacity is reached at 12,58mm while the maximum arching capacity is met at 5,96mm, as can be observed at the figure below.

The arching capacity is 24.65% and the bending action is 75.35% of the ultimate capacity. The contribution of the arching action is important at the overall performance of the slab.

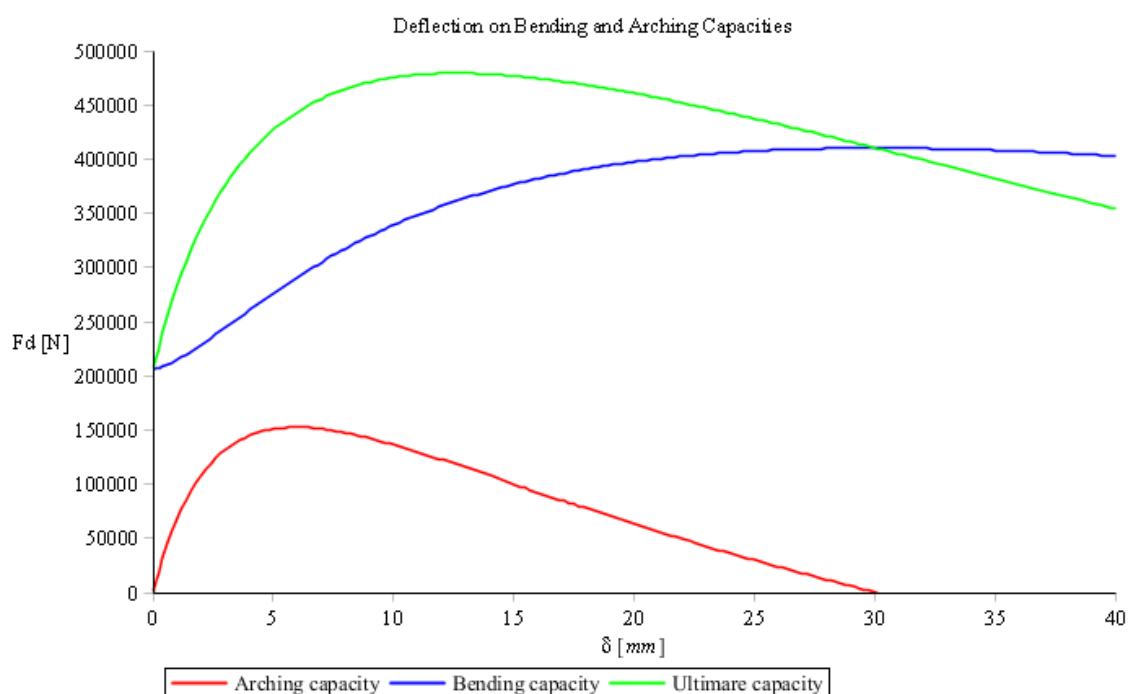


Figure 40 Deflection on Bending and Arching capacity

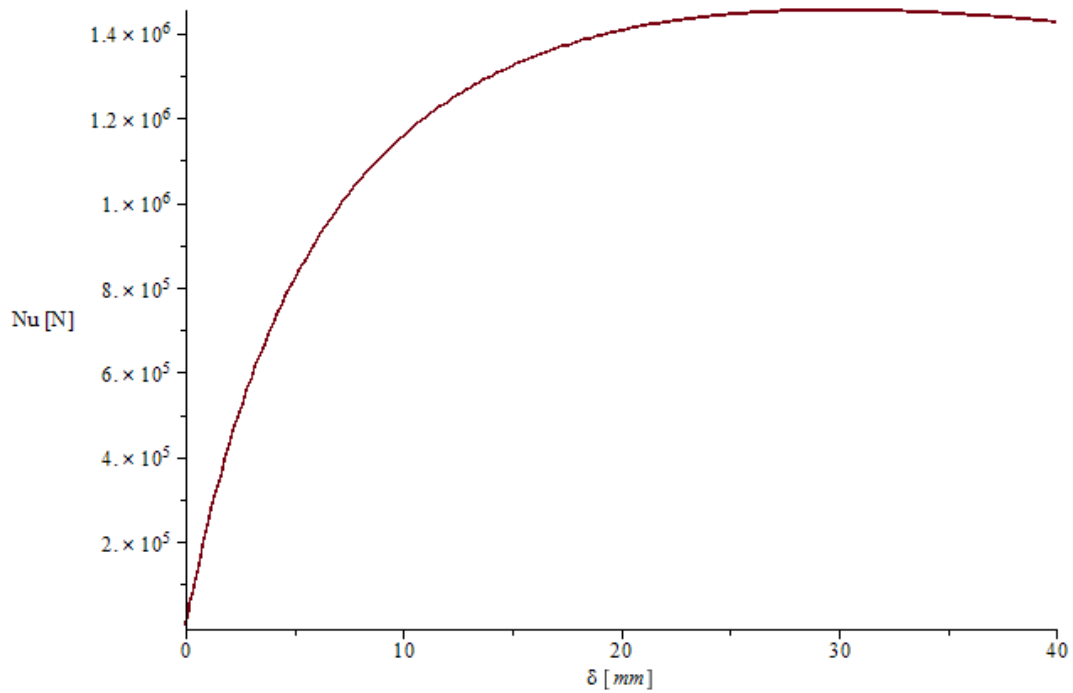


Figure 41 Compressive membrane force N_u - δ

The lateral elongation follows the profile of compressive forces.

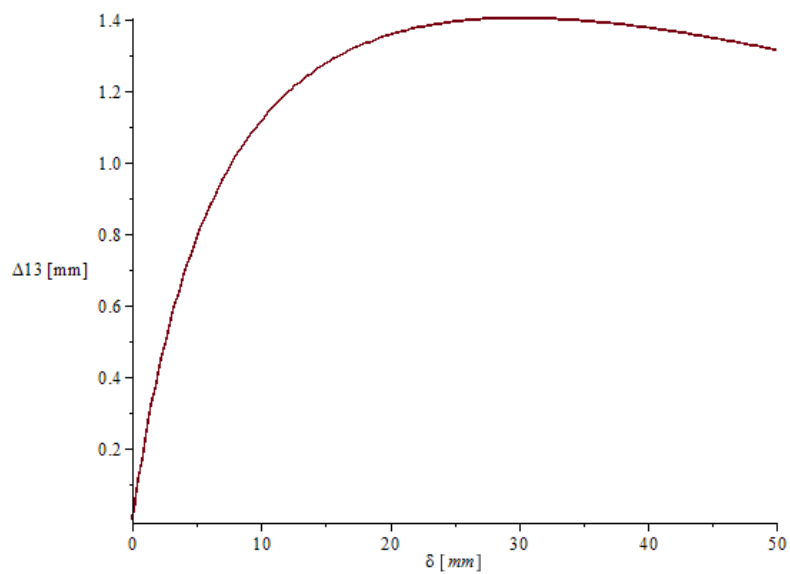


Figure 42 Lateral displacement Δ_{13} - δ

Transverse prestress level: 2.5MPa

The maximum ultimate capacity is reached at 12,23mm taking the value 484.26kN. The contribution of the arching action is important at the overall performance of the slab.

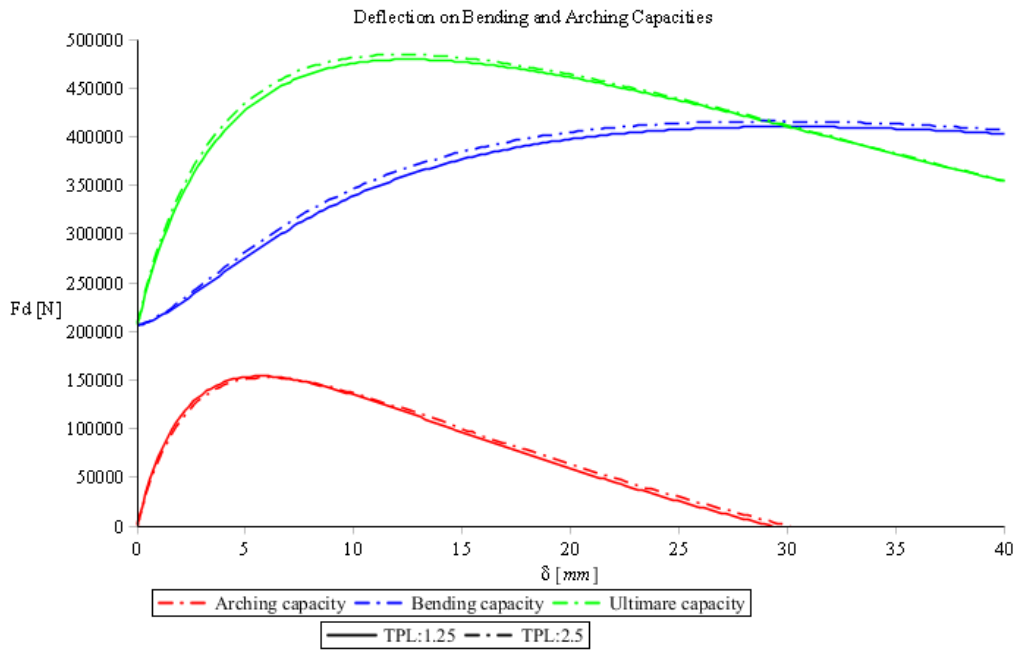


Figure 43 Comparison: Effect of TPL and Deflection on Bending and Arching Capacities

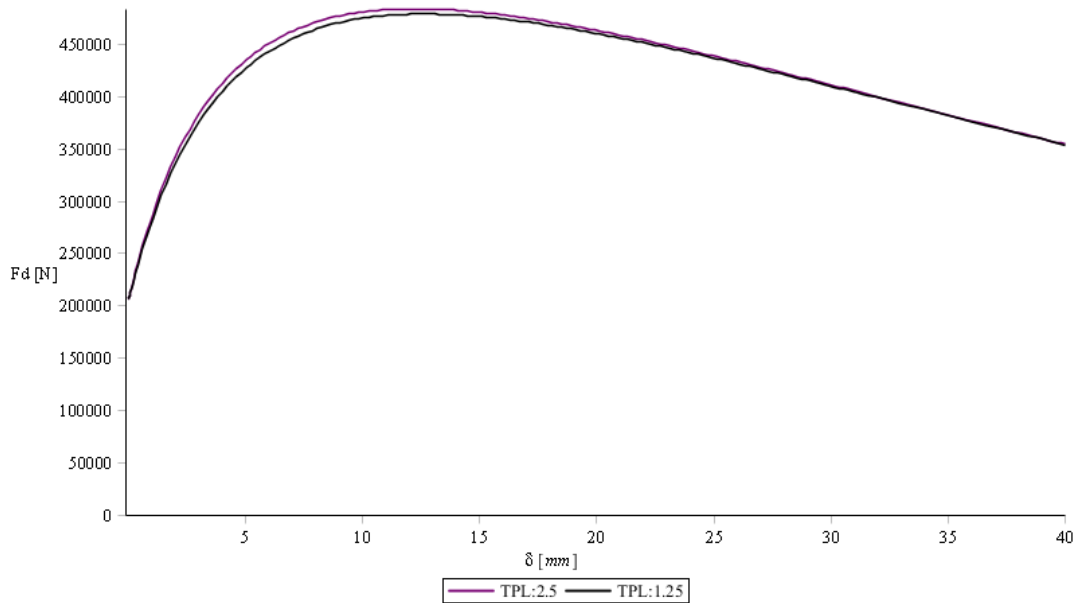


Figure 44 Comparison: Effect of TPL and Deflection on Ultimate capacity

With respect to prestress level, according to the analytical results, it can be concluded that the prestress level slightly affects the ultimate bending capacity of the slab. The additional capacity is attributed to the increase in compressive membrane force about 1.75%.

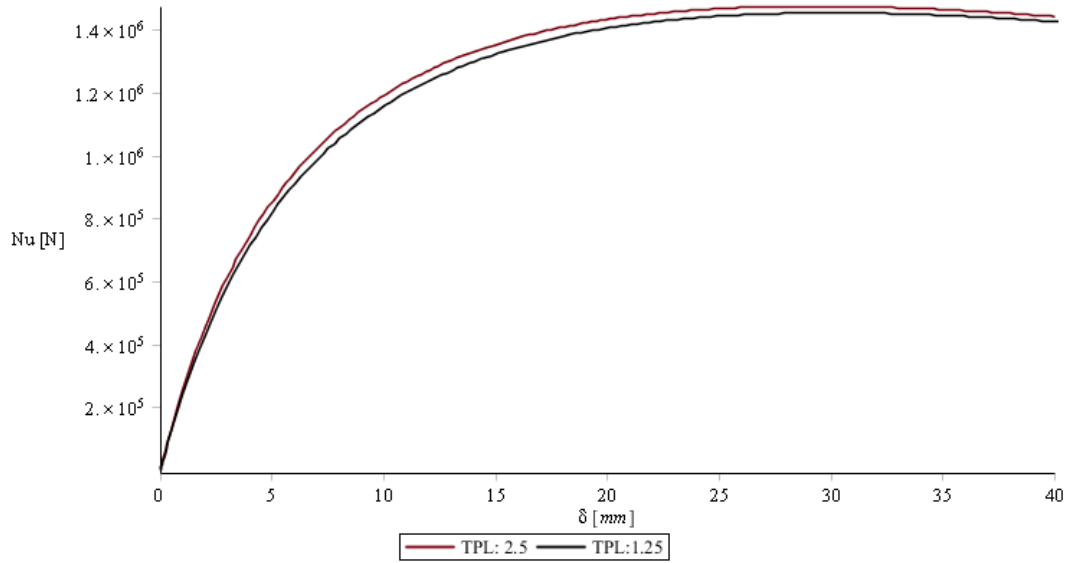


Figure 45 Comparison between compressive membrane force $Nu-\delta$ for different TPL

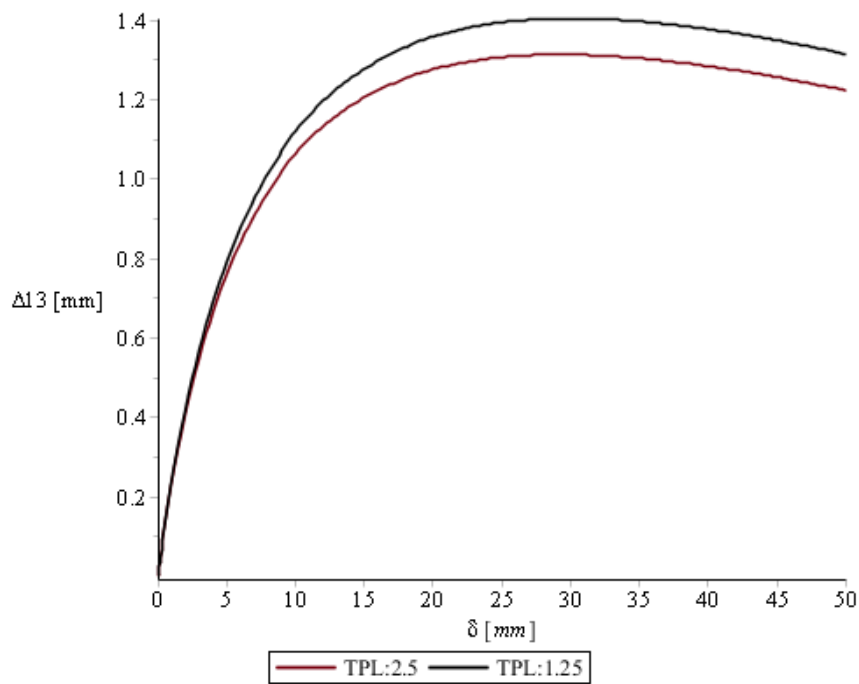


Figure 46 Comparison: Lateral displacement $\Delta l_3-\delta$ for different TPL

8.1.2. Effect of Lateral Restraint on the Ultimate capacity

Transverse prestress level: 1.25MPa

Effect of Lateral Support Stiffness on the Ultimate Capacities for the range $0 < S/S_s < 40$

The figure below illustrates the effect of lateral restraint over the ultimate capacity. At zero restraint the load is carried only by the bending action since no arching action can be developed. The abrupt increase in the ultimate capacity at small ratio of restraint is attributed mainly to arching action, which is quite intensive at the partially restrained conditions especially for values between 0.2 and 0.6. For values of ratio higher than 4 an increase in the restraint does not have any influence on the capacity. This implies that extremely stiff support is not necessary for increasing the ultimate capacity. Neither are bending action nor arching action affected by an infinitive stiff support.

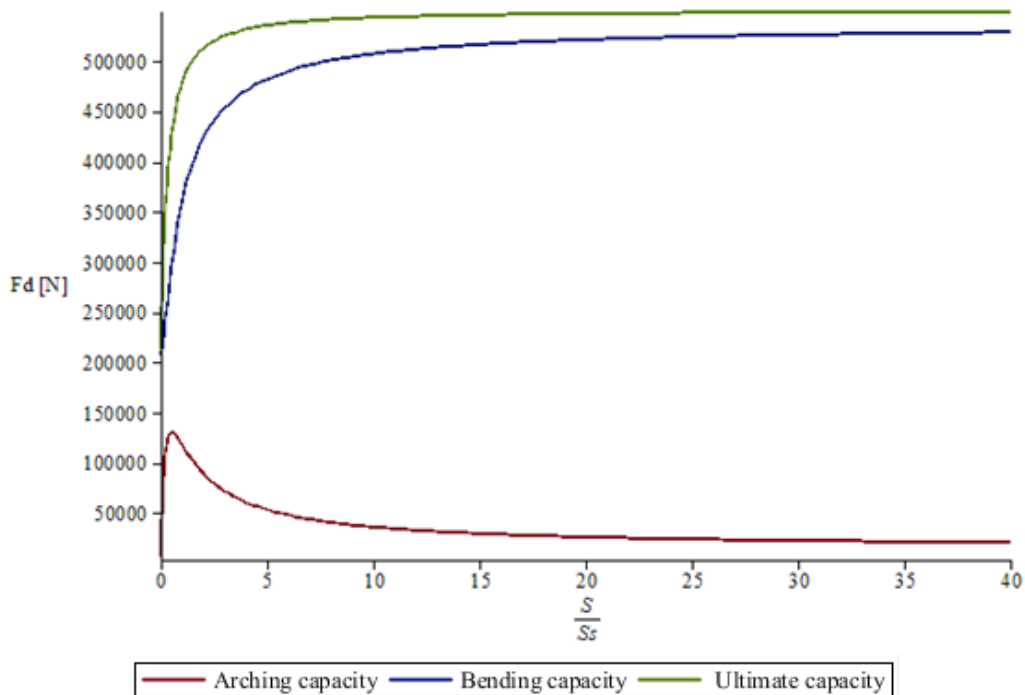


Figure 47 Ultimate capacity-Restraint ratio

Effect of Lateral Support Stiffness on the Ultimate Capacities for the range $0 < \frac{S}{S_s} < 4$

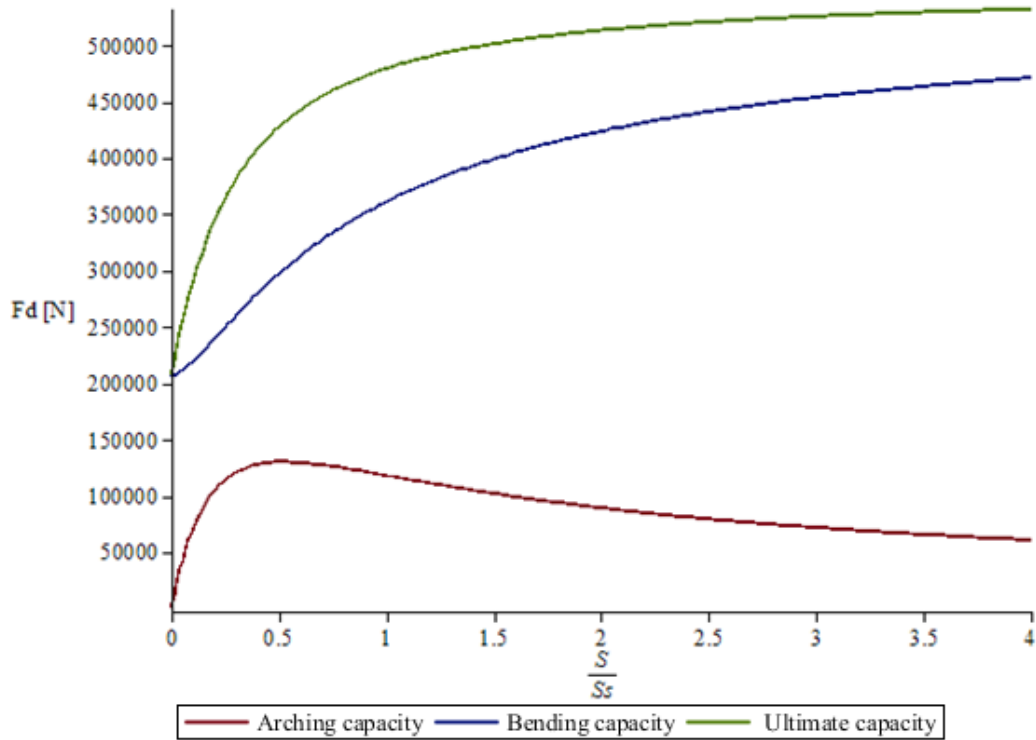


Figure 48 Ultimate capacity-Restraint ratio (in detail)

The intensive contribution of the compressive action at small values of restrained can also be illustrated by taken the ratio ultimate capacity over the bending capacity (LE). This ratio is indicative for the enhancement in the ultimate resistance solely due to arching action. thus, at small values the LE load factor reaches values more than the double ultimate capacity. That means that the **optimum restrained ratio is slightly higher than or equal to 1**, when the full stiffness is provided for lateral restraint.

Where, $LE = \text{Ultimate capacity} / \text{Bending capacity}$

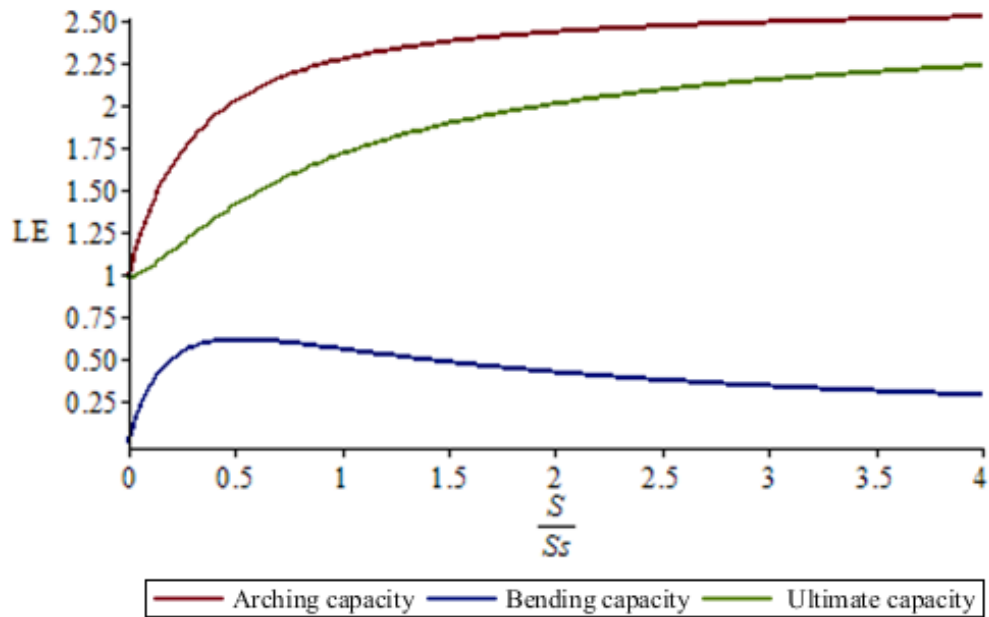


Figure 49 Enhancement factor-Restrained ratio

Furthermore, the following figure shows the ultimate capacity over the vertical displacement δ for various lateral restraint ratio S/S_s . At the case that no restraint is provided the capacity slightly changes while the vertical deflection at the midspan increases. Thus, the slab will fail due to large displacements. It is worth mentioning that as the restrained conditions increase, the slab fails at smaller deflections, which leads to the conclusion that the slab becomes **less ductile**. For values of stiffness less than the axial stiffness of the slab and the girders the slab fails at greater deflections than $L/82$ (12.85mm). According to Eurocode, at the permissible serviceability the upper limit l/h for prestressed slabs is $L/50$.

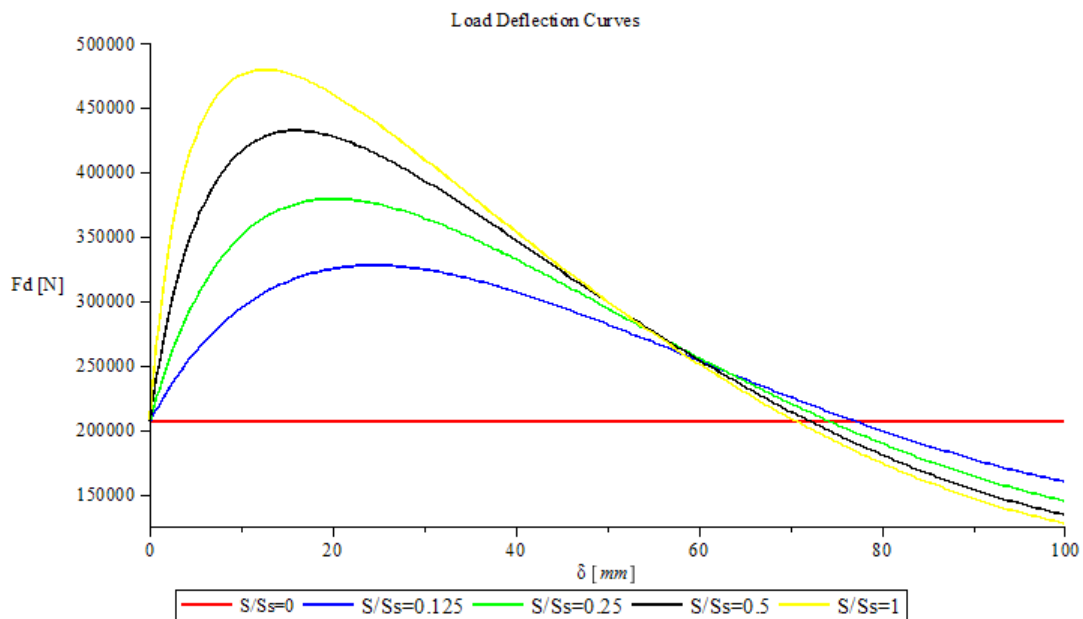


Figure 50 Load Deflections curves for varying S/S_s

The profile of the ultimate capacity is also repeated at the enhancement factor, which reaches the highest value at the stiffness ratio equal to 1. At this section at which the interior support is explained, the stiffness ratio has been considered to be equal to 1, corresponding to the yellow load deflection curve. At the aforesaid curve the load enhancement factor becomes double leading to the conclusion that at the present case the contribution of compressive membrane action at this stiffness ratio results in a double ultimate capacity.

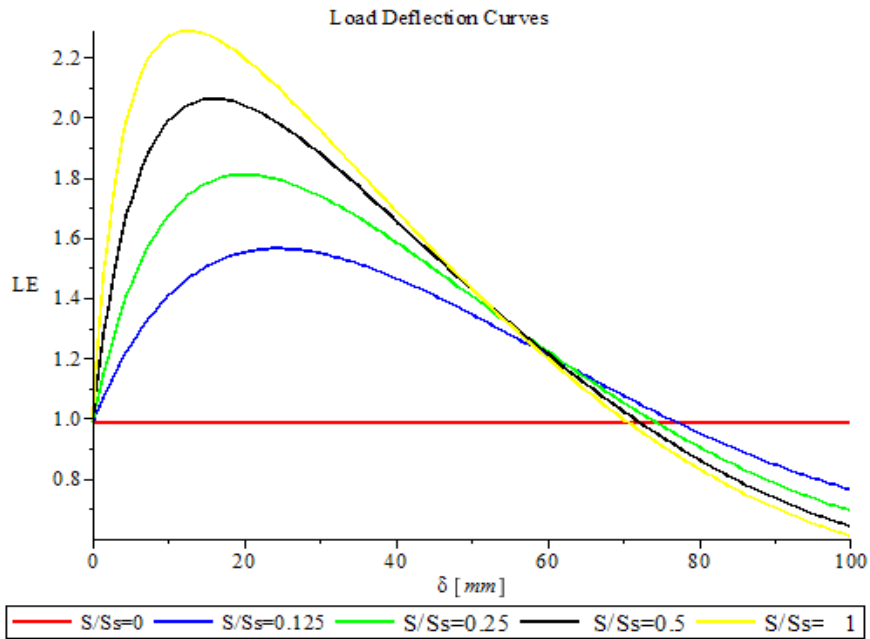


Figure 51 Enhancement load factor for varying S/S_s

Transverse prestress level: 2.5MPa

Effect of Lateral Support Stiffness on the Ultimate Capacities ($0 < S/S_s < 40$)

As can be also seen by the Table 16, the transverse prestress level hardly affects the ultimate capacity due to the fact that the prestress level is introduced as an initial imposed deformation and an increase in the effective stiffness of the prestressing steel. Both parameters do not have governing influence on the bending resistance. Therefore, there are slightly differences ranging at 1.03% between the results of the two prestress levels.

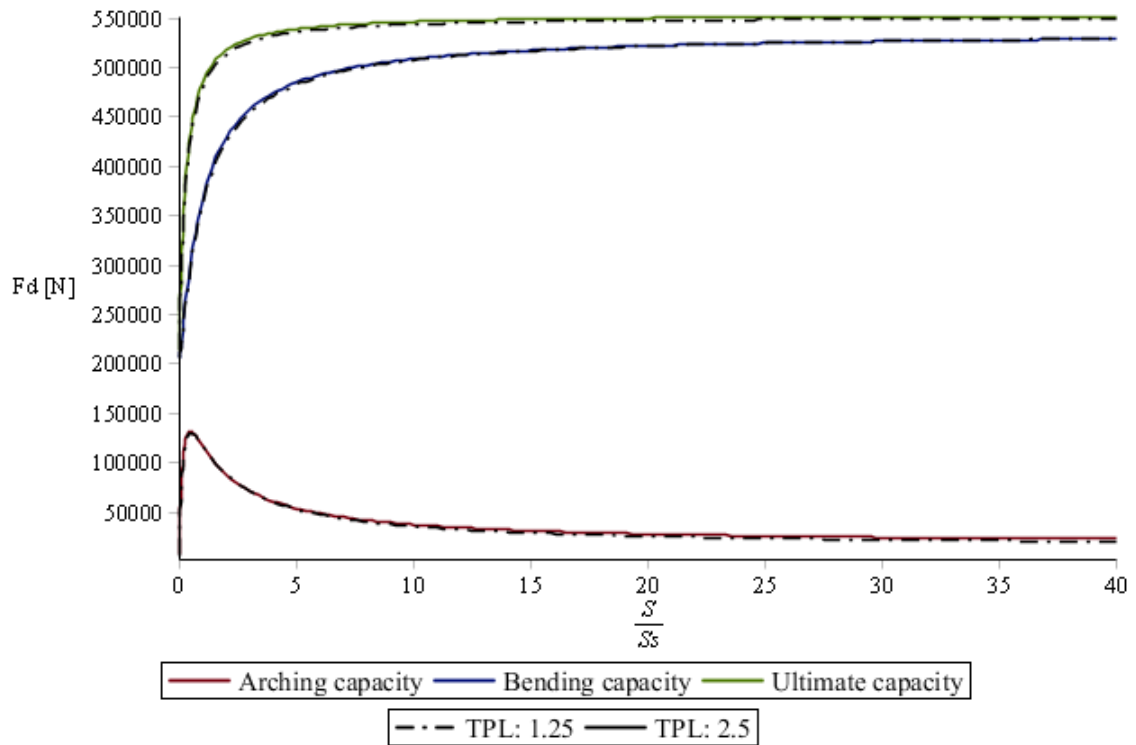


Figure 52 Comparison: Ultimate capacity-Restraint ratio for different TPL

Effect of Lateral Support Stiffness on the Ultimate Capacities ($0 < S/S_s < 4$)

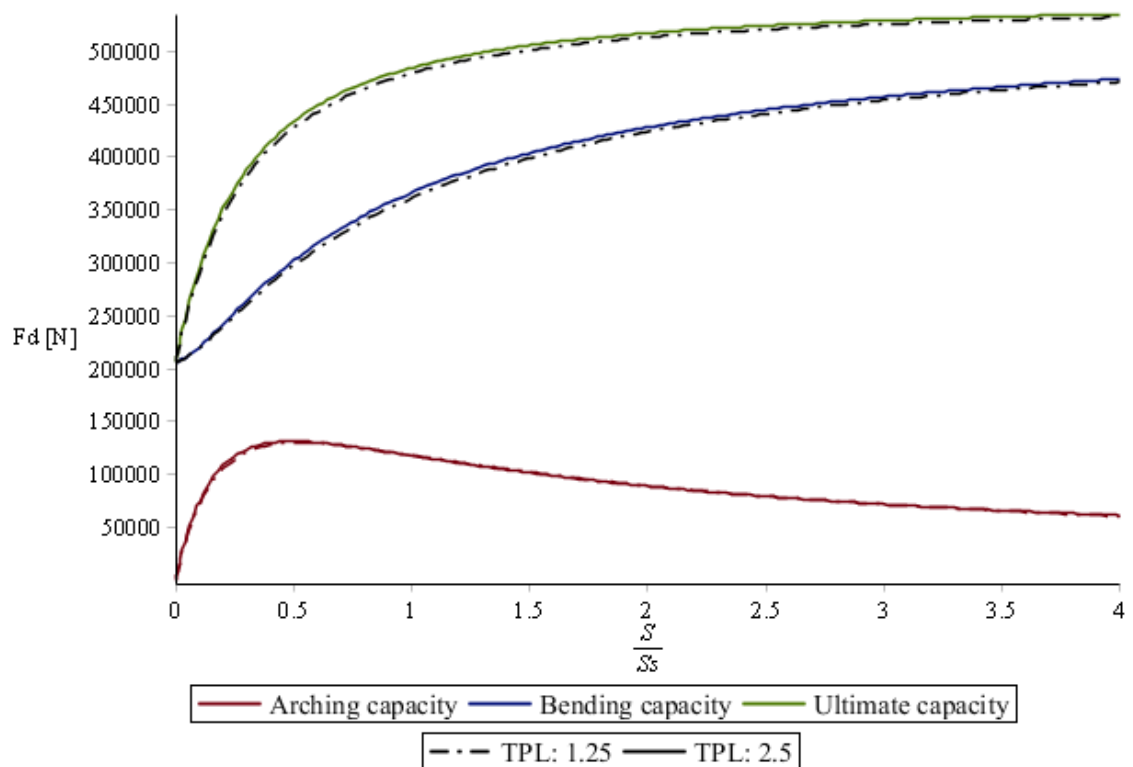


Figure 53 Comparison: Ultimate capacity-Restraint ratio for different TPL (in detail)

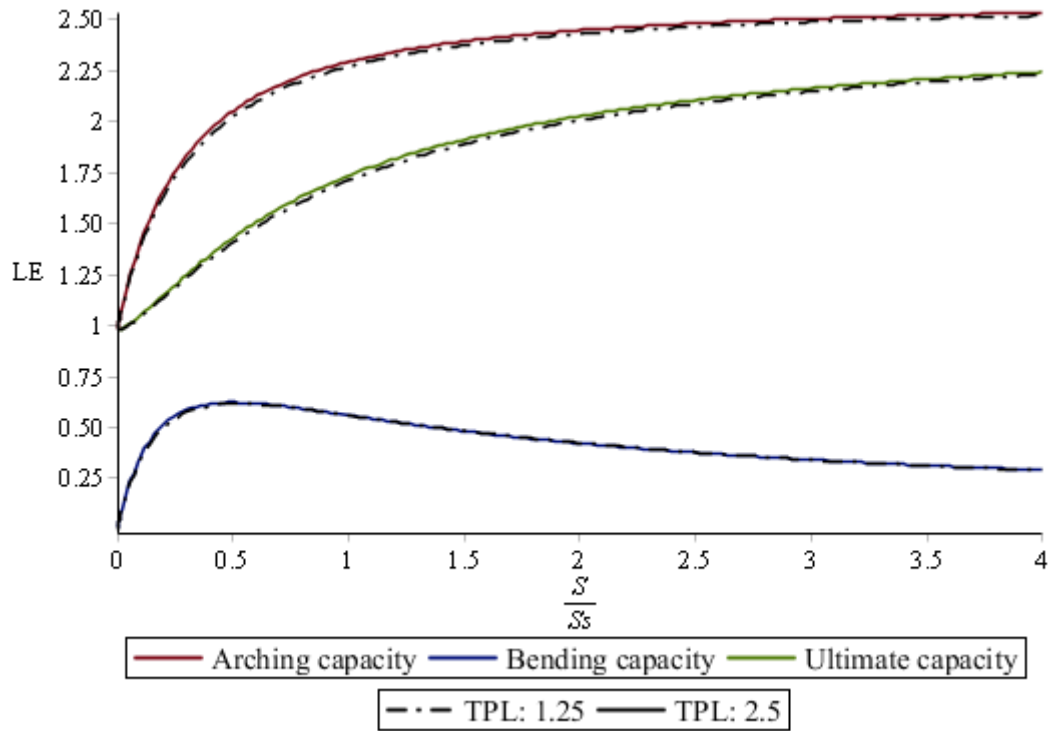


Figure 54 Comparison: Enhancement load factor for varying S/S_s for different TPL

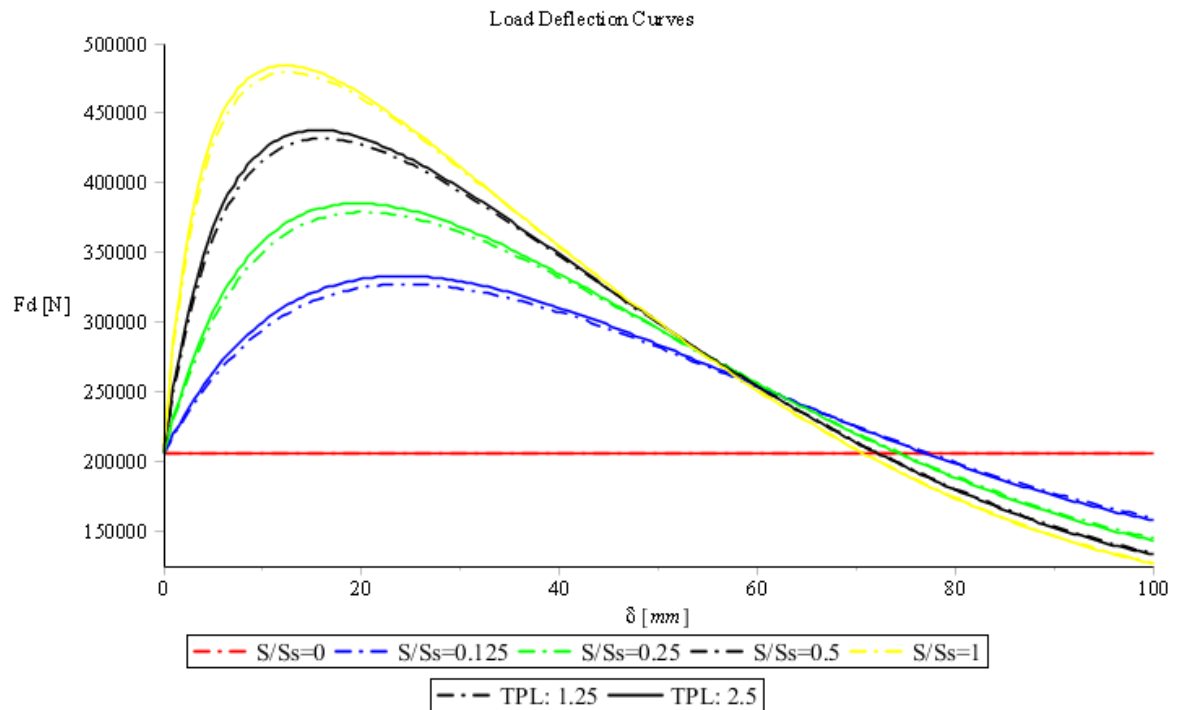


Figure 55 Comparison: Ultimate capacity for varying S/S_s for different TPL

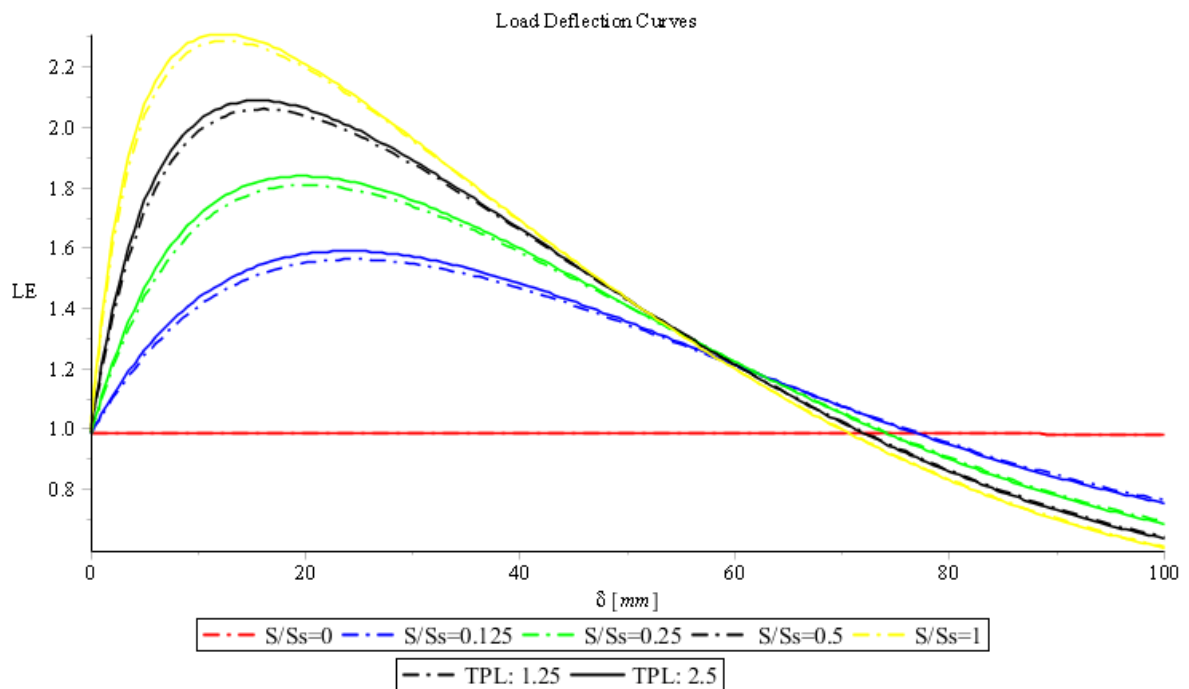


Figure 56 Comparison: Enhancement load factor for varying S/S_s

8.1.3. Capacity Enhancement Factor: Slenderness - Stiffness effect

Another important parameter which governs the performance of the slab is the slenderness l/h . At the present case this ratio is $l/h=1050/100=10.5$ while the stiffness ratio S/S_s is equal to 1. This combination results in double ultimate capacity. As expected, for small values of slenderness the arching action is more intensive due to higher compression zone. The overall performance of the slab is expressed by the blue curve, as illustrated below. On the other hand, high values of slenderness lead to a slender behaviour which weakens the compressive action. Specifically, for depth to height ratio l/h more than 15 there is no enhancement since the slab starts performing in a slender way minimizing the effect of compressive membrane action.

To estimate better the influence of slenderness and stiffness over the capacity of the slab it is wise to separate the arching and bending case. Thus, the change in the ultimate capacity will be attributed to the change in the bending or in the arching action. generally, the bending contribution determines the final value of the ultimate capacity. At Fig.61 the curves of bending action reaches the peak points at $S/S_s=1$ later than the curves of arching action $S/S_s=0.6$, Fig. 60.

As has been mentioned at previous sections, the effect of prestress hardly changes the results and the effect of the other parameters.

- I. Transverse prestress level: 1.25MPa

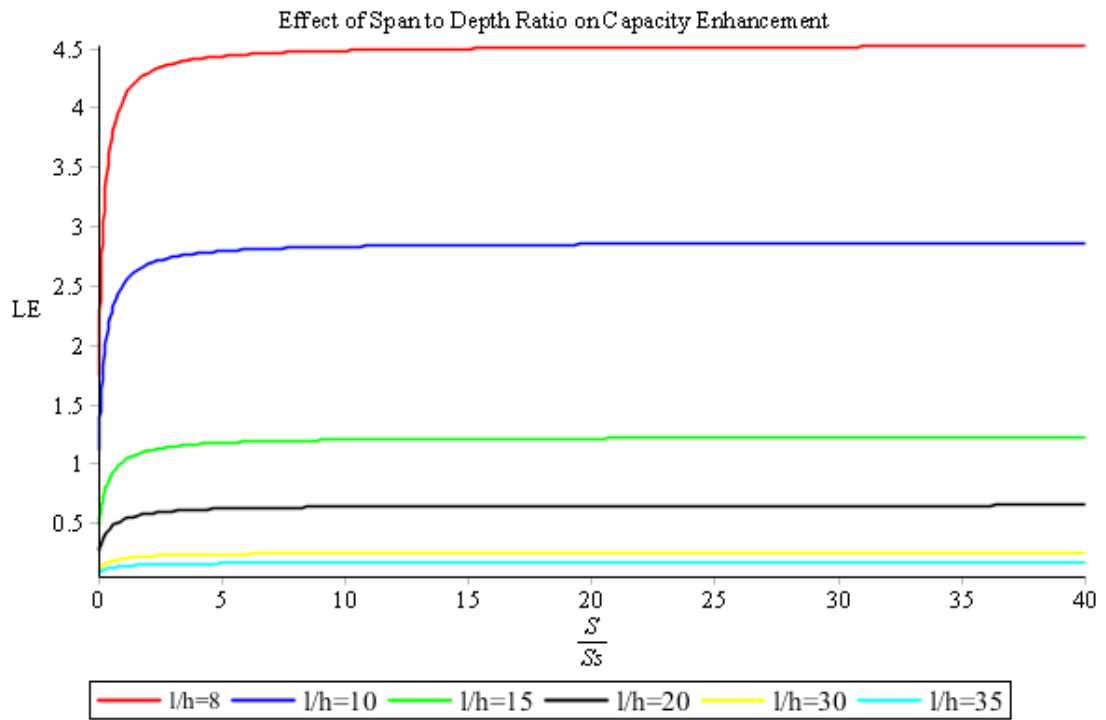


Figure 57 Enhancement load factor for varying S/S_s and varying slenderness

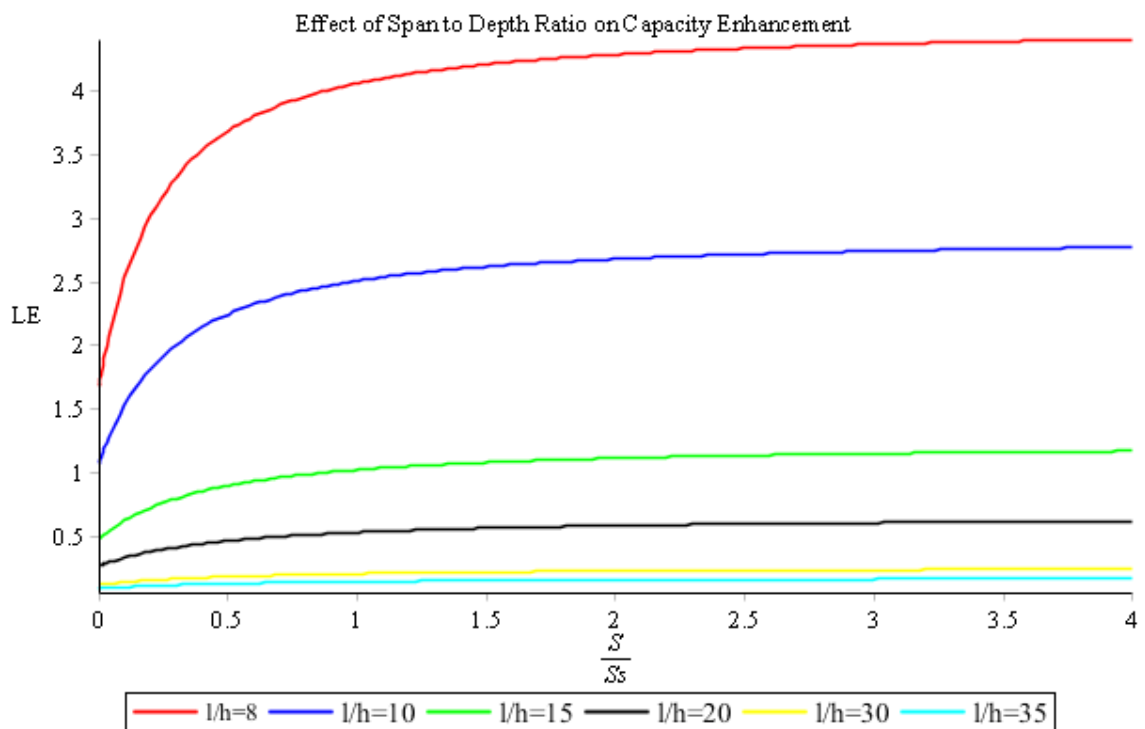


Figure 58 Enhancement load factor for varying S/S_s and varying slenderness (in detail)

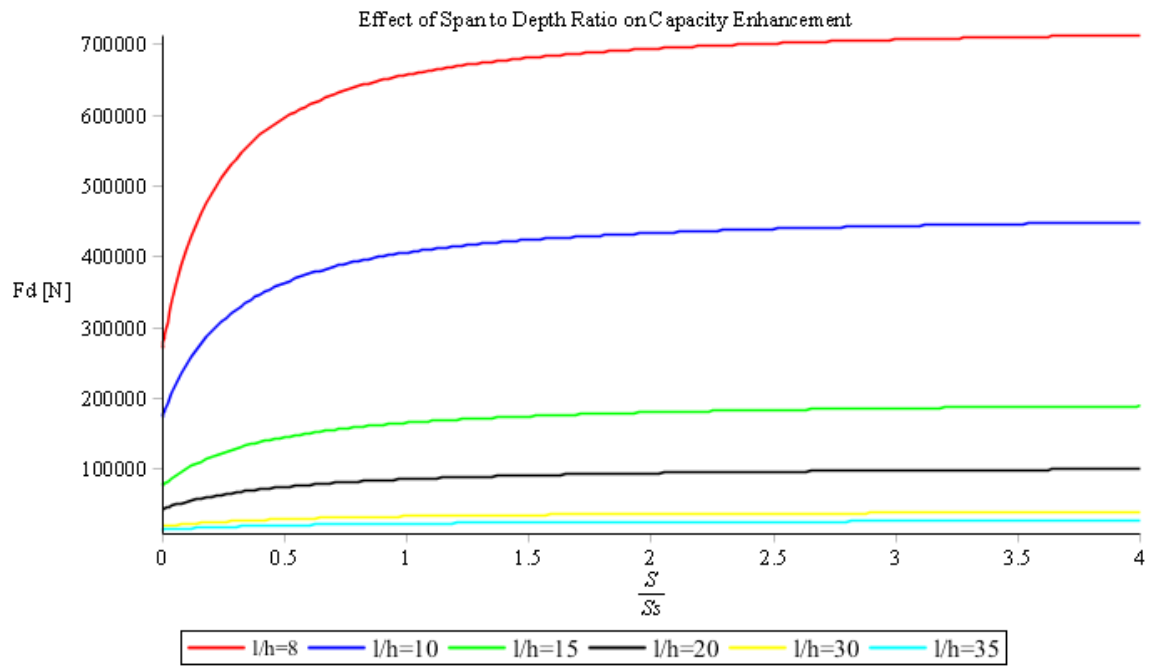


Figure 59 Ultimate capacity for varying S/S_s and varying slenderness

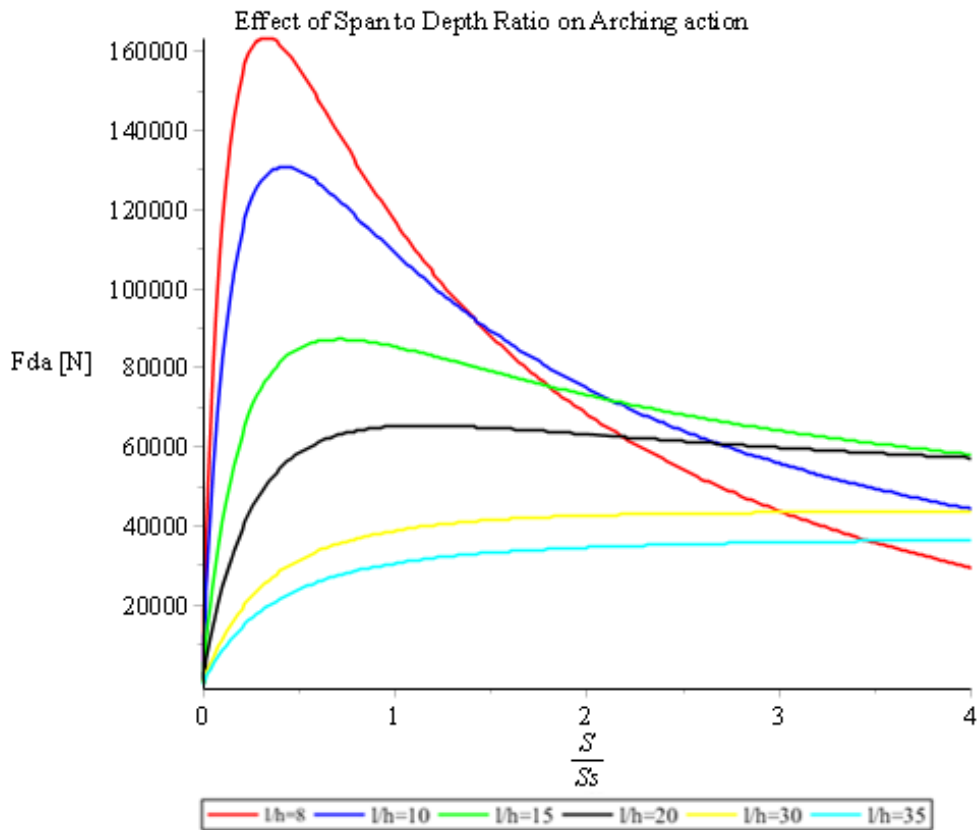


Figure 60 Arching capacity for varying S/S_s and varying slenderness l/h

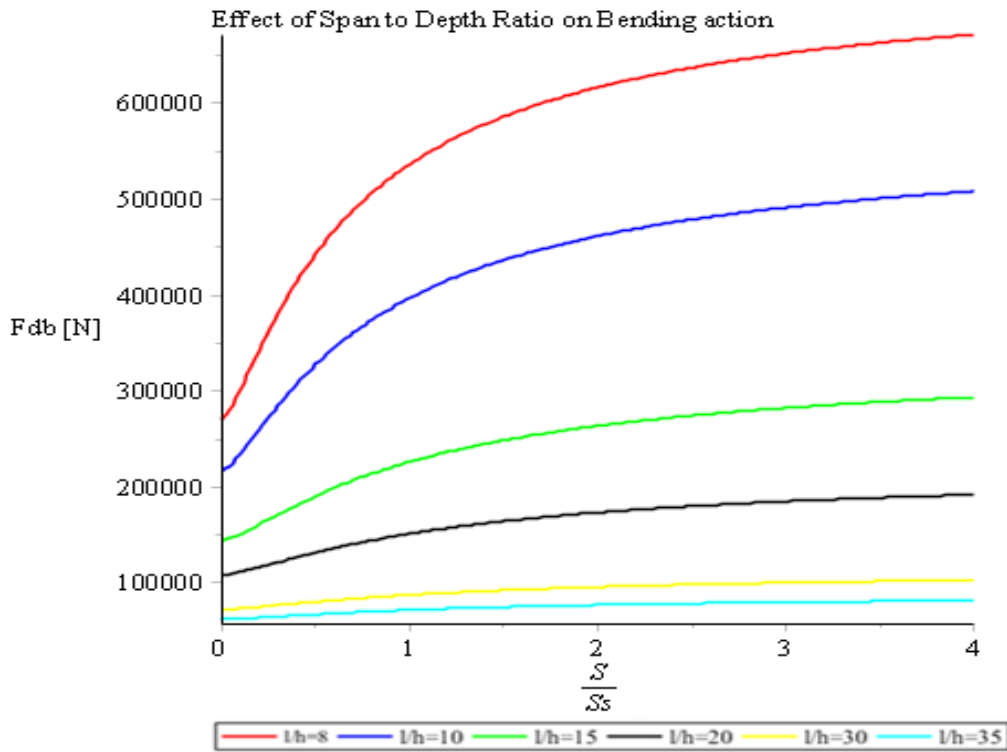


Figure 61 Bending capacity for varying S/S_s and varying slenderness l/h

II. Transverse prestress level: 2.5MPa

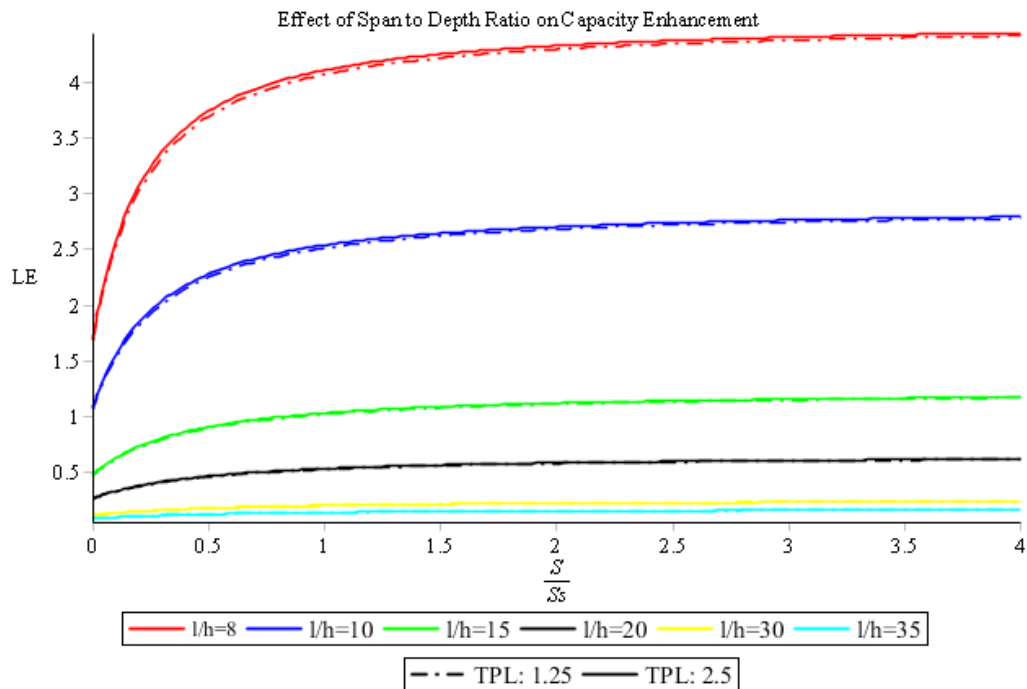


Figure 62 Comparison: Enhancement load factor for varying S/S_s and varying slenderness l/h

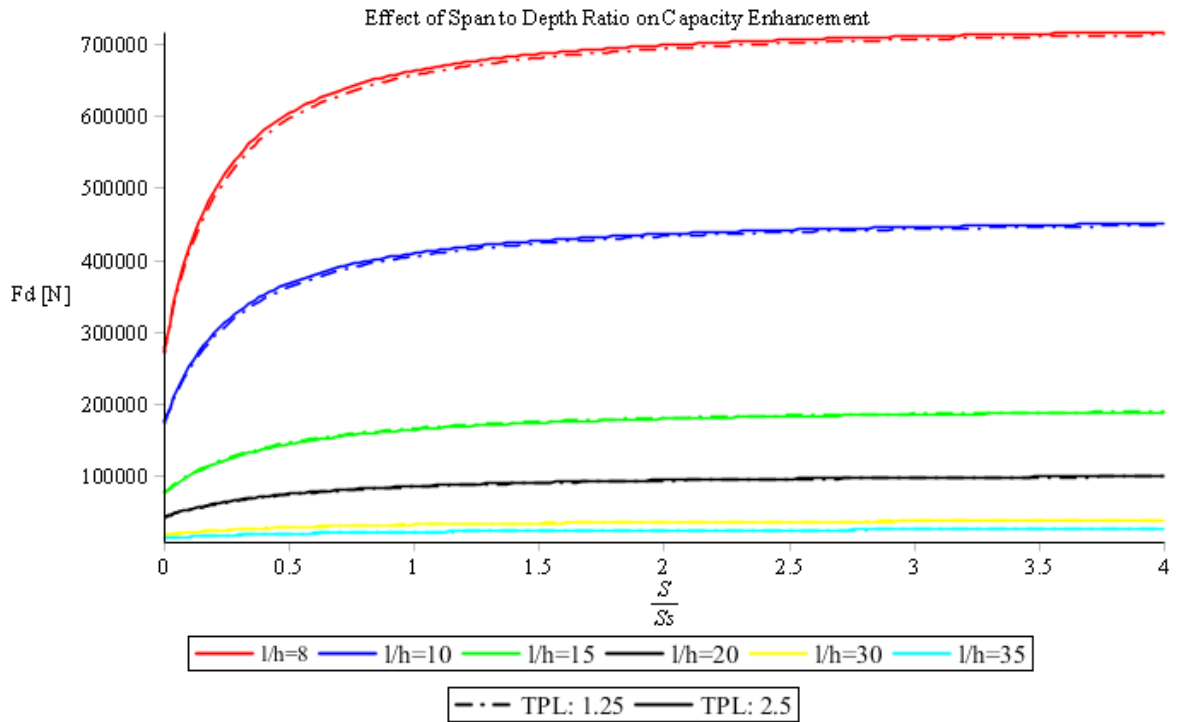


Figure 63 Comparison: Ultimate capacity for varying S/S_s and varying slenderness (in detail)

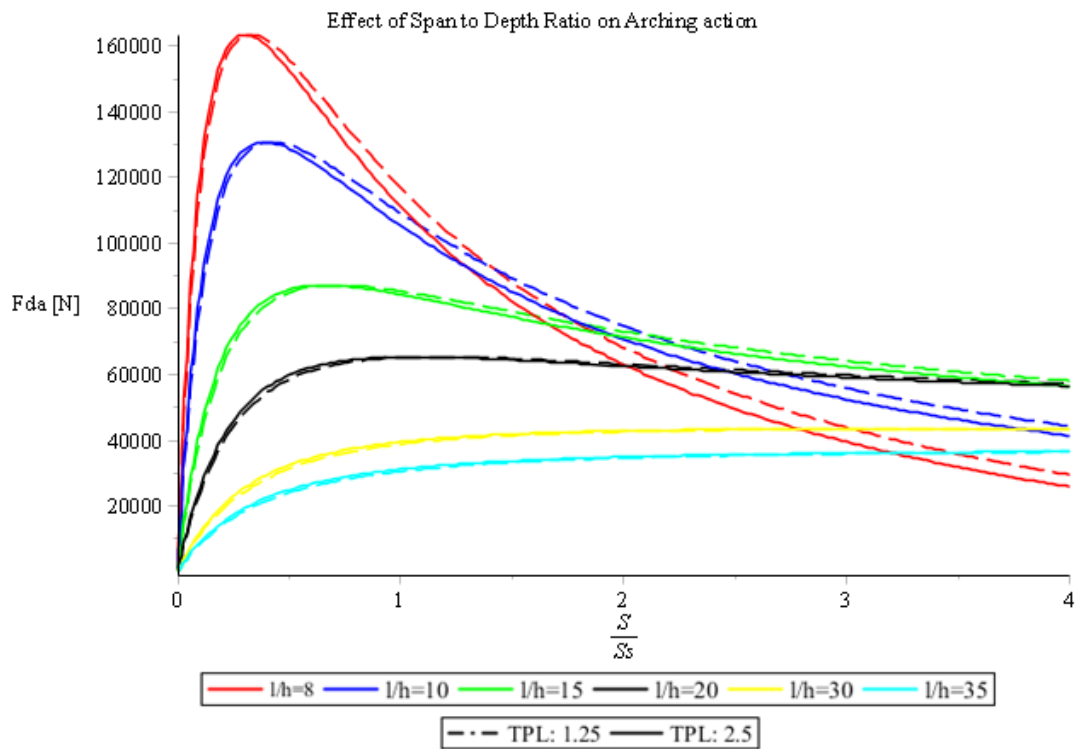


Figure 64 Comparison: Arching capacity for varying S/S_s , varying slenderness l/h and different TPL

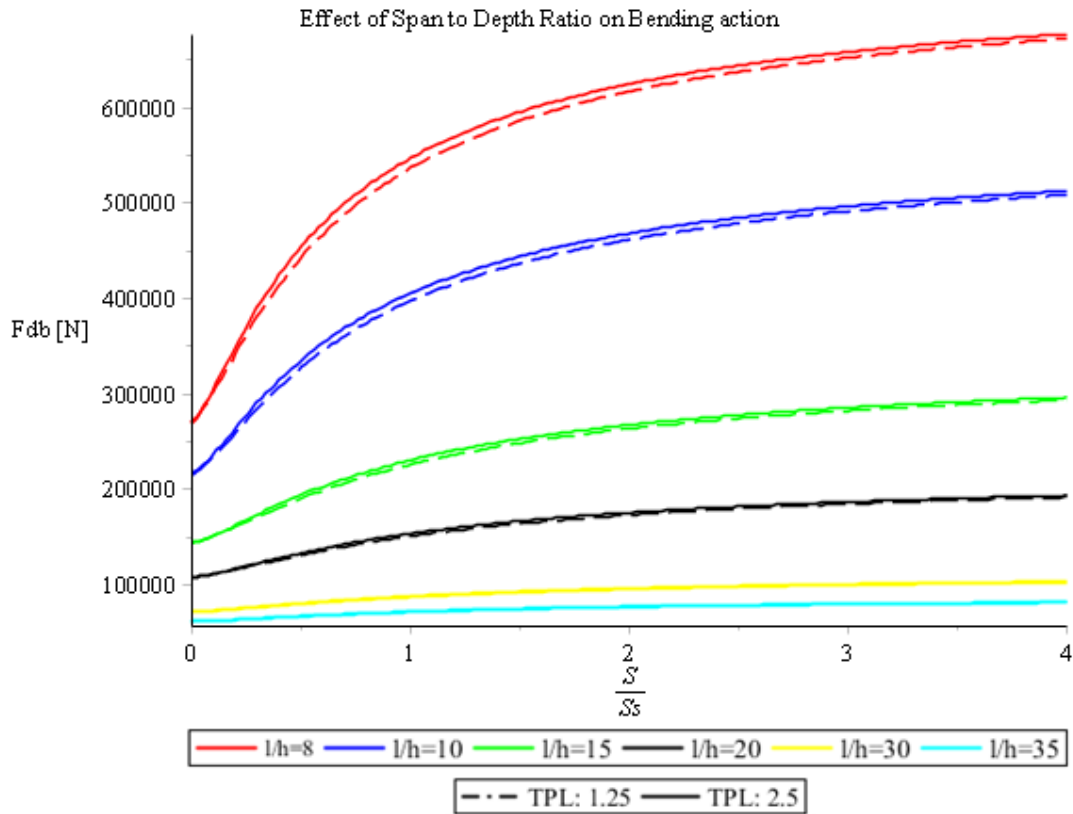


Figure 65 Bending capacity for varying S/S_s and varying slenderness l/h
8.2. Case 2: Exterior slab

Table 13 Results

EXTERIOR SLAB LOADED - 5 SLAB STRIPS USED			
Strip number [NUM]	Effective support stiffness [S]	Ultimate capacity [WU]	Load enhancement [LE]
1	622.29	0.7118	2.14
2	172.4	0.5796	1.74
3	75.9	0.4929	1.48
4	41.3	0.4437	1.33
5	29.6	0.4232	1.27

AVERAGE ULTIMATE CAPACITY IS 0.53

AVERAGE LOAD ENHANCEMENT IS 1.59

8.2.1. Effects of Compressive Membrane Action

The most advisable way to investigate the effect of compressive membrane action is to isolate the bending action and arching action. This can be achieved by calculated the ultimate capacity separately, by inserting different stiffness at the subroutine STRIP.

Load for Compressive membrane action:

$$F_{da} = \frac{2Nu(h-c_1-c_2+\beta(c_1-c_3)-\delta)}{(1-\beta)L}$$

Load for bending action

The moments M_1 , M_2 and M_3 are calculated with the axial internal forces at the level of neutral axis. They are not equal to the moments M_{u1} , M_{u2} and M_{u3} which are calculated with the axial forces at the mid-depth of the slab.

$$F_{db} = \frac{2\left(\frac{M_1}{\beta} + \frac{M_2 \cdot \beta}{1-\beta} + \frac{M_3}{1-\beta}\right)\beta}{L}$$

The moments M_1 , M_2 and M_3 can be found by converting the moments M_{u1} , M_{u2} and M_{u3} at the neutral axis according to the following expressions:

$$M_1 = M_{u1} - \left(\frac{h}{2} - c_1\right)N_u$$

$$M_2 = M_{u2} - \left(\frac{h}{2} - c_2\right)N_u$$

$$M_3 = M_{u3} - \left(\frac{h}{2} - c_3\right)N_u$$

Ultimate load: Load Bending capacity + Load Compressive membrane action

$$F_{dot} = \frac{2Nu(h-c_1-c_2+\beta(c_1-c_3)-\delta)}{(1-\beta)L} + \frac{2\left(\frac{M_1}{\beta} + \frac{M_2 \cdot \beta}{1-\beta} + \frac{M_3}{1-\beta}\right)\beta}{L}$$

According to the extracting results the F_{dot} is maximized at δ equal to 13.33mm. This is verified also numerically by taking the derivative of the above equation with respect to the δ equals to zero and solving it. Then, the displacement is found the same value with the program Fortran. This happens at every step of the increasing displacement.

The contribution of the arching and bending action in the ultimate capacity is plotted below.

Table 14 Results

TPL [MPa]	1.25	2.5
-----------	------	-----

F_{dotot} [N]	457920	4617906
F_{da} [N]	117895	1180629
F_{db} [N]	340024	3437276
M_{u1} [Nmm]	66468806	66932774
M_{u2} [Nmm]	70150624	70614592
M_{u3} [Nmm]	66468806	66932774
M_1 [Nmm]	42787345	43273349
M_2 [Nmm]	46469163	46955167
M_3 [Nmm]	42787345	43273349
N_u [N]	1163824	1180903
δ [mm]	14.1	13.8
$c_1=c_2=c_3$ [mm]	29.6	29.96
$\Delta 13$ [mm]	1.55	1.49
S_s	622.290	658.897

- Transverse prestress level: 1.25MPa

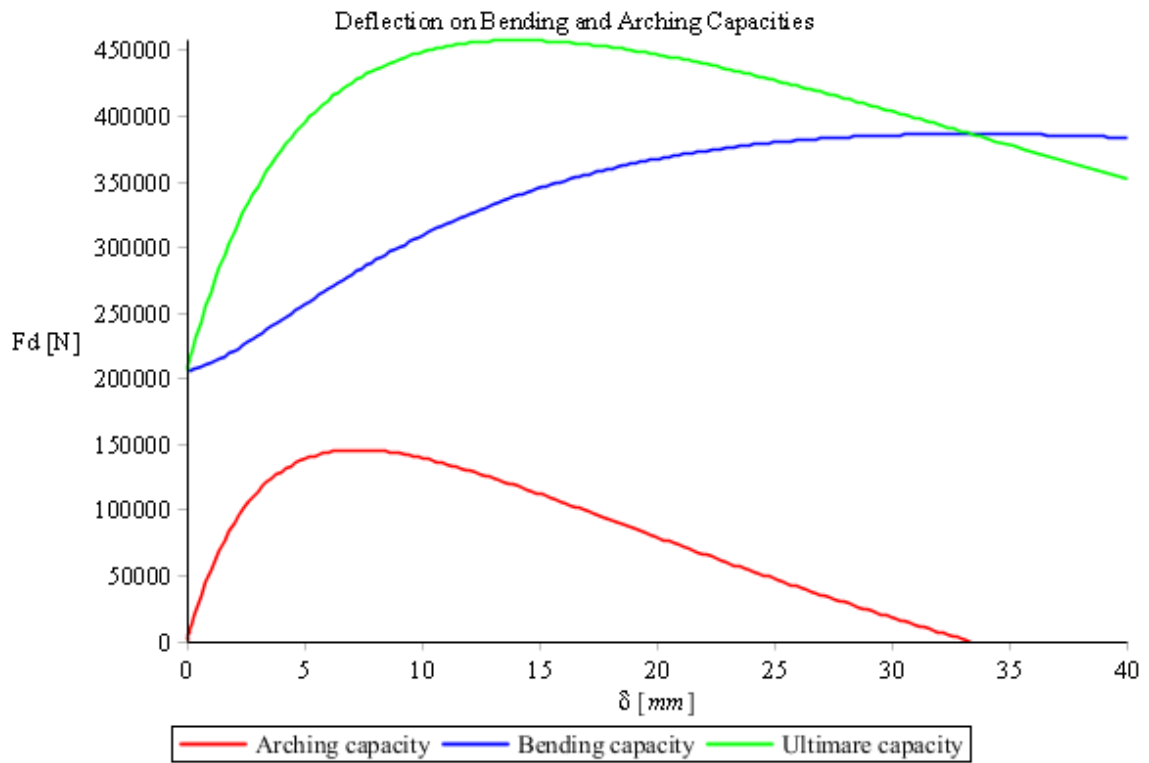


Figure 66 Effect of Deflection on Bending and Arching Capacities

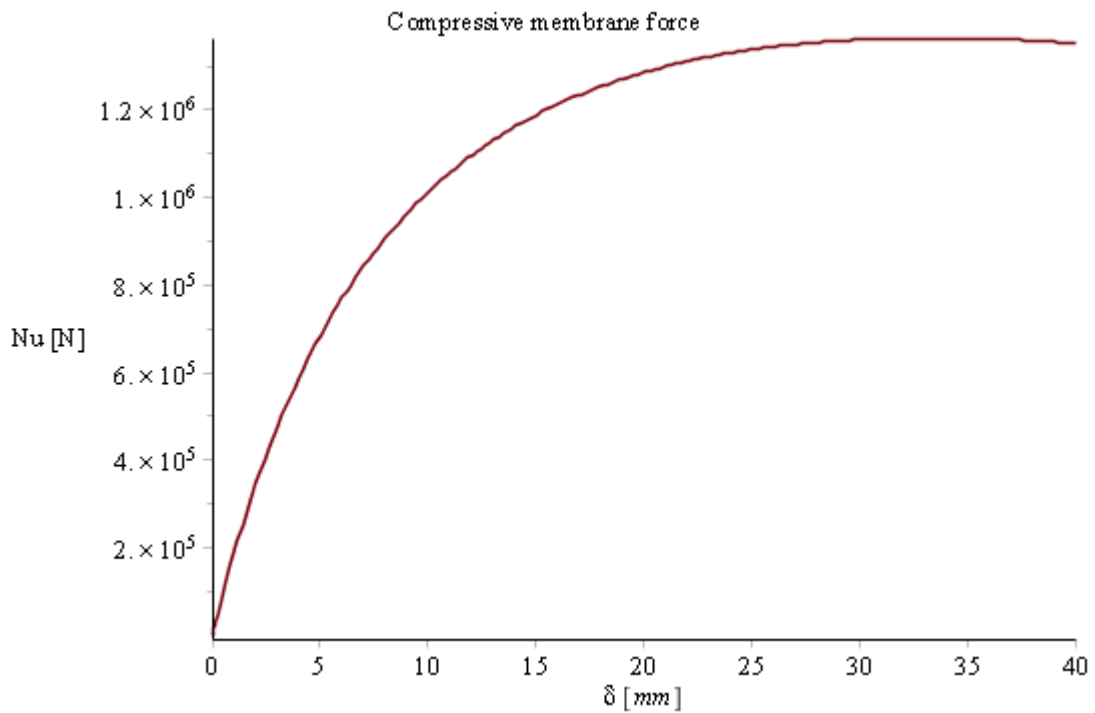


Figure 67 Compressive membrane force N_u - δ

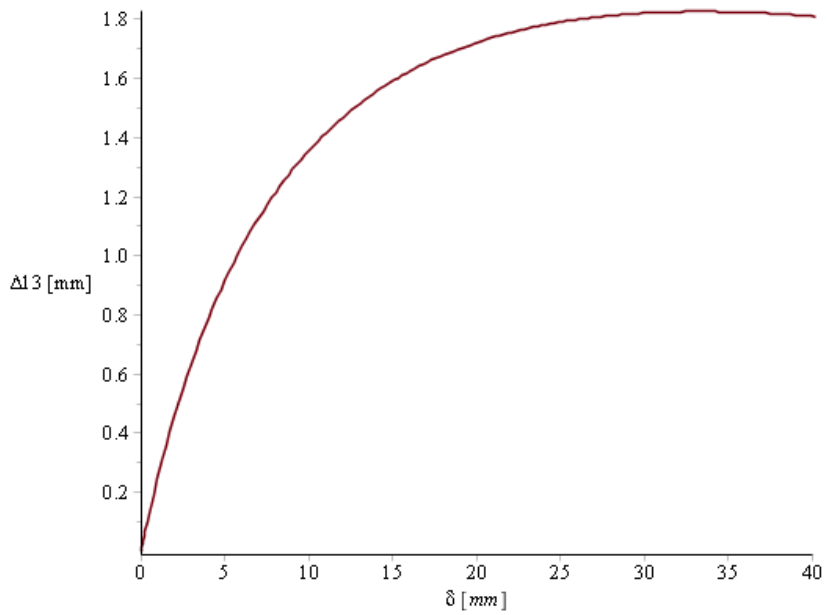


Figure 68 Lateral displacement $\Delta_{13}-\delta$

- Transverse prestress level: 2.5MPa

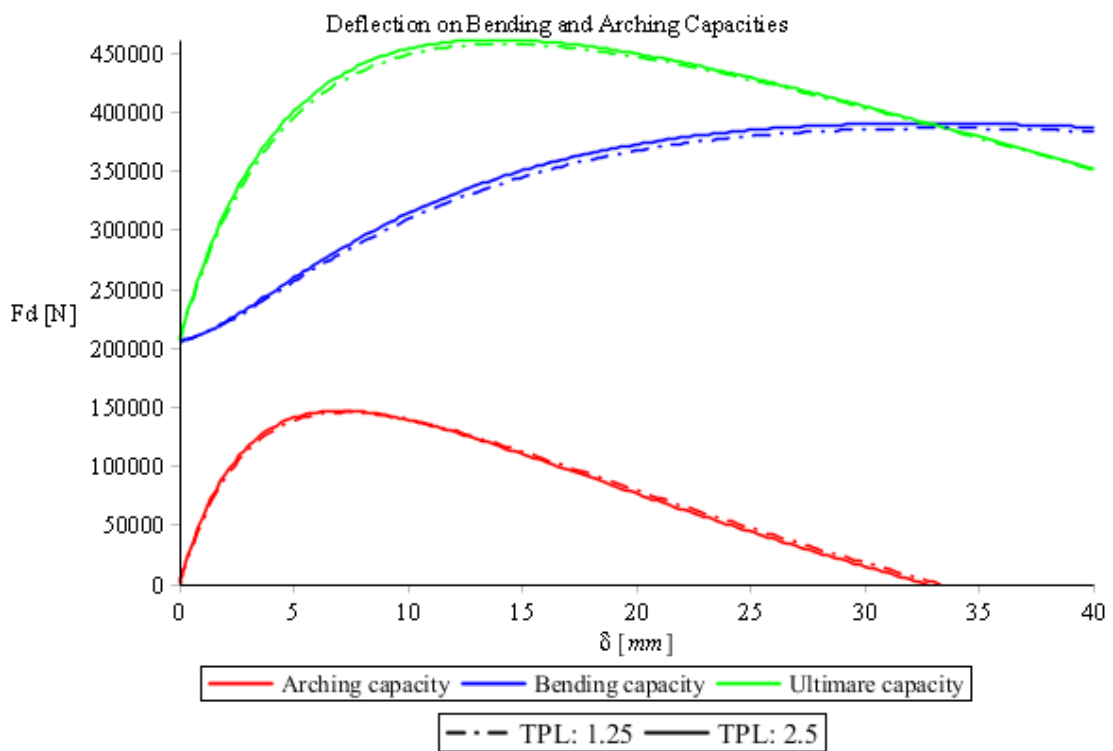


Figure 69 Comparison: Effect of Deflection on Bending and Arching Capacities for different TPL

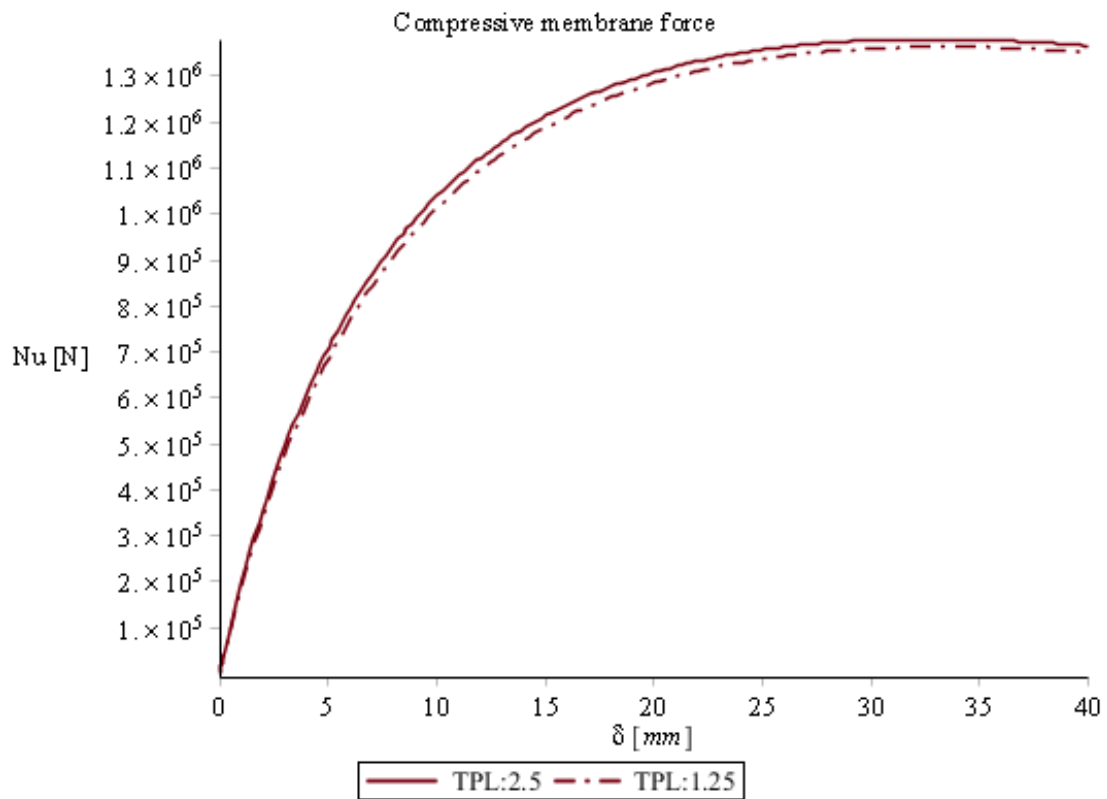


Figure 70 Comparison: Compressive membrane force Nu - δ for different TPL

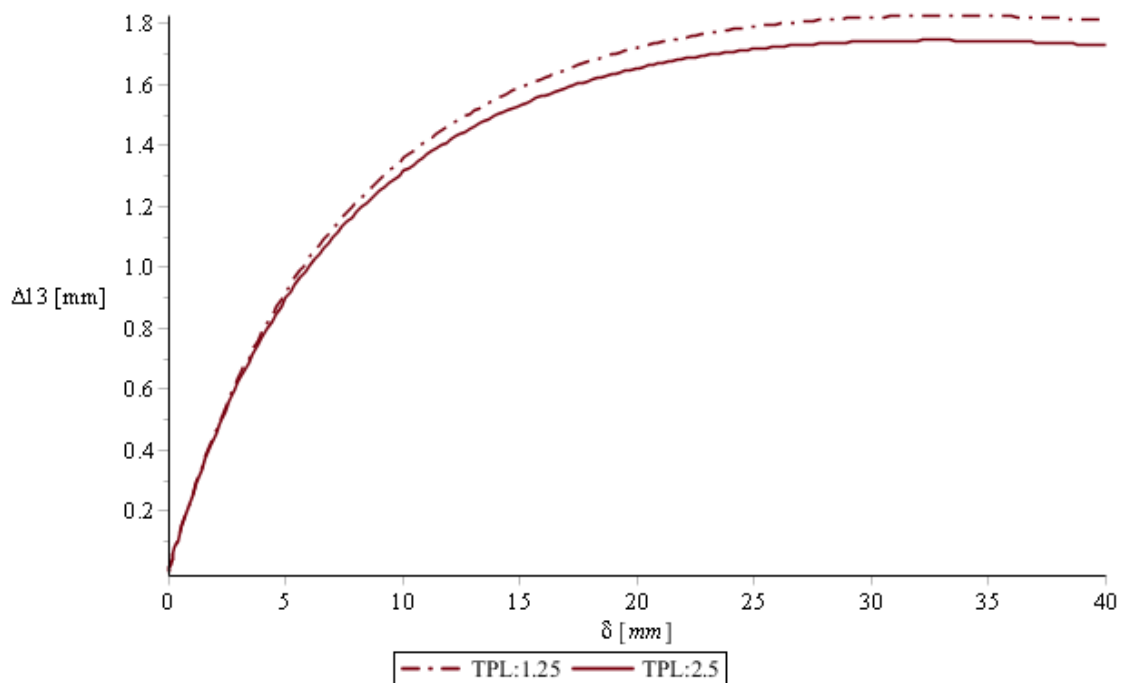


Figure 71 Comparison: Lateral displacement Δ_{13} - δ for different TPL

8.2.2. Effect of Lateral Restraint on the Ultimate capacity

- Transverse prestress level: 1.25MPa

Effect of Lateral Support Stiffness on the Ultimate Capacities ($0 < S/S_s < 40$)

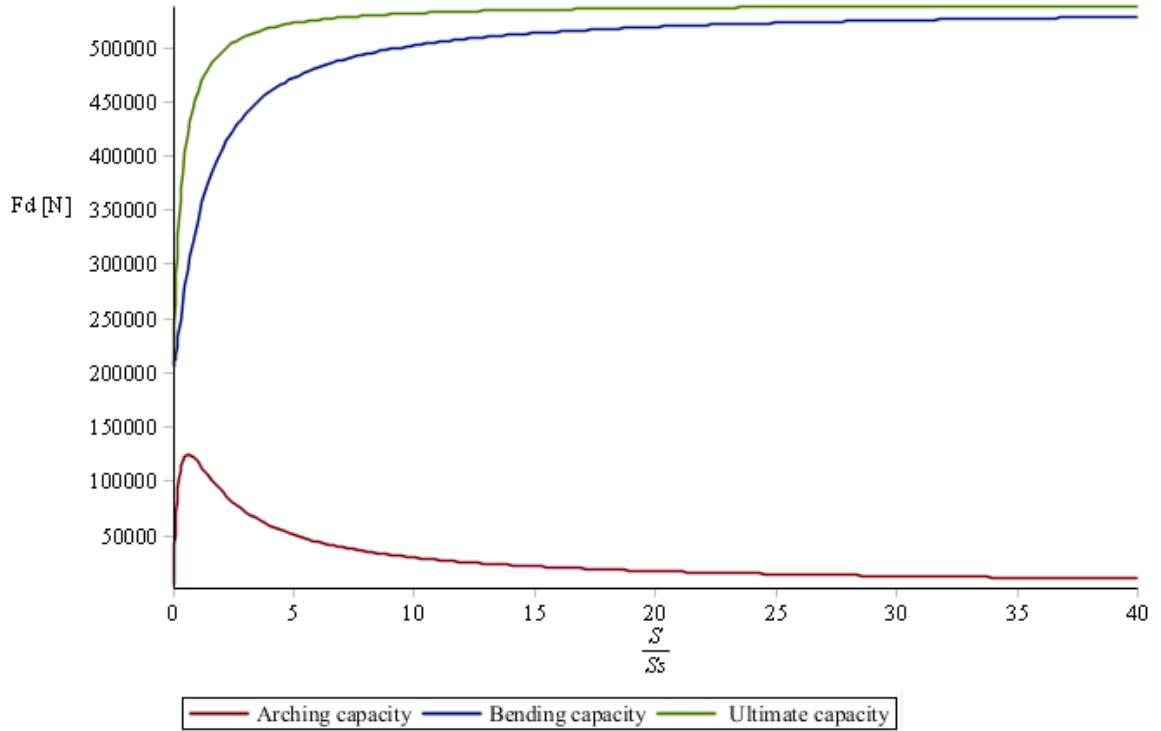


Figure 72 Ultimate capacity-Restraint ratio

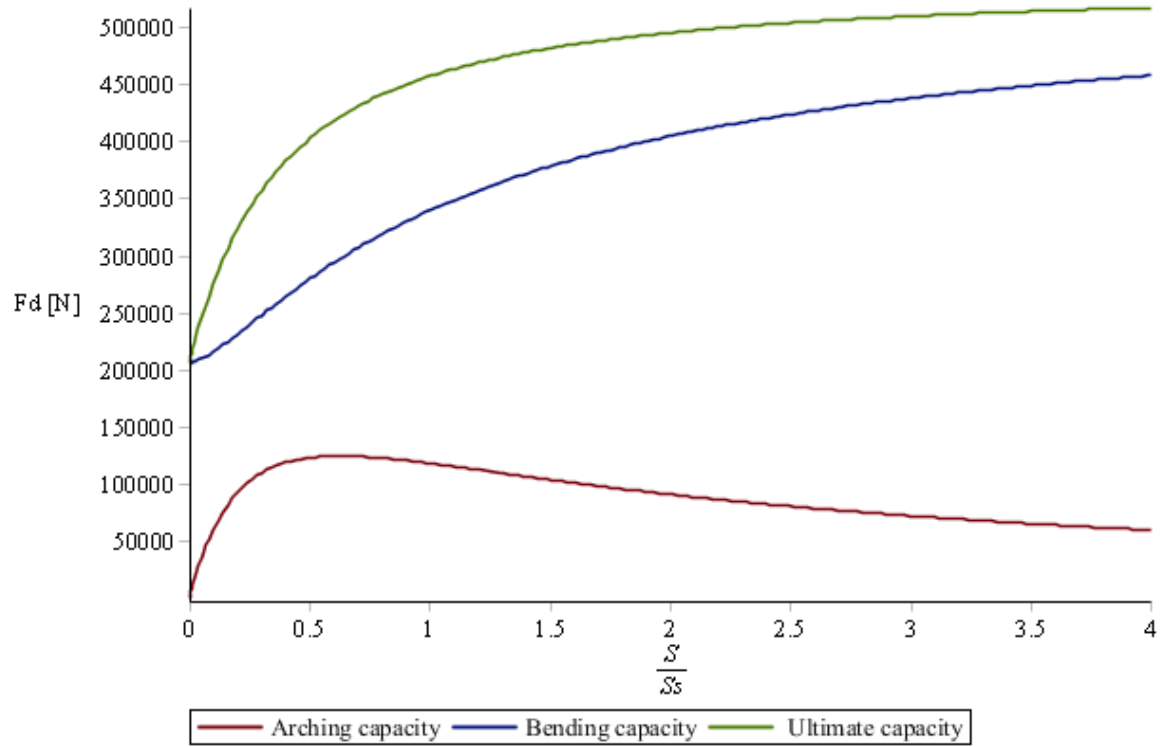


Figure 73 Ultimate capacity-Restraint ratio (in detail)

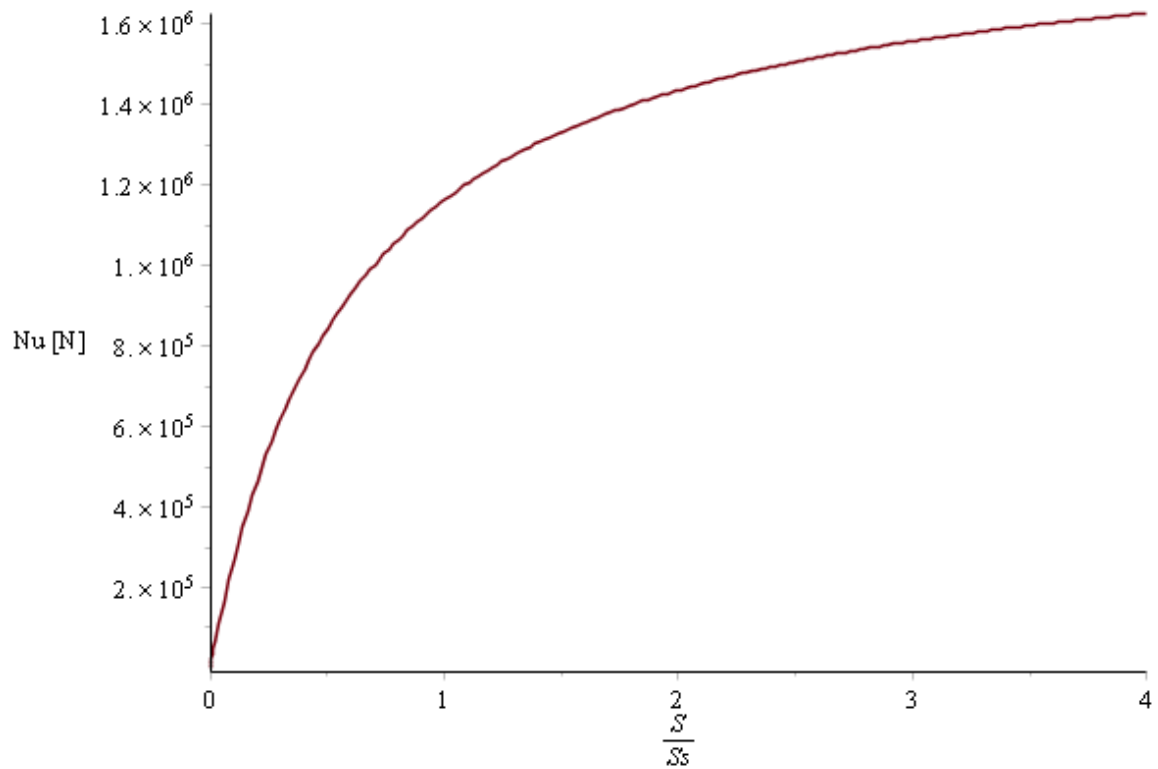


Figure 74 Effect of stiffness ratio on compressive membrane action

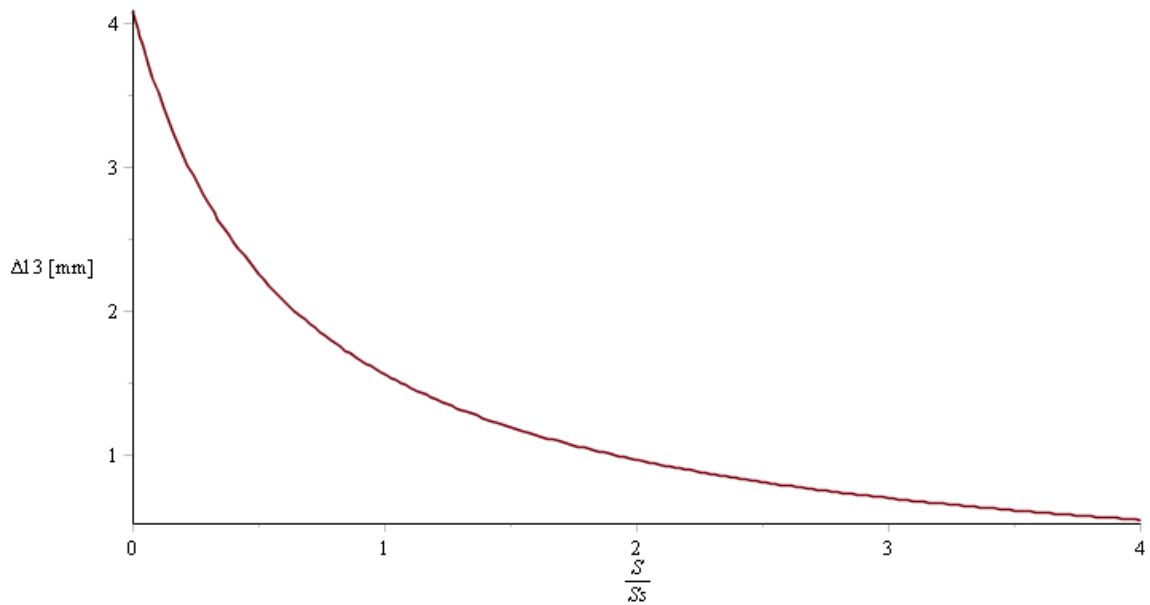


Figure 75 Effect of stiffness ratio on lateral displacement

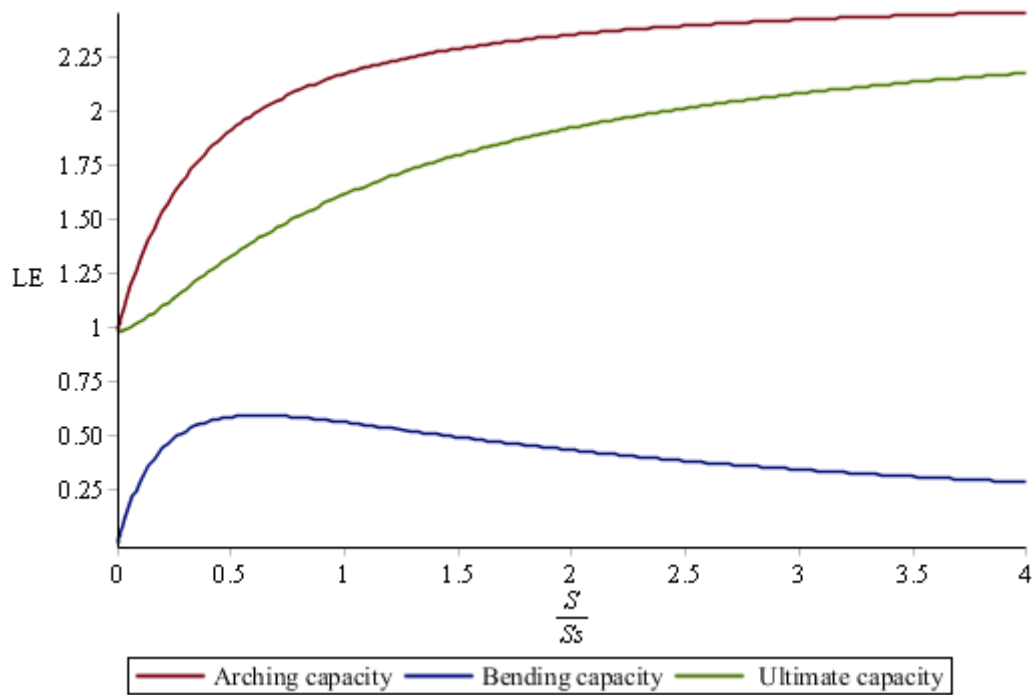


Figure 76 Effect of stiffness ratio on enhancement load factor LE

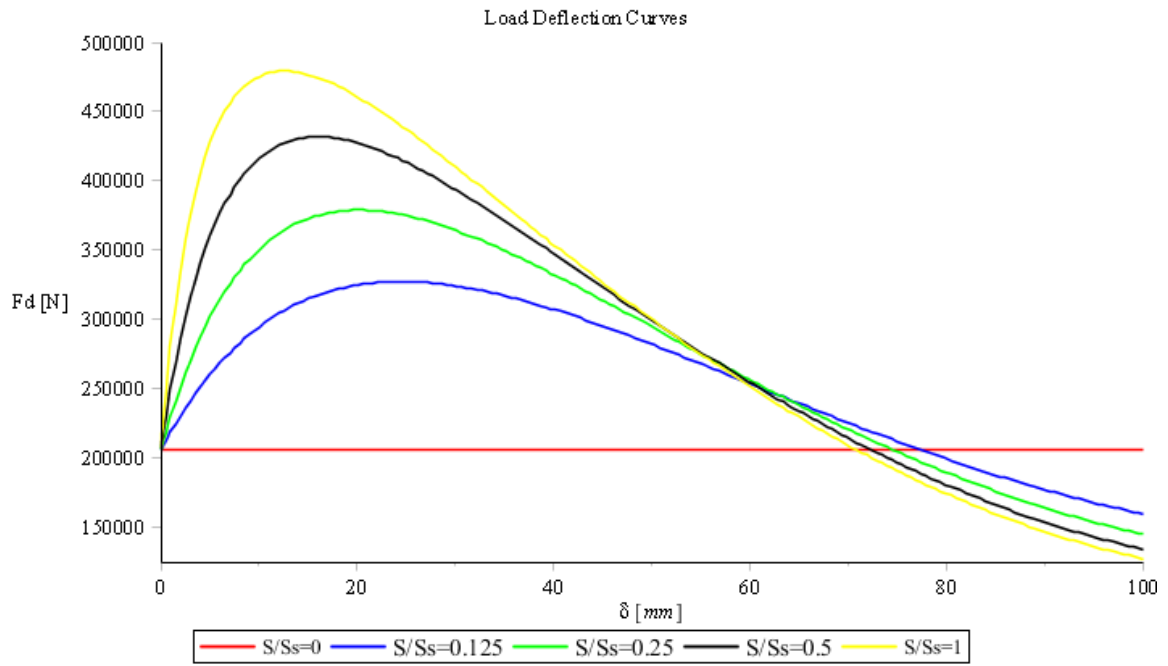


Figure 77 Load Deflections curves for varying S/S_s

- Transverse prestress level: 2.5MPa: Comparison between TPL

Effect of Lateral Support Stiffness on the Ultimate Capacities ($0 < S/S_s < 4$)

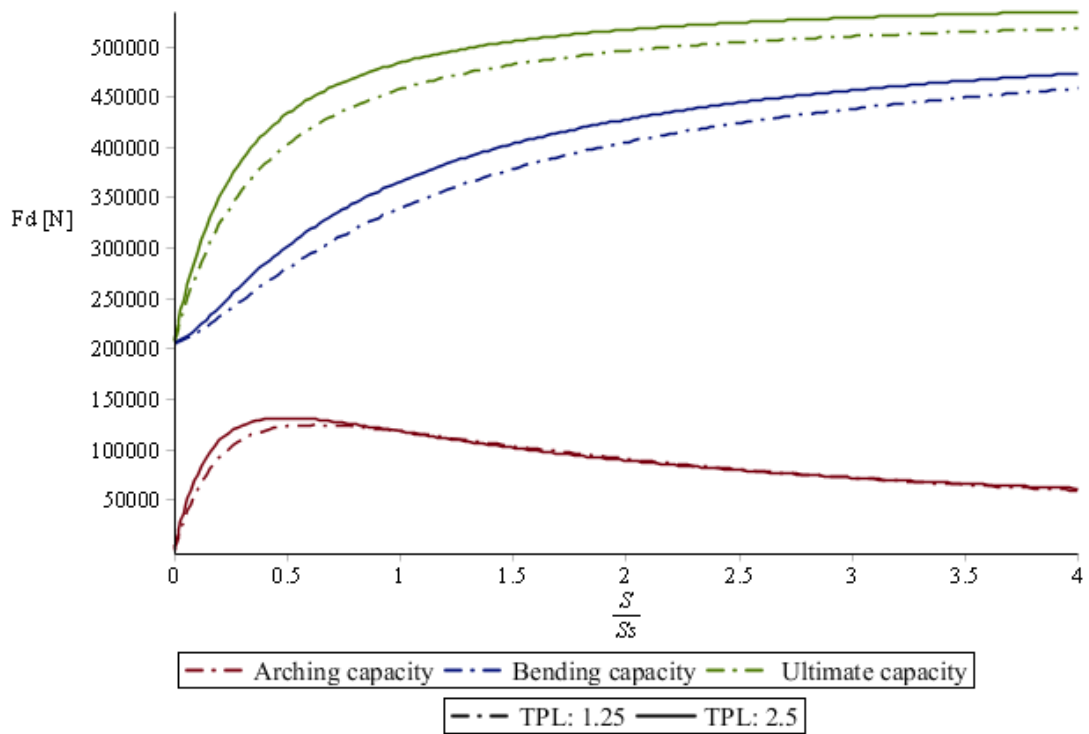


Figure 78 Comparison: Effect of Lateral Support Stiffness for different TPL

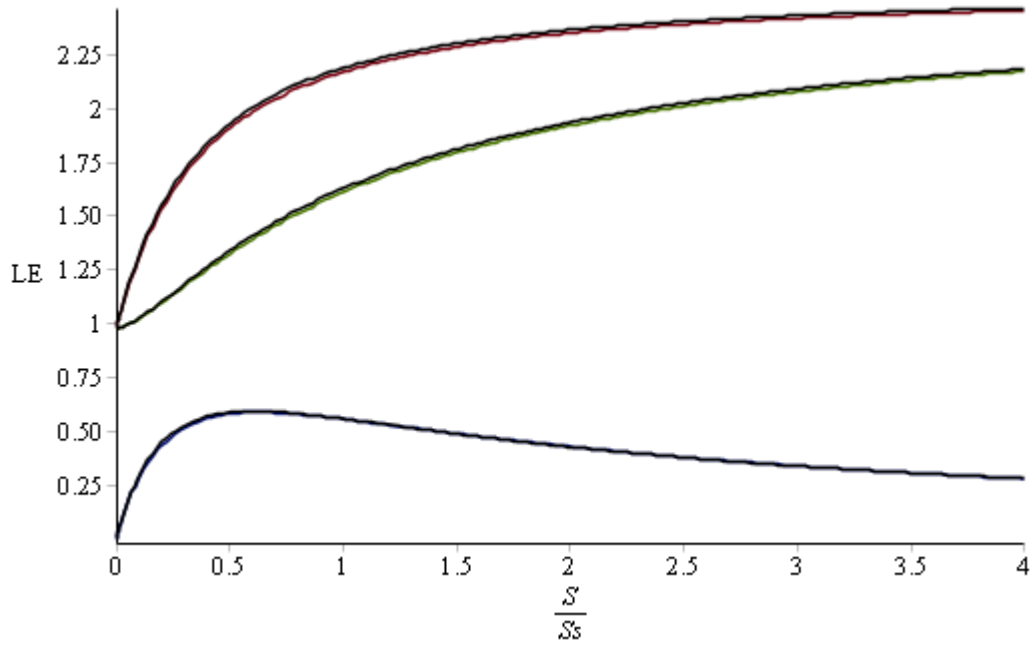


Figure 79 Comparison: Load enhancement factor for different TPL

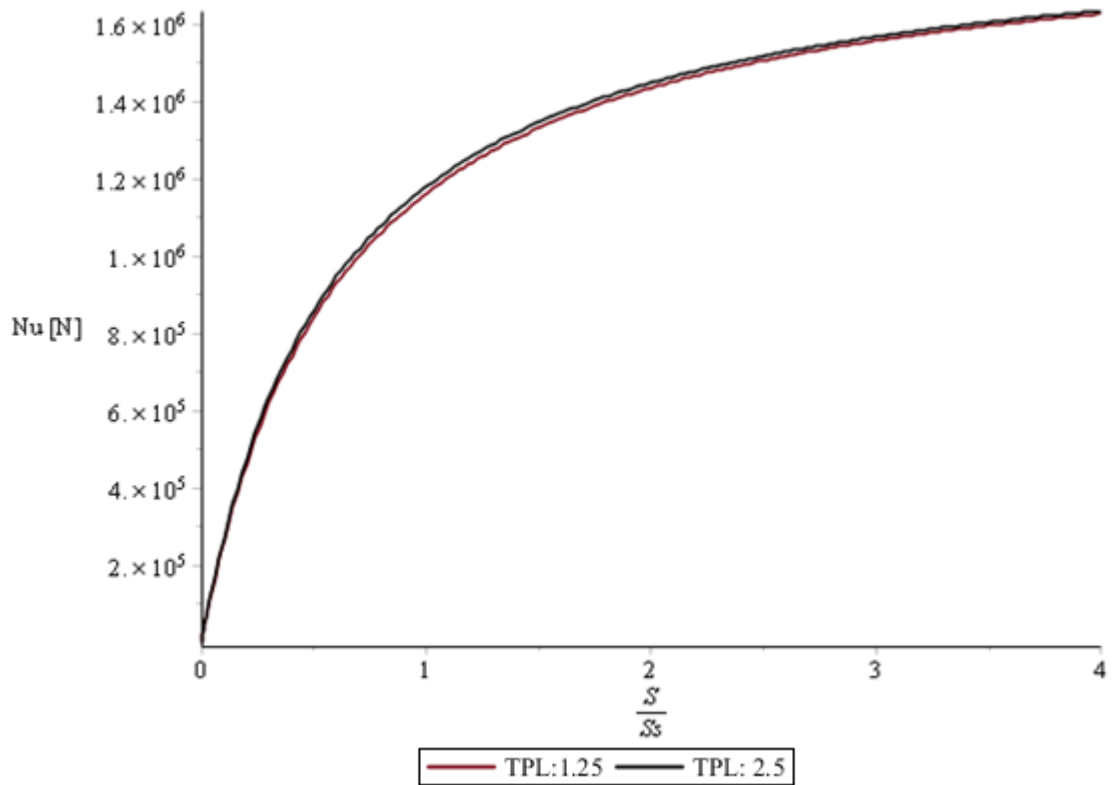


Figure 80 Comparison: Compressive membrane force for different TPL

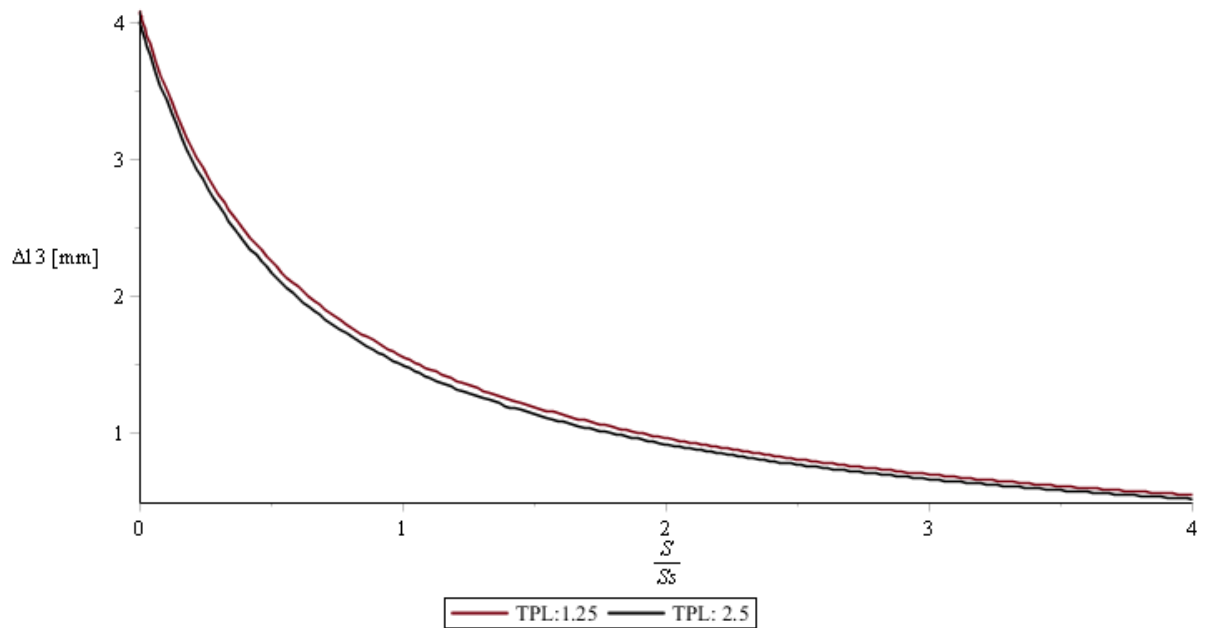


Figure 81 Comparison: Effect of stiffness ratio on lateral displacement
Load Deflection Curves

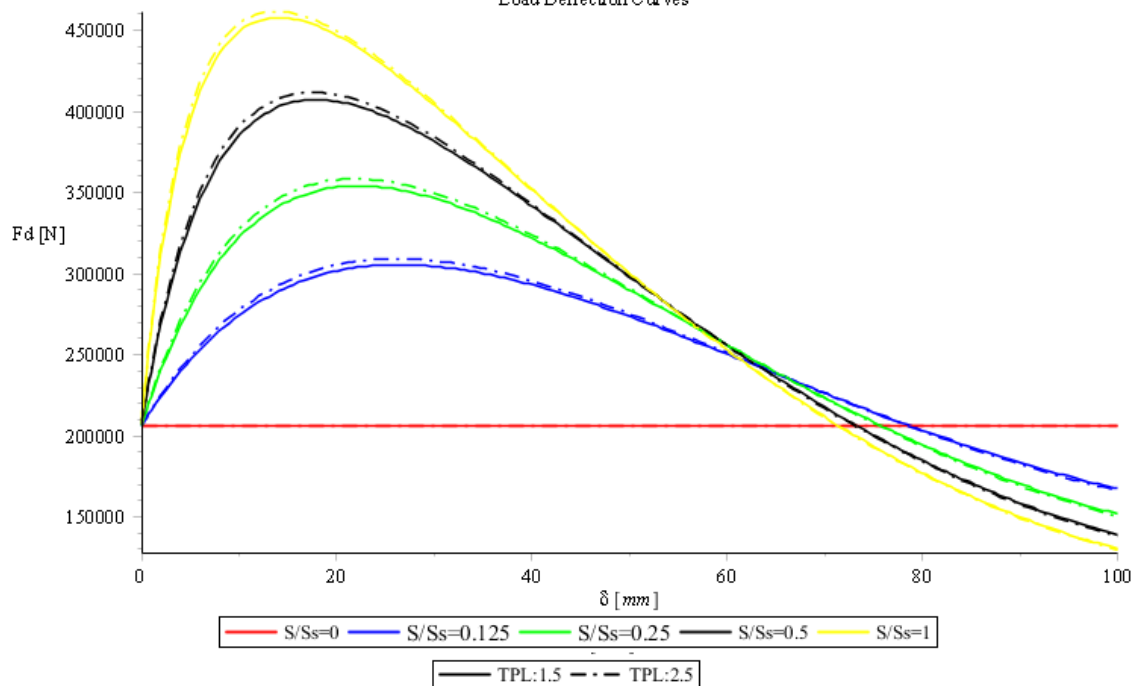


Figure 82 Comparison: Load Deflections curves for varying S/S_s and different TPL

8.2.3. Capacity Enhancement Factor: Slenderness - Stiffness effect

- **Comparison: TPL = 1.25MPa - 2.5MPa**

The slab to depth ratio is governing at the estimation of the compression membrane force. The arching action is directly dependent on the horizontal elongation, which in turn depends on the geometric characteristics of the slab. As can be observed below that as the slab to depth ratio

increases the arching action becomes rapidly less effective. The Fig. 83 shows how the ultimate capacity is affected by the slab to depth ratio with respect to the restraint ratio.

When no restraint is provided the ultimate capacity decreases considerably since the slab becomes more slender without any support stiffness to develop compressive membrane action. When lateral restraint is provided, the enhancement still decreases substantially since the slab becomes again more slender.

For ratio $l/h=8$ the enhancement factor shows that the ultimate capacity is 4 times more than that when no lateral stiffness is provided, which means that only bending action is present in the slab.

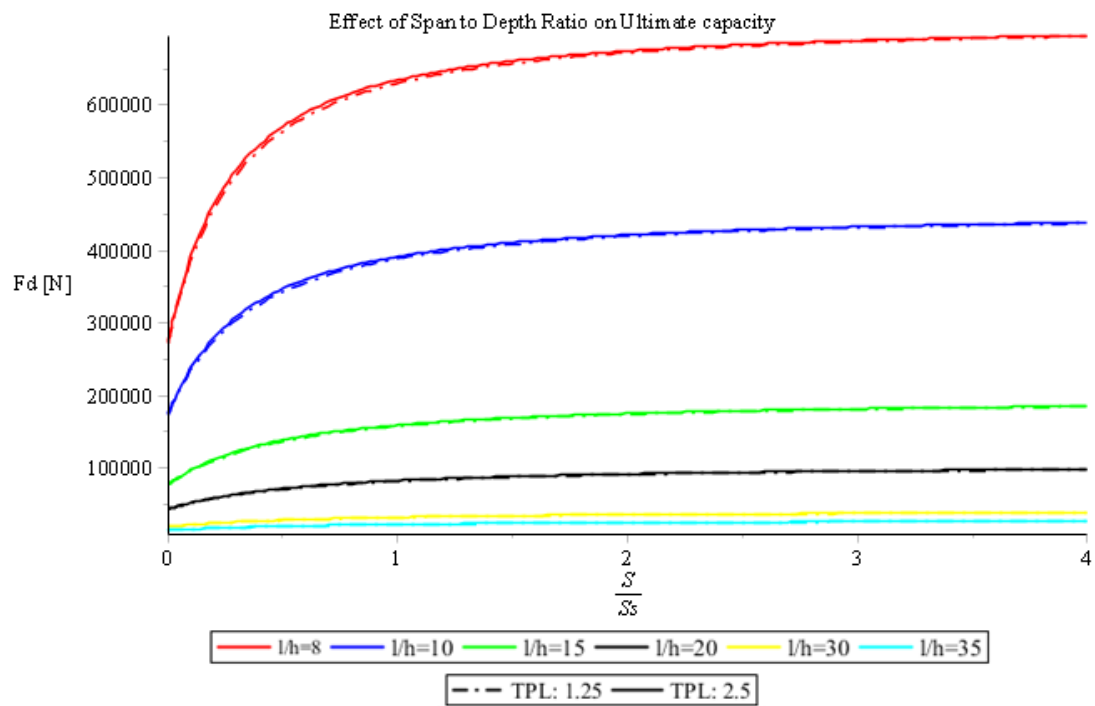


Figure 83 Comparison: Ultimate capacity for varying l/h , varying S/S_s and different TPL

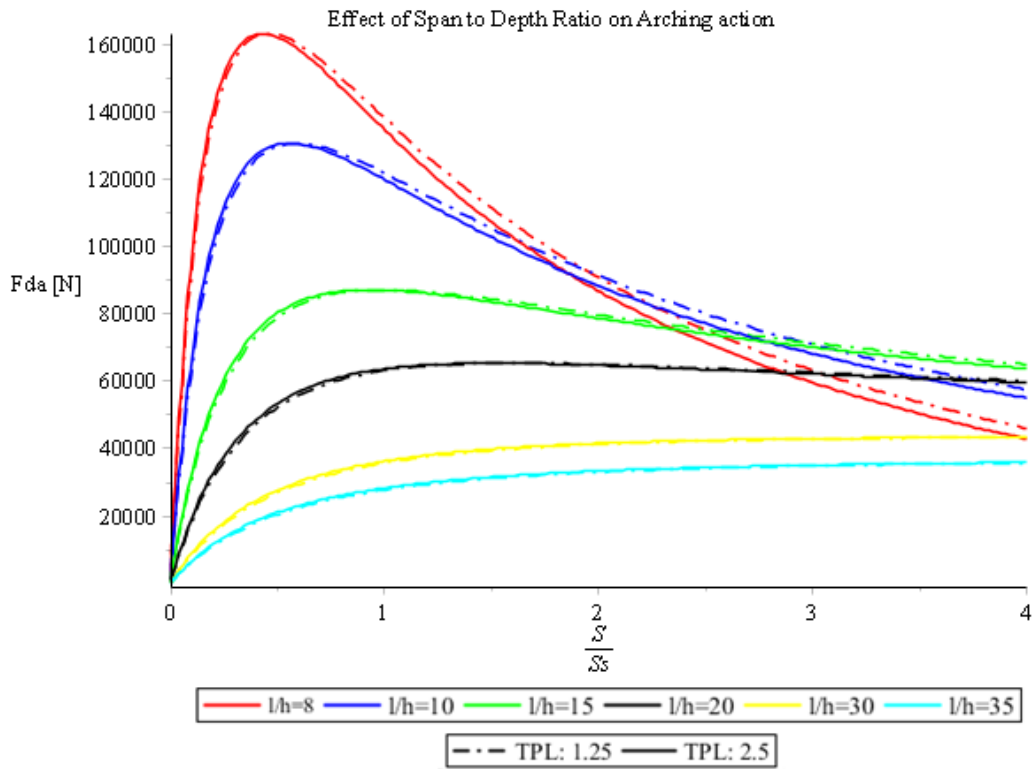


Figure 84 Comparison: Arching capacity for varying l/h , varying S/S_s and different TPL
Effect of Span to Depth Ratio on Arching action

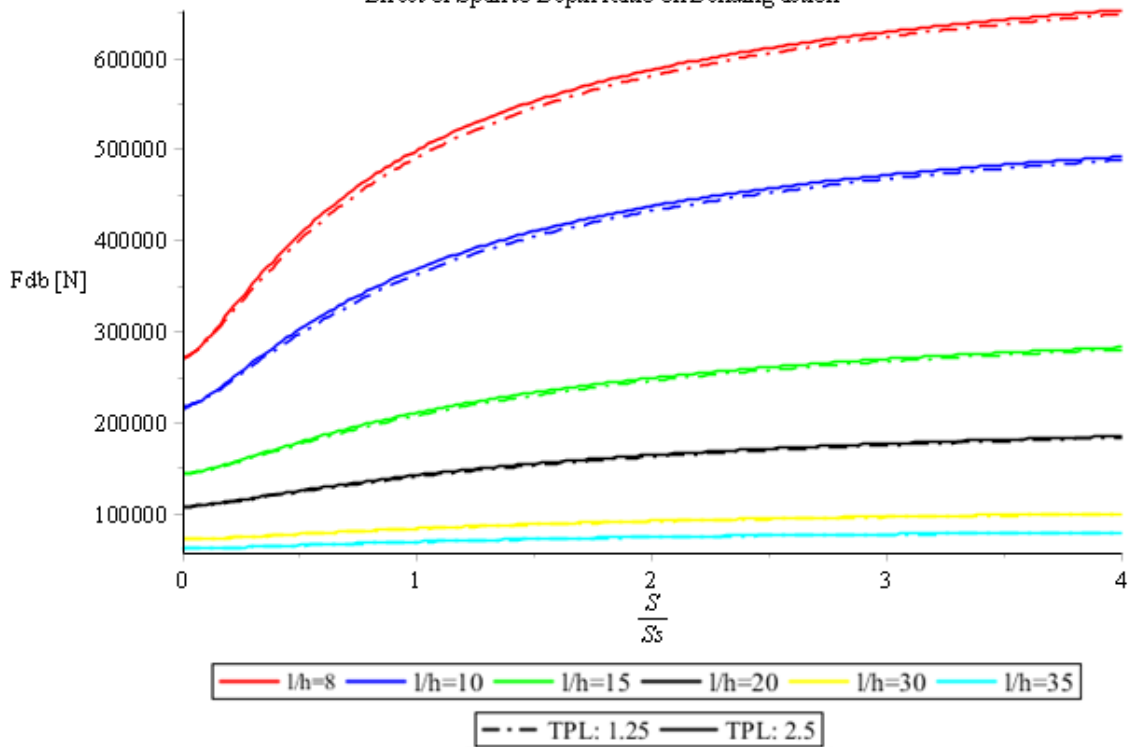


Figure 85 Comparison: Bending capacity for varying l/h , varying S/S_s and different TPL

8.2.4. Comparison: Load over Internal and External panel

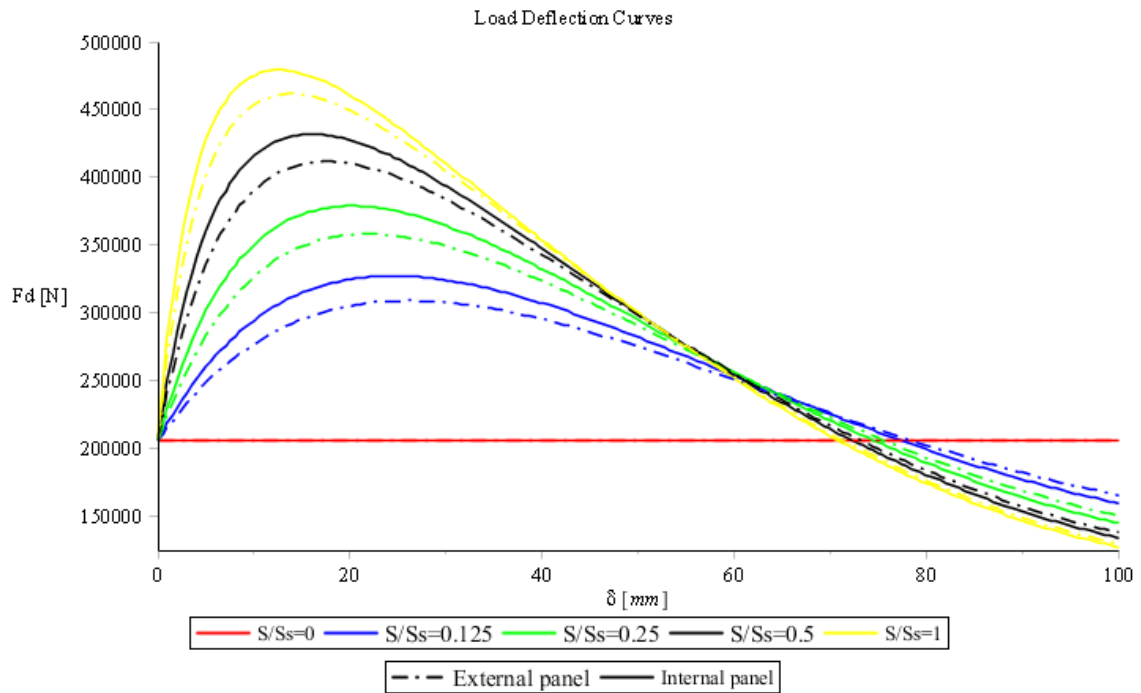


Figure 86 Comparison: Load deflection curves at Internal and External panel [TPL=2.5]

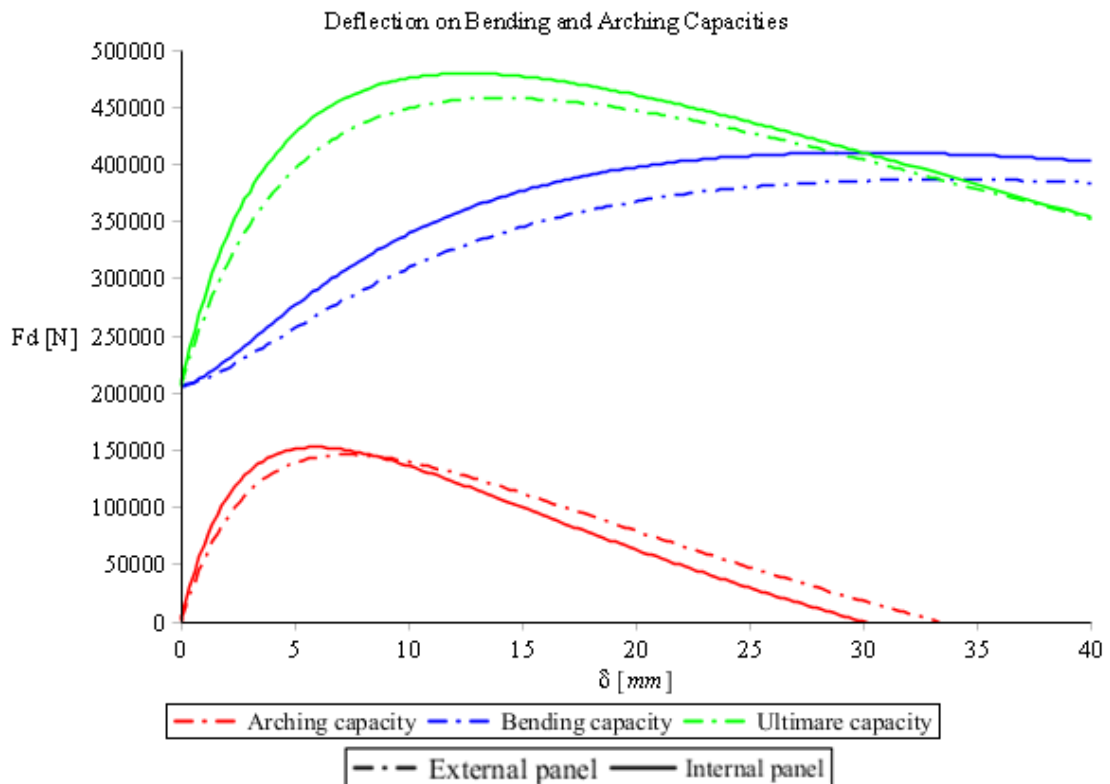


Figure 87 Comparison: Deflection on Bending and Arching Capacities at internal and external panel

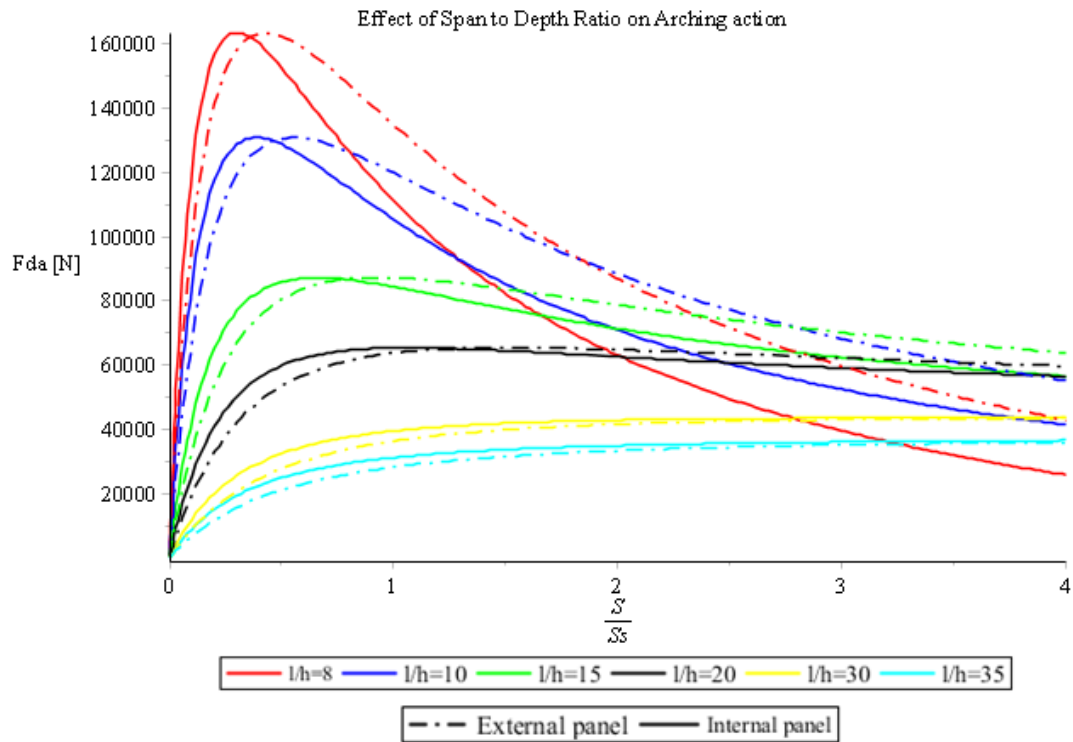


Figure 88 Comparison: Effect of slenderness and stiffness over Arching Capacities [2.5MPa]
Effect of Span to Depth Ratio on Arching action

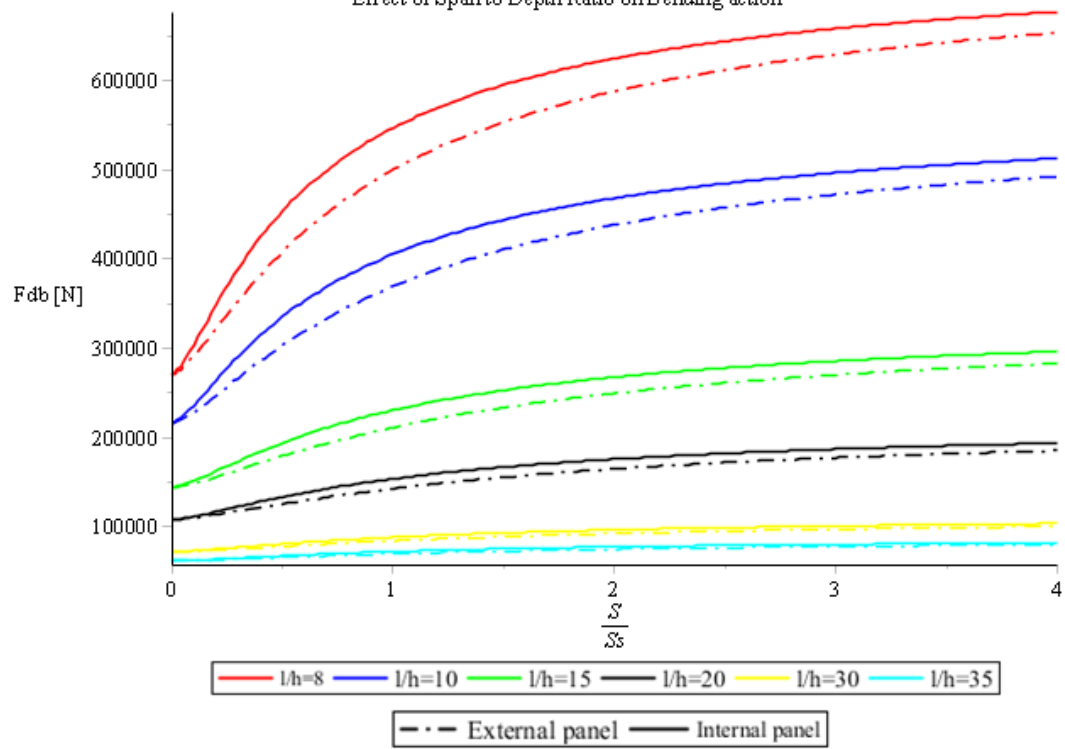


Figure 89 Comparison: Effect of slenderness and stiffness over Bending Capacities [2.5MPa]

9. COMPARATIVE STUDY

9.1. Comparison Bending results

The experimental results and the theoretical approach for bending failure are going to be compared.

Table 15 Experimental results

Experiment	TPL [N/mm²]	Load P_u [N]	Deflection δ [mm]
BB-11 [Exterior]	1.25	377850	7.11
BB-5 [Exterior]	2.5	490400	9.56

Table 16 Results of theoretical approach

Theoretical approach	TPL [N/mm²]	V_ε = P_u [N]	Deflection δ [mm]
External	1.25	457920	14.104
	2.5	461790	13.826
Internal	1.25	479287	12.5846
	2.5	484260	12.2369

Experimental results

At the specimens BB-11 and BB-5 the load is applied at the exterior panels at which there is only restrained from the edge beam and the one side panel. The main difference between the specimens is the transverse prestress level. The BB-5 has 23% higher capacity due to the greater restraint owing to higher prestress. More compressive stresses neutralize the tensile increasing the ultimate compression zone and carrying higher vertical load P_u. The exterior panels have lower effective stiffness than the interior, as a result the effect of prestress will be weaker. At the interior panels the difference in the ultimate capacity is expected to be greater.

Observations

- i. Large rotations occurred at the peak load leading to longitudinal cracks between the double loading points.
- ii. No further increase in the capacity after the failure was occurred.
- iii. The skewed interface has sufficient capacity to bear the vertical load, since no interface failure occurred during the experiments.
- iv. No significant loss of prestressing steel occurred, verifying the initial assumption to neglect the prestress losses.

Theoretical results

- At the internal panels the ultimate capacity is higher because the surrounding slabs form a confining ring, which does not occur at the exterior. At the same prestress level the punching shear capacity is higher about 5% at the interior panel than that of the exterior.
- The effect of the prestress level slightly increases the bending capacity of the slab because it is simulated as an additional stiffness of the prestressing steel area. The additional capacity is attributed to the increase in compressive membrane force about 1.75%.

9.2. Graphs

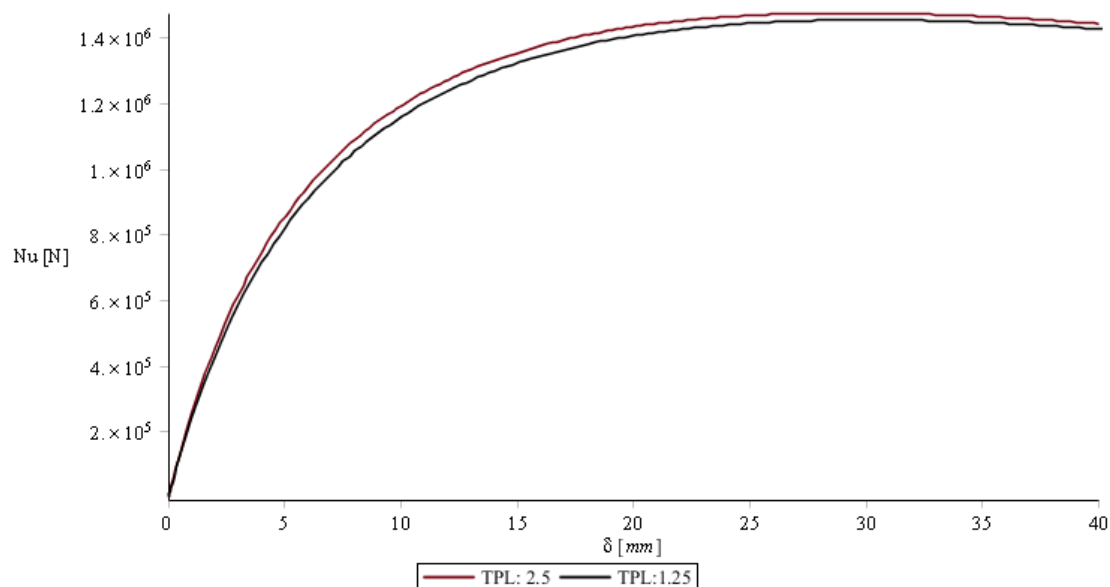


Figure 90 Compressive membrane force N_u - δ

Due to very low regular reinforcement area the total bending capacity is reached later than the maximum value of the arching capacity (Fig.91). The maximum ultimate capacity is reached at 12,5mm while the maximum arching capacity is met at 5,96mm at TPL 2.5MPa. The maximum capacity can be divided into an arching capacity of 24.65% and a bending action of 75.35% of the ultimate capacity.

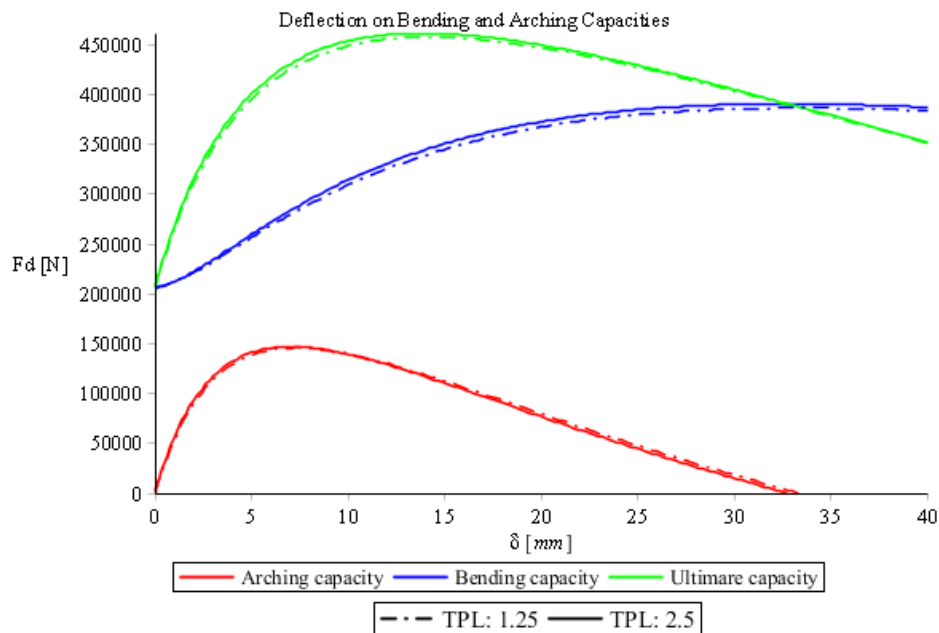


Figure 91 Comparison: Effect of Deflection on Bending and Arching Capacities for different TPL.

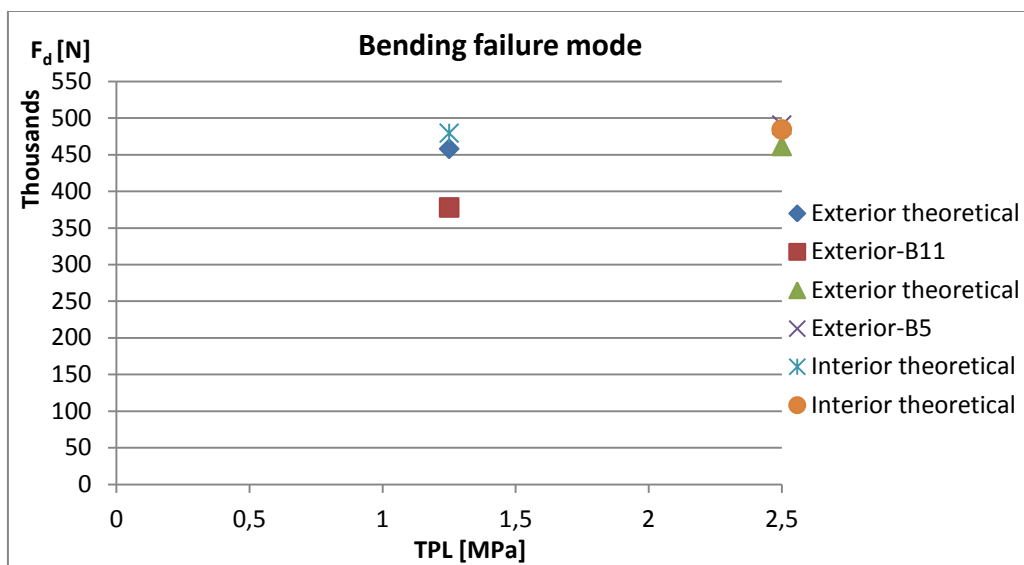


Figure 92 Ultimate capacity at bending

9.3. Comparison: Punching – Bending results

At Fig.93-95 a comparison is presented between the experimental and theoretical results of ultimate capacity at bending and punching shear for different prestress levels. According to the graphs, the bending capacity is higher than the punching shear capacity. This leads to the conclusion that the slab will fail mostly in punching shear, which is also verified by the experiments. The difference in the capacities can be attributed to the fact that the bending capacity takes into account the stiffness of the surroundings element, such as panels and girders, whereas the punching shear capacity is based only on the stiffness of the formed conical shell.

Consequently, the theoretical approach of Kinnunen and Nylander underestimates the effective stiffness provided by the adjacent elements, leading to a lower ultimate punching shear capacity.

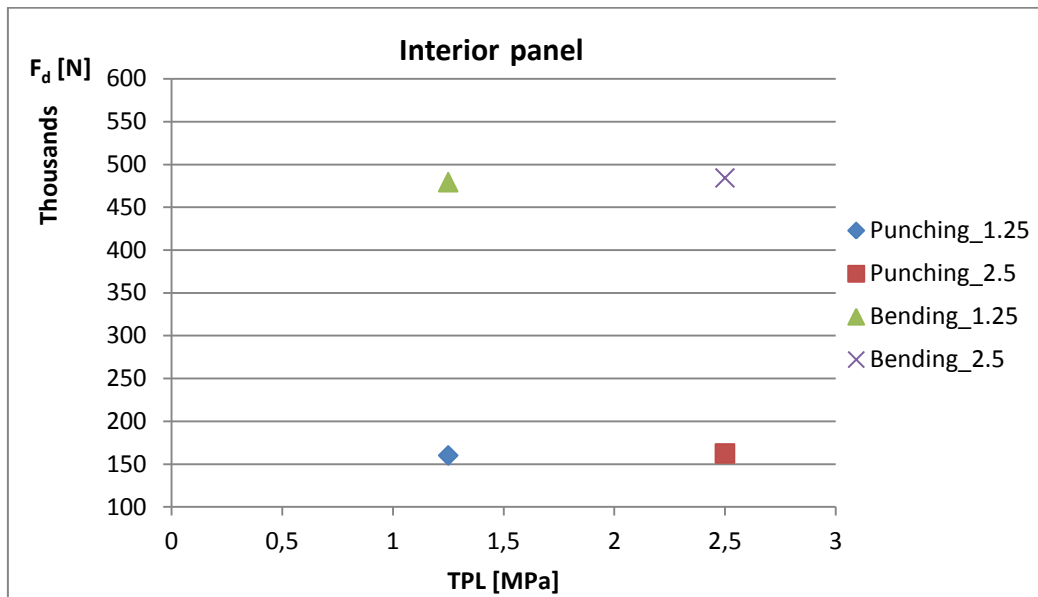


Figure 93 Comparison: Punching-Bending Results

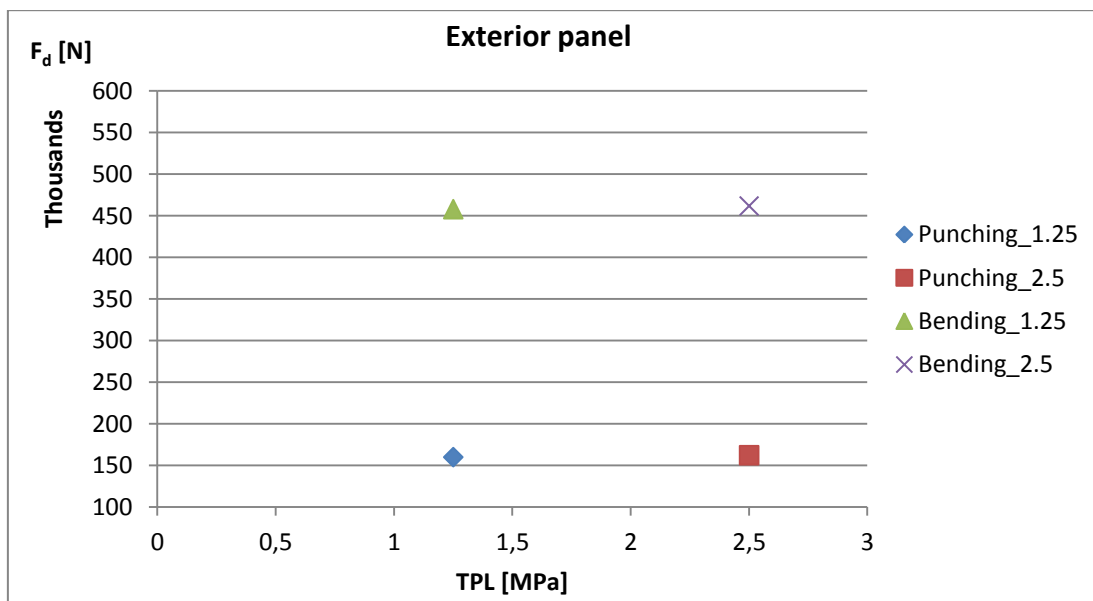


Figure 94 Comparison: Punching-Bending Results

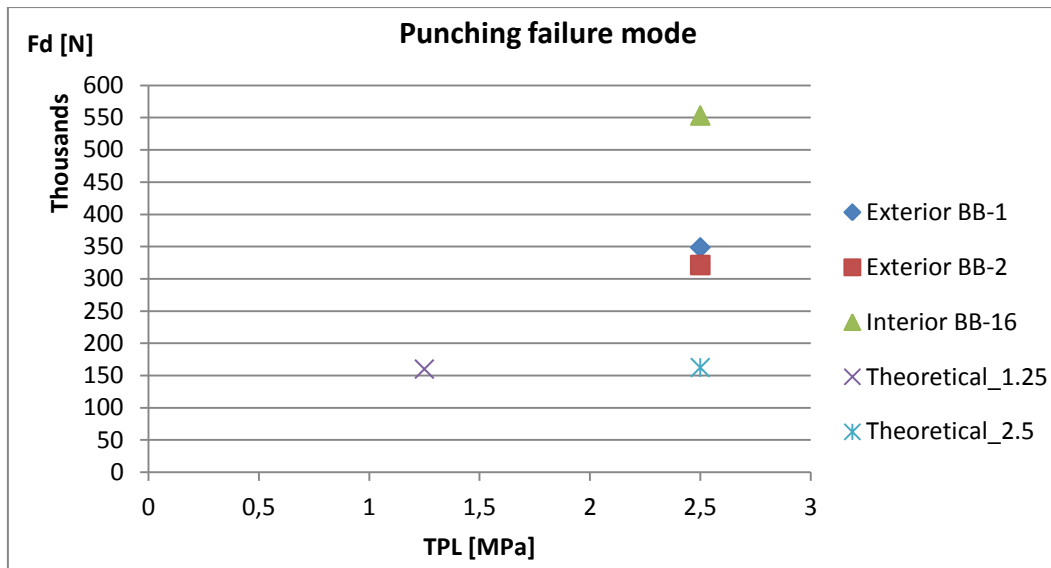


Figure 95 Punching failure mode

10. PARAMETRIC STUDY

The sensitivity of parameters is investigated and plotted in order to estimate the effect and the contribution of each parameter, such as the position of load, the restraint ratio, the slenderness and the TPL. The considering slab has the following characteristics:

- Stiffness ratio: $S/S_s=1$
- Slenderness: $L/H=10.5$
- $TP1=1.25-2.5$

Comparison: Load over Internal and External panel

1. The ratio of ultimate capacity over the bending capacity (LE) is indicative for the enhancement in the ultimate resistance solely due to arching action. Thus, at small values the LE load factor reaches values more than the double ultimate capacity. That means that the **optimum restraint ratio is slightly higher than or equal to 1**, when the full stiffness is provided for lateral restraint.
2. At the case that no restraint is provided the capacity slightly changes while the vertical deflection at the midspan increases (Fig.97). Thus, the slab will fail due to large displacements. As the restraint conditions increase, the slab fails at smaller deflections, which leads to the conclusion that the slab becomes **less ductile**. For values of stiffness less than the axial stiffness of the slab and the girders, the slab fails at greater deflections than $L/82$ (12.85mm). According to Eurocode, at the permissible serviceability the upper limit l/h for prestressed slabs is $L/50$ (21mm).

3. The load enhancement factor becomes double leading to the conclusion that at the present case the contribution of compressive membrane action at this stiffness ratio results in an almost double ultimate capacity.
4. For small values of slenderness the arching action is more intensive due to higher compression zone. The overall performance of the slab is expressed by the blue curve, as illustrated below (Fig.99-100). On the other hand, high values of slenderness lead to a slender behaviour which weakens the compressive action. Specifically, for depth to height ratio l/h more than 15 there is no enhancement since the slab starts performing in a slender way minimizing the effect of compressive membrane action.
5. Due to very low regular reinforcement area the total bending capacity is reached later than the maximum value of the arching capacity (Fig.97). The maximum ultimate capacity is reached at 12,5mm while the maximum arching capacity is met at 5,96mm at TPL 2.5MPa. The arching capacity is 24.65% and the bending action is 75.35% of the ultimate capacity.
6. At zero restraint $S/S_s=0$ the load is carried only by the bending action since no arching action can be developed (Fig.99-100). The abrupt increase in the ultimate capacity at small ratio of restraint is attributed mainly to arching action, which is quite intensive at the partially restraint conditions especially for values between 0.2 and 0.6. For values of ratio higher than 4 an increase in the restraint does not have any influence on the capacity. This implies that extremely stiff support is not necessary for increasing the ultimate capacity. Neither are bending action nor arching action affected by an infinitive stiff support.

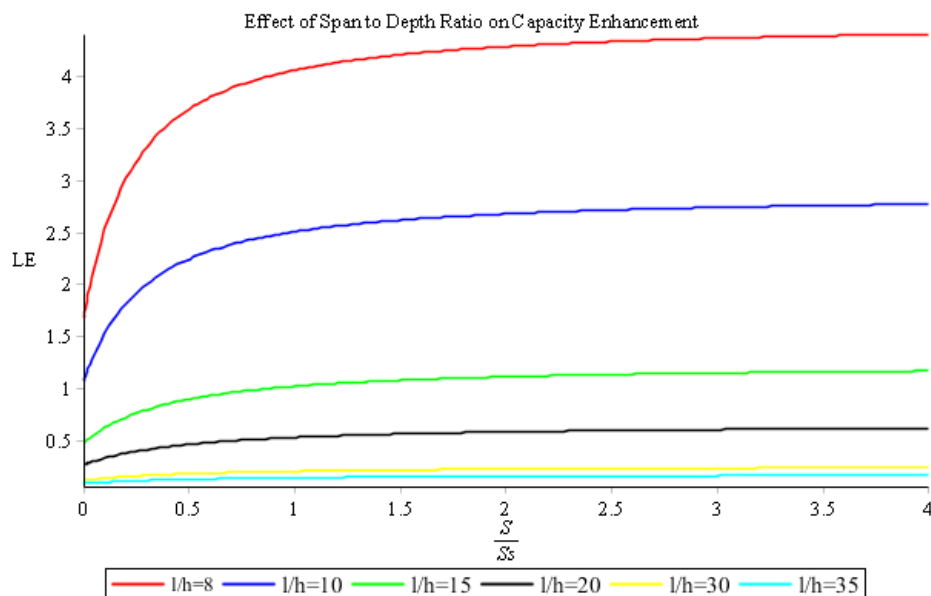


Figure 96 Enhancement load factor for varying S/S_s and varying slenderness (in detail)

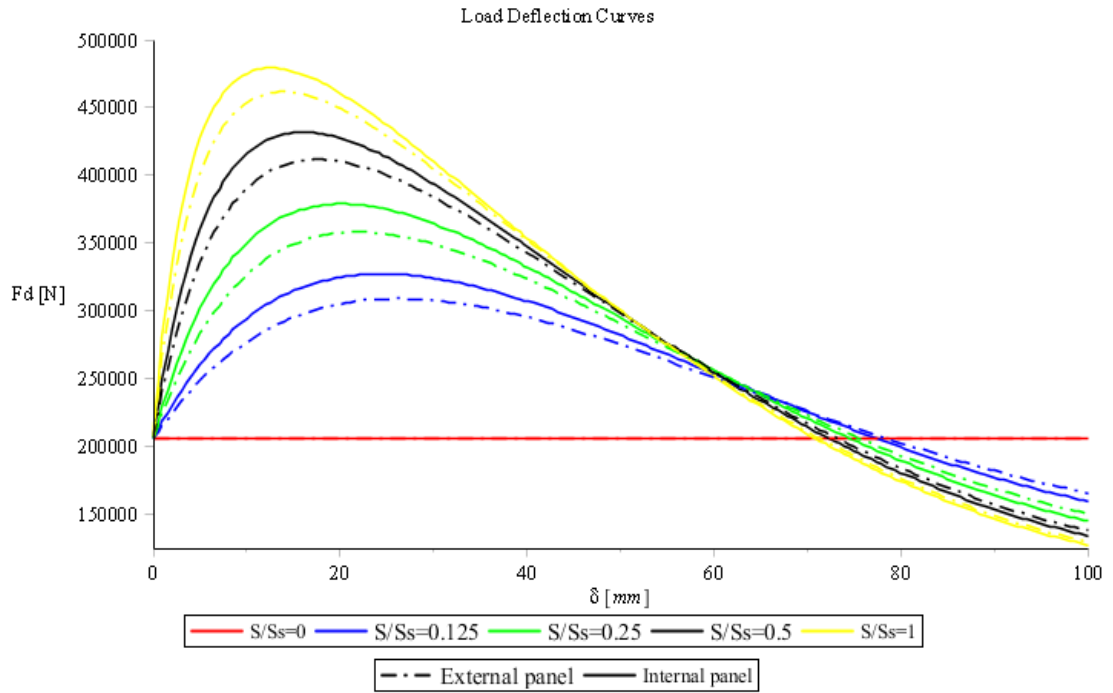


Figure 97 Comparison: Load deflection curves at Internal and External panel [TPL=2.5]

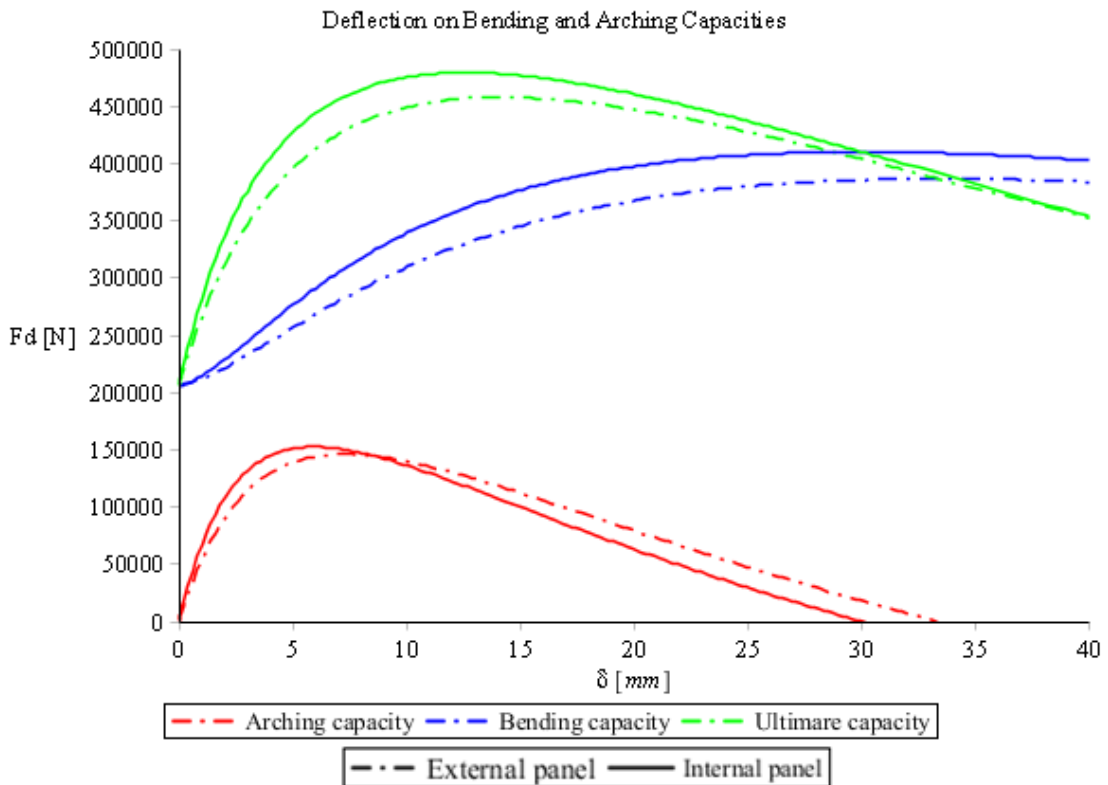


Figure 98 Comparison: Deflection on Bending and Arching Capacities at internal and external panel

To estimate better the influence of slenderness and stiffness over the capacity of the slab it is wise to separate the arching and bending case. Thus, the change in the ultimate capacity will be

attributed to the change in the bending or in the arching action. Generally, the bending contribution determines the final value of the ultimate capacity.

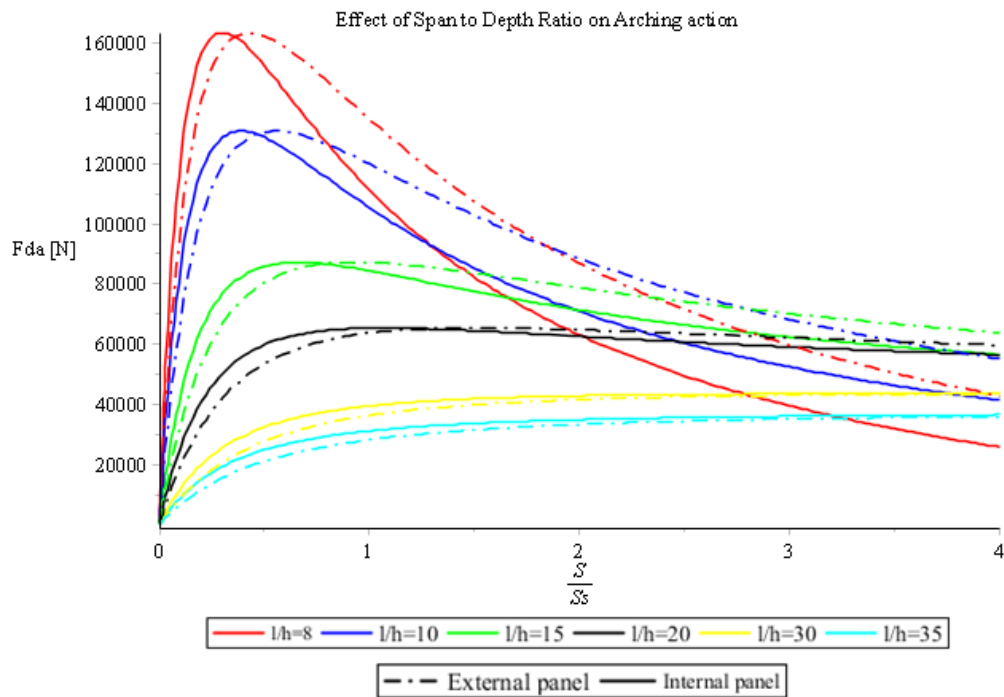


Figure 99 Comparison: Effect of slenderness and stiffness over Arching Capacities [2.5MPa]

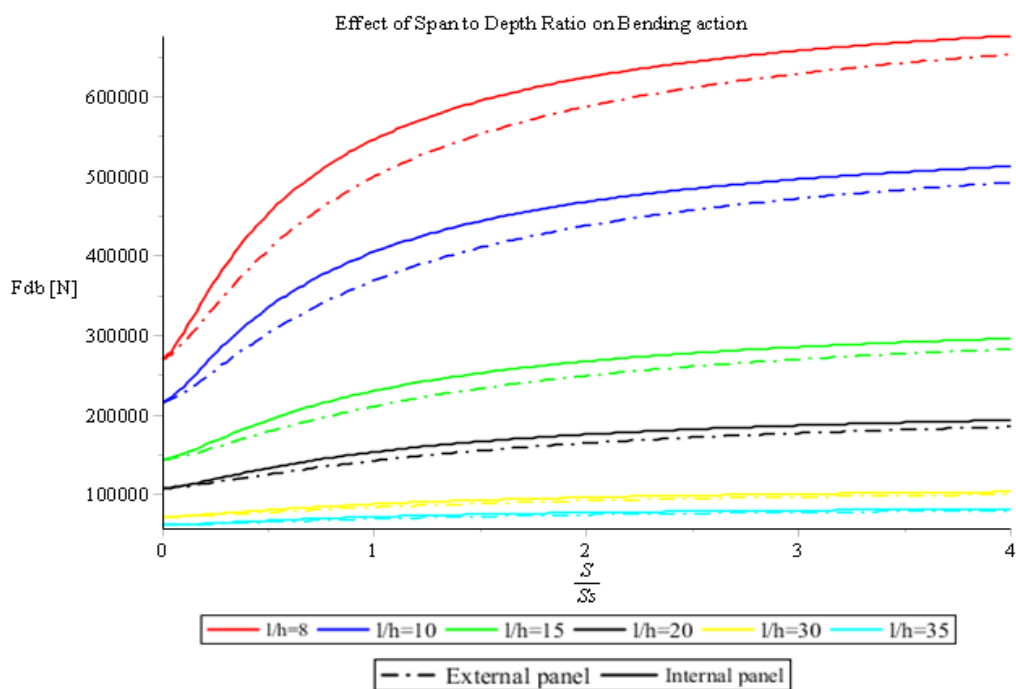


Figure 100 Comparison: Effect of slenderness and stiffness over Bending Capacities [2.5MPa]

11. CONCLUSIONS

- The Mild steel has no effect over the punching and bending capacity due to the low value of reinforcement ratio.

- The transverse prestress level has simulated as an initial imposed deformation in punching capacity and as an additional stiffness in bending capacity. In both cases the TPL slightly has a contribution in the enhancement of the capacities. This can be explained by the fact that the unbonded tendon never yields, responding elastically throughout the loading process. Therefore, the tendon has a linear elastic profile and its stress value at the ultimate stage is independent on the yielding stress because it is never reached. The TPL will delay the failure of concrete.
- The simulation of TPL as an imposed deformation underestimates the contribution of the prestress making the approach less realistic compared to experimental results.
- The ultimate capacity is considerably affected by the lateral restrained ratio S/S_s , provided by the support and the surrounding slabs. The degree of the lateral restraint governs the contribution of the compressive membrane action. The optimum restraint ratio is estimated $S/S_s=1$ at which the combination of the compressive and bending action is maximum. Stiffness ratio higher than 1 results in non ductile slabs whereas for values higher than 5 the stiffness becomes so high that there is no effect of stiffness to the ultimate capacity.
- It is not necessary to provide fully fixed conditions at the support, since for high values of stiffness ratio there is not any further enhancement. The performance of the slab under a double wheel load should be characterized by plasticity and ductility. When the stiffness ratio decreases the slab can accommodate higher displacements showing more warning cracks and avoiding a sudden failure. This can be achieved by taken the lateral restraint ratio equal to 1, leading to an economical solution and sufficient ultimate capacity.
- The length depth ratio l/h affects the overall performance of the slab. For the present case the ratio l/h is 10 which leads to a double ultimate capacity compared to lower ratios. If the slenderness increase the slab becomes more slender and as a result it decreases the effect of compressive action.
- The interior slab shows higher enhancement of the capacity compared to exterior slabs, because of the effective stiffness of the surrounding elements (slab-girders). At the case of loading the interior slab, the surrounding panels and concrete girders form a confining ring around it, increasing considerably the restraint stiffness.
- The performance of the exterior slab depends on the flexibility of the edge beam. The failure load as well as the contribution of compressive membrane action are calculated by taking into account the flexural, rotational and torsional rigidity of the edge beam.
- The shear effect can be considered to be negligible either the load is positioned at the centre of the panel or close to the edge structure. Otherwise, the horizontal

deformation should be calculated as a superposition of the support and the shear deformation.

REFERENCES

- i. Punching behaviour of composite decks with transverse prestressing
Weishi He
1992
- ii. Punching behaviour of composite bridge decks transversely prestressed with carbon fibre reinforced plastic tendons

- S. Marshe
1997
- iii. Punching behaviour of composite bridge decks transversely prestressed with carbon fibre reinforced polymer tendons
S. Marshe; M.F. Green
1999
- iv. Punching shear resistance of prestressed concrete slabs
G. D. Stefanou
University of Patras, Greece
- v. Analysis and Design of laterally restrained structural concrete one-way members
Nasser Meamarian, Theodor Krauthammer, and John O'Fallon
ACI Structural Journal Technical Paper, Title no. 91-S70
- vi. Reinforced Concrete Slabs
Robert Park and William L. Gamble, 2000
- vii. Membrane action in lateral restraint reinforced concrete slabs
WANG Gang (王刚), WANG Qing-xiang (王清湘), LI Zhong-jun (李中军)

THESIS

- viii. Membrane behaviour in one-way prestressed concrete slabs
Roger J. Miltenburg
The University of Western Ontario, Ontario August 1998
- ix. Loading capacity of laterally restrained prestressed concrete slabs
R.F.C. de Rooij
Delft University Of Technology, April 2011
- x. Experimental determination of bearing capacity transversely prestressed concrete slabs
M.W.J. Vugts,
Delft University Of Technology, June 2012
- xi. A finite element model for the deck of plate-girder bridges including compressive membrane action, which predicts the ultimate collapse load

G.J. Bakker

Delft University Of Technology, August 2008

APPENDIX I

PUNCHING SHEAR: EXPERIMENTS

To investigate the punching shear capacity of a transversely prestressed slab, a bridge has been constructed at 1:2 scale model at Stevin II laboratory, CITG faculty, Delft University of Technology. The bridge model has 12m long and 6.4m width, consisting of four precast concrete girders placed at 1800 mm c/c distance. The slab has been casted in situ and prestressed in the transverse direction with clear span of 1050mm and thickness of 100mm, as can be observed below.



Figure 101 Apparatus of bridge model

Experiment BB-1

The first test of the series was carried out on 5th February, 2013. The load was applied in 25kN increments @ 1kN/sec. The position of the load and the distances are depicted below. The applied prestress level was 2.5MPa.

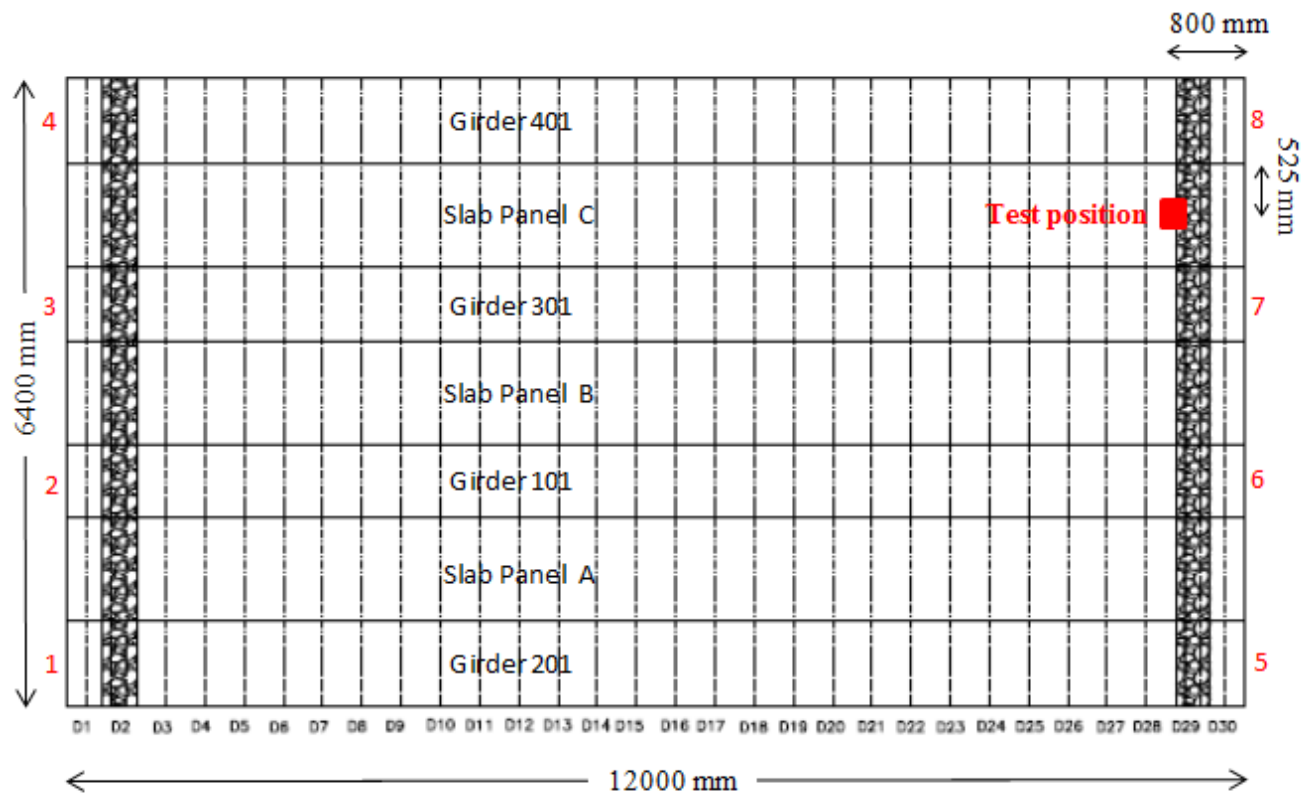


Figure 102 BB-1 Apparatus of structure and load

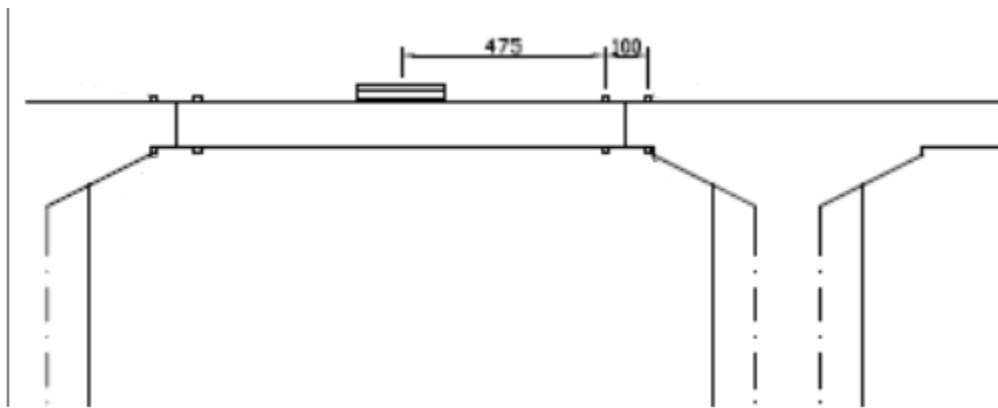


Figure 103 Detail of the load position

Table 17 Response progress

Load	Crack Width	Type	Remarks
kN	mm		
25	-	-	-
50	-	-	
75	<0.05	Bottom long/transverse	Hairline cracks directly under loading plate. Hardly visible
100	<0.05		Better visibility
125	0.05	Diagonal/Radial punching	Diagonal cracks. Widening of previous cracks
150	0.1-0.15		Spreading of radial cracks/Widening
175	0.2-0.25		
200	0.3		Max Crack width directly under load
225	0.35		Max Crack width directly under load
250	0.4-0.45		0.45 directly under load. Elsewhere 0.4
275	0.5		Max Crack width directly under load

300	0.6		Max Crack Width directly Under load. Crack observations stopped
325		Circumferential	Circumferential cracks occurred somewhere between 300kN and failure.
348.7			Punching failure. Large cracking and spalling at some places. G301(East side of panel) interface spalling at bottom. Top side punched through the loading plate.

Table 18 Summary results

Load [kN]	TPL [N/mm ²]	Deflection [mm]	Crack width [mm]
348.74	2.5	10.4	0.8

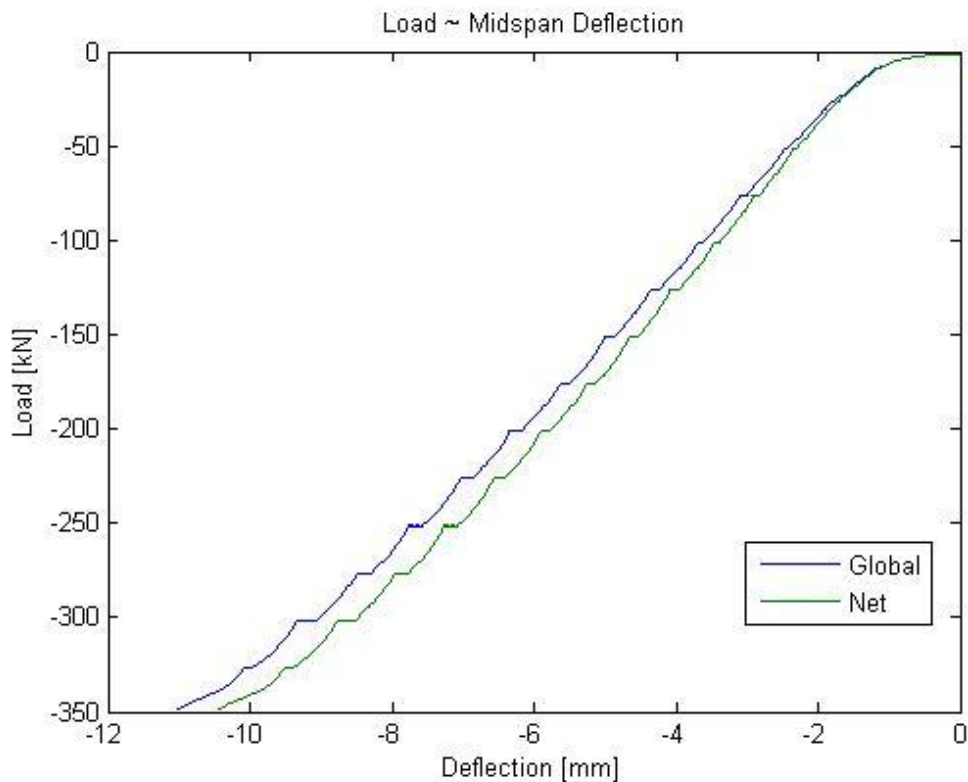


Figure 104 Load – Midspan Deflection Response



Figure 105 Bottom side of deck slab after failure

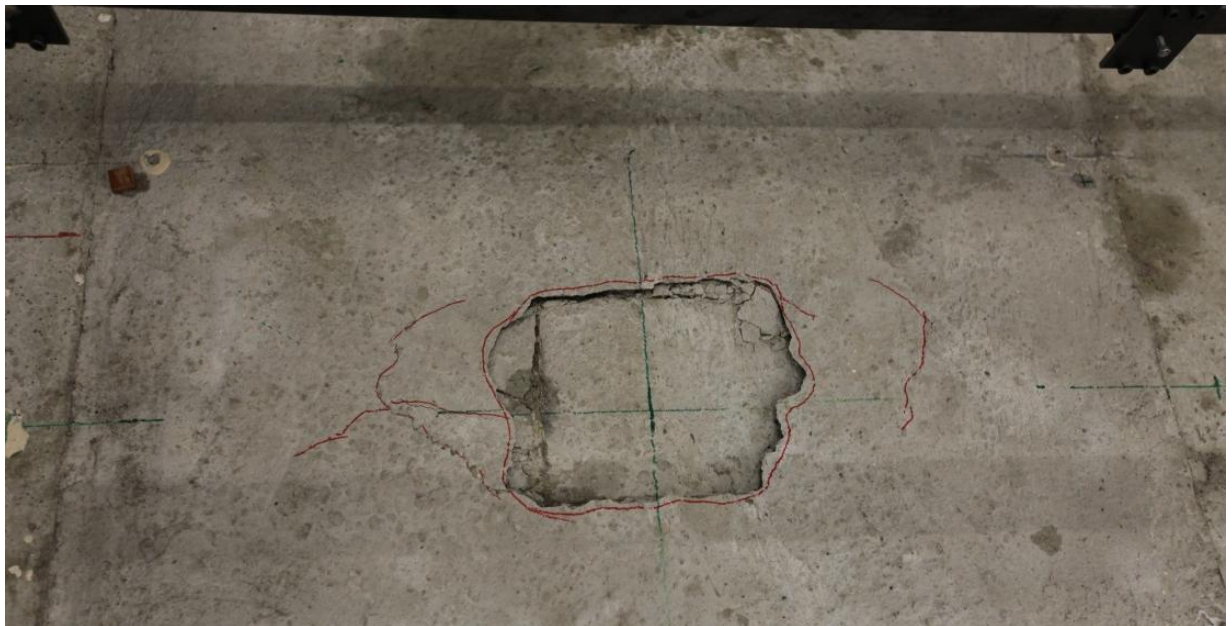


Figure 106 Top side of deck slab after failure

- Experiment BB-2

The second test of the series was carried out on 8th February, 2013 at Stevin II laboratory, CITG faculty, Delft University of Technology.

Load was applied in 75, 100, 150, 200, 250 kN steps @ 1kN/sec. Later the actuator was switched to displacement control at 0.01mm/sec till failure.

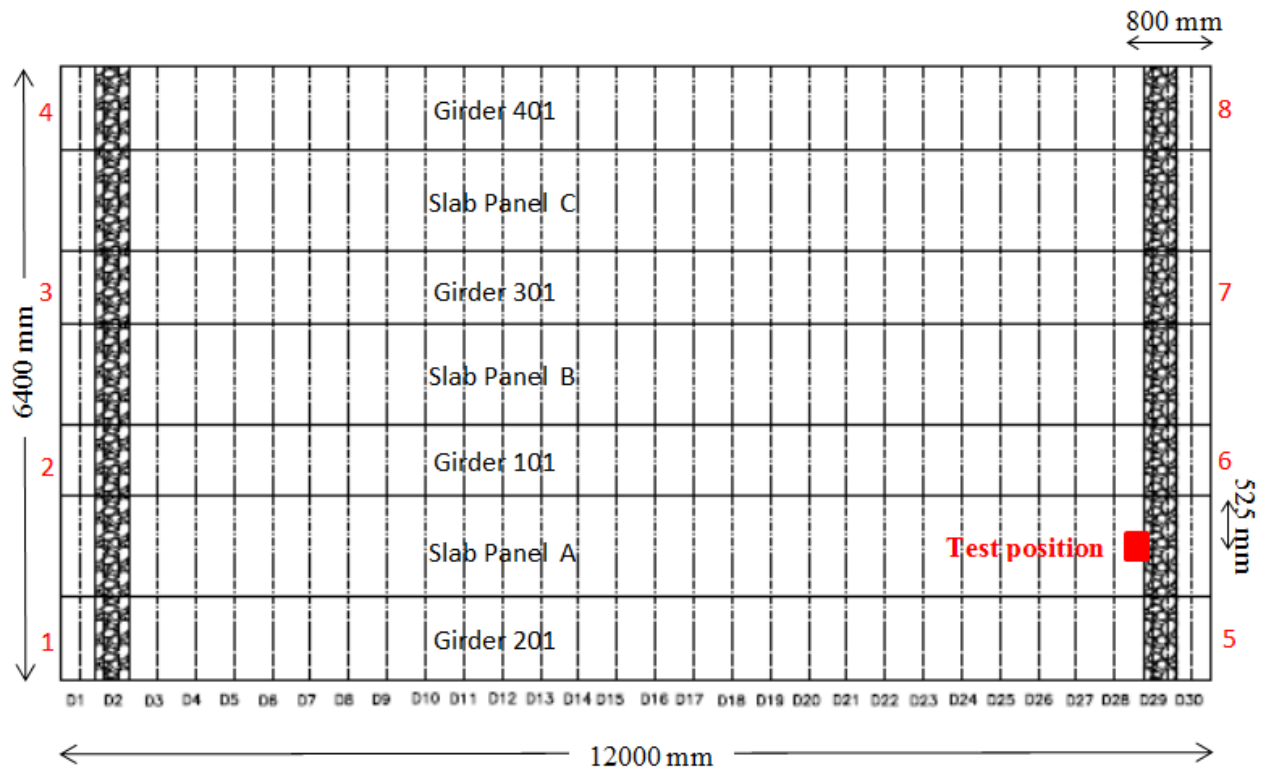


Figure 107 BB-2 Apparatus of structure and load position

Table 19 Response progress

Load F0	Crack Width	Type	Remarks
kN	mm		
75	<0.05	Bottom Diagonal/transverse	Hairline cracks. Hardly visible . Directly under the loading plate
100	0.05	Diagonal/Radial	More diagonal/radial cracking
150	0.1 - 0.15		Spreading of radial cracks/Widening of crack. First circumferential crack observed near Duct 27
200	0.25- 0.3		Propagation of cracks. Longitudinal crack at mid span extending from bottom of deck and going round the front side to the top. Max Crack width directly under load
250	0.45- 0.5		Crack propagation in all directions. Random radial cracks. More circumferential cracks observed outlining the loading plate at the bottom side of the deck.
Crack observations stopped. Load continued (displacement controlled) at 0.01mm/sec			

321.4			Punching started. Maximum load reached.
0.01mm/s			Further displacement allowed punching cone to form fully. More diagonal crack propagation . A circumferential crack appeared between duct 30 and 29.

Table 20 Summary results

Load [kN]	TPL [N/mm ²]	Deflection [mm]	Crack width [mm]
321400	2.5	9.1	0.7

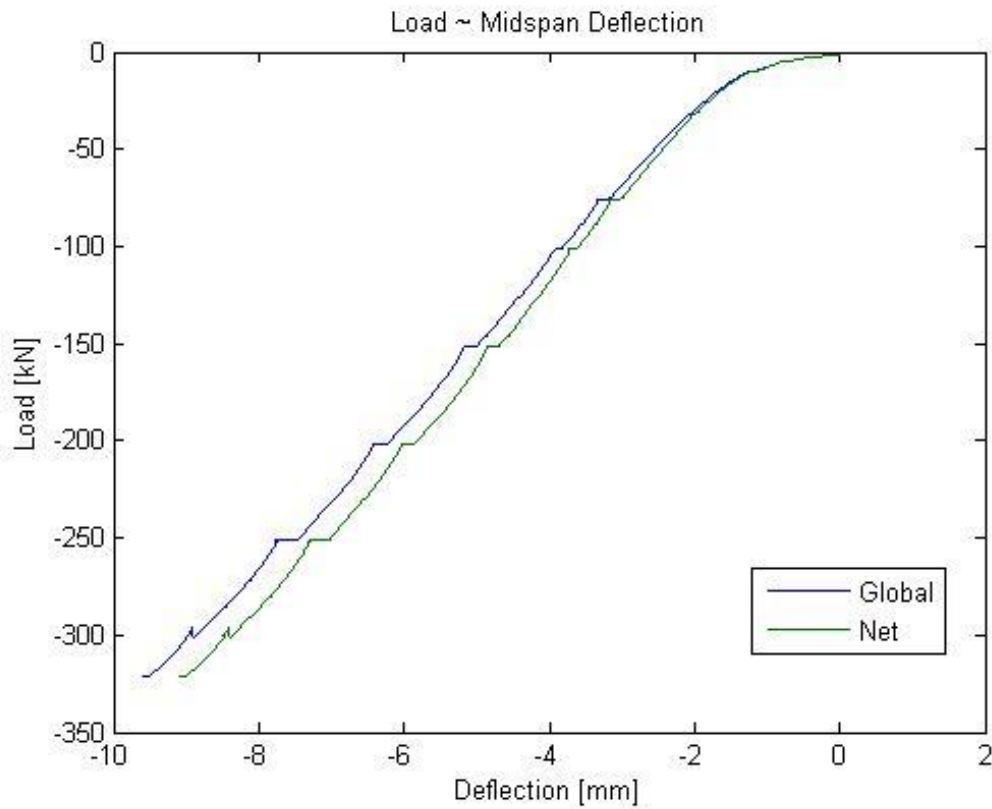


Figure 108 Load – Midspan Deflection Response

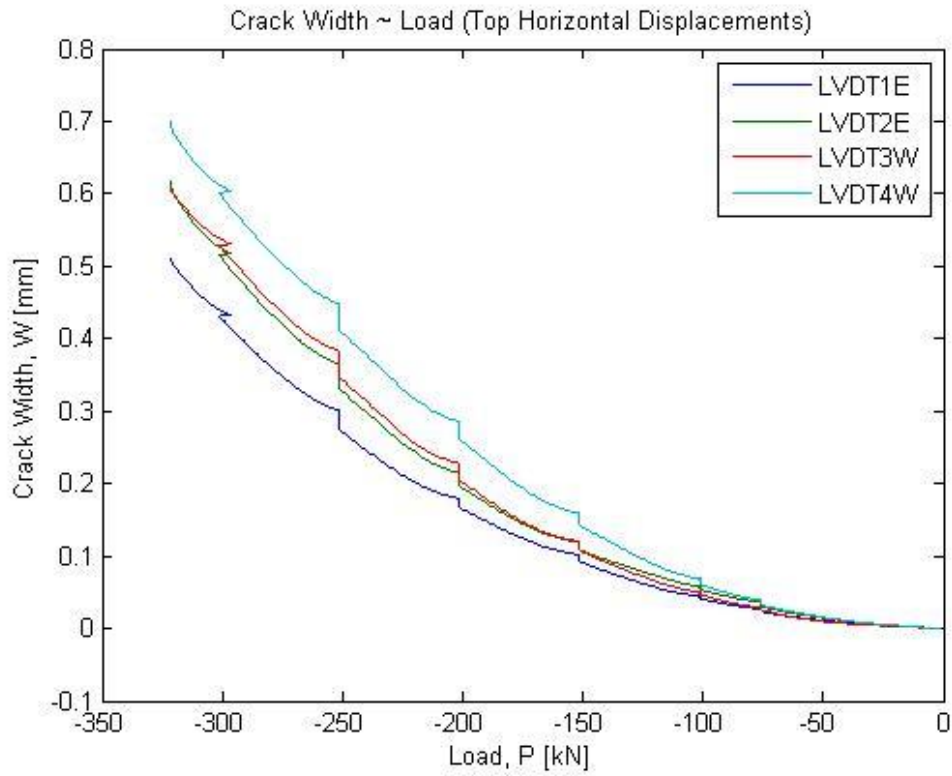


Figure 109 Crack width-Load curve

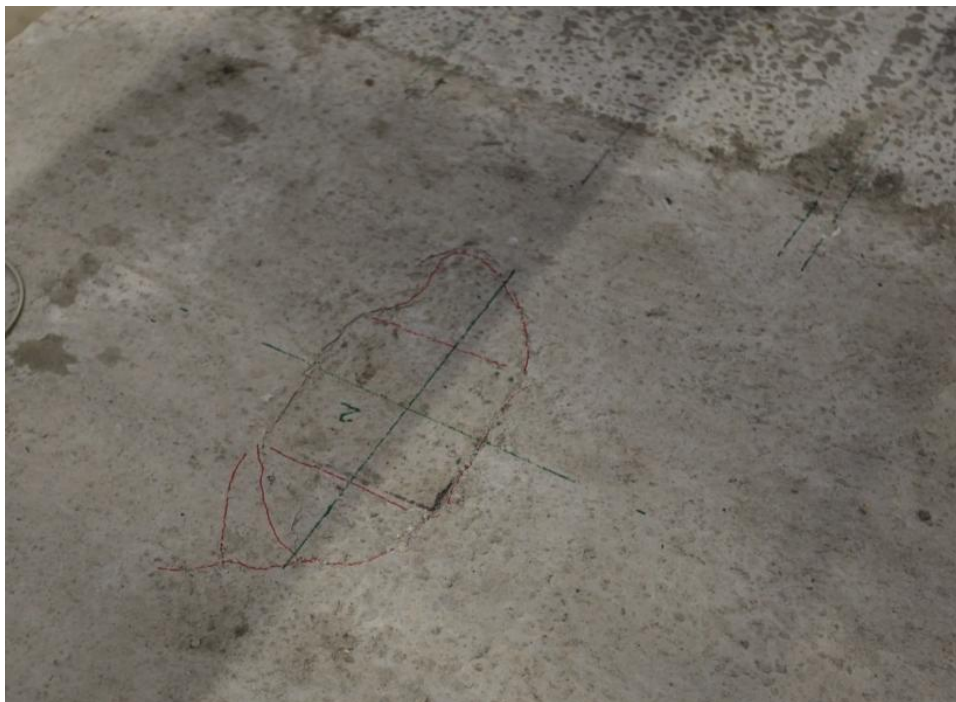


Figure 110 Top side of deck slab after failure



Figure 111 Bottom side of deck slab after failure

- Experiment: BB-16

This test was carried out on 6th May, 2013 at Stevin II laboratory, CITG faculty, Delft University of Technology.

Load was applied in 50 kN increments @1kN/sec till 400 kN. Later the actuator was switched to displacement control at 0.01 mm/sec till failure. The load was applied at two points with a c/c distance of 600 mm at the midspan.

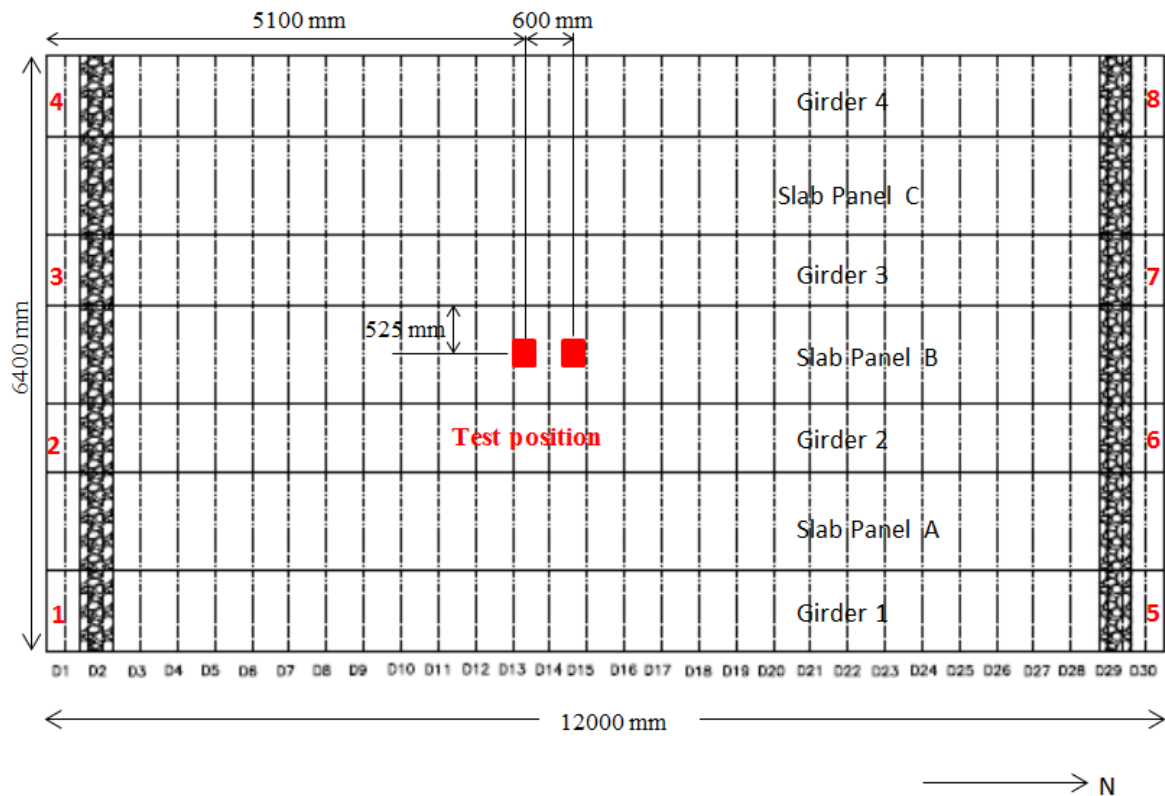


Figure 112 BB-16: Apparatus of structure and load

Table 21 Response progress

Load F_0 , kN	Crack Width [mm]	Type	Remarks
50	-	-	-
100	--	-	-
150	0.05*	Longitudinal/ Transverse/ Radial	First crack in the longitudinal crack direction between the two load points. Hairline transverse and radial cracks.
200	0.1*-0.05**- Hairline***	Longitudinal/ Radial	Propagation of initial cracks. New longitudinal and radial cracks.
250	0.2*-0.15**- 0.1***	Longitudinal/ Transverse/ Radial	More cracks in different directions,. Propagation of previous cracks.
300	0.3*-0.2**- 0.1***	Radial	More radial/diagonal cracks. Widening and propagation of previous cracks. Shrinkage crack at duct 15 widening.
350	0.45*-0.3**- 0.15***	Radial	New radial cracks. Propagation and widening of previous cracks. Shrinkage crack 0.4 mm wide.

400	0.8*-0.35**- 0.2***	Radial	
Displacement controlled load at 0.01 mm/sec. Observations stopped.			
553.4			Large rotations observed. Circumferential crack around loading point 1. Punching Shear Failure. Top side punched through the loading plate 1.

*Initial Longitudinal crack **Radial crack at load point 1 ***Transverse crack at load point 1

Table 22 Summary results

Load [kN]	TPL [N/mm ²]	Deflection [mm]	Crack width [mm]
553.4	2.5	9.97	

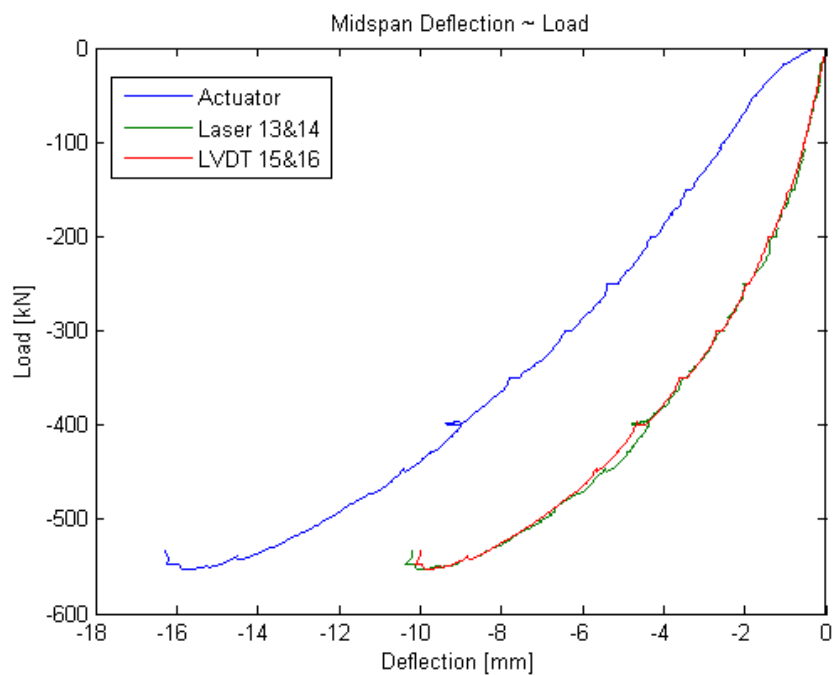


Figure 113 Load – Midspan Deflection Response3

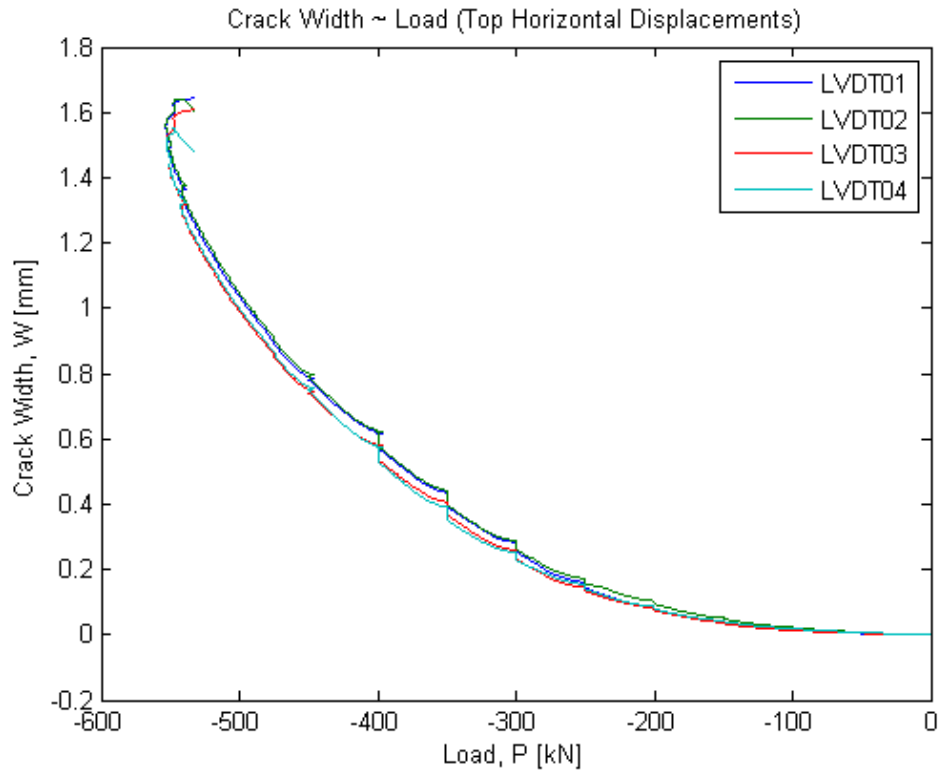


Figure 114 Load - Crack width

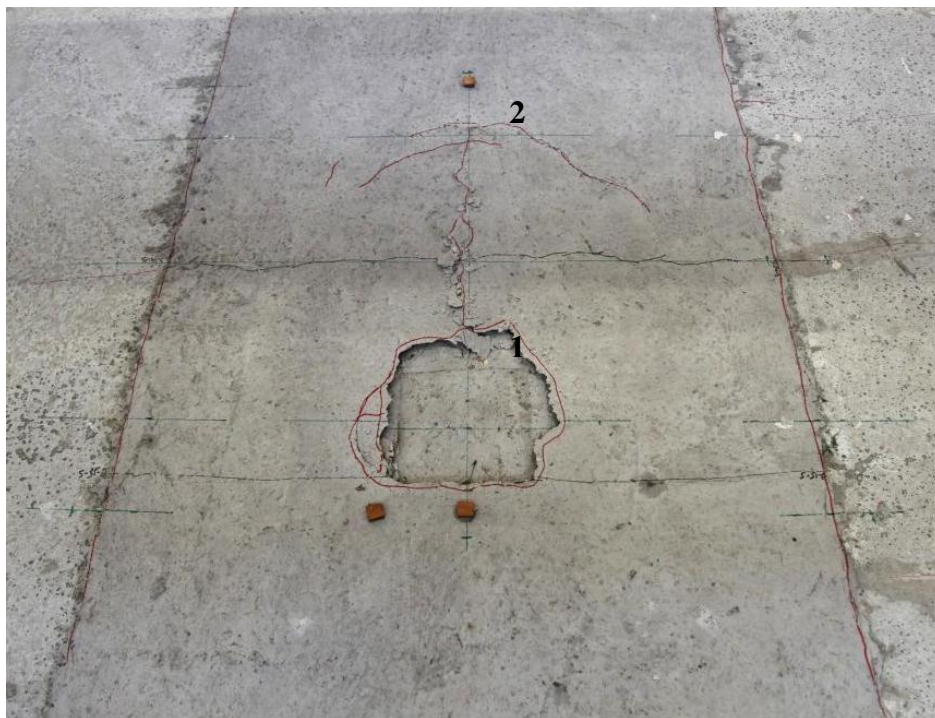


Figure 115 Top side of the deck slab

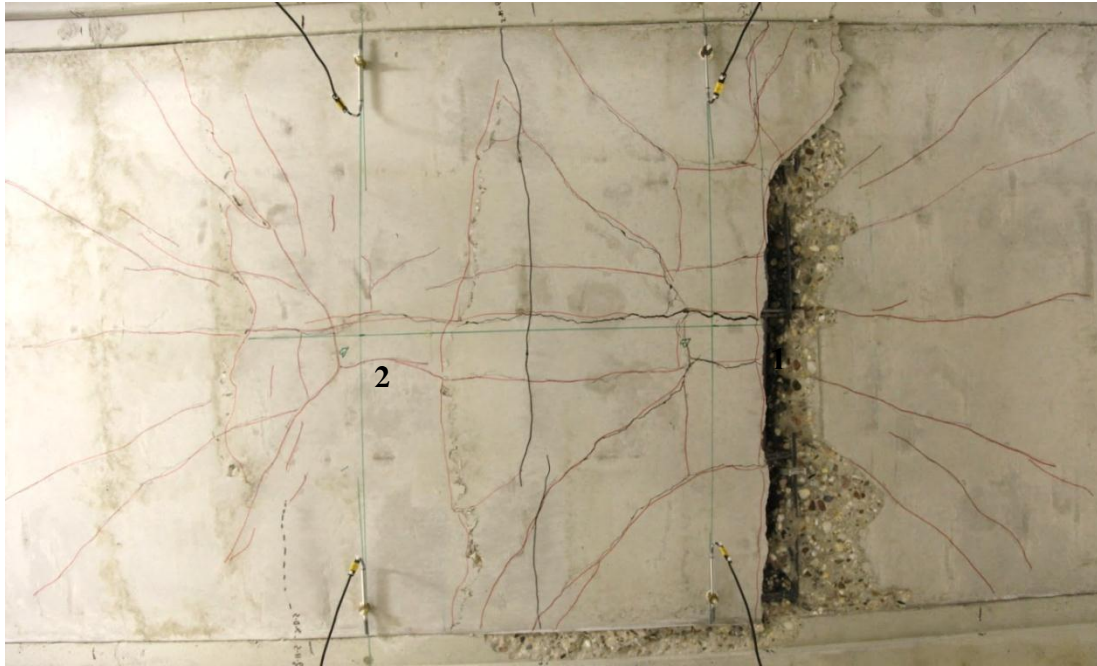


Figure 116 Bottom side of deck slab showing the cracks

BENDING: EXPERIMENTS

i. Experiment BB-5

The fifth test of the series was carried out on 25th February, 2013. The load was applied in 50kN increments @1kN/sec till 350kN. The position of the load and the distances are depicted below. The applied prestress level was 2.5MPa.

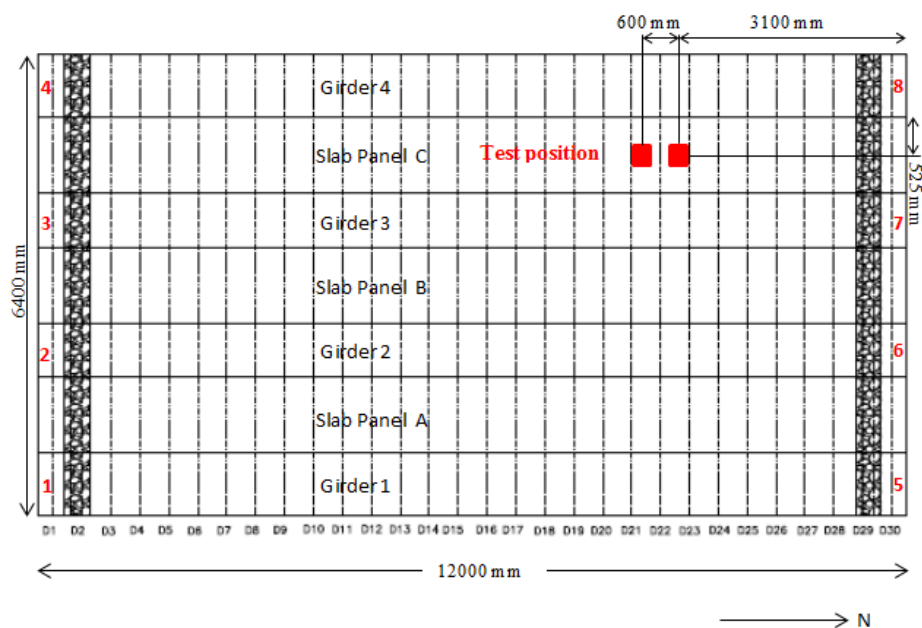


Figure 117 Apparatus of structure and load

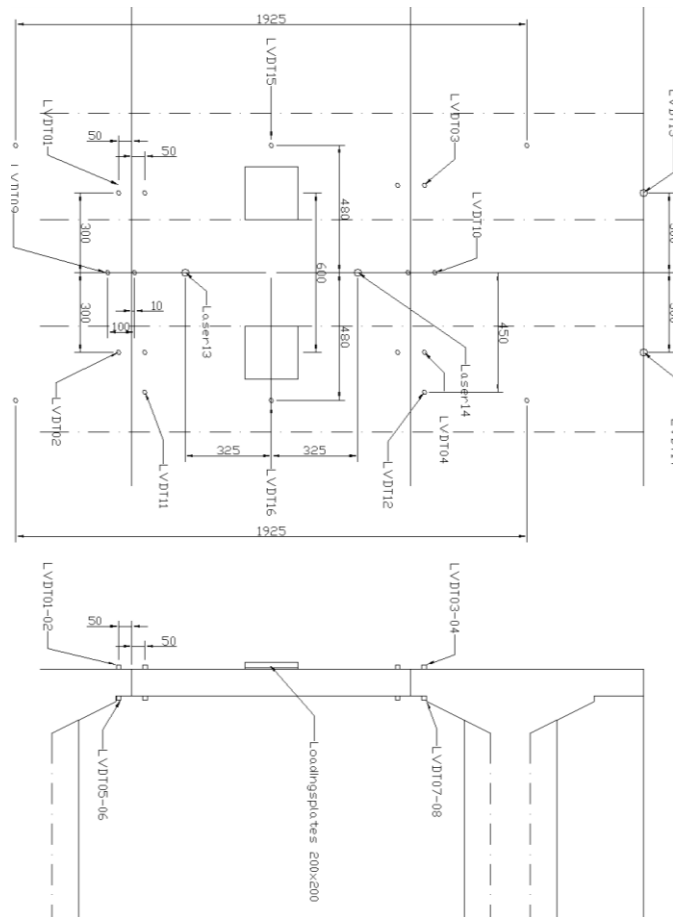


Figure 118 Detail of the load position

Table 23 Response progress

Load F_0 [Kn]	Crack Width [mm]	Type	Remarks
50			
100			
150	0.05	Longitudinal/ Transverse/ Radial	First crack in the longitudinal direction between the 2 loading points, transverse cracks at both loading points, radial crack at load point 1.
200	0.05-0.1		Propagation of the initial cracks.
250	0.15-0.2	Longitudinal/ Transverse/ Radial	More cracks in different directions, propagation of previous cracks. Maximum crack width at the initial longitudinal crack.
300	0.3	Radial	More radial/diagonal cracks. Widening and propagation of previous cracks. Maximum crack width at the initial longitudinal crack

350	0.45-0.5	Radial	More radial/diagonal cracks. Propagation of previous cracks. Longitudinal crack getting wider.
Displacement controlled load at 0.005 mm/sec, then changed to 0.01 mm/sec at 370 kN. Observations stopped.			
400			
450			
469.7			Load dropped for a while and then again started increasing at increasing deflections.
490.4			No further load increase was possible. Increase in rotation. Flexural failure with a number of radial cracks at the loading points.
250	2.5		Longitudinal crack of 2.5 mm width.

Summary results:

Load [kN]	TPL [N/mm ²]	Deflection [mm]	Crack width [mm]
490.4	2.5	9.56	2.51

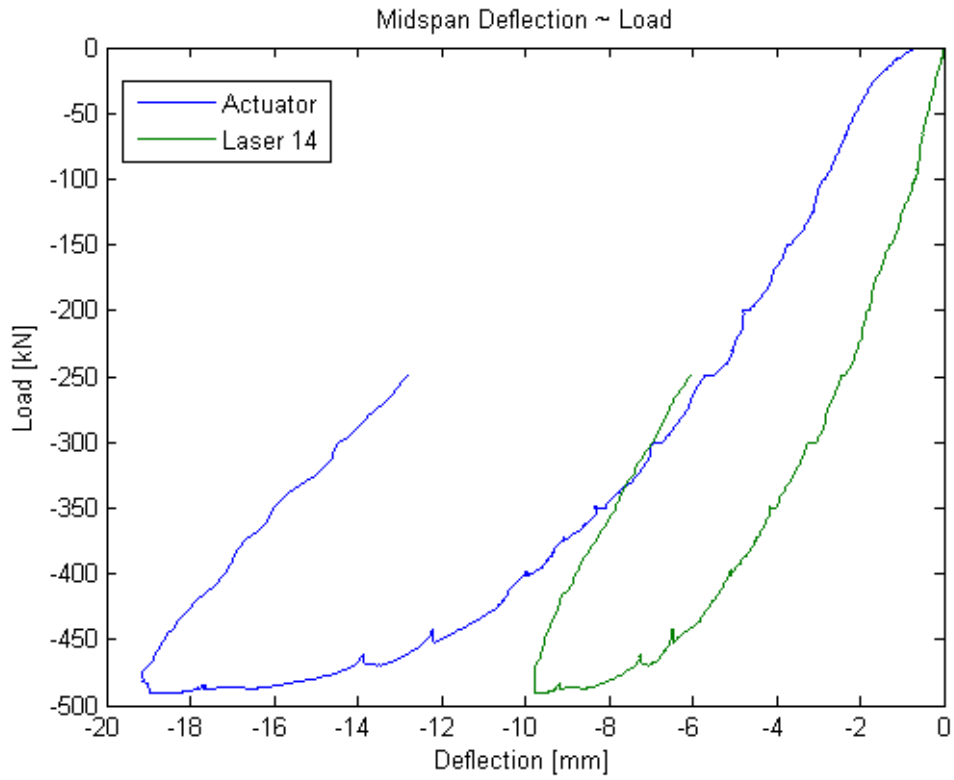


Figure 119 Load – Midspan Deflection Response



Figure 120 Bottom side of deck slab after failure



Figure 121 Top side of deck slab after failure

ii. Experiment BB-11

The eleventh test of the series was carried out on 27th March, 2013. The load was applied in 50kN increments @1kN/sec till 237kN. The position of the load and the distances are depicted below. The applied prestress level was 1.25MPa.

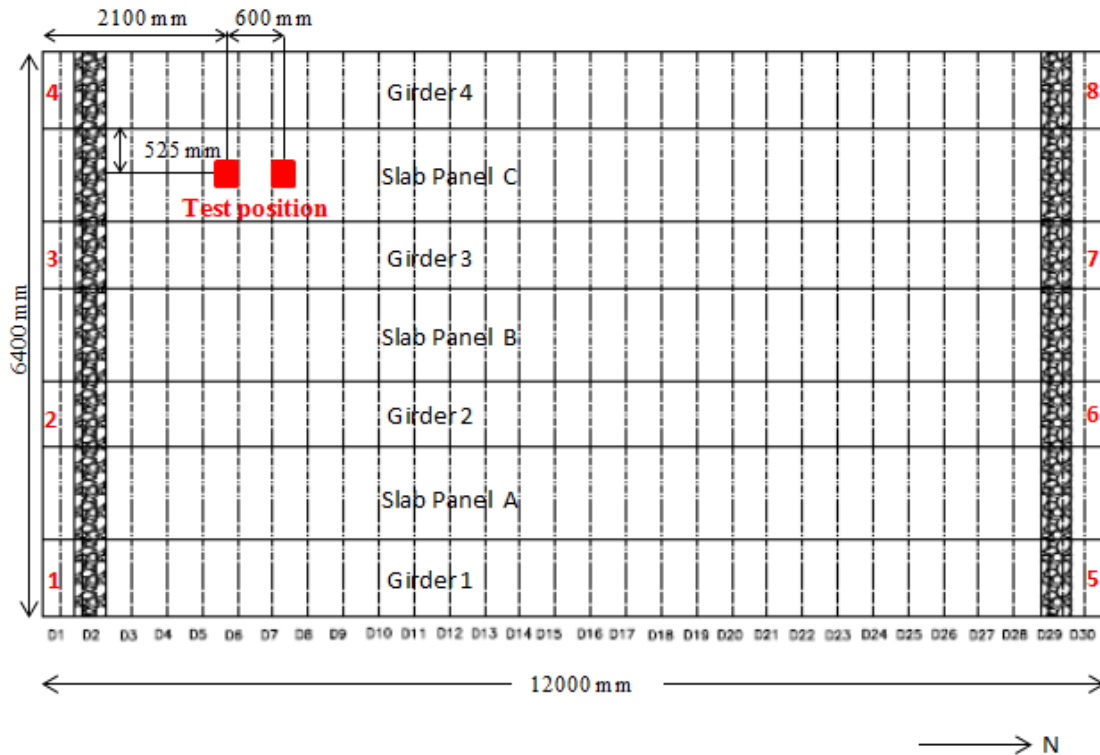


Figure 122 Apparatus of structure and load

Table 24 Response progress

Load F_0 [Kn]	Crack Width [mm]	Type	Remarks
50	Hairline	Transverse	A short transverse crack at load point 1.
100	0.05*	Longitudinal	First longitudinal crack *between two point loads. Initial transverse crack at load point 1 remains hairline.
150	0.15* Hairline** Hairline***	Transverse/ Radial	New transverse cracks at both loading points. Radial crack at load point 1. Longitudinal crack propagates further.
200	0.3*-0.05** 0.1***	Longitudinal/ Transverse/ Radial	New longitudinal cracks. New transverse crack under load point 2. Long radial cracks. Propagation of previous cracks.
Displacement controlled load at 0.01 mm/sec at 237 kN.			
250	0.9*-0.15** 0.3***	Radial	Radial cracks. Propagation of previous cracks. Maximum crack width at the initial longitudinal crack.
300	2*-0.35** 0.7***	Radial	More radial cracks. Widening and propagation of previous cracks. Maximum crack width at the

			initial longitudinal crack.
Observations stopped. Crack width of longitudinal crack at 350 kN = 5mm*			
377.85			Flexural failure with no further increase in load. Large increase in prestressing force.

Summary results:

Load [kN]	TPL [N/mm ²]	Deflection [mm]	Crack width [mm]
377.85	1.25	7.11	2.65

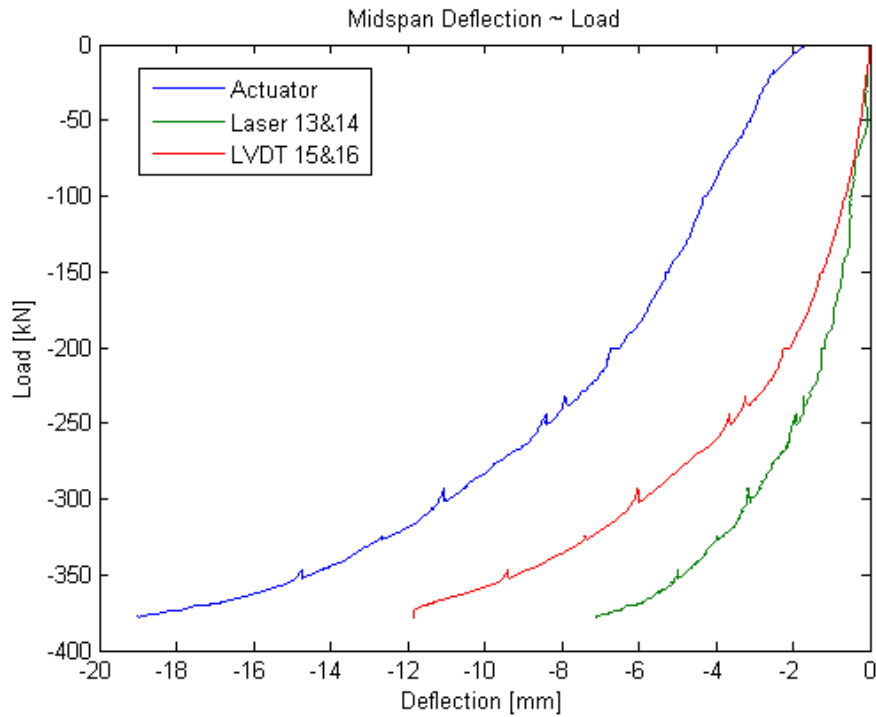


Figure 123 Load – Midspan Deflection Response



Figure 124 Bottom side of deck slab after failure

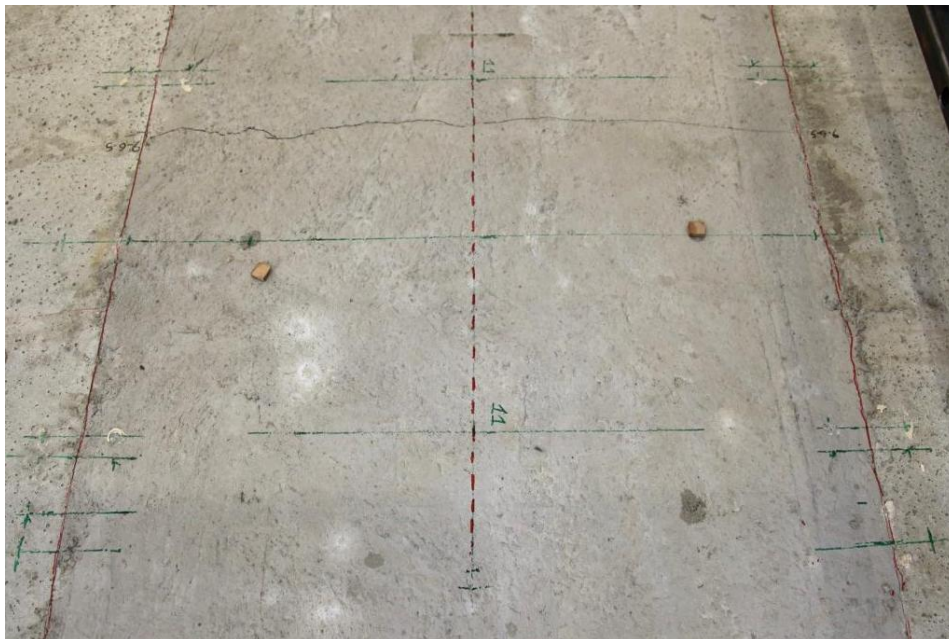


Figure 125 Top side of deck slab after failure

Conclusions:

- v. Large rotations occurred at the peak load leading to longitudinal cracks between the double loading points.
- vi. No further increase in the capacity after the failure was occurred.

- vii. The skewed interface has sufficient capacity to bear the vertical load, since no interface failure occurred during the experiments.
- viii. No significant loss of prestressing steel occurred, verifying the initial assumption to neglect the prestress losses.

APPENDIX II

- Verification of the code Fortran 95

The bending capacity of the model bridge is calculated based on numerical analysis on Fortran 95. A lot of research has been carried out in the past to estimate the bending resistance of slabs taken into account the effect of the compressive membrane action. In the Master thesis of a code casted in Fortran 75 has been used to calculate the bending capacity of a frame-slab. This code is an invaluable engineering tool for capacities of any kind of slabs, since it has taken into account the following important parameters, as well as their effects:

- Compressive membrane action (N_u)
- Effect of regular reinforcement or prestress (F_{ps})
- Strain hardening of reinforcement steel
- The position of the loaded part in the slab (case 1, case 2)
- The temperature changes, creep, shrinkage
- Symmetrical or unsymmetrical conditions at the supports

This code had to deal with the prestressed slabs in the longitudinal direction supported by columns.

At the present master thesis this code could not be applicable without modifications and adjustments.

At the first step the original code had to be re-casted in order to be compatible with the newer version Fortran 95. Some of the old commands were necessary to be replaced with new commands executing the same function. After recasting the updated code was tested before it is applied at the present case.

It gave exactly the same results with the old code, verifying the validity of the updated one.

At the second step the code had to be adjusted to the conditions of the structure of the model bridge.

The structure at the initial code has many important differences from the structure at the present case. The bridge model, constructed in the Stevin Lab II, CITG TUDelft, differs from the aforesaid structure at the next points:

- Present case: the bridge is supported laterally by the concrete girders. These girders can provide adequate restraint to the slab leading to the development of compressive membrane forces in the transverse direction. Thus, the axial and flexural stiffness are given by the girders and the surroundings panels.
Past case: it is supported by columns and cross beams. Thus, the axial and flexural stiffness are given by the beams, the columns and the surrounding panels.
- Present case: the bridge is prestressed in the transverse and longitudinal direction.
Past case: it is prestressed only in the longitudinal direction and only the effect of the regular reinforcement was taken into account employing the Modified trilinear idealization for mild steel [Sargin, 1971] to simulate the strain hardening of steel.

At the next table the results of the original code are presented, which are precisely the same with that from the relative Master thesis.

➤ Example - Analysis of Interior Slab

Tables B.1 and B.2 show input and output files, respectively, for the analysis of an interior slab in the parking structure. The input file for the analysis of Slab having a remain stiffness of 257 N/rnm², was arbitrarily chosen to demonstrate the input and output files for the analysis of an interior slab. A summary of the program execution is also given at the end of the output file to show the size of the program.

Table B.1: Input Data

INPUT FILE							
S	4840	140	16500				
L	114	26	114	26	114	26	
A	100	110	100	71950			
B	4714	4125	4714	0	0	0	2159

	30	24648	0.805	0.895
D	200000	9000	400	600
A	0.002	0.006	0.08	
T	1120	1860	200000	
A	0.025	118	10	
	0	0		
	1			
S	Case 1: Interior slab loaded			
U	257.1			
P				
P				
O				
R				
T				
DATA				

Table B.2 Output Data

INTERIOR SLAB LOADED -SINGLE SLAB STRIP USED			
EFFECTIVE	MAXIMUM		
SUPPORT	ULTIMATE	VERTICAL	LOAD
STIFFNESS	CAPACITY	DEFLECTION	ENHANCEMENT
257.1	0.0272	29.87	1.51
AXIAL	MOMENT AT PLASTIC HINGE		
FORCE	1	2	3
0.546E+07	0.738E+09	0.739E+09	0.738E+09

Numbers of Warnings 0

Numbers of Errors 0

➤ Example - Analysis of Interior Slab

Table B.3 Input Data

INPUT FILE						
S	4745	140	16500			
L	114	26	114	26	114	26

A	100	110	100	71950			
B	4714	4125	4714	0	0	0	2888
	30	24648	0.805	0.895			
D	200000	9000	400	600			
A	0.002	0.006	0.08				
T	1120	1860	200000				
A	0.025	118	10				
	0	0					
	2						
S	Case 2: Exterior slab loaded						
U	975						
P	4850	2425	375	$7.02 \cdot 10^{14}$			
P	750	300	12000	$4.16 \cdot 10^{13}$	$5.35 \cdot 10^{13}$		
O	5						
R							
T							
DATA							

Numbers of Warnings 0

Numbers of Errors 0

Table B2: Results

EXTERIOR SLAB LOADED - 5 SLAB STRIPS USED			
Strip number [NUM]	Effective support stiffness [S]	Ultimate capacity [WU]	Load enhancement [LE]
1	295.1	0.0301	1.44
2	4.3	0.0235	1.12
3	0	0.0231	1.11
4	0	0.0231	1.11
5	0	0.0231	1.11

AVERAGE ULTIMATE CAPACITY IS 0.02

AVERAGE LOAD ENHANCEMENT IS 1.18

TOTAL AXIAL FORCE APPLIED TO A COLUMN IS 0.574E+06
TOTAL MOMENT APPLIED TO AN EXTERIOR COLUMN IS 0.257E+09
TOTAL MOMENT APPLIED TO AN INTERIOR COLUMN IS 0.305E+09

APPENDIX III

NUMERICAL CODES

Hereby, the original and the updated code are given below:

ORIGINAL CODE

```
*****  
SLAB  
*****  
IMPLICIT DOUBLE PRECISION (A-Z)  
INTEGER CASE,NUM  
OPEN (1, FILE='TERMINAL')  
OPEN (5,FILE='INPUT')  
OPEN (6, FILE='OUTPUT' )  
READ (5,*) L,H,B,  
+ D1,D11,DZ,D12, D3, D13,  
+ DP1, DP2, DP3, LPS,  
+ AS1, AS2, AS3, ASP1,ASP2,ASP3,ASP,  
+ FC, EC, A1, BI,  
+ ES, ESH, FYS, FUS,  
+ EYY, ESSH, EUU,  
+ FPE, FPU, EP,  
+ AA, BB, CC,  
+ K, EST,  
+ CASE  
IF (ASP.EQ.0) THEN  
GOTO 10  
ELSE  
CALL ISTRN (EPPI, FPE, EP, AA, BB, CC)  
ENDIF  
10 GOTO (100,200,300), CASE  
100 READ(5, *) S  
CALL INT(L,H,B, D1,D11,D2,D12, D3, D13, DP1, DP2,DP3,LPS,AS1,AS2,  
+ AS3,ASP1,ASP2,ASP3,ASP,FC,EC,A1,B1,ES,ESH,FYS,FUS,  
+ EYY,ESSH,EUU,EPPI,FPE,FPU,EP,AA,BB,CC,K,EST,S)  
GOTO 400  
200 READ(5,*) S3,  
+ LC1, LCB1, WCOL, EIC1,  
+ HB1, BB1, LB1, EIB1, JGB1,  
+ NUM  
CALL EXT (L, H, B, D1, D11, D2, D12, D3,D13, DP1, DP2,  
+ DP3,LPS,AS1,AS2,AS3,ASP1, ASP2, ASP3,ASP,FC,EC,A1,  
+ B1, ES, ESH,FYS, FUS,
```

```

+      EYY, ESSH, EUU, EPPI, FPE, FPU, EP,AA, BB, CC, K, EST,
+      S3, LC1,LCB1, WCOL, EIC1, HB1, BB1, LB1, EIB1, JGB1, NUM)
GOTO 400
300 READ(5,*) S3,
+      LC1, LCB1,WCOL,EIC1,
+      HB1, BB1, LB1, EIB1, JGB1,
+      NUM
S3=1E38
EIC1=1E38
CALL EXT (L,H, B, D1, D11, D2, D12,D3, D13, DP1, DP2, DP3,
+      LPS,AS1,AS2,AS3,ASP1, ASP2,ASP3,ASP, FC, EC,A1, B1,ES,
+      ESH, FYS, FUS, EYY, ESSH, EUU, EPPI, FPE, FPU, EP,AA, BB,
+      CC, K, EST, S3, LC1, LCB1, WCOL, EIC1, HB1, BB1, LB1, EIB1, JGB1 , NUM)
GOTO 400
400 END

```

```

*****
SUBROUTINE EXT (L,H,B, D1, D11, D2,D12, D3,D13,
+      DP1,DP2,DP3,LPS, AS1, AS2,AS3,ASP1,ASP2, ASP3,ASP,FC,
+      EC,A1,B1,ES, ESH, FYS, FUS, EYY, ESSH, EUU, EPPI,
+      FPE, FPU, EP, AA, BB, CC, K, EST, S3, LC1, LCB1, WCOL, EIC1,
+      HB1, BB1, LB1, EIB1,JGB1, NUM)
*****

```

```

IMPLICIT DOUBLE PRECISION (A-Z)
INTEGER NUM, X , Z ,Y
DIMENSION DIST (15) , S1 (15) , SE (15) , F1SLAB (30) ,
+      F3SLAB (30) , CC1 (15) , CC3 (15) , WWU (15) , DDL (15) , SSMOVE (15),
+      D1SLAB (15) , RMOVE (15), VV1 (15), VV3 (15) , LE (15)
* CALCULATE WIDTH OF STRIPS AND STEEL IN STRIPS
B=B/(2* NUM)
ASP1=ASP1/(2 *NUM)
ASP2=ASP2/(2 *NUM)
ASP3=ASP3/(2 *NUM)
ASP=ASP/(2 *NUM)
AS1=AS1/(2 *NUM)
AS2=AS2/(2 *NUM)
AS3=AS3/(2 *NUM)
* CALCULATE SLAB CAPACITY NEGLECTING COMPRESSIVE MEMBRANE
* AND STRAIN HARDENING
SO=1E-30
ENSH=0
CALL STRIP(L,H,B, D1, D11, D2,D12, D3,D13,
+      DP1,DP2,DP3,LPS, AS1, AS2,AS3,ASP1,ASP2, ASP3,ASP, FC,
+      EC,A1,B1,ES, ESH, FYS, FUS, EYY, ESSH, EUU, EPPI,
+      FPE, FPU, EP, AA, BB, CC, K, EST, S, NU,
+      MU1,MU2,MU3,C1,C2,C3,WU, DL,SMOVE,BH,V1,V3)
* SET STIFFNESS OF FIRST SLAB STRIP EQUAL TO FLEXURAL
* STIFFNESS OF EDGE BEAM AT MIDDLE OF FIRST SLAB STRIP AND
* ITERATE TO GET STIFFNESS DISTRIBUTION
DO 10 X=1,NUM
S1 (X)=(1/(2/(3*EIC1*LC1**3/( LCB1**3*(LC1-LCB1)**3)) + ( LB1/
+      (4*NUM) **2 / (6*EIB1*LB1**3)* (3*LB1**3*( LB1/( 4*NUM)) -
+      LB1**3*( LB1/(4*NUM)-3*LB1**2*( LB1/( 4*NUM) )**2))) ) /B
DIST (X) =1
SE(1)=1/ (1/S1(1) +1/S3)
10 CONTINUE
140 Z=0

```

```

70  Z=Z+1
    DO 20 X=1, NUM
20  SE (X) =DIST (X) * SE (1)
* CALCULATE FORCES AND DISPLACEMENTS OF STRIPS
DO 30 X=1,NUM
S=SE (X)
CALL STRIP(L,H,B, D1, D11, D2,D12, D3,D13,
+      DP1,DP2,DP3,LPS, AS1, AS2,AS3,ASP1,ASP2, ASP3,ASP, FC,
+      EC,A1,B1,ES, ESH, FYS, FUS, EYY, ESSH, EUU, EPPI,
+      FPE, FPU, EP, AA, BB, CC, K, EST, S, NU,
+      MU1,MU2,MU3,C1,C2,C3,WU, DL,SMOVE,BH,V1,V3)
F1SLAB (X) = NU
F1SLAB (X+NUM) =MU1
CC1 (X) =C1
VV1(X) =V1
F3SLAB(X) =NU
F3SLAB (X+NUM) =MU3
CC3 (X) =C3
VV3 (X) =V3
WWU(X) =WU
LE (X) =WU/WUO
DDL (X) =DL
30 SSMOVE (X) =SMOVE
* CALCULATE MOVEMENT OF SUPPORTS
TNU=0
DO 40 X=1, NUM
40  TNU=2*F3SLAB(X)+TNU
D3SLAB=TNU/(B*2*NUM*S3)
CALL REST (H,LC1 ,LCB1 , WCOL,EIC1,HB1 , BB1 , LB1 , EIB1 , L JGB1 ,
+      F1SLAB, CC1, D1SLAB, NUM, VV1 )
50  RMOVE (X) =D1SLAB (X) + D3SLAB
* CALCULATE DISTRIBUTION OF EFFECTIVE STIFFNESS
IF(Z.EQ.1)THEN
DO 60 X=F1SLAB(X) /RMOVE(X) /(F1SLAB (1) / RMOVE (1))
ELSE
CONTINUE
ENDIF
* DEFINE POINTS ON TWO LINES TO CALCULATE COMPATIBLE STIFFNESS
IF(Z.EQ.1)THEN
SM1=SSMOVE ( 1)
RM1=RMOVE (1)
SEFF1 = SE ( 1 )
SE(1)=.7*SE (1)
GOTO 70
ELSE IF(Z.EQ.2)THEN
SM2=SSMOVE ( 1 )
RM2 =RMOVE ( 1 )
SEFF2=SE ( 1 )
ELSE
SM1=SM2
RM1 = RM2
SEFF1 =SEFF2
SM2 =SSMOVE ( 1 )
RM2=RMOVE ( 1 )
SEFF2=SE ( 1 )
ENDIF
WRITE(1,*) 'ITERATION',Z

```

```

* PREVENT POSSIBLE INFINITE LOOP
IF(Z.LT.50)THEN
GOTO 80
ELSE
WRITE (1,*) ' SOLUTION DID NOT CONVERGE'
GOTO 700
ENDIF
* CHECK IF STRIP AND RESTRAINT MOVEMENT ARE EQUAL FOR FIRST
* STRIP
80 (SSMOVE(1)-RMOVE(1)) /SSMOVE(1)) .LT.0.01)THEN
GOTO 90
ELSE
GOTO 100
ENDIF
* CALCULATE NEXT ESTIMATE OF STIFFNESS
100 SEFF=(SEFF2-SEFF1)*(RM1-SM1)/(SM2-SM1-RM2+RM1)+SEFF1
IF (SEFF . LT . 0 ) THEN
SEFF=1E-5
ELSE
CONTINUE
ENDIF
SE ( 1 ) =SEFF
GOTO 70
* CHECK IF STRIP AND RESTRAINT MOVEMENT ARE EQUAL FOR OTHER
* STRIPS
90 WRITE(1,*) 'MATCHED STRIP FIRST STRIP ... CHECKING ALL STRIPS'
Y=1
120 IF(ABS( (SSMOVE(Y)-RMOVE(Y))/SSMOVE(Y)).GT.0.01)THEN
GOTO 110
ELSE IF(Y.LT.NUM)THEN
WRITE(1,*) 'MATCHED STRIP #',Y
Y=Y+1
GOTO 120
ELSE
WRITE(1,*) 'MATCHED STRIP #',Y
GOTO 150
ENDIF
* CALCULATE NEW DISTRIBUTION OF STIFFNESS
110 DO 130 X=1,NUM
130 DIST(X)=F1SLAB(X) /RMOVE(X) /(F1SLAB(1)/RMOVE(1))
GOTO 140
150 WRITE (1,*) 'SLAB HAS CONVERGED TO A SOLUTION'
* CALCULATE TOTAL AXIAL FORCE AND MOMENT APPLIED TO COLUMNS AND
* AVERAGE LOAD CAPACITY AND LOAD ENHANCEMENT
NUT=0
MU1T=0
MU3T=0
WTOT=0
DO 160 X=1,NUM
NUT=NUT+F1SLAB (X)
MU1T=MU1T+F1SLAB (X+NUM)
MU3T=MU3T+F3SLAB (X+NUM)
160 WTOT=WTOT+WWU (X)
WAVG=WTOT/NUM
AVGLE=WAVG/WUO
* OUTPUT DATA
WRITE (6,1) NUM

```

```

DO 170 X=1,NUM
170  WRITE (6,2) X, SE(X) , WWU (X), LE (X)
WRITE (6,3)  WAVG, AVGLE, NUT, MU3T, MU1T
  1 FORMAT(/,'EXTERIOR SLAB LOADED -', I3, ' SLAB STRIPS USED ', //,
    + ' EFFECTIVE
    +,/, ' STRIP      SUPPORT      ULTIMATE
+ ' LOAD ', /, ' NUM STIFFNESS CAPACITY ',
+ ' ENHANCEMENT ' )
2 FORMAT(I3, ' ,F6.1,F18.4,F19.2)
3 FORMAT(//'AVERAGE ULTIMATE CAPACITY IS ', F6.2,//,
+'AVERAGE LOAD ENHANCEMENT IS',F7.2,///,
+'TOTAL AXIAL FORCE APPLIED TO A COLUMN IS'.
+ E17.3,//,'TOTAL MOMENT APPLIED TO AN EXTERIOR COLUMN
+ IS',E12.3,
+ //, ' TOTAL MOMENT APPLIED TO AN INTERIOR COLUMN IS ', E12.3, /)
700  CONTINUE
END

```

```

*****
SUBROUTINE INT(L,H,B, D1, D11, D2,D12, D3,D13,
+ DP1,DP2,DP3,LPS, AS1, AS2,AS3,ASP1,ASP2, ASP3,ASP, FC,
+ EC,A1,B1,ES, ESH, FYS, FUS, EYY, ESSH, EUU, EPPI,
+ FPE, FPU, EP, AA, BB, CC, K, EST, S)
*****
IMPLICIT DOUBLE PRECISION (A-Z)
SO=1E-30
ENSH=0
CALL STRIP (L,H,B, D1, D11, D2,D12, D3,D13, DP1,DP2,DP3,LPS,
+ AS1, AS2,AS3,ASP1,ASP2, ASP3,ASP, FC,EC,A1,B1,ES, ENSH,
+ FYS, FUS, EYY, ESSH, EUU, EPPI,FPE, FPU, EP, AA, BB, CC,
+ K, EST, SO, NU,MU1,MU2,MU3,C1,
+ C2,C3,WUO,DL,SMOVE,BH,VI,V3)
ENSH=0
CALL STRIP (L,H,B, D1, D11, D2,D12, D3,D13, DP1,DP2,DP3,LPS,
+ AS1, AS2,AS3,ASP1,ASP2, ASP3,ASP, FC,EC,A1,B1,ES, ESH,
+ FYS, FUS, EYY, ESSH, EUU, EPPI,FPE, FPU, EP, AA, BB, CC,
+ K, EST, S, NU,MU1,MU2,MU3,C1, C2,
+ C3,WU,DL,SMOVE,BH,VI,V3)
LE=WU/WUO
WRITE(1,*)'SLAB HAS CONVERGED TO A SOLUTION'
*OUTPUT DATA
WRITE (6,1)
WRITE(6,2) S,WU,DL, LE
WRITE(6,3)
WRITE(6,4) NU, MU1,MU2,MU3
1 FORMAT(/,'INTERIOR SLAB LOADED -SINGLE SLAB STRIP USED', //,
+ ' EFFECTIVE      MAXIMUM      ', /
+ ' SUPPORT      ULTIMATE      VERTICAL      LOAD', /,
+'STIFFNESS CAPACITY DEFLECTION ENHANCEMENT ' )
2 FORMAT(F6.1, F18.4,2F16.2)
3 FORMAT ( //, 'AXIAL      MOMENT AT PLASTIC HINGE ', /,
+ ' FORCE      1      2      3')
4 FORMAT(E9.3,3E18.3, /)
RETURN
END
*****

```

```

*****
SUBROUTINE FMILDS (F,ESS,EYY,ESSH,EUU,AS,ES,ESH,FYS,FUS)
*****
IMPLICIT DOUBLE PRECISION (A-Z)
IF(ABS(ESS).LT.EYY) THEN
F=AS*ES*ESS
ELSE IF(ESS.LE. (ESSH*(-1))) THEN
F=O
ELSE IF(ESS.LE.(EYY*(-1))) THEN
F=AS*FYS* (-1)
ELSE IF(ESS.LE.ESSH) THEN
F=AS*EYS
ELSE IF (ESS. LE. EUU) THEN
F=AS*(FYS+ESH*(ESS-ESSH)*(1-ESH*(ESS-ESSH))/(4*(FUS-FYS)))
ELSE
F=O
ENDIF
RETURN
END

```

```

*****
SUBROUTINE ISTRN (EPPI,FPE,EPAA,BB,CC)
*****
IMPLICIT DOUBLE PRECISION (A-Z)
EPPI=0
10 FP=EP*EPPI* (AA+ (1-AA) / (1+ (BB*EPPI) **CC) ** (1/CC) )
IF(FP.LE.FPE) THEN
EPPI=EPPI+0.000001
GOTO 10
ELSE
GOTO 20
ENDIF
20 RETURN
END

```

```

*****
SUBROUTINE REST(HS,LC,LCB, WCOL,EIC,HB,BB,LB,EIB, JGB,
+
FSLAB, CI,DSLAB,NUM,V1)
*****
IMPLICIT DOUBLE PRECISION (A-M, P-W)
INTEGER X, Y, NUM
DIMENSION MID(15),F(30,30), FSLAB(30),FEB(30),DEB(30),DSLAB(15),
+
C1(15) ,V1 (15)
* DETERMINE MIDPOINTS OF STRIPS
DO 10 X=1,NUM
MID(X)=LB/ (4*NUM)+ (X-1) *LB/ (2*NUM)
10 CONTINUE
* CALCULATE FLEXIBILITY MATRIX
KHC=3*EIC*LC**3/(LCB**3*(LC-LCB)**3)
KXC=EIC*LC**3/((-4)*LCB**2*LC**2+LCB*LC**3+6*LCB**3*LC
+
-3*LCB**4)
DO 20 X=1,2*NUM
DO 30 Y=1,2*NUM
IF((X.GT.NUM).AND.(Y.LE.NUM)) THEN

```

```

* EQUATION (4.29)
      F(Y,X) = 2/(6*EIC*LC**3)*(12*LCB**3*LC**2-3*LCB**2*LC**3)
+
      -15*LCB**4*LC+6*LCB**5)
ELSE IF((X.GT.NUM).AND.(Y.LE.X)) THEN
IF( (MID(Y-NUM)) .LE. (WCOL/2)) THEN
* EQUATION (4.14 A)
F(Y, X)=2/KXC
ELSE
* EQUATION (4.14 B)
F(Y,X)=(2/KXC+ (MID(Y-NUM) -0.5*WCOL) /JGB)
ENDIF
ELSE IF( (X.GT.NUM) .AND. (Y.GT.X) ) THEN
* EQUATION (4.14 C)
F(Y,X)=(2/KXC+ (MID(X-NUM) -0.5*WCOL) /JGB)
ELSE IF(Y.GT.NUM) THEN
* EQUATION (4.38)
F(Y,X)=2/(6*EIC*LC)*(-4*LC**2*LCB+15*LC*LCB**2
+
      -20*LCB**3+15*LCB**4/LC-6*LCB**5/LC**2)
ELSE IF(Y.GT.X) THEN
IF( (MID(Y) .LE. (WCOL/2)) THEN
! EQUATION (4.11 A)
F(Y,X)=2/KHC
ELSE
* EQUATION (4.11 B )
      F(Y, X)=2/KHC+ (MID(X)- 0.5 *WCOL)* **2/ (6*EIB*LB**3)*
+
      (3*LB**3*MID (Y) - LB**3*MID(X) -LB**3*WCOL-
+
      3*LB**2* (MID (Y) -0.5*WCOL) **2)
ENDIF
ELSE
! EQUATION (4.11 C)
F(Y,X)=2/KHC+(MID(Y)-0.5*WCOL)**2/(6*EIB*LB**3)*
+
      (3*LB**3*MID (X) -LB**3*MID(Y) -LB**3*WCOL-
+
      3*LB**2*MID (X)**2)
ENDIF
30   CONTINUE
20   CONTINUE
* CONVERT FORCES AT MIDEPTH OF SLAB TO FORCES AT NA OF EDGE BEAM
DO 40 X=1,2*NUM
IF(X.LE.NUM) THEN
FEB (X) =FSLAB (X)
ELSE
FEB(X) =FSLAB(X)+V1(X-NUM)*HB/2-FSLAB(X-NUM)/2 *(HB-HS)
ENDIF
40   CONTINUE
! CALCULATE DISPLACEMENTS AT NA OF THE EDGE BEAM
DO 50 X=1,2*NUM
50   DEB(X)=O
DO 60 X=1,2*NUM
DO 70 Y=1,2*NUM
DEB (X)=DEB (X) +F(X, Y) * FEB (Y)
70   CONTINUE
60   CONTINUE
! CALCULATE DISPLACEMENTS AT NEUTRAL AXIS OF SLAB
DO 80 X=1 , NUM
DSLAB(X)=DEB(X)-(HB/2-HS+CI(X)-BB/2*TAN(DEB(X+NUM)/2))*
+
      SIN (DEB(X+NWM))
80   CONTINUE

```

END

```
*****
SUBROUTINE STRIP(L,H,B, D1, D11, D2,D12, D3,D13,
+   DP1,DP2,DP3,LPS, AS1, AS2,AS3,ASP1,ASP2, ASP3,ASP, FC,
+   EC,A1,B1,ES, ESH, FYS, FUS, EYY, ESSH, EUU, EPPI,
+   FPE, FPU, EP, AA, BB, CC, K, EST, S, NU,
+   MU1,MU2,MU3,C1,C2,C3,WU, DL,SMOVE,BH,V1,V3)
*****
IMPLICIT DOUBLE PRECISION (A-W)
SET INCREMENT FOR SLAB DEFLECTION
BH=0.5
60 DLINC=H/300
DL=DLINC
WU2=0
INITIAL GUESS OF FORCES IN STEEL
T1=AS1*FYS
T2=AS2*FYS
T3=AS3* FYS
FPS=ASP* FPE
CS1=ASP1*FYS
CS2=ASP2*FYS
CS3=ASP2 FYS
* START LOOP FOR CALCULATION OF LOCATIONS OF NA AND FORCES IN STEEL
21 Y=0
20 Y=Y+1
IF(Y.EQ.15000)THEN
GOTO 7000
ELSE
CONTINUE
ENDIF
N=ES / EC
P=(AS1+AS2+AS3+ASPI+ASP2+ASP3)/(3*B*H)
BRACK=(( (1 + K ) *L/( (1+(N-1)*P)*EC*H)+1/S)*(A1*FC*B1*(H/2-DL/4+
+ ( (BH-1) *(T1-CS1) + T2-CS2-BH*(T3-CS3)+A1*FC*
+ ( (BH-1) + ASP1-ASP2-BH*ASP3)) / (2*A1*FC*B1*B)) + (CS2-T2-FPS) /B) +
+ EST*L) / (1+ (1-BH) *BH*L/ (2*DL)*A1 * F C * B 1 ) *
+ ( (1+ K)*L/ ( (1+ (N-1) * P) *EC*H) +1/S)
CALCULATE LOCATION OF NA
C1=H/2-DL/4 -(1-BH)* BH*L/ (2*DL)* BRACK+
+ ( (1+BH)' (T1-CS1)- T2+CS2-BH* (T3-CS3)+ A1 *FC* ( (BH+1) *ASP1-
+ ASP2-BH*ASP3))/(2*A1*FC*B1*B)
C2=H/2-DL/4-(1-BH)*BH*L/(2*DL)*BRACK+
+ ((BH-1)*(T1-CS1)+T2-CS2-BH*(T3-CS3)+A1*FC*((BH-1)*ASP1+
+ ASP2-BH*ASP3)) / (2*A1*FC*B1*B)
C3=H/2-DL/4-(1-BH)*BH*L/(2*DL)*BRACK+
+ ( (BH-1) * (T1-CS1)- T2+CS2+(2-BH)* (T3-CS3) +A1*FC* ( (BH-1)
+ ASP1-ASP2+ (2-BH) *ASP3)) / (2+A1*FC*B1*B)
* CALCULATE STRAINS AND FORCES IN STEEL
ECC=0.0035
ESS=EYY
ET1=ECC* ( (D1-C1) /C1)
CALL FMILDS (T12, ET1, EYY, ESSH,EUU, AS1,ES,ESH, FYS,FUS)
ET2=ECC* ( (D2-C2) /C2)
CALL FMILDS (T22, ET1, EYY, ESSH, EUU,AS2, ES, ESH, FYS, FUS)
ET3=ECC*((D3-C3)/C3)
```

```

CALL FMILDS (T32,ET1,EYY, ESSH,EUU,AS3, ES,ESH, FYS, FUS)
DL1 = (DP1-C1) / (BH*L) *DL
DL2=(DP2-C2) / (BH* (1-BH) *L) *DL
DL3=(DP3-C3) / ( (1-BH) *L) * DL
IF(ASP.EQ.0) THEN
FPS2=0
ELSE
EPP=EPP1 + (DL1+DL2+DL3) /LPS
FPS2=ASP * (EP*EPP*( AA+ (1-AA)/(1+ (BB*EPP)* *CC)* * (1/CC)))
ENDIF
IF(FPS2.GT.(FPU*ASP)) THEN
FPS2=0
ELSE
CONTINUE
ENDIF
ECS1=ECC* ( (C1-D11) /C1 )
CALL FMILDS(CS12,ET1,EYY,ESSH,EUU,ASP1,ES,ESH, FYS,FUS)
ECS2=ECC* ( (C2-D12) /C2)
CALL FMILDS (CS22, ET1, EYY, ESSH,EUU,ASP2,ES,ESH,FYS,FUS)
ECS3=ECC*((C3-D13)/C3)
CALL FMILDS (CS32, ET1, EYY, ESSH,EUU,ASP3,ES,ESH,FYS,FUS)
* COMPARE CALCULATED VALUES WITH ASSUMED VALUES
IF(T1.EQ.0) THEN
GOTO 11
ELSE IF(ABS ( (T1-T12) /T1) .GE.0.001) THEN
GOTO 10
ELSE
GOTO 11
ENDIF
11 IF(T2.EQ.0) THEN
GOTO 12
ELSE IF(ABS ((T2-TS22) /T2) .GE.0.001) THEN
GOTO 10
ELSE
GOTO 12
ENDIF
12 IF(T3.EQ.0) THEN
GOTO 13
ELSE IF(ABS((T3-T32)/T3).GE.0.001) THEN
GOTO 10
ELSE
GOTO 13
ENDIF
13 IF(FPS.EQ.0) THEN
GOTO 14
ELSE IF(ABS ((FPS-FPS2) /FPS) .GE.0.001) THEN
GOTO 10
ELSE
GOTO 14
ENDIF
14 IF(CS1.EQ.0) THEN
GOTO 15
ELSE IF(ABS((CS1-CS12)/CS1). GE.0.001) THEN
GOTO 10
ELSE
GOTO 15
ENDIF

```

```

15 IF(CS2.EQ.0) THEN
GOTO 16
  ELSE IF (ABS ( (CS2-CS22) /CS2 ) . GE. 0.001 ) THEN
GOTO 10
  ELSE
GOTO 16
16 IF(CS3.EQ.0) THEN
GOTO 17
  ELSE IF(ABS((CS3-CS32)/CS3).GE.0.001) THEN
GOTO 10
  ELSE
GOTO 17
ENDIF
10 IF(T12.EQ.0) THEN
T1=0
  ELSE
    T1=(T1+T22)/2
  ENDIF
  IF(T32.EQ.0) THEN
T3=0
  ELSE
T3= (T3+T32) /2
  ENDIF
  IF(FPS2.EQ.0) THEN
FPS=0
  ELSE
FPS= (FPS+FPS2) /2
  ENDIF
  IF(CS12.EQ.0) THEN
CS1=0
  ELSE
CS1=(CS1+CS12) /2
  ENDIF
  IF(CS22.EQ.0) THEN
CS2=0
  ELSE
CS2=(CS2+CS22)/2
  ENDIF
  IF(CS32.EQ.0) THEN
CS3=0
  ELSE
CS3=(CS3+CS32) /2
  ENDIF
  GOTO 21
17 CONTINUE
* CALCULATE FORCES AND ULTIMATE LOAD
MU1=A1*FC* (B1*C1*B-ASP1)*(0.5*H-0.5*B1*C1)+CS1
+
  0.5*H-D11) +T1*(D1-0.5*H) +FPS* (DP1-0.5*H)
NU=A1*FC*(B1*C2*B-ASP2) +CS2-T2-FPS
MU2=A1*FC*(B1*C2*B-ASP2)*(0.5*H-0.5*B1*C2)+CS2
+
  *(0.5*H-D12) +T2*(D2-0.5*H) +FPS* (DP2-0.5*H)
MU3=A1*FC* (B1*C3*B-ASP3)* (0.5*H-0.5*B1*C3)
+
  CS3*(0.5*H-D13)+T3*(D3-0.5*H)+FPS*(DP3-0.5H)
WU=2/(B*L**2)*(MU1/BH+MU2/((1-BH)*BH)+MU3/(1-BH)
+
  -NU*DL/((1-BH)*BH))
* CHECK IF ULTIMATE LOAD IS REACHED
WU1=WU2

```

```

WU2=WU
IF(WU1.GT.WU2) THEN
  DL=DL-DLINC
  GOTO 50
ELSE
  DL=DL+DLINC
GOTO 20
ENDIF
50 CONTINUE
* CALCULATE LOCATION OF HINGE 2
IF(ABS(MU1-MU3).LT.0.001) THEN
  BH2=0.5
  ELSE
  BH2=((MU1+MU2-NU*DL)-SQRT((MU1+MU2-NU*DL)**2-
+ (MU1-MU3)*(MU1+MU2-NU*DL)) ) / (MU1-MU3)
  ENDIF
IF(ABS (BH-BH2) /BH.LT.0.001) THEN
GOTO 30
  ELSE
  BH=BH2
GOTO 60
  ENDIF
30 CONTINUE
* CALCULATE TOTAL MOVEMENT OF SUPPORTS
SMOVE=NU/ (B*S)
* CALCULATE SHEAR
V1=(WU*B*(1-BH**2)*L**2-2*MU2-2*MU3+2*NU*DL)/(2*(1-BH)*L)
V3=(WU*B*(1-BH)**2*L**2+2*MU2+2*MU3-2*NU*DL)/(2*(1-BH)*L)
GOTO 6000
7000 WRITE (1,*) 'ERROR'
6000 END

```

UPDATED CODE

```

SUBROUTINE EXT (L, H, B, D1, D11, D2, D12, D3,D13, DP1, DP2, DP3,LPS,AS1,AS2, &
  AS3,ASP1, ASP2, ASP3,ASP,FC,EC,A1,B1,ES,ESH,FYS,FUS,&
  EYY, ESSH, EUU, EPPI, FPE, FPU, EP,AA, BB, CC, K, EST, S3, LC1,&
  LCB1,WCOL, EIC1, HB1, BB1, LB1, EIB1, JGB1, NUM)
IMPLICIT DOUBLE PRECISION (A-Z)
INTEGER NUM, X, Z, Y
DIMENSION DIST (15), S1 (15), SE (15), F1SLAB (30), F3SLAB (30), CC1 (15), CC3 (15)
, WWU (15), DDL (15), SSMOVE (15), &
D1SLAB (15), RMOVE (15), VV1 (15), VV3 (15), LE (15)
!CALCULATE WIDTH OF STRIPS AND STEEL IN STRIPS
B=B/(2* NUM)
ASP1=ASP1/ (2 *NUM)
ASP2=ASP2/ (2 *NUM)
ASP3=ASP3/ (2 *NUM)
ASP=ASP/ (2 *NUM)
AS1=AS1/ (2 *NUM)
AS2=AS2/ (2 *NUM)
AS3=AS3/(2*NUM)
!CALCULATE SLAB CAPACITY NEGLECTING COMPRESSIVE MEMBRANE
! AND STRAIN HARDENING
SO=1E-30

```

```

ENSH=0
CALL STRIP(L,H,B, D1, D11, D2,D12, D3,D13, DP1,DP2,DP3,LPS, AS1, AS2, &
AS3,ASP1,ASP2, ASP3,ASP, FC, EC,A1,B1,ES, ENSH, FYS, FUS,&
EYY, ESSH, EUU, EPPI, FPE, FPU, EP, AA, BB, CC, K, EST,SO, NU, &
MU1,MU2,MU3,C1,C2,C3,WUO, DL,SMOVE,BH,V1,V3)
!SET STIFFNESS OF FIRST SLAB STRIP EQUAL TO FLEXURAL
! STIFFNESS OF EDGE BEAM AT MIDDLE OF FIRST SLAB STRIP AND
! ITERATE TO GET STIFFNESS DISTRIBUTION
DO 10 X=1,NUM
S1 (X)=(1/(2/(3*EIC1 *LC1**3/( LCB1**3*(LC1-LCB1)**3)) + ( LB1/ &
(4*NUM)**2 / (6*EIB1*LB1**3)* (3*LB1**3*( LB1/( 4*NUM)) - &
LB1**3*(LB1/(4*NUM))-3*LB1**2*(LB1/(4*NUM))**2))))/B
DIST (X) =1
SE(1)=1/ (1/S1(1) +1/S3)
10 CONTINUE
140 Z=0
70 Z=Z+1
DO 20 X=1, NUM
20 SE (X) =DIST (X) * SE (1)
! CALCULATE FORCES AND DISPLACEMENTS OF STRIPS
DO 30 X=1,NUM
S=SE (X)
CALL STRIP(L,H,B, D1, D11, D2,D12, D3,D13, DP1,DP2,DP3,LPS, AS1, AS2, &
AS3,ASP1,ASP2, ASP3,ASP, FC, EC,A1,B1,ES, ESH, FYS, FUS,&
EYY, ESSH, EUU, EPPI, FPE, FPU, EP, AA, BB, CC, K,
EST,S, NU, &
MU1,MU2,MU3,C1,C2,C3,WU, DL,SMOVE,BH,V1,V3)
F1SLAB (X ) = NU
F1SLAB (X+NUM) =MU1
CC1 (X)=C1
VV1(X) =V1
F3SLAB(X) =NU
F3SLAB (X+NUM) =MU3
CC3(X) = C3
VV3 (X) =V3
WWU(X) =WU
LE (X) =WU/WUO
DDL (X)=DL
30 SSMOVE (X) =SMOVE
! CALCULATE MOVEMENT OF SUPPORTS
TNU=0
DO 40 X=1, NUM
40 TNU=2*F3SLAB(X) + TNU
D3SLAB=TNU/(B*2*NUM*S3)
CALL REST (H,LC1 ,LCB1 , WCOL,EIC1,HB1 , BB1 , LB1 , EIB1 ,JGB1 ,&
+ F1SLAB, CC1, D1SLAB, NUM, VV1 )
50 RMOVE (X) = D1SLAB (X) + D3SLAB
! CALCULATE DISTRIBUTION OF EFFECTIVE STIFFNESS
IF(Z.EQ.1)THEN
DO 60 X=1, NUM
60 DIST(X)= F1SLAB(X) /RMOVE(X) /(F1SLAB (1) / RMOVE (1))
ELSE
CONTINUE
ENDIF
! DEFINE POINTS ON TWO LINES TO CALCULATE COMPATIBLE STIFFNESS
IF(Z.EQ.1)THEN
SM1=SSMOVE(1)

```

```

RM1=RMOVE(1)
SEFF1=SE(1)
SE(1)=.7*SE(1)
GOTO 70
ELSE IF(Z.EQ.2)THEN
SM2=SSMOVE ( 1 )
RM2 =RMOVE ( 1 )
SEFF2=SE ( 1 )
ELSE
SM1=SM2
RM1 = RM2
SEFF1 =SEFF2
SM2 =SSMOVE ( 1 )
RM2=RMOVE ( 1 )
SEFF2=SE ( 1 )
ENDIF
WRITE(1,*) 'ITERATION',Z
!PREVENT POSSIBLE INFINITE LOOP
IF(Z.LT.50)THEN
GOTO 80
ELSE
WRITE (1,*) ' SOLUTION DID NOT CONVERGE'
GOTO 700
ENDIF
! CHECK IF STRIP AND RESTRAINT MOVEMENT ARE EQUAL FOR FIRST
! STRIP
80 IF (ABS((SSMOVE(1)- RMOVE(1)) /SSMOVE(1)).LT.0.01)THEN
GOTO 90
ELSE
GOTO 100
ENDIF
! CALCULATE NEXT ESTIMATE OF STIFFNESS
100 SEFF=(SEFF2-SEFF1)*(RM1-SM1)/(SM2-SM1-RM2+RM1)+SEFF1
IF (SEFF .LT. 0 ) THEN
SEFF=1E-5
ELSE
CONTINUE
ENDIF
SE(1)=SEFF
GOTO 70
!CHECK IF STRIP AND RESTRAINT MOVEMENT ARE EQUAL FOR OTHER
! STRIPS
90 WRITE(1,*) 'MATCHED STRIP FIRST STRIP ... CHECKING ALL STRIPS'
      Y=1
120 IF(ABS( (SSMOVE(Y)-RMOVE(Y))/SSMOVE(Y)).GT.0.01)THEN
GOTO 110
ELSE IF(Y.LT.NUM)THEN
WRITE(1,*) 'MATCHED STRIP #',Y
Y=Y+1
GOTO 120
ELSE
WRITE(1,*) 'MATCHED STRIP #',Y
GOTO 150
ENDIF
! CALCULATE NEW DISTRIBUTION OF STIFFNESS
110 DO 130 X=1,NUM
130 DIST(X)=F1SLAB(X) /RMOVE(X) /((F1SLAB(1)/RMOVE(1))

```

```

GOTO 140
150 WRITE (1, *) 'SLAB HAS CONVERGED TO A SOLUTION'
!CALCULATE TOTAL AXIAL FORCE AND MOMENT APPLIED TO COLUMNS AND
! AVERAGE LOAD CAPACITY AND LOAD ENHANCEMENT
NUT=0
MU1T=0
MU3T=0
WTOT=0
DO 160 X=1,NUM
NUT=NUT+F1SLAB (X)
MU1T=MU1T+F1SLAB (X+NUM)
MU3T=MU3T+F3SLAB (X+NUM)
160 WTOT=WTOT+WWU (X)
      WAVG=WTOT/NUM
      AVGLE=WAVG/WUO
! OUTPUT DATA
WRITE (6,1) NUM
DO 170 X=1,NUM
170 WRITE (6,2) X, SE(X) , WWU (X), LE (X)
WRITE (6,3) WAVG, AVGLE, NUT, MU3T, MU1T
1 FORMAT(/,'EXTERIOR SLAB LOADED - ',I3, ' SLAB STRIPS USED',/, &
'
      EFFECTIVE
      ' &
      ,/, 'STRIP          SUPPORT          ULTIMATE
      '          LOAD',/,' NUM          STIFFNESS    CAPACITY', &
      '          'ENHANCEMENT')
2 FORMAT(I3, '          ',F6.1,F18.4,F19.2)
3 FORMAT(/'AVERAGE ULTIMATE CAPACITY IS ', F6.2,/, &
+'AVERAGE LOAD ENHANCEMENT IS',F7.2,///, &
+'TOTAL AXIAL FORCE APPLIED TO A COLUMN IS', &
+ E17.3,/, 'TOTAL MOMENT APPLIED TO AN EXTERIOR COLUMN IS',E12.3, &
+ //, ' TOTAL MOMENT APPLIED TO AN INTERIOR COLUMN IS ', E12.3, /)
700 CONTINUE
END

```

```

SUBROUTINE FMILDS (F,ESS,EYY,ESSH,EUU,AS,ES,ESH,FYS,FUS)
IMPLICIT DOUBLE PRECISION (A-Z)
IF(ABS(ESS).LT.EYY) THEN
F=AS*ES*ESS
ELSE IF(ESS.LE. (ESSH*(-1))) THEN
F=0
ELSE IF(ESS.LE.(EYY*(-1))) THEN
F=AS*FYS* (-1)
ELSE IF(ESS.LE.ESSH) THEN
F=AS*FYS
ELSE IF (ESS.LE. EUU) THEN
F=AS*(FYS+ESH*(ESS-ESSH)*(1-ESH*(ESS-ESSH))/(4*(FUS-FYS)))
ELSE
F=0
ENDIF
RETURN
END

```

```

SUBROUTINE INT (L,H,B,D1,D11,D2,D12, D3, D13, DP1,DP2,DP3,LPS,AS1,AS2,&

```

```

AS3,ASP1,ASP2,ASP3,ASP,FC,EC,A1,B1,ES,ESH,FYS,FUS,
&
EYY ,ESSH,EUU,EPPI,FPE,FPU,EP,AA,BB,CC,K,EST,S)
IMPLICIT DOUBLE PRECISION (A-Z)
! effective restraint stiffness SO
SO=1E-30
! strain-hardening modulus for mild steel reinforcement ENSH is 0
! determine the ultimate capacity of the slab neglecting CMA and
! strain-hardening of the mild steel reinforcement
ENSH=0
CALL STRIP (L,H,B, D1, D11, D2,D12, D3,D13, DP1,DP2,DP3,LPS,AS1, AS2,&
AS3,ASP1,ASP2, ASP3,ASP, FC,EC,A1,B1,ES, ENSH,FYS, FUS,&
EYY, ESSH, EUU, EPPI,FPE, FPU, EP, AA, BB, CC,K, EST, SO, NU, &
MU1,MU2,MU3,C1,C2,C3,WUO,DL,SMOVE,BH,V1,V3)
CALL STRIP (L,H,B, D1, D11, D2,D12, D3,D13, DP1,DP2,DP3,LPS,AS1, AS2,&
AS3,ASP1,ASP2, ASP3,ASP, FC,EC,A1,B1,ES, ESH,FYS, FUS,&
EYY, ESSH, EUU, EPPI,FPE, FPU, EP, AA, BB, CC,K, EST, S, NU, &
MU1,MU2,MU3,C1,C2,C3,WU,DL,SMOVE,BH,V1,V3)
LE=WU/WUO
WRITE(1,*)'SLAB HAS CONVERGED TO A SOLUTION'
! OUTPUT DATA
WRITE (6,1)
WRITE(6,2) S,WU,DL, LE
WRITE(6,3)
WRITE(6,4) NU, MU1,MU2,MU3
1 FORMAT(/,'INTERIOR SLAB LOADED -SINGLE SLAB STRIP USED', //, &
'EFFECTIVE MAXIMUM ', / &
'SUPPORT ULTIMATE VERTICAL LOAD', /, &
'STIFFNESS CAPACITY DEFLECTION ENHANCEMENT ')
2 FORMAT(F6.1, F18.4,2F16.2)
3 FORMAT ( //, 'AXIAL MOMENT AT PLASTIC HINGE ', /, &
' FORCE 1 2 3')
4 FORMAT(E9.3,3E18.3, / )
RETURN
END

```

```

SUBROUTINE ISTRN (EPPI,FPE,EP, AA,BB,CC)
IMPLICIT DOUBLE PRECISION (A-Z)
! initial total prestress strain is equal to 0
EPPI=0
! FP is the stress: equation 2.36:modified Ramberg-Osgood Function
10 FP=EP*EPPI * (AA + (1-AA) / (1+ (BB * EPPI) **CC) ** (1/CC) )
IF(FP.LE.FPE) THEN
EPPI=EPPI+0.000001
GOTO 10
ELSE
GOTO 20
ENDIF
20 RETURN
END

```

```

SUBROUTINE REST (HS,LC,LCB, WCOL,EIC,HB,BB,LB,EIB, JGB, FSLAB,
C1,DSLAB,NUM,V1)
IMPLICIT DOUBLE PRECISION (A-M, P-W)
INTEGER X, Y, NUM
DIMENSION MID(15),F(30,30), FSLAB(30),FEB(30),DEB(30),DSLAB(15), C1(15) ,V1 (15)
!DETERMINE MIDPOINTS OF STRIPS

```

```

DO 10 X=1,NUM
MID(X)=LB/ (4*NUM)+ (X-1) *LB/ (2*NUM)
10 CONTINUE
!CALCULATE FLEXIBILITY MATRIX
KHC=3*EIC*LC**3/(LCB**3*(LC-LCB)**3)
KXC=EIC*LC**3/((-4)*LCB**2*LC**2+LCB*LC**3+6*LCB**3*LC-3*LCB**4)
DO 20 X=1,2*NUM
DO 30 Y=1,2*NUM
IF ((X.GT.NUM).AND.(Y.LE.NUM)) THEN
! EQUATION (4.29)

$$F(Y,X) = 2/(6*EIC*LC**3)*(12*LCB**3*LC**2-3*LCB**2*LC**3 - 15*LCB**4*LC+6*LCB**5)$$

ELSE IF((X.GT.NUM).AND.(Y.LE.X)) THEN
IF( (MID(Y-NUM)) .LE. (WCOL/2)) THEN
!EQUATION (4.14 A)
F(Y, X)=2/KXC
ELSE
!EQUATION (4.14 B)
F(Y,X)=(2/KXC+ (MID(Y-NUM) -0.5*WCOL) /JGB)
ENDIF
ELSE IF( (X.GT.NUM) .AND. (Y.GT.X) ) THEN
!EQUATION (4.14 C)
F(Y,X)=(2/KXC + (MID(X-NUM)-0.5*WCOL) /JGB)
ELSE IF(Y.GT.NUM) THEN
! EQUATION (4.38)

$$F(Y,X)=2/(6*EIC*LC)*(-4*LC**2*LCB+15*LC*LCB**2 -20*LCB**3+15*LCB**4/LC-6*LCB**5/LC**2)$$

ELSE IF(Y.GT.X) THEN
IF( (MID(Y)) .LE. (WCOL/2)) THEN
!EQUATION (4.11 A)
F(Y,X)=2/KHC
ELSE
! EQUATION (4.11 B )

$$F(Y,X)= 2/KHC + (MID(X)- 0.5 * WCOL) **2/ (6*EIB*LB**3)*(3*LB**3*MID(Y) - LB**3*MID(X) -LB**3*WCOL-3*LB**2*(MID(Y) - 0.5*WCOL) **2)$$

ENDIF
ELSE
! EQUATION (4.11 C)

$$F(Y,X)=2/KHC+(MID(Y)-0.5*WCOL)**2/(6*EIB*LB**3)*(3*LB**3*MID (X) - LB**3*MID(Y) -LB**3*WCOL- 3*LB**2*MID (X)**2)$$

ENDIF
30 CONTINUE
20 CONTINUE
!CONVERT FORCES AT MIDEPTH OF SLAB TO FORCES AT NA OF EDGE BEAM
DO 40 X=1,2*NUM
IF(X.LE.NUM) THEN
FEB (X) =FSLAB (X)
ELSE
FEB(X) =FSLAB(X)+V1(X-NUM)*HB/2-FSLAB(X-NUM)/2 *(HB-HS)
ENDIF
40 CONTINUE
!CALCULATE DISPLACEMENTS AT NA OF THE EDGE BEAM
DO 50 X=1,2*NUM
50 DEB(X)=0
DO 60 X=1,2*NUM
DO 70 Y=1,2*NUM
DEB (X)=DEB (X) +F(X, Y) * FEB (Y)

```

```

70 CONTINUE
60 CONTINUE
!CALCULATE DISPLACEMENTS AT NEUTRAL AXIS OF SLAB
  DO 80 X=1 , NUM
DSLAB(X)=DEB(X)-(HB/2-HS+Cl(X)-BB/2*TAN(DEB(X+NUM)/2))* SIN
(DEB(X+NUM))
80 CONTINUE
END

```

PROGRAM SLAB

```

IMPLICIT DOUBLE PRECISION (A-Z)
INTEGER CASE,NUM
OPEN (1, FILE = 'TERMINAL')
OPEN (5, FILE = "C:\\example\\EXPL\\inputcase11.txt",STATUS ='OLD')
OPEN (6, FILE='OUTPUT' )
READ (5,*)   L,H,B,&
              D1,D11,D2,D12, D3, D13,&
              DP1,DP2,DP3,LPS,&
              AS1,AS2,AS3,ASP1,ASP2,ASP3,ASP,&
              FC,EC,A1,B1, &
              ES,ESH,FYS,FUS,&
              EYY,ESSH,EUU, &
              FPE,FPU,EP, &
              AA,BB,CC,&
              K,EST, &
              CASE
IF (ASP.EQ.0) THEN
GOTO 10
ELSE
CALL ISTRN (EPPI, FPE, EP, AA, BB, CC)
ENDIF
10 GOTO (100,200,300),CASE
100 READ(5, *) S
CALL INT(L,H,B,D1,D11,D2,D12, D3, D13, DP1,DP2,DP3,LPS,AS1,AS2,&
+ AS3,ASP1,ASP2,ASP3,ASP,FC,EC,A1,B1,ES,ESH,FYS,FUS, &
+ EYY ,ESSH,EUU,EPPI,FPE,FPU,EP,AA,BB,CC,K,EST,S)
GOTO 400
200 READ(5,*) S3, &
  LC1, LCB1, WCOL, EIC1,&
  HB1, BB1, LB1, EIB1, JGB1,&
  NUM
CALL EXT (L, H, B, D1, D11, D2, D12, D3,D13, DP1, DP2, DP3,LPS,AS1,AS2, &
+ AS3,ASP1, ASP2, ASP3,ASP,FC,EC,A1,B1,ES,ESH,FYS,FUS,&
+ EYY, ESSH, EUU, EPPI, FPE, FPU, EP,AA, BB, CC, K, EST, S3, LC1,&
+ LCB1,WCOL, EIC1, HB1, BB1, LB1, EIB1, JGB1, NUM)
GOTO 400
300 READ(5,*) S3, &
  LC1, LCB1, WCOL, EIC1,HB1, BB1, LB1, EIB1, JGB1,&
  NUM
S3=1E38
EIC1=1E38
CALL EXT (L, H, B, D1, D11, D2, D12, D3,D13, DP1, DP2, DP3,LPS,AS1,AS2, &
+ AS3,ASP1, ASP2, ASP3,ASP,FC,EC,A1,B1,ES,ESH,FYS,FUS,&
+ EYY, ESSH, EUU, EPPI, FPE, FPU, EP,AA, BB, CC, K, EST, S3, LC1,&
+ LCB1,WCOL, EIC1, HB1, BB1, LB1, EIB1, JGB1, NUM)
400 END

```

```

SUBROUTINE STRIP (L,H,B, D1, D11, D2,D12, D3,D13, DP1,DP2,DP3,LPS,AS1, AS2,&
    AS3,ASP1,ASP2, ASP3,ASP, FC,EC,A1,B1,ES,ESH,FYS, FUS,&
    EYY, ESSH, EUU, EPPI,FPE, FPU, EP, AA, BB, CC,K, EST, S, NU, &
    MU1,MU2,MU3,C1,C2,C3,WU,DL,SMOVE,BH,V1,V3)
IMPLICIT DOUBLE PRECISION (A-W)
!SET INCREMENT FOR SLAB DEFLECTION
! IDEALISED PLASTIC FAILURE
    BH=0.5
! APPLY INCREMENTAL DEFLECTION
    60 DLINC=H/300
        DL=DLINC
        WU2=0
! INITIAL GUESS OF FORCES IN MILD STEEL: STEEL YIELDS (BUT NO STRAIN
HARDENING)
    T1=AS1*FYS
    T2=AS2*FYS
    T3=AS3*FYS
! INITIAL PRESTRESS FORCE= EFFECTIVE PRESTRESS FORCE
    FPS=ASP*FPE
! INITIAL COMPRESSIVE STEEL FORCE IN MILD STEEL (NO ADDITIONAL STRAIN
DUE TO DEFORMATION)
    CS1=ASP1*FYS
    CS2=ASP2*FYS
    CS3=ASP3*FYS
! START LOOP FOR CALCULATION OF LOCATIONS OF NA AND FORCES IN STEEL
UNTIL F<0.1%
    21 Y=0
    20 Y=Y+1
        IF (Y.EQ.15000) THEN
            GOTO 7000
        ELSE
            CONTINUE
        ENDIF
        N=ES/EC
! P IS THE REINFORCEMENT RATIO
        P=(AS1+AS2+AS3+ASP1+ASP2+ASP3)/(3*B*H)
! BRACKET IN EQUATION 2.41-2.43
        BRACK= (((1+K)*L/((1+(N-1)*P)*EC*H)+1/S)*(A1*FC*B1*(H/2-DL/4+((BH-1)*(T1-
CS1)+T2-CS2-BH*(T3-CS3)+ &
        A1*FC*((BH-1)*ASP1-ASP2-BH*ASP3))/(2*A1*FC*B1*B))+ (CS2-T2-FPS)/B)+
EST*L)/(1+ &
        (1-BH)*BH*L/(2*DL)*(A1*FC*B1)*((1+K)*L/((1+(N-1)*P)*EC*H)+1/S))
! CALCULATE LOCATION OF NA : 2.41-2.43
!START WITH ASSUMED VALUES AND CALCULATE NA FOR EACH ITERATION
        C1=H/2-DL/4-(1-BH)*BH*L/(2*DL)*BRACK+ &
        ((1+BH)*(T1-CS1)-T2-CS2-BH*(T3-CS3)+A1*FC*((1+BH)*ASP1-ASP2-
BH*ASP3))/(2*A1*FC*B1*B)
        C2=H/2-DL/4-(1-BH)*BH*L/(2*DL)*BRACK+ &
        ((BH-1)*(T1-CS1)+T2-CS2-BH*(T3-CS3)+A1*FC*((BH-1)*ASP1+ASP2-
BH*ASP3))/(2*A1*FC*B1*B)
        C3=H/2-DL/4-(1-BH)*BH*L/(2*DL)*BRACK+ &
        ((BH-1)*(T1-CS1)-T2+CS2+(2-BH)*(T3-CS3)+A1*FC*((BH-1)*ASP1-ASP2+(2-BH)*ASP3)
)/(2*A1*FC*B1*B)
!CALCULATE STRAINS AND FORCES IN STEEL : EQ 2.25-2.37
!CALCULATE NEW FORCES FOR THE NEW NA
        ECC=0.0035
        ESS=EYY

```

```

! STRAIN IN TENSION EQ 2.25 FOR EACH PLASTIC HINGE
  ET1=ECC*((D1-C1)/C1)
    CALL FMILDS (T12,ET1,EYY, ESSH, EUU, AS1, ES,ESH,FYS,FUS)
  ET2= ECC*((D2-C2)/C2)
    CALL FMILDS (T22,ET1, EYY, ESSH, EUU, AS2, ES,ESH,FYS,FUS)
  ET3=ECC*((D3-C3)/C3)
    CALL FMILDS (T32,ET1, EYY, ESSH, EUU, AS3, ES,ESH,FYS,FUS)
!INCREASE LENGTH OF TENDON pi: eq 2.32
  DL1=(DP1-C1)/(BH*L)*DL
  DL2=(DP2-C2)/(BH*(1-BH)*L)*DL
  DL3=(DP3-C3)/((1-BH)*L)*DL
  IF (ASP.EQ.0) THEN
    FPS2=0
  ELSE
    EPP=EPPI+(DL1+DL2+DL3)/LPS
    ! steel force PRESTRESS: eq 2.36
    FPS2=ASP*(EP*EPP*(AA+(1-AA)/(1+(BB*EPP)**CC)**(1/CC)))
  ENDIF
  IF (FPS2.GT.(FPU*ASP)) THEN
    FPS2=0
  ELSE
    CONTINUE
  ENDIF
  ECS1=ECC*((C1-D11)/C1)
    CALL FMILDS (CS12,ET1,EYY, ESSH, EUU, ASP1, ES,ESH,FYS,FUS)
  ECS2=ECC*((C2-D12)/C2)
    CALL FMILDS (CS22,ET1,EYY, ESSH, EUU, ASP2, ES,ESH,FYS,FUS)
  ECS3=ECC*((C3-D13)/C3)
    CALL FMILDS (CS32,ET1,EYY, ESSH, EUU, ASP3, ES,ESH,FYS,FUS)
! COMPARE CALCULATED VALUES WITH ASSUMED VALUES
  IF (T1.EQ.0) THEN
    GOTO 11
  ELSE IF (ABS((T1-T12)/T1).GE.0.001) THEN
    GOTO 10
  ELSE
    GOTO 11
  ENDIF
11 IF (T2.EQ.0) THEN
  GOTO 12
  ELSE IF (ABS((T2-T22)/T2).GE.0.001) THEN
    GOTO 10
  ELSE
    GOTO 12
  ENDIF
12 IF (T3.EQ.0) THEN
  GOTO 13
  ELSE IF (ABS((T3-T32)/T3).GE.0.001) THEN
    GOTO 10
  ELSE
    GOTO 13
  ENDIF
13 IF (FPS.EQ.0) THEN
  GOTO 14
  ELSE IF (ABS((FPS-FPS2)/FPS).GE.0.001) THEN
    GOTO 10
  ELSE
    GOTO 14

```

```

ENDIF
14 IF (CS1.EQ.0) THEN
    GOTO 15
    ELSE IF (ABS((CS1-CS12)/CS1).GE.0.001) THEN
        GOTO 10
    ELSE
        GOTO 15
    ENDIF
15 IF (CS2.EQ.0) THEN
    GOTO 16
    ELSE IF (ABS((CS2-CS22)/CS2).GE.0.001) THEN
        GOTO 10
    ELSE
        GOTO 16
    ENDIF
16 IF (CS3.EQ.0) THEN
    GOTO 17
    ELSE IF (ABS((CS3-CS32)/CS3).GE.0.001) THEN
        GOTO 10
    ELSE
        GOTO 17
    ENDIF
10 IF (T12.EQ.0) THEN
    T1=0
    ELSE
        T1=(T1+T12)/2
    ENDIF
    IF (T22.EQ.0) THEN
        T2=0
        ELSE
            T2=(T2+T22)/2
        ENDIF
        IF (T32.EQ.0) THEN
            T3=0
            ELSE
                T3=(T3+T32)/2
            ENDIF
            IF (FPS2.EQ.0) THEN
                FPS=0
                ELSE
                    FPS=(FPS+FPS2)/2
                ENDIF
                IF (CS12.EQ.0) THEN
                    CS1=0
                    ELSE
                        CS1=(CS1+CS12)/2
                    ENDIF
                    IF (CS22.EQ.0) THEN
                        CS2=0
                        ELSE
                            CS2=(CS2+CS22)/2
                        ENDIF
                        IF (CS32.EQ.0) THEN
                            CS3=0
                            ELSE
                                CS3=(CS3+CS32)/2
                            ENDIF

```

```

GOTO 21
17 CONTINUE
! CALCULATE FOCRES AND ULTIMATE LOAD
MU1=A1*FC*(B1*C1*B-ASP1)*(0.5*H-0.5*B1*C1)+CS1*(0.5*H-D11)+T1*(D1-
0.5*H)+FPS*(DP1-0.5*H)
NU=A1*FC*(B1*C2*B-ASP2)+CS2-T2-FPS
MU2=A1*FC*(B1*C2*B-ASP2)*(0.5*H-0.5*B1*C2)+CS2*(0.5*H-D12)+T2*(D2-
0.5*H)+FPS*(DP2-0.5*H)
MU3=A1*FC*(B1*C3*B-ASP3)*(0.5*H-0.5*B1*C3)+CS3*(0.5*H-D13)+T3*(D3-
0.5*H)+FPS*(DP3-0.5*H)
WU=2/(B*L**2)*(MU1/BH+MU2/((1-BH)*BH)+MU3/(1-BH)-NU*DL/((1-BH)*BH))
! CHECK IF ULTIMATE LOAD IS REACHED
WU1=WU2
WU2=WU
IF (WU1.GT.WU2) THEN
DL=DL-DLINC
GOTO 50
ELSE
DL=DL+DLINC
GOTO 20
ENDIF
50 CONTINUE
!CALCULATE LOCATION OF HINGE 2
IF (ABS(MU1-MU3).LT.0.001) THEN
BH2=0.5
ELSE
BH2=((MU1+MU2-NU*DL)-SQRT((MU1+MU2-NU*DL)**2-(MU1-
MU3)*(MU1+MU2-NU*DL)))/(MU1-MU3)
ENDIF
IF (ABS(BH-BH2)/BH.LT.0.001) THEN
GOTO 30
ELSE
BH=BH2
GOTO 60
ENDIF
30 CONTINUE
!CALCULATE TOTAL MOVEMENT OF SUPPORTS
SMOVE=NU/(B*S)
! CALCULATE SHEAR
V1=(WU*B*(1-BH**2)*L**2-2*MU2-2*MU3+2*NU*DL)/(2*(1-BH)*L)
V3=(WU*B*(1-BH)**2*L**2+2*MU2+2*MU3-2*NU*DL)/(2*(1-BH)*L)
7000 WRITE (1,*) 'ERROR', Y
6000 END

```

PUNCHING SHEAR CAPACITY

MATLAB CODE

```

% scp=2,5MPa- CRACKED EI
function [Fb]=Fb (c,B,y,d,Es,fsy,rho,P,TA)
% Starting Assumption
c = 1050;
r1 = 200;
r2 = 200;
B = (r1 * r2)^0.5;
Ap =0.583871669;
h = 100;
rho = Ap / h;

```

```

d = 0.5*0.45*h;
fck = 70.16;
fcube = 82.54;
sigmap = 2.5;
%Fp = sigmap * h; NOT CRACK WIDTH
fpk = 1100;
fsy = 762.7144350; % unbonded tendon
Es = 2.05 * 10^5;
Ec = 34297.30;
yel=12.07355402;% mm only for the uncracked stiffness
y= 10.41; % mm
P= 162367;% N
ecpu=3.57E-03; % total strain = concrete and pretress
[TA] = calTA(B,y,d,fcube,P)
TA1=real(TA);
A = 1/4.7*(1+y/B)*log(c/(B+2*y));
kz = ((A + (1 - TA1)/(1+TA1*TA1))*(1+TA1*TA1)/(TA1*(1-TA1)))% [-]
fcurv=ecpu/y;
me=P*(2*log(c/B)+1-(B^2/c^2))/(8*pi);
EI=me/fcurv % cracked stiffness
if B / d < 2
tasi = 0.0035 * (1 - 0.22*(B/d))*(1 + B/(2*y));
else
tasi = (P/(4*pi))*(1-B^2/c^2)*(c/(2*EI));
end
rs = Es / fsy * tasi * (d - y);
C0 = B/2 + 1.8 * d;
if rs > C0 % mm
R1 = (rho * fsy * d * ((rs - C0) + rs * log(c/(2 * rs)))/1000; %kNmm
R2overBeta = rho * fsy * d * C0/1000;% kNmm
else % it is else
R1 = (rho * fsy * d * rs * log(c/(2*C0)))/1000 ;%kNmm
R2overBeta = rho * fsy * d * rs/1000; % kNmm
end
[Mb] = Mb(P,y,B,c,TA1,d)
Fb = (P*kz/(2*pi)- R1*1000 - R2overBeta*1000)*(2/c) % N
function [TA] = calTA(B,y,d,fcube,P)
if B/d < 2
ft = 825 * (0.35 + 0.3 * (fcube/150))*(1 - 0.22 * (B / d));
else
ft = 460 * (0.35 + 0.3 * (fcube/150));
end
falpa = P / (pi * (B / d) * (y / d) * (B + 2 * y) / (B + y) * ft * d * d);
TA = (1 - sqrt(1-4*(falpa+1)*falpa)) / (2*(falpa+1));
TA1=real(TA);
% calculation of Fbmax and Mbmax
c = 1050;
r1 = 200;
r2 = 200;
B = (r1 * r2)^0.5;
Ap =0.583871669;
h = 100;
rho = Ap / h;
d = 0.5*0.45*h;
fck = 70.16;
fcube = 82.54;
sigmap = 2.5;

```

```

Fp = sigmap * h;
fpk = 1100;
fsy = fpk - (Fp / Ap);
Es = 2.05 * 10^5;
Ec = 34297.30;
yel=12.07355402;% mm only for the uncracked stiffness
y= 10.41; % mm
P= 162367;% N
ecpu=3.57E-03; % total strain = concrete and pretress
fcurv=ecpu/y;
me=P*(2*log(c/B)+1-(B^2/c^2))/(8*pi)
EI=me/fcurv % cracked stiffness EI
if B / d < 2
tasi = 0.0035 * (1 - 0.22*(B/d))*(1 + B/(2*y));
else
tasi = (P/(4*pi))*(1-B^2/c^2)*(c/(2*EI))
end
delta =1/2* tasi*(c-B) %mm
Fc = 0.75 * 0.721 *0.842* fck * (h/2 - delta/4);
Ft = d * rho * fsy;
Fbmax = Fc - Ft %N
Mbmax = Ft * (2 * d - h) - Fc * (d - 13*h/16 - 3 * delta/32)%Nmm
[Mb] = Mb(P,y,B,c,TA1,d);
eta1=Mb/Mbmax;
function [Mb] = Mb(P,y,B,c,TA1,d)
A = 1/4.7*(1+y/B)*log(c/(B+2*y));
ky = 3*(c - B)/(2*(3*d - y));
kz = ((A + (1 - TA1)/(1+TA1*TA1))*(1+TA1*TA1)/(TA1*(1-TA1)));
X = (4*(3*d-y)/3)*(ky-kz)/1000 ;%mm
% Calculate Mb [N m]
Mb = P * X / (4*pi);

```